8-2010

Studies on the Role of Vitronectin and Plasminogen-Activator Inhibitor-1 Complexes Beyond Inhibiting Proteases: Binding to the Extracellular Matrix, Cell Interactions and Pathogenesis

Sumit Goswami
sgoswam1@utk.edu

To the Graduate Council:

I am submitting herewith a dissertation written by Sumit Goswami entitled "Studies on the Role of Vitronectin and Plasminogen-Activator Inhibitor-1 Complexes Beyond Inhibiting Proteases: Binding to the Extracellular Matrix, Cell Interactions and Pathogenesis." I have examined the final electronic copy of this dissertation for form and content and recommend that it be accepted in partial fulfillment of the requirements for the degree of Doctor of Philosophy, with a major in Biochemistry and Cellular and Molecular Biology.

<div align="right">Cynthis B. Petesron, Major Professor</div>

We have read this dissertation and recommend its acceptance:

Jeff Becker, John Koontz, Andreas Nbenfuhr, Jay Wimalasena

<div align="right">Accepted for the Council:</div>

<div align="right">Carolyn R. Hodges</div>

<div align="right">Vice Provost and Dean of the Graduate School</div>

(Original signatures are on file with official student records.)

To the Graduate Council:

I am submitting herewith a thesis written by Sumit Goswami entitled "Studies on the Role of Vitronectin and Plasminogen-Activator Inhibitor-1 Complexes Beyond Inhibiting Proteases: Binding to the Extracellular Matrix, Cell Interactions and Pathogenesis."
I have examined the final electronic copy of this thesis for form and content and recommend that it be accepted in partial fulfillment of the requirements for the degree of Doctor of Philosophy, with a major in Biochemistry Cellular and Molecular Biology.

Cynthia B. Peterson, Major Professor
_____

We have read this thesis
and recommend its acceptance:

Jeff Becker
_____

John Koontz
_____

Andreas Nebenfuhr
_____

Jay Wimalasena
_____

Accepted for the Council:

Carolyn R. Hodges
_____

Vice Provost and Dean of the Graduate School

(Original signatures are on file with official student record)

Studies on the Role of Vitronectin and Plasminogen-Activator Inhibitor-1 Complexes Beyond Inhibiting Proteases: Binding to the Extracellular Matrix, Cell Interactions and Pathogenesis

A Thesis Presented for the

Doctor of Philosophy

Degree

The University of Tennessee, Knoxville

Sumit Goswami

August 2010

<u>DEDICATION</u>

This dissertation is dedicated to

my parents

Jiban Krishna Goswami and Uma Goswami

my wife

Sukanya Bhattacharya

my advisor

Dr. Cynthia B. Peterson

and my daughter

Shreeja Goswami

ACKNOWLEDGEMENTS

First of all I would like to thank the Biochemistry Cellular and Molecular Biology (BCMB) Department for accepting me as a graduate student and providing me an opportunity to earn a PhD. I am grateful to this department as it has always provided an excellent learning environment. I have also a special reason to be thankful to my department. I had to borrow a laptop from the department as my personal computer crashed when I was in the middle of writing my thesis. This BCMB laptop got stolen from the Hodges library carrel. I was fortunate enough to have my department and my mentor Dr. Cynthia Peterson beside me at that point and I did not have to pay any compensation. I was allowed to have another laptop from the department which I used for the rest of my thesis writing and currently using to write this acknowledgement.

I was fortunate to have Dr. Cynthia B. Peterson as my mentor. I would like to thank her both as my advisor and as an administrator who has successfully run the department for the last few years. Under her supervision I have seen a lot of improvements that have happened in our department. She is an open-minded professor who believes in the importance of education. Both inside the lab and within the department, I have seen her as a person who is sincerely engaged in the maintenance of proper learning environment. I had tremendous opportunity of expanding my technical expertise and knowledge base under her guidance. My primary research project has been extremely difficult for various reasons requiring extensive unanticipated troubleshooting phases. There were moments when I felt frustrated and lost faith in me but Dr. Peterson always showed faith in me. Rather, she allowed me to work on more than one projects and was always supportive. When I look back and try to evaluate the decisions that I have taken in my life I find

daughter when my wife and I were struggling to manage our graduate student life and our

daughter. The love and care that my daughter received from them was invaluable. I will remain

grateful to these people forever. I find myself privileged when I think of the tremendous help and

love that I have received from so many people! I honestly apologize if I am forgetting to

acknowledge someone and I also hope that in the future, I will be able to be equally helpful to

my friends and colleagues.

<u>ABSTRACT</u>

Plasminogen activator inhibitor-1 (PAI-1), a member of the serine protease inhibitor (serpin) superfamily of proteins, circulates in blood in a complex with vitronectin (VN). These two proteins are also found localized together in the extracellular matrix in many different pathophysiological conditions. Both of these proteins are involved with a number of physiologically important processes. Though PAI-1 is a well-known inhibitor of serine proteases, more emphasis is now geared towards its protease independent functions. VN, on the other hand, is a binding protein that exists in the circulation in a preferred monomeric conformation. However, in the extracellular matrix, VN exists as multimer with altered conformation. Though the exact reason for such conformational alterations and compartmentalization is unknown, there are a number of biomolecules, including PAI-1 that are proposed to cause such alterations. In last few years, sufficient experimental evidence has been gathered to confirm this protease-independent effect of PAI-1 by which it induces multimerization of VN in a concentration-dependent fashion. It has been observed also that PAI-1 remains associated with this multimeric complex for several hours. A major focus of this dissertation work was to extend our understanding of the mechanism of the interaction between these proteins and to explore the physiological relevance of the multimeric complexes formed by their interaction on cellular adhesion and migration. In our study, emphasis has been given to the presence of an appropriate microenvironment so that the role of the multimeric complexes could be investigated in a relevant biological setting. Our findings indicate the importance of the surrounding microenvironment in establishing the specific role of the VN/PAI-1 complex in cell-matrix interactions. In a previous study from our lab, it was found that vitronectin knock-out mice were

more resistant to *Candida* infection compared to wild type C57Bl/6 mice. One of the goals of this dissertation work was to provide a mechanistic explanation for their increased survival of the vitronectin knock-out mice upon *Candida* infection. Another important aspect of this work was to establish biophysical methods for understanding the structural changes that happen in PAI-1 naturally or due to ligand binding.

TABLE OF CONTENTS

LIST OF FIGURES

LIST OF TABLES

CHAPTER-1

General Background

1.1. Vitronectin

1.1. a. Localization & Biosynthesis

Vitronectin (VN) is a glycoprotein that was initially termed as 'serum spreading factor' because of its presence in human serum and involvement in cellular attachment [1]. Originally it was purified from serum using glass bead chromatography columns [1]. This protein, when isolated from human serum, could support cell growth and spreading of fibroblast and epithelial cells under serum-free conditions [2-3]. Podack et al. first reported a method of purification of this protein from plasma [4]. The concentration of VN in the circulation is about 0.2-0.4 mg/ml (0.3-0.6μM) [5-6]. The presence of VN in the extracellular matrix and tissue was first reported by Ruoslahti and his group [7]. With specific monoclonal antibody staining, this group clearly showed the presence of vitronectin in fetal membrane tissue and in the extracellular matrix associated with the surface of fibroblast cells [7]. They were the first to denote 'serum spreading factor' as 'vitronectin' because of its glass-binding and cell-adhesive properties. S-protein is another circulatory protein that was identified as part of a soluble complement complex, known as the SC5b-9 complex [8]. Later, cDNA sequence analysis and immunological/functional studies confirmed that VN and S-protein were identical proteins [9-12]. In blood, VN circulates mainly as a monomer [13-14], but in the extracellular matrix it exists as a multimer. The source of extracellular matrix-associated VN has been thought to be mainly from the plasma. While the

exact mechanism for its compartmentalization is unknown, it is accepted that vitronectin has specific and distinct functions in the blood and extracellular matrix.

The primary site of VN synthesis is the liver, and a severe reduction in the plasma level of VN has been observed in patients with cirrhosis of liver and liver failure [5, 15-16]. The presence of VN has been observed in the medium of cultured hepatoma cell lines, e.g. HepG2 and Hep3B [13, 17]. VN is expressed at a high level in tumors also [13-14]. Endodermal sinus tumor cells (yolk sac carcinoma cells resembling parietal endoderm) derived from human testicular teratoma have also been found to secrete VN, and they do not require serum for attachment and growth [18]. Hetland et al. reported that monocytes and macrophages could also synthesize and secrete VN in the culture medium [19]. The other major site of VN synthesis is the platelet. Parker et al. first reported the intracellular storage of VN in platelets [20]. Later in the same year, Preissner et al. quantified the amount of VN present in platelets (8.1 +/- 4.6μg/10platelets) [21].

1.1. b. Structural Organization and Post-translational Modification

While VN is an important protein involved in several physiological processes, it is unfortunate that no high-resolution structure for full-length vitronectin has yet been solved. The protein appears to be organized into distinct domains: the N-terminal SMB (somatomedin-B) domain, the central domain and the C-terminal domain as shown in **Figure-1.1**. A crystal structure of the recombinant SMB domain in complex with recombinant PAI-1 has been determined [22]. The structure of this SMB domain has been included in **Figure-1.1**. There are three other NMR solution structures available for the SMB domain (a recombinant SMB domain, SMB domain isolated from purified monomeric VN from blood and recombinant SMB domain
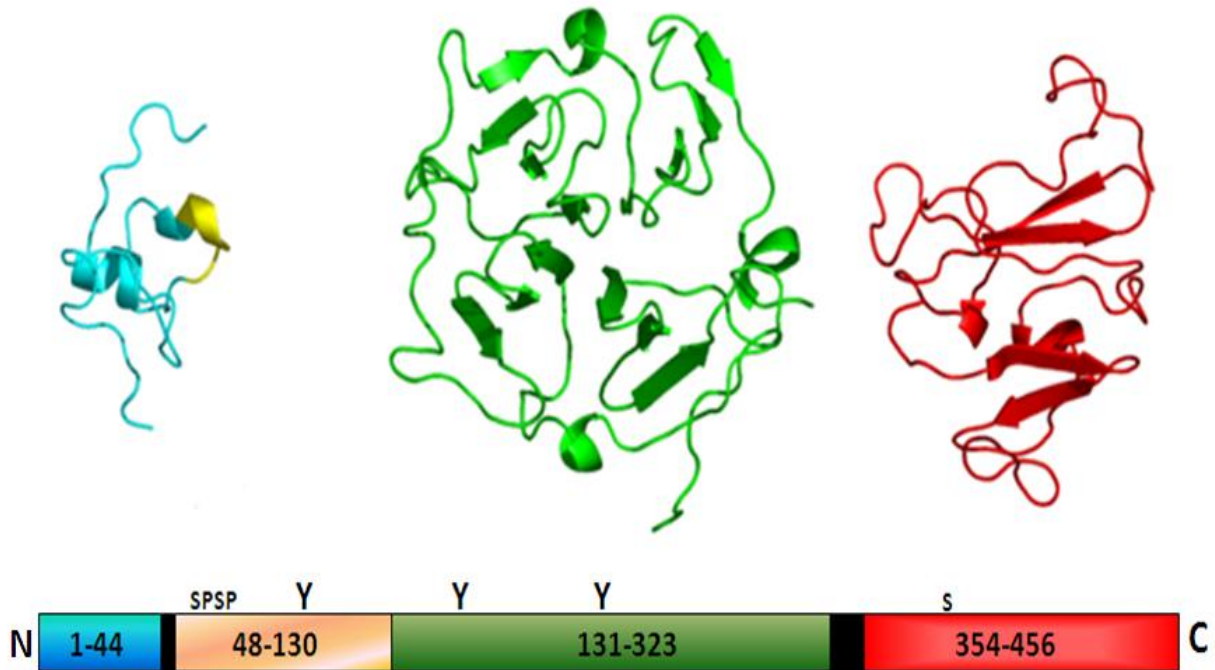
Figure 1. 1: Domain organization of VN

Figure-1.1: The structural model of VN includes several domains. Cyan: crystal structure of SMB domain (1-44 aa) [22], Amber: Intrinsically disordered domain (48-130 aa) predicted by PONDR, Green: Central domain predicted to be four bladed β-propellers (131-323 aa), Red: C-terminal domain, predicted to have half of four bladed β-propellers (354-456 aa), yellow: region in SMB that contacts with PAI-1 [26-27]. 'S' indicates sulfations, 'P' indicates phosphorylation and 'Y' indicates glycosylation.

expressed in *Pichia*) [23-25]. Though certain differences exist among all of these solved structures in terms of disulfide bond arrangements, folding and secondary structure, the main similarity that they share is the presence of a surface exposed patch of hydrophobic residues (encompassing Phe13, Val15, Leu24, Tyr27 and Tyr28) responsible for ligand binding (PAI-1, urokinase Plasminogen Activator Receptors). For all the other domains in VN, only computationally predicted models are available [26]. These models indicate that the central domain adopts a full four-bladed β-propeller fold like that described in hemopexin and gelatinase [26]. The C-terminal domain is predicted to contain half of that four-bladed β-propeller fold. We also know from bioinformatic analysis with PONDR that the region between the SMB domain and central domain (residues 54-130) is intrinsically disordered [27] asdepicted in **Figure-1.1**. A lower resolution structure of full length monomeric VN was proposed by the Peterson laboratory using small angle X-ray scattering data [27]. This model indicates that the entire molecule possesses a peanut-shaped bi-lobed structure that remains extended in solution (maximum length of about 110Å).

VN contains a total of 14 cysteine residues. Out of these, eight are present within the SMB domain and form four disulfide linkages. Though there were controversies related to the arrangement of these four disulfide bonds, a recent publication from Li et al. claimed that the correct arrangements of the disulfide linkages in the SMB domain of native VN are: Cys5–Cys21, Cys9–Cys39, Cys19–Cys32, andCys25–Cys31 [28]. Such extensive disulfide bridging makes this SMB domain strongly resistant to proteolysis [29]. Six other cysteine residues (Cys-137, 161, 196, 274, 411, 453) are located within the central and C-terminal domains. Cys-274 and Cys-453 are known to be disulfide linked [5]. This disulfide linkage has an important role in

the formation of the two-chain form of VN. VN in circulation exists in two different forms: a single chain and a two-chain form [7, 30-32]. This results from the genetic polymorphism that exists at residue 381 of VN. Tollefsen et al. found that the presence of Thr instead of Met at position 381 makes the protein more susceptible to proteolytic cleavage at R379 [33] and results in the formation of the two-chain form of VN connected by a disulfide linkage between Cys274 and Cys453. Cys137 and Cys161 within the central domain form the intra-domain disulfide linkage. Cys196 and Cys411 are free but remain buried within the folded structure [26, 34].

VN also contains several other post-translational modifications, including glycosylation, sulfation and phosphorylation. There are three N-linked glycosylations at residues N67, N150 and N223 [5, 35]. Recently Sano et al. reported that reducing the extent of glycosylation on VN increased multimerization and also collagen binding [36]. Tyrosine residues at position 56 and 59 have been found to be sulfated by the action of a membrane enzyme in the Golgi which is a tyrosylprotein sulfotransferase [37]. The presence of these sulfated-tyrosines within the relatively acidic region (residue 53-64) of VN has been proposed to be important for interaction with the thrombin-antithrombin complex. VN is phosphorylated at many different sites, which include Thr60, Thr67, Ser362 and Ser378. There are several different kinases implicated in the phosphorylation of these residues. Korc-Grodzicki et al. reported that a cyclic-AMP dependent kinase (PKA) released from platelets upon thrombin activation could specifically phosphorylate VN at Ser378 [38]. Though phosphorylation by PKA was mainly limited to the single chain form, the presence of heparin apparently caused phosphorylation of the two-chain form also [39]. Phosphorylation at this residue appears to lower the binding affinity of vitronectin for PAI-1 and plasminogen and thus has been implicated in fibrinolysis [40]. Seger et al. reported

phosphorylation of Thr50 and Thr57 by casein kinase II (CK2), which is found in blood and on the surface of blood cells like neutrophils, platelets etc. Phosphorylation at these residues has been implicated in cell adhesion/spreading and also in induction of αvβ3-mediated cell signaling [41-42]. Phosphorylation at Ser262 is thought to be mediated by protein kinase-C (PKC) and is implicated in providing resistance to plasmin cleavage [43].

1.1. c. Physiological Function of Vitronectin

VN is an important protein involved in several physiological processes; the multifunctional nature of this protein results from its ability to recognize various ligands including the thrombin-antithrombin complex (T-AT) [44-45], heparin [46-48], PAI-1 [49-51], complement proteins [52], and several cell surface receptors, including integrins and the urokinase plasminogen activator receptor (uPAR) [53-59]. VN exhibits functions that are specific to its localization. For example, in blood it has a role in the regulation of thrombus formation, coagulation and fibrinolysis, whereas in the tissue or extracellular matrix, it has an important role in regulating pericellular proteolysis, wound healing, inhibition of the membrane attack complex, and cellular adhesion/migration.

The regulation of thrombus formation, coagulation, fibrinolysis, wound healing and pericellular proteolysis by VN is mediated by its interaction with heparin, the T-AT complex and PAI-1 [60-66]. Coagulation is mediated by thrombin, which transforms fibrinogen into fibrin. There are a number of serine protease inhibitors (serpins) that control the amount of active thrombin in the circulation. Among those, the most important is antithrombin-III [5]. This inhibitor by itself causes slow inactivation of thrombin (T), whereas in the presence of heparin, the inactivation rate is significantly accelerated [67-69]. Heparin binding to antithrombin-III

(AT) causes a conformational change in the inhibitor, which stabilizes the complex by decreasing the dissociation constant [70-71]. Bound heparin on antithrombin-III acts as a bridge to bring the inhibitor and the protease spatially close to each other which increases the rate of the reaction [70]. After the formation of the T-AT complex, heparin is released; the formation of the protease-inhibitor complex results in a further conformational change in the inhibitor that reduces its affinity for heparin [72-73]. Released heparin can then cause further rounds of thrombin inactivation. VN acts a heparin scavenger and thus regulates the rate of antithrombin inactivation of thrombin [74-75]. Furthermore, VN has been found to bind to the T-AT complex. Binding to the TAT complex occurs through thrombin and appears to be stabilized by disulfide linkage [45, 75-76]. Binding induces a conformational change in VN that can be probed by a conformationally specific antibody [44, 77]; this change results in an increase in the affinity for heparin. Thus, it has been proposed that the pro-coagulant nature of VN requires the presence of the T-AT complex in the blood [31, 74]. It has been also proposed that VN plays a role in the clearance of the T-AT complex when it binds and forms the ternary complex. It appears that the VN-T-AT complex interacts with the surface of HepG2 cells and then can be internalized and degraded. This clearance is inhibited by heparin, indicating the involvement of heparin binding domain of VN [78].

Plasminogen activator inhibitor-1 (PAI-1) is a biomolecule that plays an important role in the regulation of plasminogen activation to form its active counterpart plasmin. Regulation is achieved by the ability of PAI-1 to inhibit tissue-Plasminogen Activator (tPA) and urokinase-Plasminogen Activator (uPA), the two common serine proteases that are involved in the activation of plasmin [79-80]. By regulating activation of plasmin, PAI-1 participates in the

regulation of fibrinolysis, pericellular proteolysis and wound healing. VN has been found to contribute to such regulation in two ways. First of all, VN increases the half-life of PAI-1 and thus keeps it stable for a longer time [81-82]. As a result, PAI-1 remains active in its inhibitory form for a longer period of time. VN is also known to localize PAI-1 to its specific site(s) of action. For example, VN was found to localize PAI-1 in the fibrin clot and thus influence the role of PAI-1 in fibrinolysis. The presence of VN in the fibrin clot increased the affinity of PAI-1 binding to the clot site and also kept PAI-1 stable for longer period of time [61].

VN acts as an inhibitor of the membrane attack complex (MAC) formed by the assembly of complement proteins. MAC forms a pore by inserting into the membrane of target cells and causes their lysis. MAC is built by the sequential assembly of various complement proteins, including C5b, C6, C7, C8 and C9 [83-85]. Each of these individual units is hydrophilic, but their assembly results in the formation of an amphiphilic complex. Once the complex between C5b, C6 and C7 is formed, the initial hydrophilic-to-amphiphilic transition happens [86-87] and this complex is targeted to the membrane. Membrane-inserted C5b-7 complex binds to C8, and the resulting complex catalyzes polymerization of C9; the entire C5b-9 complex adopts an amphiphilic, membrane pore forming, tubule-like structure that causes cytolysis [88-90]. VN can regulate the formation of this active membrane attack complex. It binds to the C5b-7 complex and inhibits the hydrophilic-amphiphilic transition and renders the complex soluble (SC5b-7). Though the subsequent binding of this complex to C8 and C9 can occur, polymerization of C9 does not happen and thus the entire complex becomes inactive [8, 91].

Regulation of cellular adhesion/migration comes from the ability of VN to act as a matrix protein that can bind to different cell surface receptors like uPAR (urokinase plasminogen

activator receptor) and certain subclasses of integrins [92].VN has been found to regulate

adhesion and migration properties of different cell types, e.g. fibroblasts, endothelial cells,

megrakaryocytes, platelets, tumor cells, etc [92]. VN modulation of cellular adhesion and

migration has been implicated in various physiological processes, including angiogenesis [66].

Integrins are heterodimeric cell surface receptors that are known to establish a link between the

extracellular matrix and cytoskeleton. There are approximately 24 different types of integrins

that can recognize a variety of extracellular matrix components [93]. Many of them can interact

with VN, including αvβ1, αvβ3, αvβ5, αvβ6, αvβ8 and αIIbβ3 [13, 94]. Recently Mac1 (αMβ2)

has been added to the growing list of vitronectin partners [95]. Out of all these, αvβ3 and αvβ5

are thought to be the two most common cell surface receptors for VN and have been found to be

overexpressed in activated endothelial cells undergoing angiogenesis [96-97]. Several

antagonists of these two integrins are currently being studied for the inhibition of angiogenesis as

a possible treatment strategy for cancer [98-99]. Most of these integrins recognize VN via an

RGD sequence (residues 45-47) that is located immediately after the SMB domain. uPAR is

another cell surface receptor that is anchored to the membrane via a GPI

(glycosylphosphatydylinositol) link. The primary function of uPAR is to bind and localize uPA

at the cell surface and regulate pericellular proteolysis [100]. uPAR has three distinct domains

(DI, DII and DIII), which together form a central cavity that contains the uPA binding site [101-

102]. The VN binding site is located on the outside of this cavity along the outer surface of the

protein [103]. Thus, uPA binding does not block VN binding; rather binding of uPA causes an

increase in the affinity of uPAR binding to VN. The uPAR-binding site on VN is located within

the SMB domain. **Figure-1.2** summarizes the variety of interactions of cell surface receptors with matrix-associated VN. A major focus of this study is to understand the role of VN in regulating cellular adhesion and migration in relation to its interaction with Plasminogen Activator Inhibitor-1 (PAI-1).

As mentioned above, VN exists as monomer in the circulation, but the preferred conformation of its matrix-associated form is multimeric. Multimeric and monomeric VN exhibit distinct functional properties. Multimeric VN was found to bind more to collagen compared to monomeric VN [104]. Multimeric VN also appears be endocytosed through an αvβ5-dependent process in skin fibroblast cells; this was not observed with monomeric VN [105-106]. Another example is that only multimeric VN was found to induce tyrosine phosphorylation by binding to αvβ3 on the endothelial cells [107].

In the last few years, researchers have begun to understand the importance of VN in pathogenic infections. For example, *Candida albicans* was found to possess αvβ3-like or αvβ5-like receptors for VN binding, and it was also shown that binding of *Candida* to endothelial cells was VN mediated [108]. One of the major aims of this research is also to compare *Candia* infection and pathogenesis between vitronectin knock-out mice and wt C57BL/6 mice.
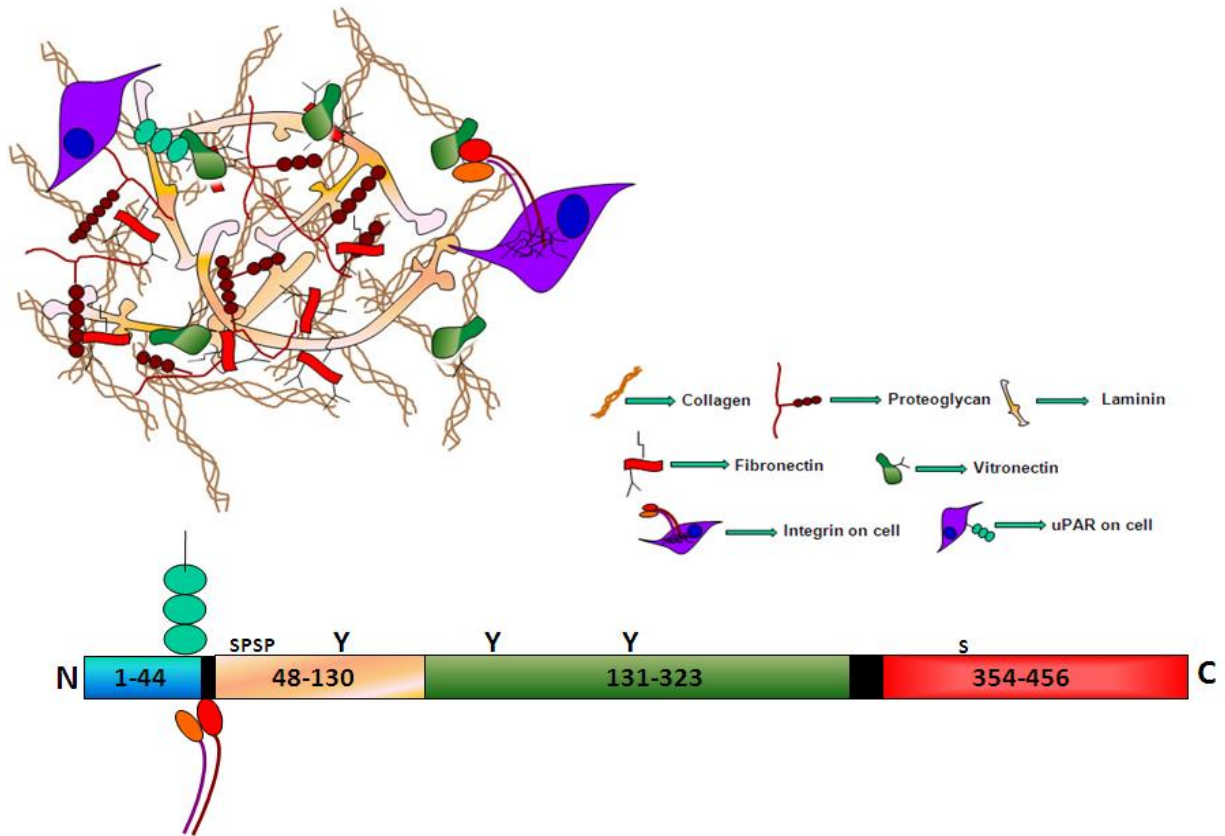
Figure 1. 2: Vitronectin as a part of the ECM interacting with cell surface receptors

Figure-1.2: A simplistic representation of the extracellular matrix comprised of a few major components, including collagen, laminin, proteoglycan, vitronectin and fibronectin is shown. Cell surface receptors (uPAR & integrins) interacting with VN associated with the extracellular matrix are shown. The domain organization of vitronectin with proposed binding sites for both uPAR and integrins is also shown.

1.2. Plasminogen Activator Inhibitor-1 (PAI-1)

1.2. a. Expression and Regulation

PAI-1 is another member of the serpin family of proteins. Like VN, it is found to be present in the circulation and extracellular matrix. In the circulation, PAI-1 concentration varies between 5-20ng/ml. Under normal physiological conditions PAI-1 is released into the circulation by a number of cells, including platelets, smooth muscle cells (SMCs), hepatocytes and adipocytes [109]. In addition, under many pathological conditions, high expression of PAI-1 is observed in other cell types, e.g. vascular endothelial cells and tumor cells. Plasma concentrations of PAI-1 can be dramatically increased in several inflammatory disease conditions, including atherosclerosis, severe sepsis etc [109-110]. An elevated plasma concentration of PAI-1 has been also observed in various thrombotic disorders, including myocardial infarction and deep vein thrombosis [111-113]. High levels of PAI-1 are positively correlated with the invasiveness of several different types of cancers [114]. In an immunohystochemical study of more than a hundred breast cancer patients, Dublin et al. showed that high levels of PAI-were positively correlated with both the grade and invasiveness of the various breast tumors. They also found that PAI-1 expression was elevated in the stromal fibroblasts associated with the tumors [115]. It appears that visceral abdominal adipocytes express high level of plasma PAI-1 in patients with central obesity [116-117]. Both obesity and insulin resistance are now known to be associated with high levels of PAI-1 in plasma [118-119].

The expression of PAI-1 can be regulated by inflammatory mediators like lipopolysaccharide (LPS). Cultured endothelial cells showed increased expression of PAI-1 in the presence of LPS [120]. Various inflammatory cytokines also cause induction of PAI-1

expression. TGF-β1 is one of the most potent inducers. Vascular injury causes release of TGF-β1 from the α-granules of platelets, and then the local expression of PAI-1 becomes elevated. TGF-β1 and PAI-1 mutually control expression of each other via a feed-back mechanism [109, 121-123]. Interleukin-1 (IL-1) and TNF-α are also implicated in transcriptional activation of PAI-1 in endothelial cells and fibrosarcoma [109]. Plasma levels of PAI-1 are elevated in type-II diabetes patients with hyperglycemia [124]. In vitro studies showed that addition of glucose and insulin to the culture medium increased PAI-1 expression by vascular endothelial cell and SMCs [125-126]. Besides insulin, its precursor molecules, such as proinsulin and split-insulin, have also been found to cause induction of PAI-1 expression in cultured endothelial cells [127]. Cultured hepatocytes showed increased expression of PAI-1 by free fatty acid (FFA, elevated in diabetes mellitus) and very-low-density lipoprotein (VLDL, elevated in hypertriglyceridemia) [109, 128]. Another important factor that has been found to be involved in the up-regulation of PAI-1 is angiotensin-II [129]. Activation of the renin-angiotensin system is associated with increased risk of ischemia, which appears to be mediated by elevation of PAI-1 expression in plasma [130-131].

1.2. b. PAI-1 as a Member of the Serpin Family of Proteins

The primary function of PAI-1 is to regulate the cleavage of plasminogen to yield its active counterpart, plasmin. Regulation is achieved by PAI-1 inhibiting the proteases, tPA & uPA. Studies with bovine PAI-1 indicate that it can also inhibit plasmin directly [132]. Indeed, PAI-1 can act on other proteases, but with low efficiency [133]. Serpin molecules contain a reactive center loop (RCL) that acts as bait for the serine proteases. RCLs of all serpins contain a scissile bond (termed the P1-P1$'$ peptide bond) recognized by specific target proteases. For PAI-1, R346-

M347 forms this P1-P1$'$ scissile bond [134]. The residues located at the N-terminal side of the scissile bond are denoted as Px (where, x=1, 2, 3.etc). In other words the residues at the N-terminal side of the scissile bond are termed as P1$'$, P2$'$, P3$'$, P4$'$ etc. The residues that are located at the C-terminal side are termed as Px$'$ (where, x=1, 2, 3….etc.). In other words the residues at the N-terminal side of the scissile bond are termed as P1, P2, P3, P4 etc. The general reaction mechanism for serpin-mediated inhibition involves these steps (see **Figure-1.3**, [135]): <u>a.</u> formation of a non-covalent Michaelis complex between the serine protease and the P1-P1$'$ scissile bond, <u>b</u>. cleavage of the P1-P1$'$ scissile bond and formation of a covalent acyl intermediate between the serine residue of the protease and the P1 residue of the serpin. This is shown as the loop-bound acyl enzyme in **Figure-1.3**, <u>c</u>. pre-insertion of the RCL bound protease indicated as loop-displaced acyl-enzyme complex, <u>d</u>. insertion of the N-terminal portion of the RCL (from P1 residue) into the central β-sheet A region of the serpin body. During this insertion, the covalently linked protease is translocated via a major conformational change so that it moves ~70Å to the opposite face of PAI-1. With this translocation, the structure of the protease is also perturbed, leading to disruption of the active site conformation of the protease [136-140]. For a usual serine protease reaction, formation of the acyl enzyme intermediate is followed by the substrate release step and regeneration of the active site. In contrast, when the active site conformation of the serine protease is disrupted due to this dramatic translocation, the substrate release step of the serine protease reaction is hindered. As a result, the serpin involved in this reaction is permanently consumed and the protease is also permanently inhibited. Because of this, serpins are called suicide inhibitors.
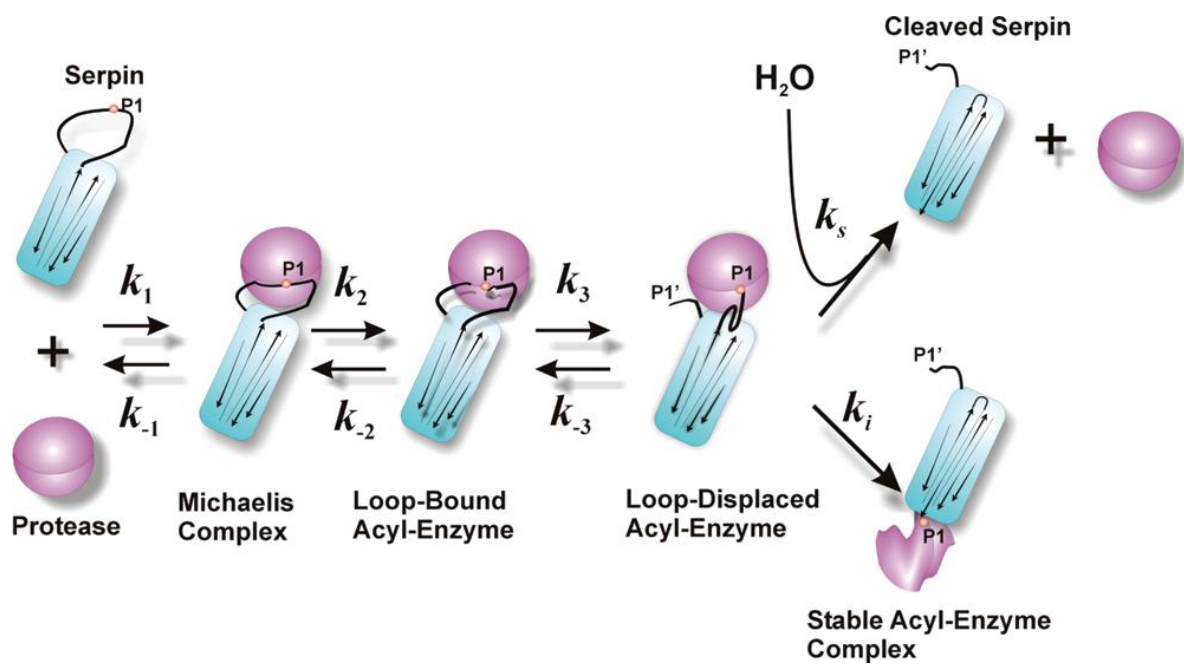
Figure 1. 3: Basic scheme of the serpin reaction mechanism

Figure-1.3: The basic scheme of serpin reaction mechanism includes formation of noncovalent michaelis complex (step-a), cleavage of the RCL with covalent attachment of the protease with the serpin (step-b), pre-insertion of the RCL with the bound protease (step-c). At this point the serpin reaction may take two pathways. It can act as a substrate which results in the release of active protease with permanent cleavage of the serpin or the serpin may act as an inhibitor. In the inhibitor pathway,y the protease undergoes a 70Å translocation to the opposite face of the serpin followed by the permanent destruction of the protease active site (step-d) [134].

Figure-1.4 shows the structure of the Michaelis (non-covalent) complex formed between α_1-proteinase inhibitor (PI)-Pittsburg (a natural variant of antithrombin, containing a Met to Arg mutation at P1) and trypsin [141]. Since the formation of the Michaelis complex between the serpin and the target protease is typically transient and not amenable to crystallization, seven stabilizing mutations (to prevent polymerization) were introduced in α_1-PI-Pittsburg. Also, the C232S mutation was introduced in order to prevent formation of an intermolecular disulfide linkage. The active site serine of trypsin has also been changed to alanine (S195A), to yield catalytically inactive trypsin). With all of these changes, Demetiev et al. could solve the only crystal structure of the non-covalent complex between a serpin and its target protease [141]. This structure shows minimum contact between the serpin and the protease. The P1 Arg side chain was inserted into the S1 specificity pocket of the protease and thus made extensive contacts. Other than that, there were hydrogen bonds formed between the backbone residues $P2^{/}$-P2 of the serpin and the backbone residues of the trypsin. **Figure-1.5** on the other hand, shows the structure of a covalent complex between α_1-antitrypsin and trypsin [142]. This structure shows that the protease portion of the complex experiences a major translocation of $\sim 71A^0$ towards the opposite pole of the serpin after forming the covalent bond. In this study, Huntington et al. also found that the formation of this covalent linkage and the subsequent translocation caused significant loss in the structural integrity of the protease molecule (including distortion of the active site), rendering it more sensitive towards destruction by protease. Although we do not have the structure of PAI-1 in its active conformation or in its protease bound form, it is believed that PAI-1 follows the same inhibitory mechanism of the serpin family of proteins represented by the α1-antitrypsin-trypsin pair. With an environmentally sensitive fluorescent probe (NBD)

16
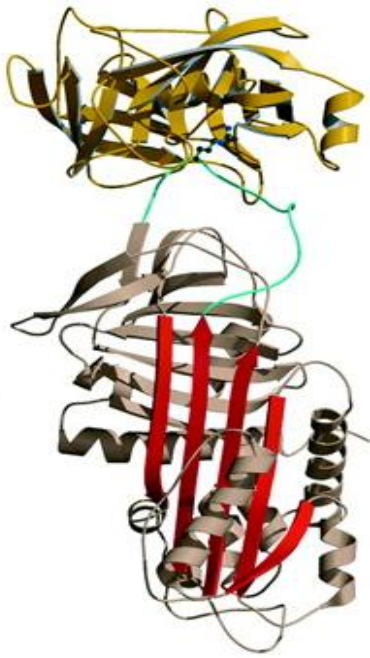
Figure 1. 4: Non-covalent complex between trypsin and serpin
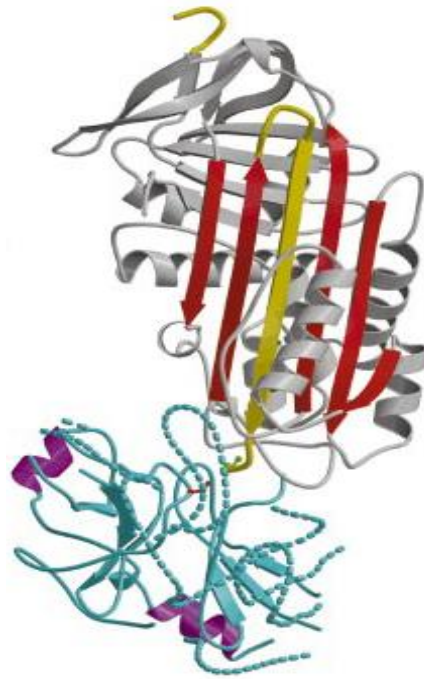
Figure 1. 5: Covalent complex between trypsin and serpin

Figure-1.4: A noncovalent complex (Michaelis complex) between S195A trypsin (shown in gold) and α1-proteinase inhibitor Pittsburgh (containing seven stabilizing mutation and C232S mutation, shown in brown) [141]. Figure-1.5: A covalent complex between active trypsin (shown in turquoise) and α1-antitrypsisn (shown in gray color). Dotted region within covalently linked trypsin indicates disordered structure from conformational transition [142]. This structure also shows a 71A^0 translocation of P1 Met of α1-antitrypsisn (covalently linked with trypsin) and insertion of the cleaved reactive center loop as 4th β-strand (shown in yellow) of the central β-sheet (shown in

placed at P9 position, Lawrence et al. showed that the inhibition of protease by PAI-1 involves the formation of an initial covalent complex and a subsequent movement of the RCL loop towards the central β-sheet region along with the protease [137]. Egelund et al. later showed that the linkage formed between PAI-1 and uPA is an ester linkage, as found with other serpin-protease partners [143].

1.2. c. PAI-1 and its Inherent Structural Flexibility

The presence of the reactive center loop (RCL) makes the serpins special. The RCL acts as substrate bait for the protease attack. The RCL is a highly mobile structure with a great deal of conformational flexibility. Several different conformations of the RCL have been found to exist in nature [144-145]. Ovalbumin is a noninhibitory serpin characterized by an RCL that contains a 3-turn α-helix. The RCL in this protein is completely exposed [146-147] and acts simply as substrate, and the reaction with protease is not followed by an insertion of the RCL to the central beta sheet region for ovalbumin. Many groups have proposed that the RCL needs to be at least partially inserted in order for serpins to be effective inhibitors. This requires flexibility in the region spanning the base of the RCL [144, 148-149]. Mutation in the base region residues, especially at the conserved P12 residue (Ala for all inhibitors), causes severe impairment to the inhibitory activity. For example, mutation of the P12 (Ala) residue by glutamate completely disrupted the inhibitory activity of C1-inhibitor [150]. The conclusion was that the flexibility in the base region is required for the partial insertion of the RCL loop in order to maintain inhibitory properties. Lawrence et al. reported that mutation of the P14 residue (Thr333) of PAI-1 to a charged residue caused a total loss of the inhibitor activity towards uPA & tPA but maintained the protease binding activity [138]. It has been proposed that the presence of a

charged residue at this position retarded the insertion of the RCL and thus impaired the inhibitor function by precluding the large conformational change upon inhibition of the protease. At times, cleavage of the RCL at, or outside of, the P1-P1$^/$ sequence by some non-target proteases may leave the serpin in a proteolytically cleaved inactive form. Such cleaved serpins also exhibit insertion of the newly generated C-terminal end of the RCL loop (corresponding to the P1 position) into the central β-sheet region [149, 151-152]. Translocation of the RCL in these cleaved forms also causes a separation of the P1 and P1$^/$ residue by 70A^0. Structural flexibility of the RCL is thus closely connected with the inhibitory function of serpins. Furthermore, insertion of the RCL requires a conformational change in other parts of the serpin. A prerequisite for successful insertion is a sliding movement of the β1-3A of the central β-sheet and helix-F away from the structure so that the groove region between strand 3A and 5A is opened for the RCL insertion [153]. Egelund et al. performed a thorough study on different forms of PAI-1 (active, latent, cleaved and complex with protease) and showed that with each separate form there were specific conformational changes associated in different region of the protein other than in the RCL and central β-sheet [154].

With some serpins the conformational lability can be so pronounced that the RCL can undergo self-insertion into the central β-sheet region without the involvement of any protease. Such a conformation in serpins is called a latent form, reflecting the absence of anti-protease activity in this structure. For example, there is a natural variant of antithrombin that can be found in patients exhibiting premature thrombosis, where mutation of Thr85 (situated at the main opening of the central β-sheet) to Lys has made the RCL extremely labile so that spontaneous self insertion is observed. As a result, the serpin converts to a latent form and permanently loses

its protease inhibition function. This variant is called antithrombin Wobble [155]. Patients

carrying this variant of antithrombin show onset of thrombosis near the age of 10. Another

variant of antithrombin is antithrombin Wibble, which contains the Thr85Met mutation. The

phenotype of this variant is normal overall, but the presence of this mutation makes the RCL

highly susceptible to spontaneous insertion under the influence of stress conditions such as a

mild increase in temperature. There are other examples of serpins that exhibit susceptibility to

loop insertion upon exposure to denaturants or high temperature. α1-antitrypsin was found to be

converted in to its loop-inserted latent form upon treatment with 0.5M citrate at 60^0C [156].

Wild-type antithrombin was also found to be converted in to its latent form upon similar

treatment [157]. Among all the serpins, PAI-1 is special, as it exhibits the highest susceptibility

towards this large conformational transition in its native form. The half-life of this latency

transition for PAI-1 ranges between 1-2hrs at 37^0C [158-159]. No mutation or denaturant is

required for initiating the self-insertion of the RCL for PAI-1.

Mottonen et al. were the first to report the crystal structure of latent PAI-1 [160]. Later

Stout et al. reported a high resolution crystal structure [161] of this form. **Figure-1.6** shows the

high-resolution crystal structure of latent PAI-1 from Stout et al. Both of these structures clearly

indicate that in latent PAI-1, the RCL is inserted to form the fourth strand of the central β-sheet-

A, and the conformation of the inserted RCL closely resembles what was found with other

cleaved serpins. This latent form is thermostable and protected from the target protease attack as

the P1$^/$-P1 bond is buried inside the core body of the protein. Denaturation/renaturation or

treatment with negatively charged phospholipids has been found to cause partial conversion of

the latent PAI-1 into its active form [162-163].
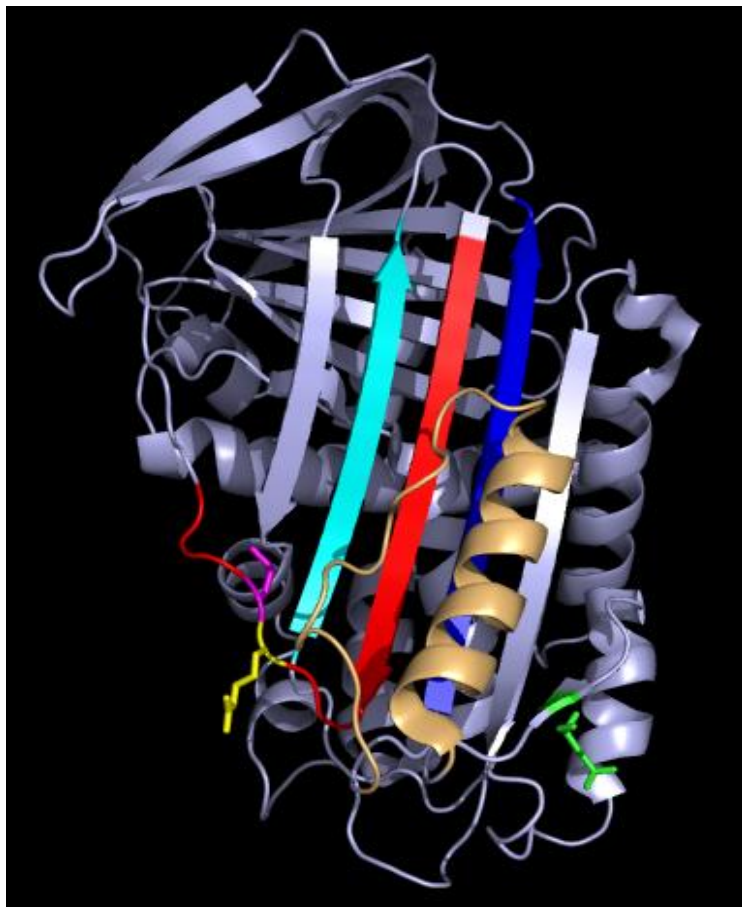
Figure 1. 6: Crystal structure of latent PAI-1

**Figure-1.6: High resolution structure of latent PAI-1 [161].
Structure shows RCL (in red), β-strand-3A (in blue), β-strand-5A
(in turquoise), helix-F (in gray), P1 residue (in yellow), P1′ residue
(in magenta), Q123 residue (in green).**

1.2. d. Factors Affecting Stability of PAI-1

Inherent conformational instability is presumably the reason why there is not yet available any crystal structure of active wt-PAI-1. Different groups have attempted to strategically introduce different sets of mutations to stabilize the structure [159, 164]. So far the highest stabilization obtained is a half-life of about 145hrs. This stabilization is exhibited by a mutant of PAI-1 that is thus constitutively active and referred to as the 14-1-B form; it contains four different mutations: N150H, K154T, Q319L and M354I [164]. The crystal structure of this mutant [165] along with all the mutated residues is depicted in **Figure-1.7**. As demonstrated in this example, stabilization of PAI-1 by altering the conformational flexibility has remained a subject of great interest. It seems that the slightest change in the structure can cause a difference in the half-life of PAI-1 stability. It is well known that stabilization of the structure is obtained with lowering of temperature. It has also been found that lowering of pH or an increase in concentration of salt in the buffer has a dramatic stabilizing effect on the structure [166-167]. Sensitivity to pH and salt indicates that it is not just the RCL or portion of the β-sheet-A that are flexible, but rather the entire body of the protein possesses inherent flexibility; a slight conformational change in one region may cause a subsequent change in the conformation or dynamics of another portion of the molecule. Such change, in turn, may affect the stability of the molecule.

His364 has been implicated in the pH dependent stability of the molecule [167]. This residue is located at the distal C-terminal end of the molecule. A change in pH alters the ionization status of this residue, which in turn causes structural changes in the molecule responsible for lowering the insertion rate of RCL. Blouse et al. showed that mutation of the
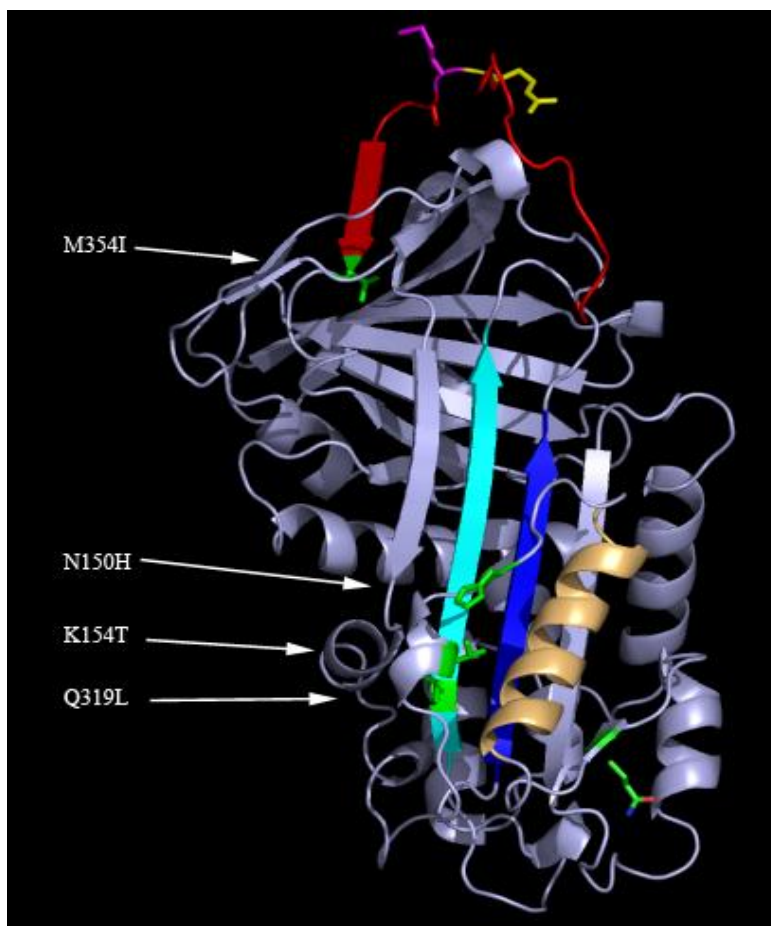
Figure 1. 7: Crystal structure of stable mutant (14-1-B) of PAI-1

Figure-1.7: Crystal structure of stable mutant of PAI-1 with all the stabilizing mutations [165]. Structure shows RCL (in red), β-strand-3A (in blue), β-strand-5A (in turquoise), helix-F (in gold), P1 residue (in yellow), P1$'$ residue (in magenta), four stabilizing mutations (in green) and Q123 residue (in green with color of elements) [165].

conserved Tryptophan residue (Trp175) with a replacement by Phe increased the inherent

stability of the structure from a half-life of about 2hrs to 22hrs [135]. Trp175 is located in the

hydrophobic pocket of the breach region of the molecule. The location of this breach region

close to the base region of the RCL is critical for the initial insertion of the loop. Thus, the

conservative change from Trp to Phe interfered significantly with the rate of RCL insertion and

increased the half-life. All these studies point toward how much conformational lability exists in

the whole structure of PAI-1.

Ligand binding to PAI-1 has also been found to affect the stability of this molecule. VN

is one of the major binding partners of PAI-1 and is known to cause a moderate stabilization of

the structure. We have shown that the stability with VN in a buffer of 100mM Tris, 1mM EDTA,

1% BSA (pH-7.4) increases by 33%, with a change in half-life of PAI-1 from 1.14hr to 1.5hr.

VN binding to PAI-1 has been proposed to interfere with the RCL insertion by blocking the

sliding movement of s1A and s2A toward the gap between helix-E & F. A crystal structure

(**Figure-1.8**) of the complex containing recombinant SMB domain of VN and the 14-1-B stable

form of PAI-1 provided convincing evidence for this mechanism for structural stabilization [22].

Once again, it is noted   that a conformational change at one region of the structure may perturb

another part of the molecule. Although this study was done with SMB domain, full-length VN

interacts with PAI-1 with an even larger surface [168], and thus the interaction between PAI-1

and VN extends beyond SMB domain of VN. This conformational flexibility and the

corresponding change in the stability of PAI-1 resulting from ligand binding are fascinating and

require more careful investigation. One of the areas of focus in this dissertation study has been to

probe the conformational change in PAI-1 that occurs due to ligand binding. This has been
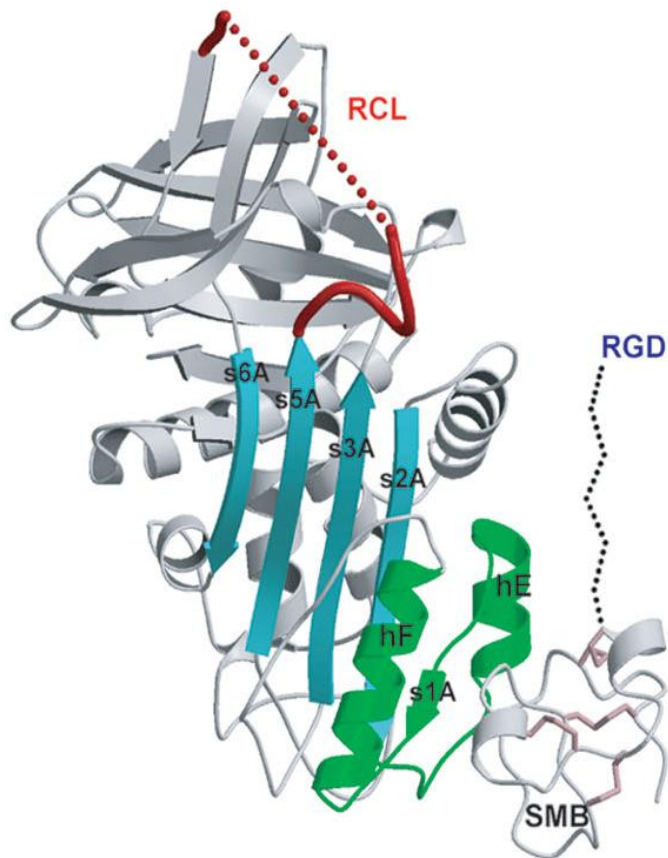
Figure 1. 8: Crystal structure of 14-1-B & SMB domain

Figure-1.8: Crystal structure of stable mutant of PAI-1 in complex with recombinant SMB domain [22]. Structure shows RCL (in red), central β-sheet (in turquoise), helix-E & F and β-strand-1A (in green). Somatomedin domain is shown in gray with pink disulfide bridges. Dotted regions indicate disordered structure in the RCL and residues leading the RGD sequence of SMB domain [22] which could not be resolved by X-ray crystallography.

approached by strategically placing a nitroxide spin label and following changes in electron paramagnetic resonance that occur with structural changes in PAI-1.

Recently our lab has found that different metals can significantly affect the stability of PAI-1. Type-II metal ions (Co, Cu, Ni) were found to largely destabilize the active conformation of PAI-1, whereas type-I (Mg, Ca) metal ions conferred instead a slight stabilization. When the effect of these metal ions was tested in the presence of VN, it was found that type-I metals did not show much difference in the absence or presence of VN, but type-II metals had completely opposite effects. In presence of VN, type-II metals dramatically stabilized PAI-1. **Figure-1.9** shows the effect of different metals on the stability of PAI-1 in the absence/presence of VN (Thompson et al., submitted). Significant progress has been made in terms of unraveling mechanistic aspects of these differential metal effects by studying binding and ensuing structural changes. My goal in this study has been to characterize the binding interaction between PAI-1 and different metals using biophysical techniques.

1.2. e. Physiological Role of PAI-1

PAI-1 is an essential biomolecule. The importance of PAI-1 is evident from its involvement in several important biological processes, including fibrinolysis, extracellular proteolysis, cell-matrix interaction etc. The physiological function of PAI-1 can be broadly classified into two main categories- **protease dependent** and **protease independent activities**. Under protease-dependent functions, PAI-1 is mainly involved in the inactivation of tissue-plasminogen activator (tPA) and urokinase-plasminogen activator (uPA) and thus regulates activation of plasmin [79-80]. The primary function of uPA and tPA is to cause formation of plasmin from inactive plasminogen as shown in **Figure-1.10**. While uPA is involved in the activation of plasmin
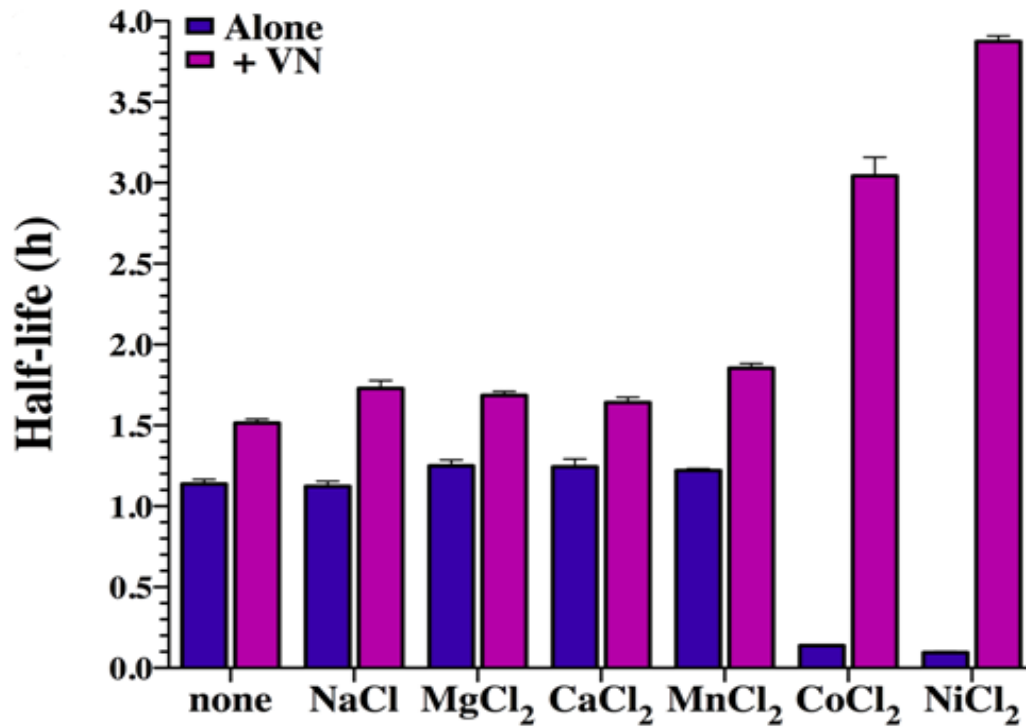
Figure 1. 9: Metal effect on the stability of PAI-1

Figure-1.9: Half life of wild type active PAI-1 with (purple) or without VN (blue) in the presence of different type-I (Mg, Ca) and type-II (Mn, Co & Ni) metals. It also includes the half life of PAI-1, measured in the absence of metal but in the presence of equivalent amount of chloride.
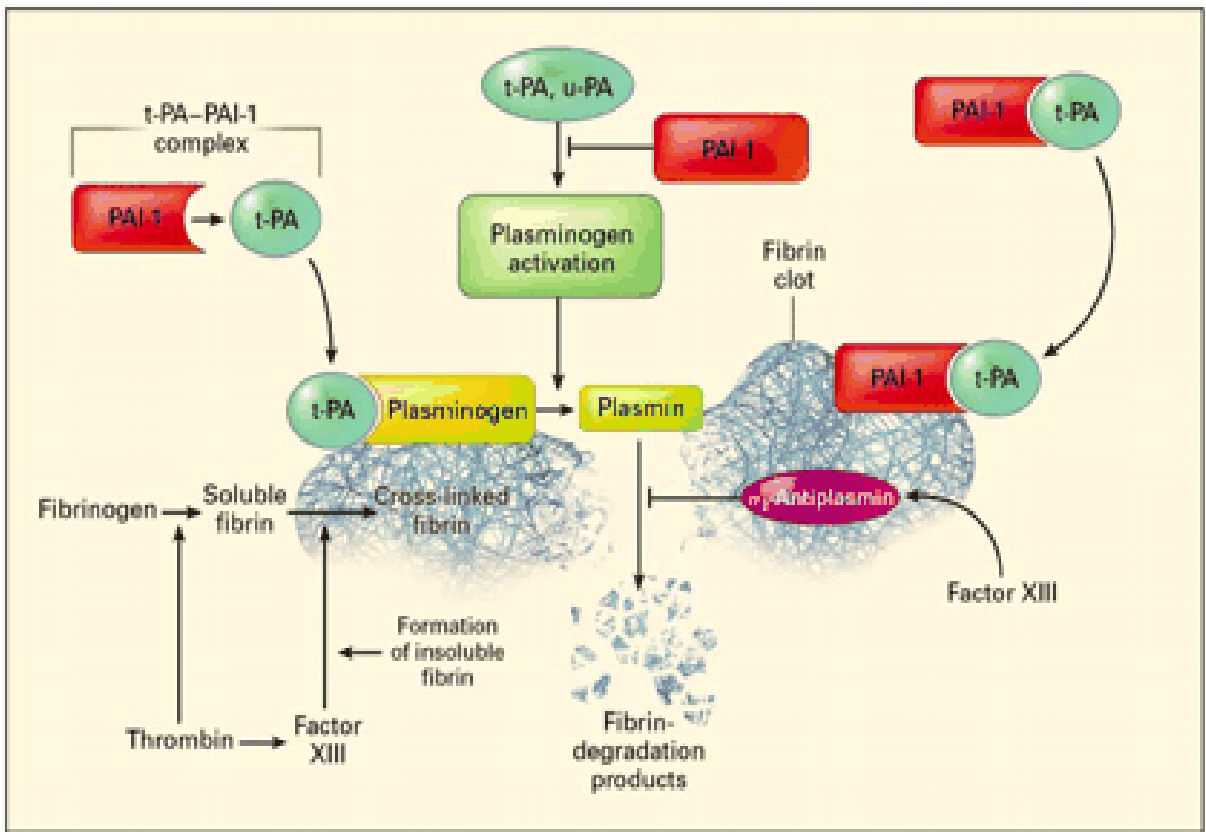
Figure 1. 10: Activation of the fibrinolytic pathway

Figure-1.10: Activation of the fibrinolytic pathway adapted from the journal published by Kohler et al., New Eng J Med, 2000 [112]. Activation of plasmin occurs by tPA when plasminogen is bound to the fibrin clot. PAI-1 bound to the fibrin clot maintains tPA inactivation activity. Factor-XIII causes formation of insoluble fibrin by crosslinking [112].

mainly on the cell surface, tPA on the other hand causes activation of plasmin in the extracellular matrix [169]. In the terminal steps of the coagulation cascade, activated thrombin causes formation of soluble fibrin from fibrinogen. Soluble fibrin then polymerizes to form the fibrin clot, which can be further stabilized by activated factor-XIII-mediated crosslinking [112]. Fibrinolysis is a process in which degradation of the fibrin clot happens by the tPA/uPA mediated activation of plasmin. tPA and inactive plasminogen are known to bind to the fibrin polymer. Fibrin-bound tPA causes activation of plasmin on the clot surface, and activated plasmin causes lysis of the clot [170-171]. PAI-1 is also known to associate with the fibrin clot and causes inactivation of tPA on the clot surface and thus inhibits fibrinolysis [172]. As a result, PAI-1 plays an important role in the regulation of coagulation and fibrinolysis which is depicted in **Figure-1.10** [112].

Activated thrombin has been found to cause activation of platelets [112]. Thrombosis is characterized by the aggregation of the activated platelets on fibrin mesh. The presence of PAI-1 is connected with the regulation of thrombolysis by virtue of its ability to inhibit the plasminogen activation system. Activation of the thrombolytic system remains a major strategy for the treatment of myocardial infarction. However, the major problem with such treatment is the thrombotic reocclusion of the initially treated blood vessel [173-174]. Platelet aggregation has been found to play a major role in such thrombotic reocclusion. It has been found that each activated platelet contains 4000-8000 PAI-1 molecules [175-176]. Activated platelets release PAI-1 from α-granules, and as a result, the local concentration of PAI-1 is elevated to around 50-100μg/ml [175, 177]. Thrombin can induce the release of PAI-1 from endothelial cells [178]. Such locally elevated PAI-1 concentrations protect the platelet-rich thrombi from thrombolysis.

Platelet-rich thrombi have been found to be more readily degraded by the application of tPA in mice deficient in PAI-1 [178]. Levi et al. reported that inhibition of PAI-1 activity by a monoclonal antibody blocked extension of thrombus formation in an experimental model of thrombosis [177]. The ability to influence the process of fibrinolysis and thrombolysis by virtue of its protease dependent function has put PAI-1 at the centerpiece of various coronary artery diseases. A strong positive correlation has been found between high levels of plasma PAI-1 and the risk of development of coronary sclerosis, restenosis, myocardial infarction, and deep vein thrombosis [109, 113, 179]. The ability to interfere with the plasminogen activation system also has implicated PAI-1 in other diseases that involve fibrosis resulting from increased fibrin deposition. Such inflammatory lung diseases that involve pulmonary fibrosis include adult respiratory distress syndrome, bronchopulmonary dysplasia; elevated PAI-1 concentrations have been found in bronchoalveolar lavage fluid from disease tissue [109]. A high concentration of PAI-1 has also been associated with renal diseases such as nephritic syndrome and hemolytic uremic syndrome [109].

Protease-independent functions of PAI-1 have recently grown in prominence. These functions refer to the activities of PAI-1 that are not directly related to its ability to inhibit proteases. Instead, these functions depend on the ability of PAI-1 to interact with other binding partners. For example, binding of PAI-1 to receptor-bound uPA on the cell surface causes internalization of the ternary complex of PAI-1/uPA/uPAR [180-181]. This internalization requires the interaction of PAI-1 within the ternary complex with the α2-macroglobulin receptor/low density lipoprotein receptor-related protein (α2-MR-LRP) or epithelial glycoprotein-330 or very low density lipoprotein (VLDL) receptor on the cell surface [182-185].

Formation of the complex with uPA opens up a cryptic high affinity LRP binding site on PAI-1 [186]. While the internalized uPA-PAI-1 complex undergoes lysosomal degradation, uPAR is recycled back to the cell surface [187]. PAI-1 also appears to be involved in the internalization of the tPA/PAI-1 complex via the α2-MR-LRP endocytic receptor [188]. Thus, such protease-independent activities of PAI-1 play important roles in the turnover of its target proteases.

Another important protease-independent function of PAI-1 is the regulation of cell matrix interactions. Involvement of PAI-1 in such processes is largely mediated by its ability to interact with VN. (A detailed discussion of this protease independent effect of PAI-1 on cell-matrix interaction is given in the following section.) In fact, understanding the interaction between PAI-1 and VN and how such interaction affects their ability to regulate cell-matrix interaction is a major focus of this dissertation work. High PAI-1 expression has been found to be positively correlated with the increased invasiveness and metastatic spreading of different types of cancer. Tumor extracts from several types of cancers showed high expression of PAI-1 [189-190]. PAI-1-deficient mice appear to be inefficient in supporting invasion of cancer cells [191]. This creates a paradox, as cancer cell invasion requires proteolysis at the pericellular region and high expression of PAI-1 at the tumor site is expected to work against invasion by virtue of its anti-proteolytic property. Such apparent contradictions may be explained, at least in part, by the protease-independent functions of PAI-1.

1.3. Interaction between VN and PAI-1

1.3. a. Structural Aspects of the Interaction

PAI-1 is one of the major interacting partners of VN. In blood, PAI-1 circulates in a complex with VN [81, 192]. VN also serves as the primary binding protein for PAI-1 in the

ECM [193]. Interaction between vitronectin and PAI-1 has remained an interesting subject in the area of protein-protein interactions. A primary interaction site involves the SMB domain of VN [194], as first demonstrated by Seiffert et al. using a recombinantly expressed version of the SMB domain. Deng et al. used alanine scanning mutagenesis and reported that each of the cysteine residues within the SMB domain is important for proper folding, maintaining the three-dimensional topology required for binding to PAI-1 [195]. Alanine scanning mutagenesis and antibody binding studies also reported that residues G12, D22, L24, Y27 and Y28 at the SMB domain are important for maintaining the PAI-1-binding property of vitronectin [195-196]. Several groups have used site-specific mutagenesis studies to localize the complementary VN-binding site on PAI-1. Lawrence et al. reported five point mutants in PAI-1 that had low affinity for VN. Out of these, three (Q55P, L116P and Q123K) had ten times lower affinity for VN binding compared to wild type [197]. Magdolen and his group used site directed mutagenesis to demonstrate the importance of residues in the helix-E and F region of PAI-1 for VN binding [51]. Several other groups have performed domain-swapping experiments between PAI-1 and PAI-2 (another serpin molecule) to localize the VN binding site on PAI-1. These studies indicated that a broad region between amino acids 91 to 167, encompassing helices-E and F and part of the central β-sheet is responsible for VN binding [198-199]. Zhou et al. reported a crystal structure of the recombinant SMB domain bound with 14-1-B, the stable mutant of PAI-1 (**Figure-1.8**). This structure shows a single-turn 3_{10} α-helix of SMB interacting with helices-E and F and part of the central β-sheet (strand 1A) of the 14-1-B mutant form of PAI-1 [22]. Most of the residues on the SMB domain that were previously considered important for PAI-1 binding

from mutagenesis studies were found to be involved in the interaction with PAI-1 in the crystal structure.

Binding of the two proteins has been conventionally considered to follow a 1:1 stoichiometry, mediated thorough the SMB domain of vitronectin. However the possibility of the presence of a lower affinity binding site outside the SMB domain of VN has been proposed by a number of groups. Mimuro et al. reported such a site in the intrinsically disordered domain (residues G115 to E131) [200]. Other groups have suggested the presence of another PAI-1-binding site in the C-terminal region of vitronectin (residue K348-K370) [201-202]. In the last few years, our lab has devoted considerable effort toward understanding the details of this interaction, and these efforts have shown that the vitronectin-PAI-1 interaction is more complex than it was previously perceived. Our research has produced evidence that indicates that, although the primary high affinity (Kd~1nM) binding site of PAI-1 lies within the SMB domain of vitronectin, there is an additional binding site (of comparatively lower affinity, Kd~100nM) that lies outside of the SMB domain [203]. Direct evidence for this second binding site was obtained after a recombinant VN lacking the SMB domain was generated. This deletion mutant was found to maintain its PAI-1 binding property with a relatively lower affinity of 100nM [204].

1.3. b. Interactions Leading to Formation of Higher-Order Complexes and Multimerization of Vitronectin

There are a number of biomolecules that may initiate the process by which VN transitions to the multimeric conformation, e.g. the thrombin-antithrombin-III (TAT) complex and the

terminal complement complex (C5b-C7) [44, 205]. PAI-1 binding to VN is the molecule which has been most extensively evaluated for causing conformational changes and multimerization of monomeric plasma VN [206]. Seiffert et al. showed that PAI-1, while mixed with monomeric plasma VN, caused multimerization [206]. This interaction also exposed the conformationally sensitive epitope (for 8E6 monoclonal antibody), usually only found in multimeric VN. The exact cause of the multimerization of VN in biological systems remains one of the unresolved issues to the present day.

VN released from platelets is multimeric in nature [77, 207]. Though PAI-1 concentration in plasma is about 600-1000 fold lower than that of VN (4nM vs. 2.5-4μM), their \concentration within platelets is similar [176, 207-208]. This locally elevated concentration of PAI-1 has been contemplated as a cause for the transformation into a conformationally altered, multimeric form of VN within platelets. In last few years our lab has made significant progress towards understanding this process of PAI-1 mediated multimerization of VN. By size exclusion HPLC and analytical ultracentrifugation studies, we have confirmed that PAI-1 can induce multimerization of VN in a concentration-dependent fashion [203, 209-210]. We have observed that initiation of this multimeric complex starts with the formation of a heterotrimer containing two molecules of PAI-1 and one molecule of VN, confirmed by FRET and a multi-signal sedimentation velocity study [204, 211]. We are also confident that PAI-1 remains associated with this multimeric complex for several hours [209, 211]. With these data in support, we hypothesize that PAI-1 acts a biological partner for the transformation of VN into the matrix-associated form. Furthermore, we propose that the multimeric complexes formed by the interaction between these two proteins significantly influence their matrix-associated roles. In

34

this study, we have emphasized a more complete understanding of the mechanism of complex formation between VN and PAI-1.

1.3. c. Functional Aspects of the Interaction Between VN and PAI-1

The interaction between these two proteins is a subject of great interest in the field. These two proteins are co-localized in a number of pathological conditions, such as atherosclerosis, hepatic fibrosis, and membranous nephropathy [212-214]. While PAI-1 is mainly known as an inhibitor of uPA and tPA, the interaction with VN expands its inhibitory properties to target other proteases, e.g. thrombin and activated protein-C (APC) [215-216]. APC has been proposed to act as a profibrinolytic substance by virtue of its ability to neutralize PAI-1 in circulation. Rezaie et al. showed that while the direct inactivation of APC by PAI-1 proceeds very slowly, interaction of VN with PAI-1 increases the rate of such inactivation by 300-fold. Furthermore, in the presence of VN, PAI-1 becomes the most effective inhibitor of APC [216]. Interaction between PAI-1 and VN has been implicated in the profibrinolytic property of thrombin also. Ehrlich et al. showed that endothelial cell matrix-associated PAI-1, while bound to VN, can inhibit thrombin [215, 217]. This alternative targeting toward proteases may also deplete active PAI-1 from the circulation and ECM, and thus protect plasminogen activators and promote activity of the plasminogen activation system. Stefansson et al. later reported that PAI-1 mediated inactivation of matrix-associated thrombin, which occurs in the presence of VN, has an important role in the cellular clearance of the protease in an LRP-dependent process [218]. The presence of VN and PAI-1 in the atherosclerotic vessel wall has been shown by many groups [110, 219]. There are studies that indicate that active thrombin is also present in the atherosclerotic lesion [220]. Stoop et al. showed that VN, PAI-1 and active thrombin are co-

localized in the atherosclerotic lesion and they have proposed that interaction of VN and PAI-1 in the vessel wall is important for the regulation of thrombin activity, since the natural regulator of thrombin (antithrombin-III) is not present in the deeper region of atherosclerotic lesion [212].

PAI-1 has been found to be associated with VN in the subcellular matrix of endothelial cells and platelets [21, 192-193]. Owensby et al. showed that binding of PAI-1 to the extracellular matrix of HepG2 cells is exclusively mediated by matrix-associated VN [49]. Such VN-mediated localization of PAI-1 to the extracellular matrix appears to be required for the effect of PAI-1 in fibrotic renal diseases. These diseases are characterized by increased fibrin deposition and accumulation of matrix [133, 221]. The plasminogen activation system has a major role in maintaining the proper balance of matrix turnover [222], and this balance is compromised in renal fibrotic diseases. PAI-1 expression is highly elevated in renal fibrotic conditions and thus is thought to be one of the major causes for loss of such balance [223-224]. In these disease conditions, VN plays an important role in localizing PAI-1 within the fibrotic matrix [225].

PAI-1 also plays a role in regulating cellular adhesion and migration. In fact, a significant portion of the protease-independent functions of PAI-1 is mediated through its interaction with VN. PAI-1 interferes with the interaction of cell surface receptors with VN. The PAI-1-binding site on the SMB domain of VN overlaps with the uPAR binding site, and thus PAI-1 competes for uPAR binding to the SMB domain of VN [226-227]. A recent crystal structure of uPAR in complex with the SMB domain and uPA shows that many residues of the SMB domain that were found to be involved in PAI-1 binding are also involved in uPAR binding [103]. Waltz et al. showed that uPAR mediated binding of TGFβ1/Vitamin-D3 stimulated U937 cells and uPAR

transfected 293 cells to VN could be blocked by PAI-1 [226]. In a similar approach, Kanse et al.

showed that PAI-1 could block uPAR-mediated binding of VN to endothelial cells [53]. PAI-1

mediated blocking of the uPAR-VN interaction was found to **promote migration** of U937 and

melanoma cells [226, 228]. Such a promigratory effect of PAI-1 has been ascribed to the lack of

cell adhesion.

PAI-1 interferes with integrin binding to VN also. Stefansson et al. showed that αvβ3

binding to immobilized VN was blocked by PAI-1 in a dose-dependent manner [229]. The

integrin binding site on VN lies beyond the SMB domain (within the RGD motif, residues 45-

47), as seen in the crystal structure of 14-1-B and the SMB domain (**Figure-1.8**) [22]. So

structural overlap is not the direct cause of PAI-1 interference of αvβ3 binding to VN.

Nevertheless, exogenously added PAI-1 inhibited αvβ3 mediated smooth muscle cell (SMC)

binding to VN [229]. In the same study PAI-1 was found to **block migration** of SMC through

VN. In another study Kjøller et al. showed that PAI-1 could **block migration** of WISH and Hep2

cell lines through VN, and this inhibition was due to PAI-1 mediated blockage of αvβ3 binding

to VN [230]. Though in all these studies PAI-1 blocked cell binding to VN, the effect on

migration is contradictory.

There are studies that show that PAI-1 is proangiogenic and protumorigenic. Mice

deficient in PAI-1 showed reduced angiogenesis, tumor invasion and tumor formation [191,

231]. On the other hand in a separate study Stefansson et al. reported that addition of PAI-1

inhibited basic-fibroblast growth factor (bFGF) induced angiogenesis [232]. They also found that

such inhibition of angiogenesis was mediated through interaction of PAI-1 with VN. In an effort

to explain such apparent contradiction, McMahon et al. reported a study where they showed that

the PAI-1 mediated effect on tumor formation and angiogenesis is dose-dependent. While at low concentrations PAI-1 acted in a pro-angiogenic manner, at high concentrations it was anti-angiogenic [233]. Thus PAI-1 appears to play a regulatory role in the processes like, angiogenesis, tumorigenesis. A major focus of this study is to understand the role of PAI-1/VN interactions in the regulation of cell binding and migration.

1.4. Research Goals

Vitronectin and Plasminogen Activator Inhibitor-1 (PAI-1) are two important circulatory proteins, that are also found in the extracellular matrix (ECM). As discussed above, each of these proteins is involved in a variety of physiological and pathophysiological processes by virtue of their ability to interact with a wide variety of ligands. For PAI-1, conformational flexibility is closely connected with its function, and conformational flexibility can be influenced by ligand binding. In addition, interactions between these two proteins have been implicated in several biologically important processes such as cell binding and migration. We have seen that the interaction between vitronectin PAI-1 is much more complicated than a simple 1:1 binding. While we have made considerable progress towards understanding the mechanism of this interaction, more work is needed. The major goals of this research are:

I.   To understand how the interaction between VN and PAI-1 influences their functional roles in the extracellular matrix

II.   To understand the structure and dynamics of PAI-1 in the presence of binding partners like VN and various metals.

III.   To understand the role of vitronectin in mediating infection by comparing the

pathogenesis of *Candida albicans* infection between C57BL/6 mice and vitronectin

knock-out mice.

CHAPTER-2

Developing Methods to Investigate the Structure and Dynamics of PAI-1 and Effects of Cofactors

2.1. Introduction

Conformational flexibility is an important property for serpins. Mobility of the reactive center loop is directly connected to the inhibitory property of serpins. Insertion of the RCL requires a conformational change in other parts of the protein also. A prerequisite for successful insertion of the RCL is a sliding movement of the β1-3A strand of the central β-sheet and helix-F away from the structure so that the groove region between strand 3A and 5A is opened [153]. Egelund et al. performed a thorough study on different forms of PAI-1 (active, latent, cleaved and the complex with protease) and showed with each form that there were specific conformational changes associated in different regions of the protein other than RCL and central β-sheet [154]. PAI-1 is probably the most conformationally sensitive among all the serpins, with an inherent tendency of the RCL of PAI-1 to insert into the central β-sheet region of the molecule. This conformational change transforms active PAI-1 into latent PAI-1. The half-life of this latency transition for PAI-1 ranges between 1-2hrs at 37^0C [158-159]. Binding of ligands has been found to influence the latency transition. VN is one of the major binding partners of PAI-1 and is known to cause moderate stabilization of PAI-1 to slow down this conversion to the latent form. Our lab has showed that VN can cause an increase in half-life of PAI-1 from1.14 hr to 1.51 hr (Thompson et al., submitted to Biochemistry). This VN binding to PAI-1 is proposed to interfere with the RCL insertion by causing blockage to the sliding movement of the s1A and

s2A towards the gap between helix-E and F. A crystal structure of the recombinant SMB domain of VN and the 14-1-B stable mutant form of PAI-1 supports this mechanism of structural stabilization [22].

Though binding of VN to PAI-1 is primarily mediated through the SMB domain, there are a number of important questions regarding this interaction that are still unanswered. For example, are the functional effects of the SMB domain binding to PAI-1 equivalent to the binding of full-length vitronectin? In other words, is the interaction of PAI-1 and vitronectin solely mediated by the SMB domain? Recently, pre-steady state kinetic analyses have revealed some unique features of the vitronectin/PAI-1 interaction. Stopped-flow experiments done under conditions where only 1:1 binding is possible between strategically labeled (fluorescent) PAI-1 and vitronectin, show a concentration dependent biphasic binding of a single PAI-1 molecule to VN followed by a conformational change step [168]. Binding between PAI-1 and the isolated SMB domain, on the other hand, was monophasic. These data indicate that interaction with full-length VN is more complex and involves multiple interactions. Addressing this conformational flexibility and the corresponding change in the stability of PAI-1 is an aim of this study. One of the goals is to probe the conformational change that occurs in PAI-1 due to ligand binding by strategically by placing nitroxide spin labels within the RCL of VN. Also, there is evidence that suggests that the interaction between VN and PAI-1 causes formation of higher order of multimeric complexes [206, 209-211]. We believe that the interaction between PAI-1 and VN that extends beyond the SMB domain is critical for this multimeric complex formation. In this study we have also focused on understanding mechanistic aspects of this multimerization process using sedimentation velocity experiments in the analytical ultracentrifuge.

In addition, our lab has recently observed that different metals can significantly affect the stability of PAI-1. Type-II metal ions (Co, Cu, Ni) were found to largely destabilize the active conformation of PAI-1, whereas type-I (Mg, Mn, Ca) metal ions slightly stabilized it. Progress has been made in the mechanistic aspects of these differential effects by studying binding and ensuing structural changes. The goal in this study is to characterize the binding interaction between PAI-1 and different metals using biophysical techniques.

2.2. Materials and methods

2.2. a. Materials

PAI-1 cloned into the pET 24d expression vector was obtained from Dr. Grant Blouse (Henry Ford Health Sciences Center Detroit, MI) as a gift. Anti-PAI-1 polyclonal antibody (ASHPAI) and octa-peptide (PEP-1-M1660s Inc) (TVASSSTA) were bought from Molecular Innovations Inc, Southfield, MI. Pentapeptide (TVASS) was gift from Dr. Peter Andreasen's lab at Aarhus University, Denmark. Rosetta2(DE3)pLysS was purchased from EMD Biosciences Gibbstown, NJ. The QuikChange XL II kit for mutagenesis was purchased from Stratagene Inc Cedar Creek, TX. Primers for the PCR-mutagenesis reaction was purchased from Invitrogen. Protease inhibitor cocktail P8465 was purchased from Sigma Aldrich Corp. St. Louis, MO. SP Sepharose FF, chelating Sepharose FF and high-resolution Sephacryl S100 were purchased from GE Healthcare Piscataway, NJ. The MTSL spin label was purchased from Toronto Research Chemical Inc. The C18 reverse-phase HPLC column (250*4.6mm, 300 A^0 pore size), Proteo RP-HPLC column (4µm bead diameter, 250 A^0 pore size) and their companion guard columns were purchased from Phenomenex, Torrance, CA. Trypsin Gold mass spectrometry grade was purchased from Promega, Madison, WI. The NTA chip, CM5 chip, amine-coupling kit and HBS-

EP buffer were purchased from GE Healthcare Piscataway, NJ. The Biomax-10 column for concentrating protein solutions was purchased from Millipore. All other chemical reagents (buffer & salt) were purchased from Fisher Scientific (unless otherwise specified).

2.2. b. PCR mutagenesis, expression and purification of P9 mutant of PAI-1

In order to mutate Ser338 (P9 residue) to Cys, a PCR mutagenesis reaction was carried out on the cDNA encoding PAI-1 cloned into the pET 24d expression vector. The primer used for this mutagenesis reaction is shown below:

Forward: 5$^{/}$- gtggcctcctcatgcacagctgtcatagtc -3$^{/}$

Reverse: 3$^{/}$- caccggaggagtacgtgtcgacagtatcag -5$^{/}$

Pfu Ultra HF DNA-polymerase was used for the PCR reaction. PCR reaction conditions are shown below:
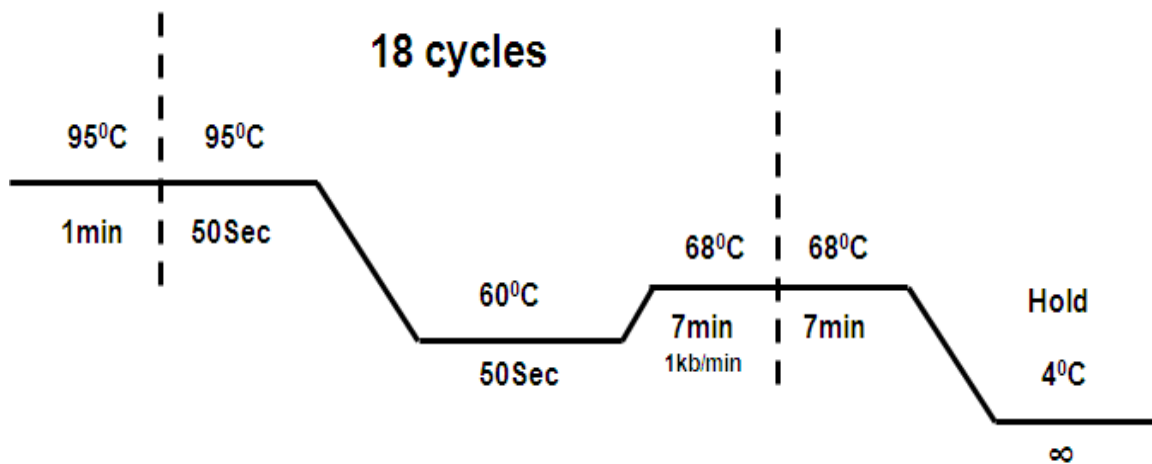
Template DNA was digested using DPN-I, and the final product was transformed into XL10-GOLD competent cells (Stratagene Inc) following manufacturer's instructions. Transformed cells were plated on Kanamycin containing TB-agar plates and incubated overnight at 37^0C for colony formation. On the next day, an isolated single colony was used for subculturing. Subculturing was performed in 50ml Falcon tubes, each containing 10ml of Terrific Broth (TB) with kanamycin. Tubes were shaken overnight at 250rpm at 37^0C. Cell pellets were then collected from each tube by centrifugation, and plasmid purification was carried out using the Promega Wizard Plus miniprep DNA purification system. The presence of the desired mutation was confirmed by DNA sequencing.

For expression purposes, the plasmid containing the mutation was transformed into Rosetta2(DE3)pLysS cells following manufacturer's instructions. Transformed cells were plated on TB-agar plates containing kanamycin (34µg/ml) and chloramphenicol (50µg/ml) and grown overnight at 37^0C. An isolated single colony was used for subculturing into a conical flask containing 200ml TB with kanamycin (34µg/ml) and chloramphenicol (50µg/ml). This subculture was grown overnight at 28^0C with shaking at 250rpm. The 28^0C temperature was used to maintain growth within the 0.5-1 OD range at 600nm within the overnight time frame. After the overnight incubation, the subculture was transferred into flasks containing 1L TB with kanamycin (34µg/ml) and chloramphenicol (50µg/ml) using an inoculum volume to give an OD at 600 nm for the 1L culture of ~ 0.01. The 1L cultures were grown at 37^0C with 300rpm shaking until the OD became 0.1. At 37^0C the Rosetta strain has a doubling time of about 25min. The temperature of the incubator was reduced to 15^0C and growth continued until the temperature was stabilized (about 1-2hr). Expression of PAI-1 was induced by adding 1ml IPTG (1M stock

concentration) to each of the 1L cultures and subsequent growth overnight at 15^0C. The cells were harvested by centrifugation and stored at -80^0C.

For purification of the P9 mutant, the cell pellet was resuspended in lysis buffer (50 mM NaH_2PO_4, 1 mM EDTA, 1mM DTT, pH 6.5) with stirring at room temperature for ~ 1hr. 10ml of lysis buffer was used for each gram of pellet. During stirring, 10 mg of Protease cocktail Inhibitor P8465 was added per gram of pellet. Resuspended cells were lysed by sonication (each cycle had 30sec pulse and 1min pause, 20 total cycles) in an ice bath with stirring. Cell debris was removed by centrifugation (15000g for 15min). In order to maintain PAI-1 in an active form, the entire purification was performed at $4\ ^0$C. The cell lysate was loaded onto an SP Sepharose FF column (2.5 x 25 cm). Prior to loading of the cell lysate, the column was equilibrated with lysis buffer containing 80mM $(NH_4)_2SO_4$. Following loading, the column was washed with the same lysis buffer containing 80mM $(NH_4)_2SO_4$. Elution was carried out with a linear gradient of 80-500 mM $(NH_4)_2SO_4$ in the same lysis buffer (total elution volume was 800ml, 13ml fraction size). SDS-PAGE and Western blotting were performed on the elution fractions to confirm the presence of PAI-1. Selected fractions were pooled and dialyzed overnight against imidazole buffer (50 mM NaH_2PO_4, 500 mM NaCl, 20 mM imidazole, 1mM DTT, pH 7.0). A chelating Sepharose FF column (1.0 x 12 cm) was loaded with Ni according to manufacturer's protocol and equilibrated with imidazole buffer without DTT. (DTT causes reduction of Ni with a color change from bluish green to blackish brown.) Just before PAI-1 was loaded on to the column, DTT was added to the imidazole buffer and equilibration was continued for about one column volume and then PAI-1 was loaded. Then the chelating Sepharose FF column was washed with the imidazole buffer containing DTT. PAI-1 was eluted with a 20-

200mM imidazole gradient (total volume of 400 ml) in the same buffer containing 1mM DTT.

The appropriate fractions were chosen to be pooled according to the SDS-PAGE and Western

blot analysis. Pooled fractions were concentrated to ~3 ml, and then loaded onto a high-

resolution Sephacryl S-100 column (2.5 x 115 cm) equilibrated with gel-filtration buffer (50 mM

NaH_2PO_4, 300 mM NaCl, 1 mM EDTA, 1mM DTT, pH 6.25). Elution was carried out at

0.5ml/min with the same buffer (fraction size- 3ml). PAI-1 eluted as a single peak. The presence

of PAI-1 was once again confirmed by SDS-PAGE and Western blotting. Fractions were pooled,

concentrated, and stored at -80 ^{0}C. Protein identity was confirmed by MALDI-MS. PAI-1

concentration was determined by absorbance at 280 nm using $\varepsilon_{280} = 0.93$ ml$^\bullet$mg^{-1}$^\bullet$cm^{-1} [234]

and a molecular weight = 43760 g/mol (calculated from the amino acid sequence).

2.2. c. Spin labeling of the P9 mutant

A nitroxide spin label, MTSL [(1-oxyl-2,2,5,5-tetramethylpyrroline-3-methyl)-

methanethiosulfonate], was chosen for labeling the P9 mutant. This methanethiosulfonate type of

spin label requires a free sulfahydryl group for labeling. The scheme of the labeling reaction is

shown in **Figure-2.1**. The labeling reaction was performed at 4^0C. Before labeling, DTT was

removed from the mutant protein in storage buffer (50 mM NaH_2PO_4, 300 mM NaCl, 1 mM

EDTA, 1mM DTT, pH 6.25) using a PD-10 column. Initially, the PD-10 column was

equilibrated with storage buffer without DTT. The mutant PAI-1 was diluted to 2.5ml in this

equilibration buffer and loaded on to the PD-10 column. After loading of PAI-1, 3ml

equilibration buffer was utilized for elution by gravity flow. MTSL was added to the mutant

PAI-1 at a 10-fold molar excess, and the reaction was conducted on ice for 4hrs.
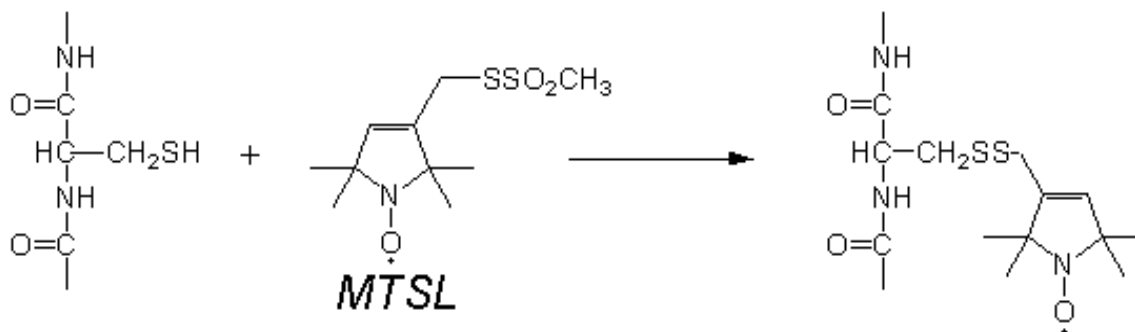
Figure 2. 1: Reaction mechanism for MTSL labeling

Figure-2.1: The reaction mechanism for MTSL labeling involves oxidation that happens between the thiosulfonate group of MTSL with the free sulfahydryl group of the cysteine side chain on the protein. This reaction results in the net loss of 184Da mass.

The MTSL/PAI-1 mixture was loaded on to another fresh PD-10 column pre-equilibrated with equilibration buffer in order to remove unbound MTSL. MTSL-labeled PAI-1 was eluted using 3ml equilibration buffer. Labeled PAI-1 was concentrated using a Biomax-10 spin column (10Kd cut off) centrifuged at 12000rpm for 18min. Analysis of the labeled-PAI-1 sample on a RP-HPLC (C4) column showed a single peak that analyzed by MALDI in order to confirm the presence of the label.

2.2. d. Isolation of the SMB domain by trypsin digestion and RP-HPLC purification

The recombinant SMB-IDD domain was used for isolating the SMB domain. The SMB-IDD was dialyzed against 100mM NH_4HC0_3 buffer (pH-7.8). For trypsin digestion, the required pH is in between 7-9. Trypsin-Gold was dissolved in HPLC-grade water to a final concentration

of 1mg/ml and mixed with the SMB-IDD sample at a ratio of 1:50 (w/w). As a control, the same amount of trypsin was mixed with 0.1M NH_4HCO_3. The reaction was performed at 37^0C and stopped by adding 1%TFA in water, so that the final concentration of TFA is 0.1%. Trypsin digestion time, which was standardized to maximize production of the SMB domain, was 140 min. The reaction mixture was separated on a Proteo RP-HPLC column with 24-28% Acetonitrile (ACN) gradient over a 30min time period at 0.5ml/min flow rate. The gradient was standardized in order to maximize the separation of peptides after digestion. HPLC peaks were collected for mass analysis by MALDI. Multiple injections were made (each 50µl) on the Proteo column, and the peak that corresponds to SMB domain was collected. The mass of this collected peak was again confirmed by MALDI. Collected fractions were combined, lyophilized in a Speed-Vac and frozen at -80^0C. The lyophilized sample was resuspended in 1XPBS, and the concentration was measured by absorbance at 276nm wavelength. using $\varepsilon_{276} = 4,500$ $M^{-1} \bullet cm^{-1}$ [235] and a molecular weight of 5678.26Kd (calculated from the amino acid sequence including 4 disulfide bonds).

2.2. e. Electron paramagnetic resonance measurements

EPR-spectroscopy was performed on this Labeled P9-mutant in a Bruker-EMX machine. For titration with VN or the SMB domain, 3µM of the labeled PAI-1 mutant was mixed with varying concentrations of vitronectin or the SMB domain. Each mixture was incubated at room temperature for 15minutes, and then 60µl of the reaction mixture was loaded in a quartz capillary for data collection. Spectra were collected at room temperature using incident microwave power at 2.158mW and a 100 kHz field modulation of 4Gauss. A total of 8 scans were accumulated for each sample; for each scan, a 100gauss scan-width centered at 3514.31Gauss was used. The

recorded spectra were analyzed using WIN-EPR software from Bruker. The intensity of the middle peak was measured, and the normalized intensity was plotted against the ratio of ligand to PAI-1 concentration.

For half-life measurements, the temperature of the instrument was maintained at 37^0C by using the nitrogen gas driven temperature control device. 7µM of the labeled PAI-1 mutant was loaded into the quartz capillary tube, and the tube was capped using a Teflon plug on both sides to avoid leakage. Spectra were collected at 37^0C, using incident microwave power at 2.16mW and a 100 kHz field modulation of 4Gauss. Two scans were added for each time point; for each scan, a 100gauss scan-width centered at 3365.31Gauss was used. Spectra were collected starting from the zero-time point and continued for a period of 22hr. A multiple-field-sweep (MFS) strategy was used for collecting spectra at different time intervals. Proper tuning of the instrument was maintained between scans. The absolute area of the middle peak at each time point was measured by WIN-EPR software from Bruker. Area was plotted against time and fit to a single exponential decay equation using GraphPad Prism software.

2.2. f. Surface plasmon resonance measurement

In order to confirm the proper function of the isolated SMB domain, SPR experiments were performed on a Biacore-3000 instrument. About 4000 response unit (RU) of monomeric Vitronectin (25µg/ml) was covalently immobilized (acetate buffer with pH-4.5) on a CM5 chip following 1-ethyl-3-(dimethylaminopropyl)carbodimide hydrochloride/*N*-hydroxysulfosuccinimide coupling chemistry (EDC/NHS coupling). 25nM of wtPAI-1 in HBS-EP buffer (10 mM HEPES, 150mM NaCl, 3 mM EDTA, 0.005% surfactant P20, pH 7.4) was flowed over the VN-chip in the presence and absence of equimolar concentration of isolated

SMB domain. The conditions for this experiment were a10µl/min flow rate with protein, with a 3min association followed by 3min dissociation phase with a flow of buffer alone. The chip was regenerated with 50mM HCl at 10µl/min flow rate for 1min.

For metal binding experiments with PAI-1, the NTA chip was used. The structure of NTA is shown in **Figure-2.2**. Freshly prepared (filtered and degassed) Tris buffer (50mM Tris, 200mM NaCl, pH-7.4) was used as running buffer. For each metal a highly concentrated stock solution was made in water and stored at 4^0C under low pH. Before each experiment a solution of 0.5mM (unless otherwise specified) was made from the stock solution using the running buffer. For regeneration, a 350mM EDTA solution was made in running buffer. For washing the loosely bound metal from the microfluidic channel and the chip, a 50µM EDTA solution was made in running buffer. All the reagents were filtered and degassed before the experiment. No reagent was used for more than two days. PAI-1 was dissolved in running buffer (filtered, degassed) at the desired concentration, and the final mixture was filtered before loading on the chip. The basic scheme of the experiment is shown in **Figure-2.3**. Metal was loaded on FC2 (or FC4) at a 10µl/min flow rate for 0.7min. Loosely bound metal was flushed out of the system by a brief injection of (1.5min) 50µM EDTA on both the metal loaded and reference flow cells at a 10µl/min flow rate. PAI-1 was loaded on to the chip (on both flow cells) at 10µl/min flow rate for 2 min and the dissociation was monitored for 3 min. Specific binding of PAI-1 to metal was obtained by subtracting the background binding on the reference flow-cell. Steady state response units were determined using the BIA-evaluation software, plotted against PAI-1 concentration and fit to a single-site specific binding model in Graphpad-Prism to obtain the affinity constant.
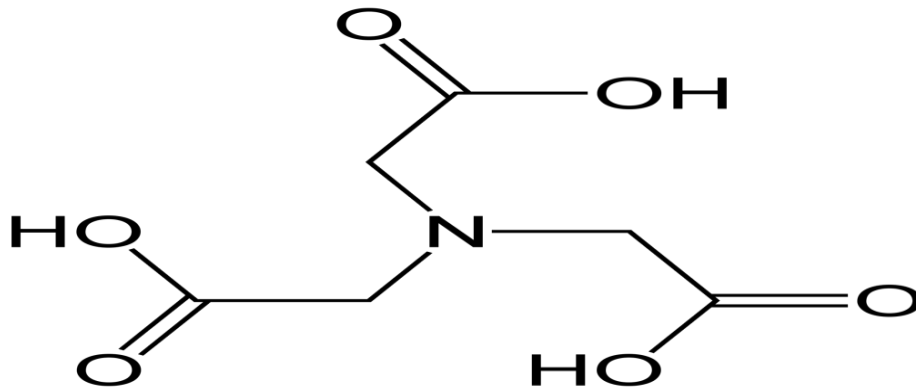
Figure 2. 2: Nitrilotriacetic acid

Figure-2.2: The structure of nitrilotriacetic acid shows
three carboxy-methylene groups are attached with the
central nitrogen atom
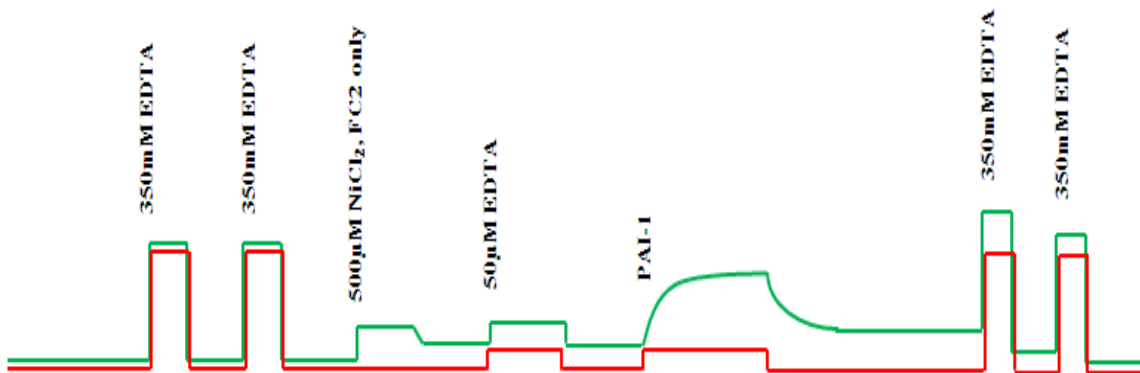
Figure 2. 3: Basic scheme for the Biacore experiments of PAI-1 binding to metal

Figure-2.3: The basic scheme for PAI-1 binding experiment to the
immobilized metal on NTA chip. The change in response unit (RU) for
each injection over both the test flow cell (in green) and the reference
flow cell (in red) is represented schematically.

51

For competition experiments, a fixed concentration of PAI-1 was mixed with varying concentrations of $MgCl_2$. The mixture of PAI-1 and $MgCl_2$ was then injected at a 20 µl/ml flow rate over both nickel-bound and reference flow cells for 2 min. Competition of magnesium with NTA-bound nickel for binding to PAI-1 was measured by the decrease in steady-state response units. For this competition experiment, response curves obtained at each concentration of $MgCl_2$ were plotted with that of PAI-1 by itself. Free metal ion concentration was calculated according to the following equation: $M_f = M_t - [(M_t + B_t + K_d) - ((M_t + B_t + K_d)^2 - 4 \cdot B_t \cdot M_t)^{1/2}]/2$ where M_f = free metal concentration, M_t = total metal concentration, B_t = total buffer concentration, and K_d = buffer/metal dissociation constant. The specific affinity information between a metal ion and the buffer was obtained from the previous work done by other groups [236-238]. By using the known buffer/metal affinity values ($\beta 1$) as described in these articles, the dissociation constants of the metals in the Tris buffer were calculated following the equation: $\beta 1 = K_a = 1/K_d$.

2.2. g. Sedimentation velocity experiments

Sedimentation velocity experiments were carried out in an Optima XL-I analytical ultracentrifugation instrument. Both interference and absorbance optics were utilized. When interference optics was used, proteins were dialyzed against a common buffer overnight at 4^0C. For example, when experiments were performed to characterize the multimerization between VN and PAI (wild type and its variants- 14-1-B & W175F), each of these proteins were loaded into Slide-A-lyzer dialysis cassettes (10Kd cut off). Each of these cassettes was then dialyzed overnight against 1XPBS in the same dialysis chamber in order to match the buffer composition between the various samples. VN and PAI-1 (or its variants) were mixed at the required concentrations and the mixture was incubated at 37^0C for 1hr. A volume of 390µl of the mixture

was loaded into the sample sector of a double-sector charcoal-filled epon (12mm path length) centerpiece inside the centrifugation cell. For interference optics, buffer from the dialysis chamber was used in the reference sector of the centrifuge cell in order to match the buffer composition between reference sector and sample sector. For absorbance optics buffer matching was not as critical. For experiments with RCL peptide mimics, only absorbance optics was used. Peptides at required concentrations were mixed with PAI-1 and incubated at 37^0C for 1hr. Following this incubation, VN was added, and incubation was continued for an additional hour at 37^0C. Samples were loaded on to centrifugation cell as described above.

Centrifugation cells were properly aligned inside an 8-hole An50 Ti rotor and the rotor was subject to temperature equilibration inside the centrifuge under vacuum. Temperature equilibration was continued for at least 1hr at 25^0C. For interference data collection, proper temperature equilibration is very critical. For interference scans, radial calibration was carried out before starting the data collection. Sedimentation velocity experiments were performed at 50,000 rpm at 25°C. Analysis of the sedimentation velocity data was carried out using the continuous c(s) distribution model described by the Lamm equation with the freely available software, SEDFIT [239-240]. The built-in integration tool of SEDFIT was used to calculate the amount of loading signal present within a specific sedimentation coefficient range.

2.3. Results

2.3.I. Characterizing the Interaction between Vitronectin and PAI-1 by Strategic Placement of a Spin Label in PAI-1

2.3.I.a. Isolation of the Correctly Folded SMB Domain

Expression of the SMB domain (first 44aa of vitronectin) in a recombinant system is challenging because of the likelihood of producing misfolded protein due to improper disulfide bridge formation. The SMB domain has 8 cysteine residues that form 4 disulfide bonds. The correct formation of these four disulfide bonds yields a structure that is resistant to protease digestion. However, expression in a bacterial system results in the formation of several different disulfide bonded species. In a separate study, a segment from vitronectin containing both the SMB and IDD domains (i.e., the first 130aa of VN) of VN was expressed in our lab. Following is the sequence of the piece that was expressed as SMB-IDD. The first four amino acids of the

GSAMDQESCKGRCTEGFNVDKKCQCDELCSYYQSCCTDYTAECKPQVTRGDVFTMPED
EYTVYDDGEEKNNATVHEQVGGPSLTSDLQAQSKGNPEQTPVLKPEEEAPAPEVGASKP
FGIDSRPETLHPGRPQP

sequence (**GSAM**) are an extra portion that resulted from the cloning strategy. The portion highlighted in green is the SMB domain, and the portion highlighted in yellow is the IDD domain with a RGD sequence in between them. A method was developed to use a trypsin digestion method to isolate and purify the correctly folded SMB domain from the expressed recombinant SMB-IDD pool (which presumably contains a mixture of species due to various disulfide arrangements). The working hypothesis was that the correctly folded form will be resistant to such digestion. Following trypsin digestion for ~ 140 min at 37^0C, reverse phase HPLC purification was pursued on the digested proteins, using a C18 Proteo column.

Figure-2.4 represents the elution profile of the digested SMB-IDD by HPLC. Various peaks were collected, and their mass was checked by MALDI. If the SMB domain remains resistant to trypsin digestion then a digestion after R49 residue will result in the release of the isolated SMB domain with a calculated mass of 5506Da including GSAM at the N-terminus. The peak that eluted at 10.11min showed a mass of 5505.339Da, close to the expected mass. Large scale trypsin digestion was carried out, and the peak corresponding to the undigested and intact SMB domain was collected upon multiple injections of the digested sample. Again, several collected fractions were selected and were tested along with the target fraction by MALDI to confirm the mass. **Figure-2.5** represents the mass chromatogram obtained from the target fraction, and the observed mass was once again very close to calculated mass for the isolated SMB domain. All of the collected peaks were combined, freeze-dried and reconstituted in 1XPBS and stored at 4^0C.

Confirmation of the correct folding of the purified SMB was performed by carrying out a SPR-based competition assay in the BIACORE instrument. A CM5 chip was covalently coupled with monomeric vitronectin. Mixtures of PAI-1 and the isolated SMB domain were passed over the VN-chip. The SMB domain, at equimolar concentrations with PAI-1, (25nM:25nM) was observed to completely block PAI-1 binding to VN chip. **Figure-2.6** shows the sensogram data with PAI-1 run over the chip alone or in combination with the SMB sample. While PAI-1 by itself showed a steady state response unit (RU) of about 500, the addition of the SMB domain reduced the binding close to baseline. These data clearly confirm the proper function of this SMB preparation.
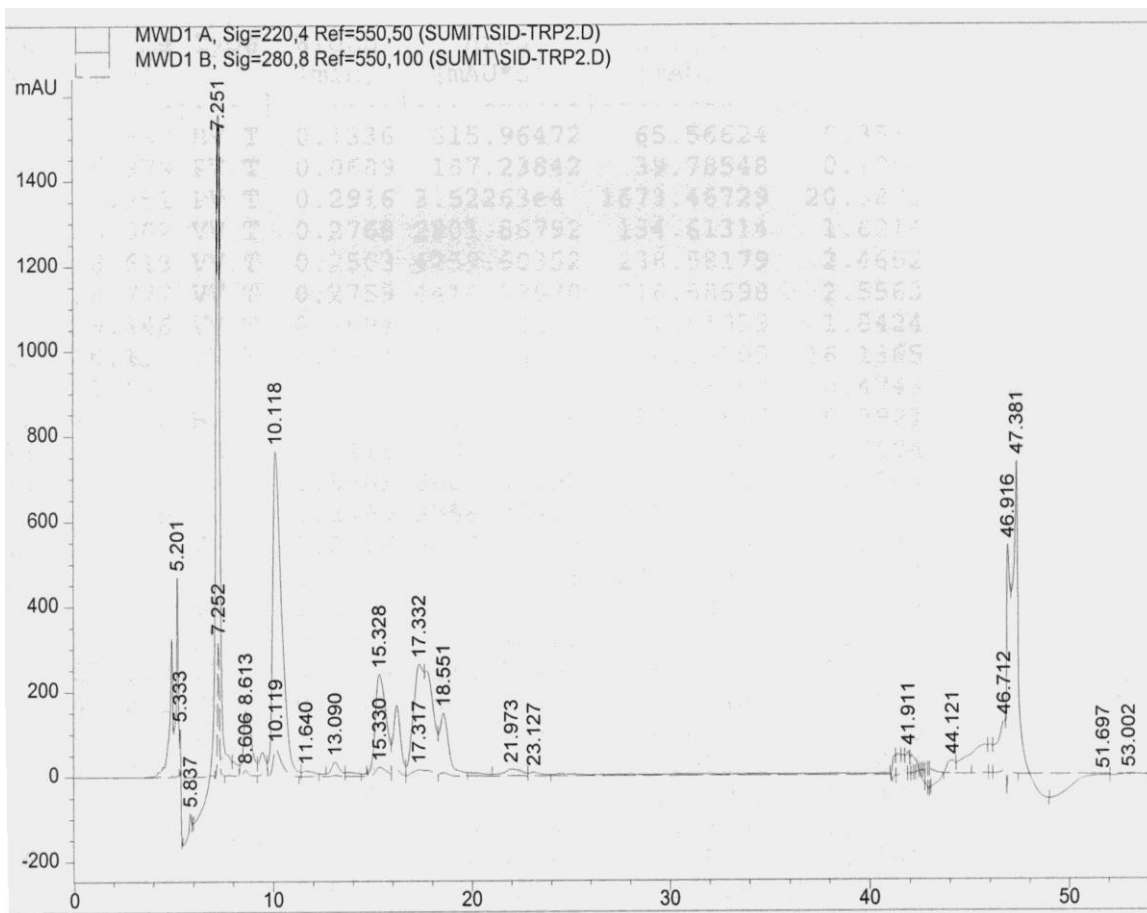
Figure 2. 4: HPLC elution profile of trypsin digested SMB-IDD

Figure-2.4: Digestion of SMB-IDD was carried out for 140min at 37⁰C in NH₄HCO₃ buffer at pH-8. 50μl of the digested sample was loaded on a Proteo-RP column and separated using a 24-28% gradient run for 30min at 0.5ml/min flow rate. The peak that eluted at 10.118min represented undigested SMB domain. The numbers indicated in the elution profile are the time points (in minutes) of the appearance of each peak.
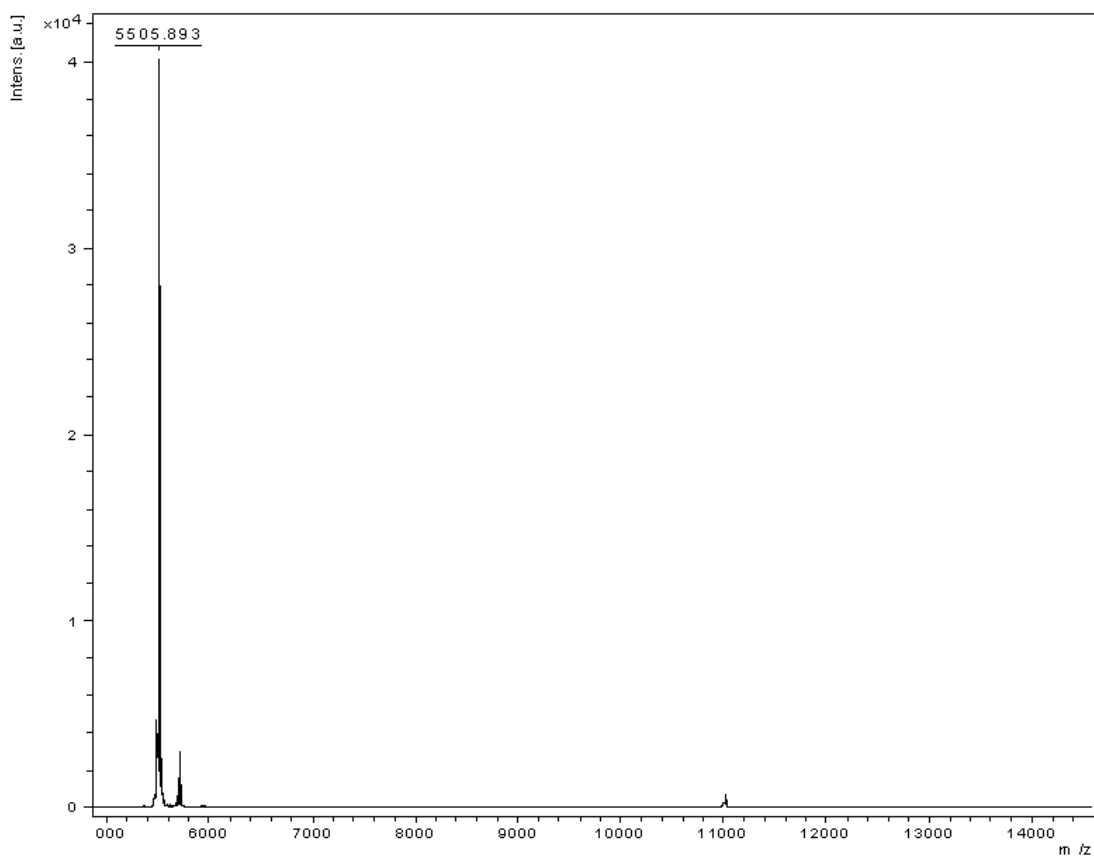
Figure 2. 5: Confirmation of the mass of the isolated SMB domainby MALDI

Figure-2.5: The SMB-IDD domain was digested with trypsin at 37^{0}C in NH$_4$HCO$_3$ buffer at pH-8. Samples were injected on to RP-HPLC. The peak eluted at 10.11min for each injection was collected. This peak represented undigested SMB. Some of the fractions were randomly selected and checked by MALDI. This figure shows the mass information obtained from one of those samples. The observed mass (5505.893) nicely matches up with the calculated mass.
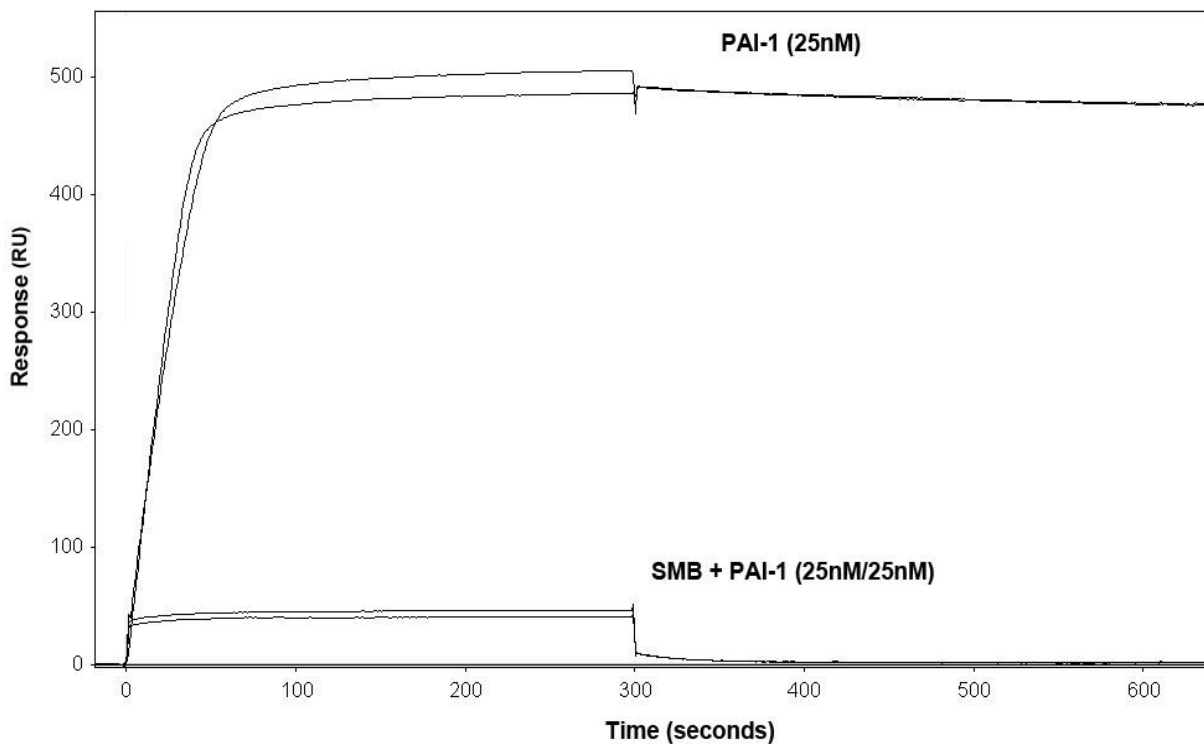
Figure 2. 6: Confirmation of the PAI-1 binding activity of the SMB by SPR

Figure-2.6: A competition experiment of SMB domain with full length VN for PAI-1 binding was designed. Monomeric VN was immobilized on a CM5 chip. Injection was carried out for 5min at 30μl/min followed by a 5min dissociation phase. PAI-1 (25nM) alone showed a response unit change of around 500. However, addition of equimolar SMB decreased the change in response units to nearly baseline, demonstrating effective competition of the SMB domain with full length VN for PAI-1 binding. This figure shows results from duplicate injections of each sample.

2.3.I.b. MTSL-labeled PAI-1 Accurately Reports the Transition to the Latent Form

Use of spin labels has been found to be quite useful in the understanding of structural changes upon protein-protein interaction. Spin labels are extremely sensitive to changes in the local environment and can provide valuable information on conformational changes. PAI-1 has an inherent advantage in that it does not have any cysteine residues in its primary structure. This allows us incorporating a single cysteine at any location within PAI-1 by site-specific mutagenesis, and thus in turn permits us to put a spin label at our position of choice. In this study, the Serine-338 residue in the RCL (known as the P9-residue), was chosen to be spin labeled. The S338C mutant of PAI-1 was successfully expressed and purified, and the purified mutant was successfully labeled with MTSL spin-label following the reaction mechanism shown in **Figure-2.1**. Incorporation of a single label was confirmed by MALDI (**Figure-2.7**). This result confirms that the observed mass (42784.043Da) of the purified mutant (S338C) agrees with the calculated mass which is 42785.45Da. If the reaction with MTSL at a single position has been achieved then the increase in mass should be 184Da. Our result shows an increase in 184.7Da.

Once the labeling was confirmed, we aimed to verify our idea that strategically placed spin-labels in PAI-1 would be sensitive to changes in the local environment. Placement of the fluorescent probe at the P9 position has been successfully utilized to probe the insertion of the RCL during the transition of PAI-1 to the latent conformation [241]. Likewise, it was predicted that this spin-label at P9 position could successfully report the insertion of the RCL. 8μM MTSL-labeled PAI-1 was loaded into the EPR tube, and scans were collected at different time intervals. Temperature inside the EPR cavity was maintained at 37^0C throughout the experiment. At each time point, two scans were collected, and the absolute area of the middle peak of the
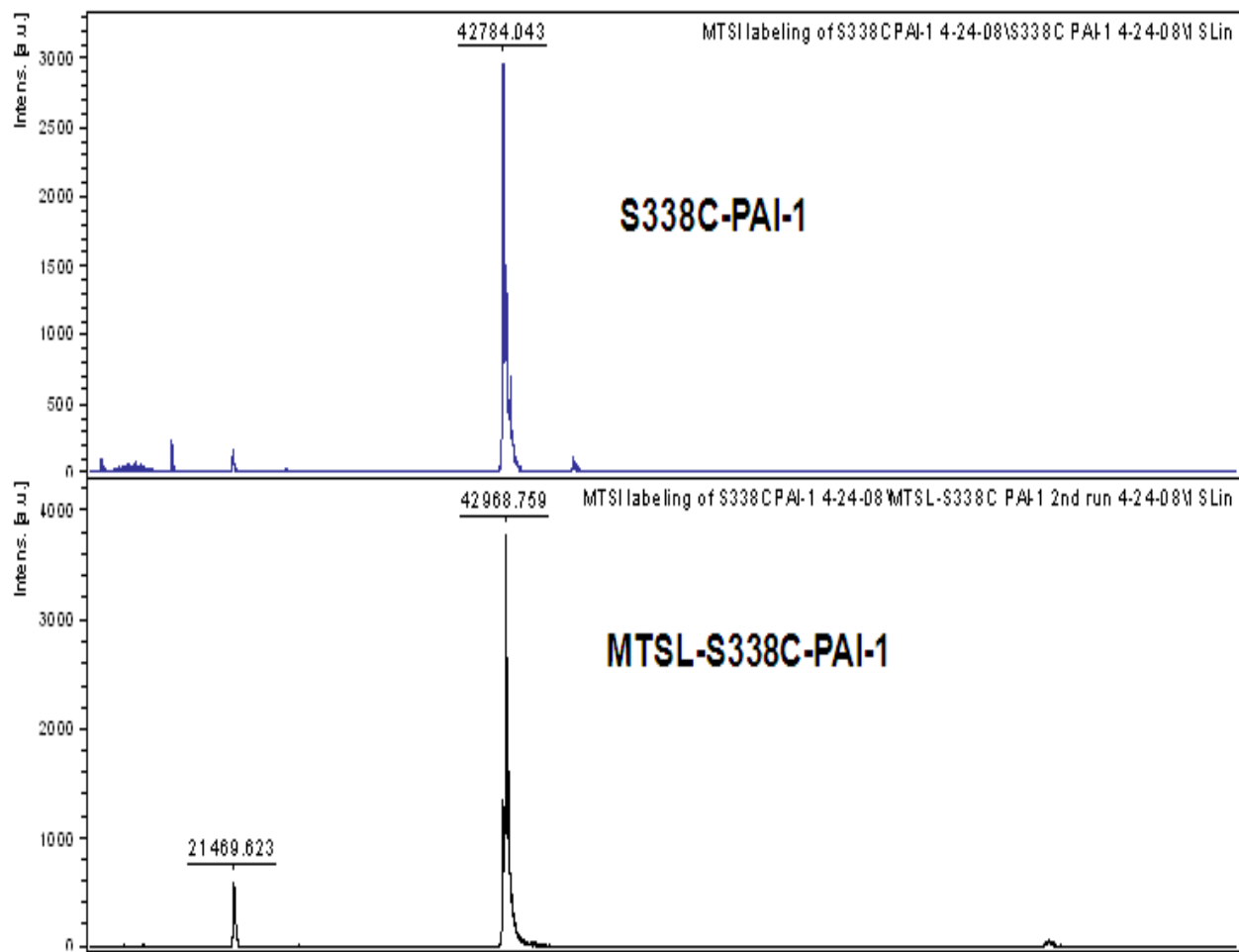
Figure 2. 7: Conformation of MTSL labeling of S338C PAI-1 by MALDI

Figure-2.7: MALDI analyses for comparing the mass of S338C-PAI-1 and MTSL-labeled S338C-PAI-1. The top panel shows the mass of purified S3368-PAI-1, and the bottom panel shows the mass of S3368-PAI-1 with the spin label attached. The major peak in the spectrum represents the average molecular weight of each species. The observed increase in mass (184.7Da) nicely corresponds to the presence of a single label on PAI-1

EPR-spectrum was calculated. Peak area was plotted against time and fitted to a single exponential decay equation. With increasing time, the peak area decreased until it reached a plateau. **Figures-2.8** and **2.9** show the spectrum collected at time zero and at 22hr respectively. **Figure-2.10** shows the area vs. time curve. The half-life of the signal change was ~ 85 min, which is similar to the half-life of the latency transition found in the literature (1-2hrs) [158-159]. This indicates that the method can effectively sense the change occurring at a structural level.

2.3.I.c. The Effect of VN or the SMB Domain Binding on MTSL-Labeled PAI-1

An experiment was designed to check the effect of the binding of the isolated SMB domain or full length VN on MTSL-labeled PAI-1. A titration experiment was carried out in the Bruker-EMX EPR instrument, using varying concentrations of vitronectin or the SMB domain mixed with a fixed concentration of MTSL-S338C PAI-1 (3μM). **Figure-2.11** shows the data from this experiment. Four scans from each sample were collected, and the peak height of the second (middle) peak of the MTSL-labeled PAI-1 was calculated using WINEPR software (from Bruker-EMX). The peak height of each sample was normalized with respect to the peak height obtained from MTSL-PAI-1 alone. The normalized data were plotted against the concentration of the ligand. This titration analysis shows an interesting difference in the interaction comparing the isolated SMB domain and full-length, intact vitronectin with PAI-1. While the addition of increased concentrations of SMB to PAI-1 did not cause much change in the spin label, addition of VN to PAI-1 caused a decrease in the signal intensity. These results provide another indication that the interaction of full length VN with PAI-1 is more extensive than that exhibited by the SMB domain by itself.
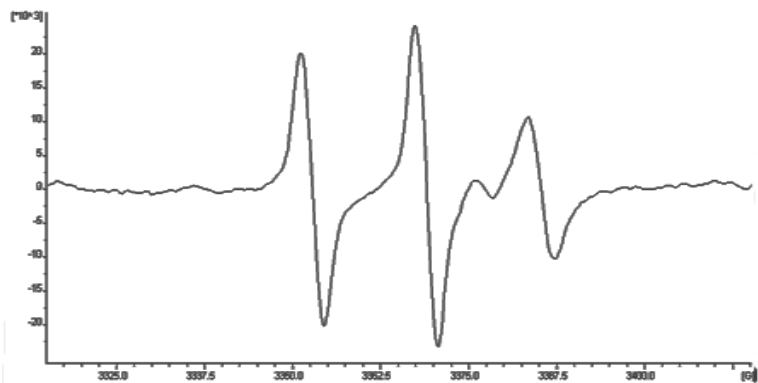
Figure 2. 8: Spectrum of MTSL labeled PAI-1: at time zero
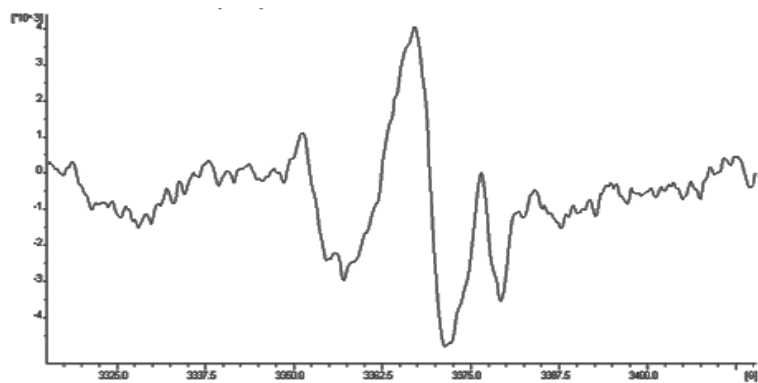
Figure 2. 9: Spectrum of MTSL labeled PAI-1: at 22hr

Figure-2.8-2.9: EPR spectra of MTSL-S338C PAI-1 at time zero (Figure-2.8) and at 22hr (Figure-2.9). MTSL-labeled PAI-1 was tested at an 8µM concentration, and each spectrum at the respective time points represents the addition of two scans.
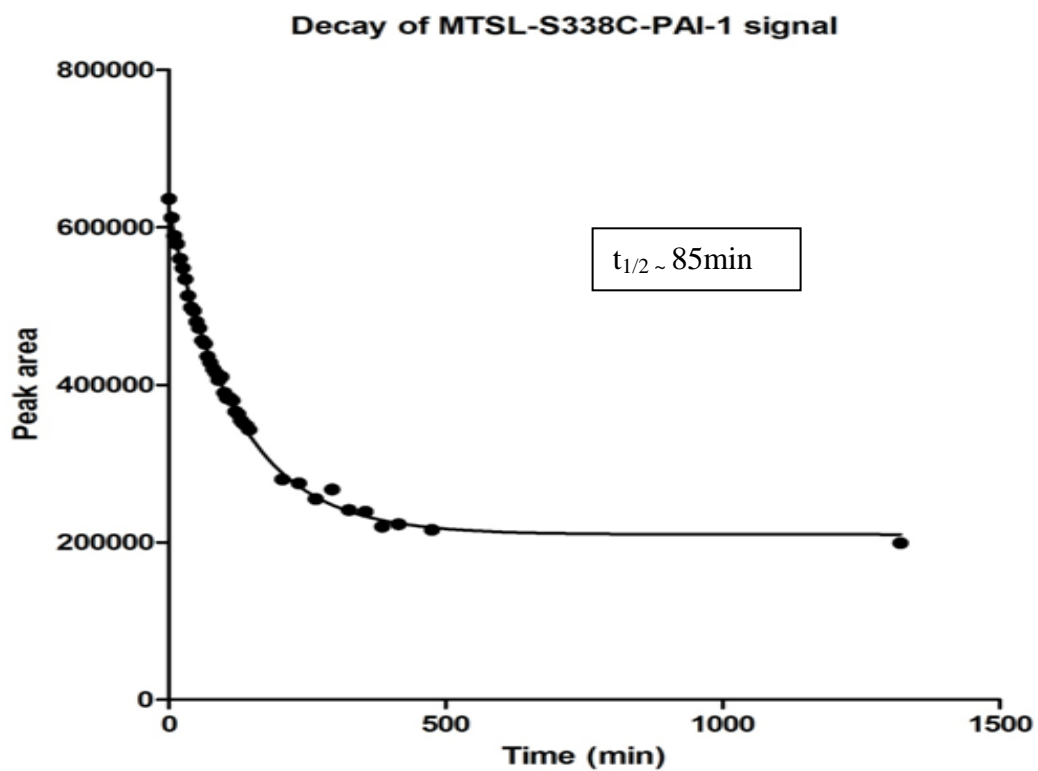
Figure 2. 10: Exponential decay of EPR signal of labeled PAI-1with time at 370C

Figure-2.10: The absolute area of the middle peak from the EPR spectra at each time point was calculated and plotted against time interval. Data have been fit to a single exponential decay equation. The half-life obtained from this study was 85min.
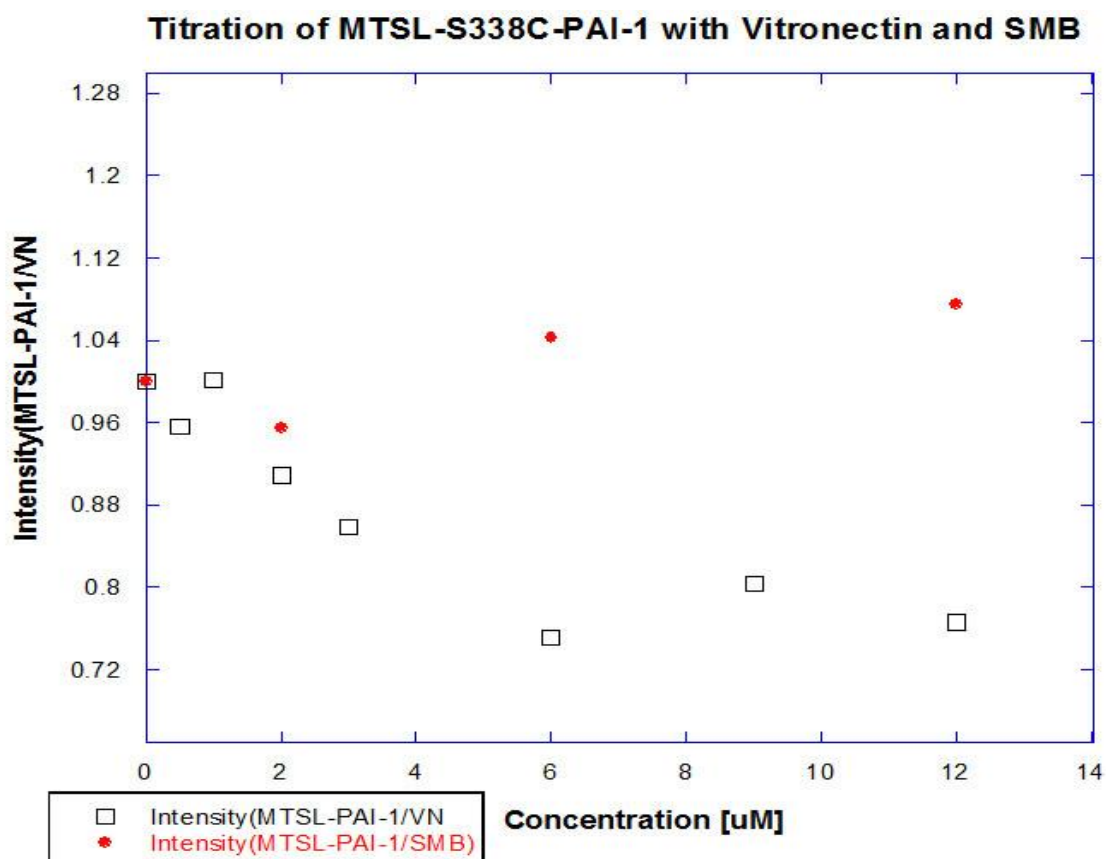
Figure 2. 11: Comparison of VN and SMB binding to S338C-PAI-1by EPR

Figure-2.11: Titration of MTSL-S338C PAI-1 (3μM) with varying concentrations of SMB and VN. Four scans for each sample were collected. The peak height of the middle peak of each sample was calculated and normalized with respect to the peak height obtained from MTSL-labeled S338C-PAI-1 alone. Normalized data have been plotted against ligand concentration. Solid circles (red) show the titration with SMB and open squares indicate the titration with VN.

2.3. II. Characterizing the Mechanism of Formation of Complexes Between VN and PAI-1

2.3.II.a. Comparison of Formation of Higher-order PAI-1/VN Complexes with Wild-type and Stable Mutant Forms of PAI-1

Sedimentation velocity experiments are routinely done in our lab to understand the association process for VN and wtPAI-1. **Figure-2.12** shows the formation of the multimeric complexes between VN and PAI-1 (mixed at equimolar concentration, 6μM) from a sedimentation velocity experiment. Absorbance data were collected and analyzed using the c(S) continuous size distribution model described by the Lamm equation using SEDFIT [240]. A distribution plot is generated relating the concentration of various species (y-axis) and their sedimentation coefficient ((s) plotted on the y-axis). Monomeric VN and PAI-1 have a characteristic sedimentation coefficient of ~ 4.5S and 3.5S respectively [210]. The appearance of higher-order multimeric species becomes evident when these two proteins are mixed together. **Figure-2.12** shows the multimeric species (with S-values greater than 6); integrating the area between specific sedimentation coefficient values allows us to quantify the relative amount of protein mass present within that range. When PAI-1 and VN are mixed together (6μM:6μM) about 65% of the total loading signal is present within the range of 6S to 60S as higher-order multimeric complexes.

We next evaluated association of vitronectin with two mutants of PAI-1 (14-1-B and W175F) that are known to have much higher stability than wild type active PAI-1 [135, 164].
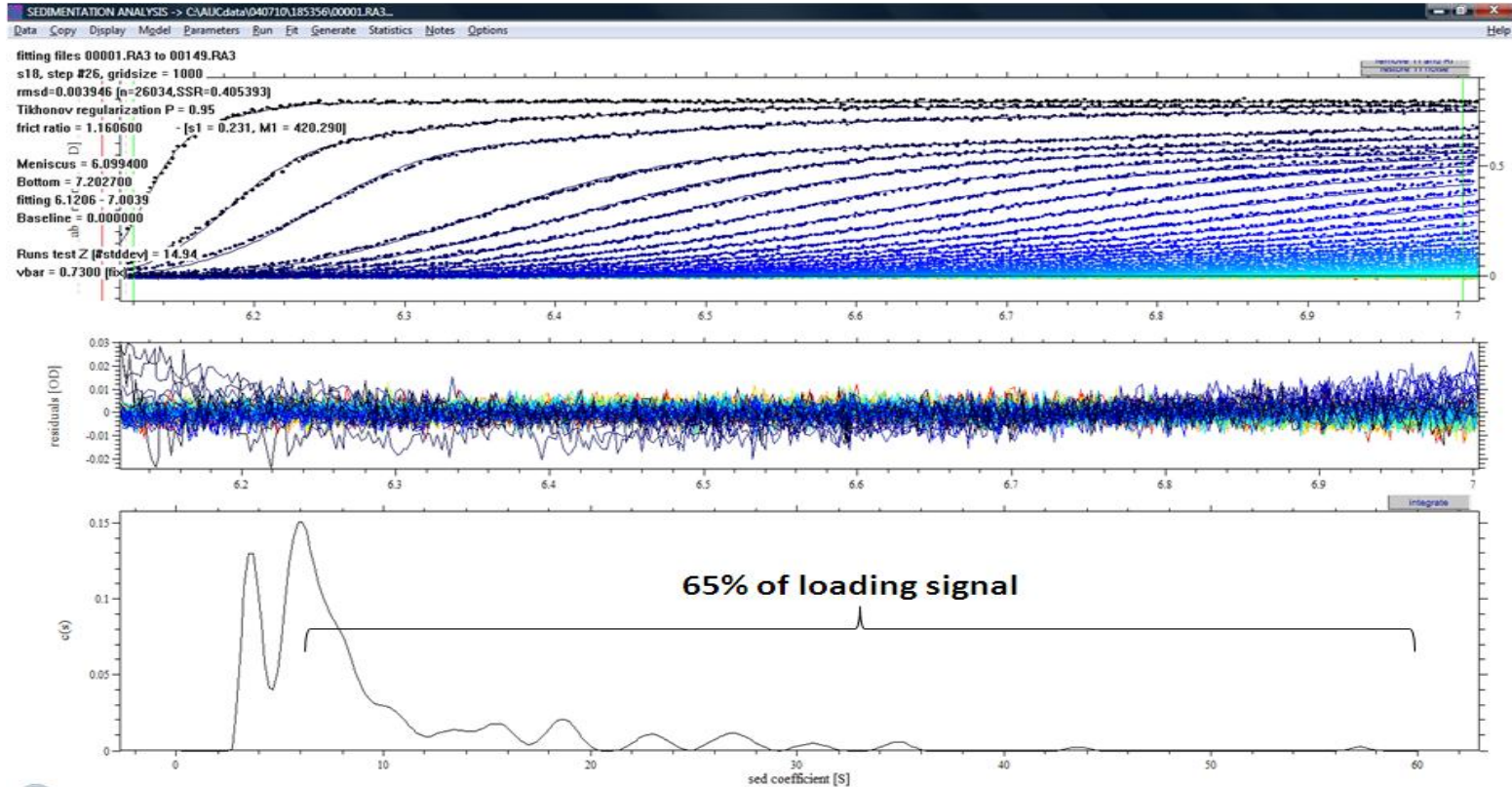
Figure 2. 12: Sedimentation velocity study of oligomeric complex formation between VN and wtPAI-1

Figure-2.12: Proteins (VN and PAI-1) were mixed at an equimolar concentration (6μM) at 37^{0}C for 1hr and loaded into the centrifuge cells. Absorbance data were collected at 50000rpm at 25^{0}C and fitted to a c(S) distribution model using SEDFIT. The top-panel indicates the RI noise and TI noise subtracted data fitted to the c(S) distribution model. The numbers indicate the fitted parameters referring to the model. The middle-panel indicates the residual of the fit. The bottom-panel is the distribution plot of different sedimenting species (c(S) vs. S). Integration of the distribution between 6S and 60S indicates that 65% of the loading concentration was present as higher order complexes.

Mutations at these different positions apparently cause structural changes that oppose the spontaneous insertion of the RCL. In a previous study done by our lab, it was found that the W175F mutant had a greatly decreased affinity (Kd>10μM) for binding to VN at the site situated outside of the SMB domain [242]. Therefore, a significant functional difference exists between wild type PAI-1 and theses mutants. Our goal was to further compare the functional properties of these two mutants with wild type active PAI-1. Although these two mutants are showing stabilizing effect on PAI-1 by bringing structural alteration, important question remains regarding their ability to form multimeric complexes with VN. Sedimentation velocity experiments were performed to compare the amount of higher-order multimeric complexes generated with VN. **Figure-2.13** shows the comparison of the distribution of higher order multimeric species formed by the interaction of VN with equimolar amounts of wild type active PAI-1 or either of the mutants. Integration of the distribution range between sedimentation coefficients of 7S to 45S demonstrates that about 50% of the loading signal from all the variants was present within this range. Thus, the total amount of higher order multimers formed between active PAI-1 and the mutants was not much different. If we carefully observe the size distribution profile it appears that with the 14-1-B mutant, formation of higher order multimers was largely limited to sedimentation values of <20S. The relative amount of higher order species present beyond that range was much lower compared to the other mutant and wild-type protein.

2.3.II.b. Studies to Address the Way in which VN and PAI-1 Interact within Multimeric Complexes

We have generated evidence in our lab that indicates that the multimerization between VN and PAI-1 is initiated by the formation of a heterotrimeric complex (1:2 stoichiometry) that
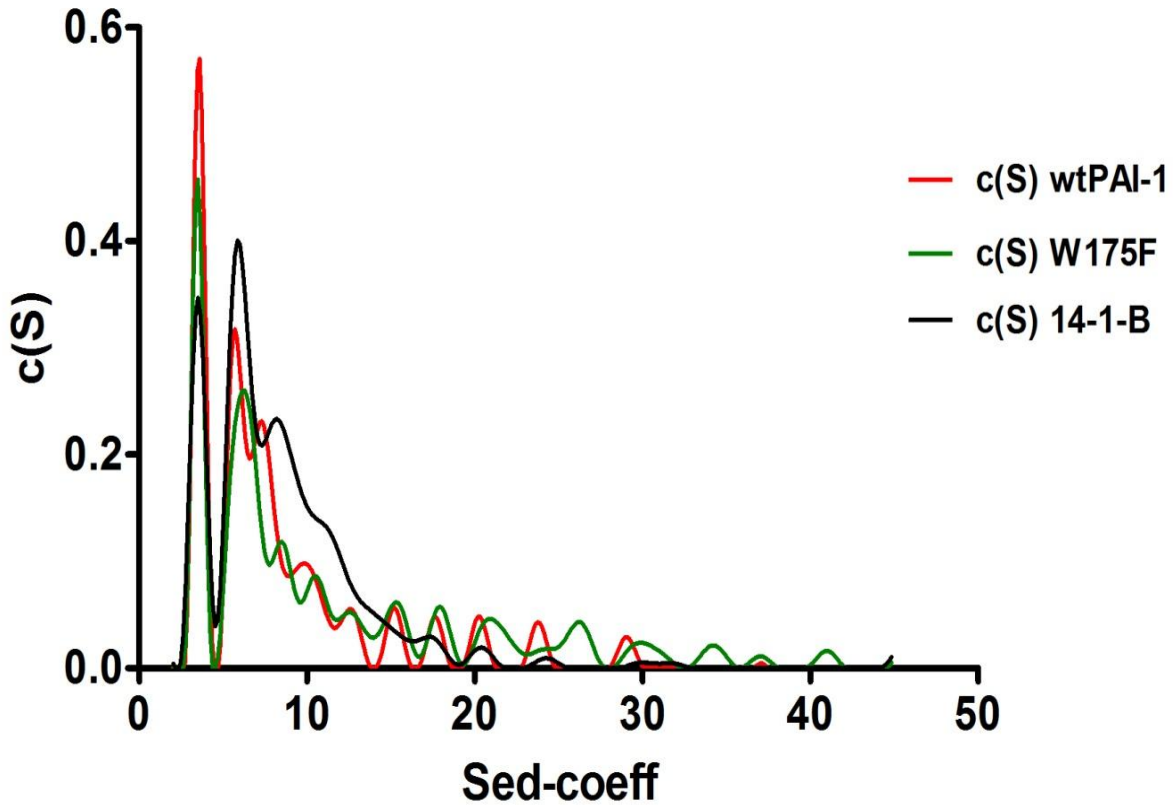
Figure 2. 13: Sedimentation velocity study: comparison of oligomerization between wtPAI-1 and its stable mutants with VN

Figure-2.13: Comparison of multimeric complex formation between wtPAI-1 (red) and mutant forms of PAI-1, W175F (green) and 14-1-B (black). Interference data were collected at 50000rpm and fitted to a c(S) distribution model using SEDFIT. Each variant of PAI-1 was mixed at an equimolar concentration with VN (6μM) and incubated for 1hr at 37^0C before loading into the centrifuge cells for the analysis.

contains one VN molecule and two PAI-1 molecules. Although our idea was that two PAI-1

molecules bind to one VN directly within the 2:1 complex, we did not have direct evidence to

validate this hypothesis. Several approaches have been pursued to address this idea. For one, we

have an ongoing collaboration with scientists at the Oak Ridge National Lab (ORNL) to study

the mechanism of complex formation between VN and PAI-1 by performing small angle neutron

scattering (SANS). These studies have been performed with a complex of monomeric VN and

perdeuterated W175F. A model of full-length VN previously generated from a small angle x-ray

scattering (SAXS) study [27] and the crystal structure of 14-1-B have been used to fit the data

obtained from these SANS studies. This has resulted in the generation of an intriguing model of

how VN and PAI-1 interact within 1:2 complexes as shown in **Figure-2.14**. This model indicates

that within the 2:1 complex, only one PAI-1 molecule is in direct contact with the VN molecule.

The second PAI-1 molecule has no connection with VN; instead, it forms direct contacts with the

first PAI-1 molecule that directly interacts with VN. This model points us in new directions

regarding the interaction between VN and PAI-1. Obviously, a direct interaction between VN

and PAI-1 is important for initiating the process; this means that use of a PAI-1 variant that

completely lacks the ability to interact with VN will be expected to fail in forming multimeric

complexes. Another interesting aspect of this model is the interaction between the PAI-1

molecules within the complex. It appears that PAI-1/PAI-1 interactions make a significant

contribution in the multimerization process. Indeed, PAI-1/PAI-1 interactions in a

polymerization process have been observed previously. For example, serpins are known to

exhibit intermolecular interactions via their reactive center loop; polymerization of serpins (α1-

antitrypsin, antithrombin, C1-inhibitor etc.) has been implicated in several diseases like, cirrhosis
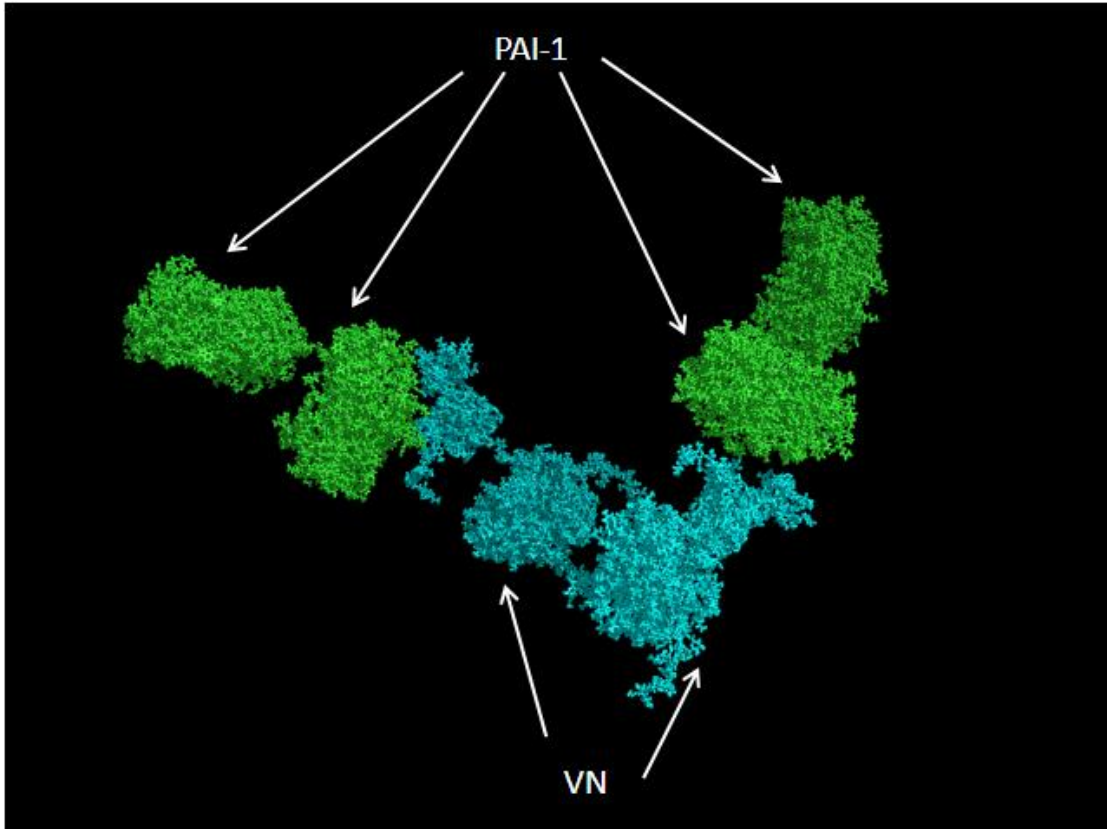
Figure 2. 14: Model of interaction between VN and W175F-PAI-1: result from SANS study

Figure-2.14: SANS (Small Angle Neutron Scattering) study for understanding the interaction between VN and W175F-PAI-1 (Peterson lab, unpublished). Within this model, four PAI-1 molecules (blue) and two VN molecules (green) are indicated by arrows. Within the 1:2 complex, PAI-1 is connected with VN by another PAI-1 molecule. Connection between two 1:2 complexes is mediated by VN.

of liver, thromboembolism, angioedema [243-245]. There are a few potential ways in which the RCL of one molecule can be inserted into the β-sheet of another serpin to initiate the process of multimerization. **Figure-2.15** indicates three possible mechanisms for loop insertion that have been proposed [246]. Insertion can occur and form the 4th β-strand or 7th β-strand of the central β-sheet A, or it may occur in a way that forms an additional strand of β-sheet C.

Replacing glutamate-123 in PAI-1 with arginine has been found to weaken the affinity for the primary site interaction within the SMB domain of VN [197]. **Figure-2.16** shows the result of sedimentation velocity study done between monomeric VN and Q123K-PAI-1 mixed at equimolar concentration (4μM). Only 10.3% of the total loading signal was present between sedimentation coefficient ranges of 6S to 37S, whereas a control experiment done between VN and native PAI-1 under similar condition had 37% of the total loading signal present within the same distribution range. This result shows that disrupting the primary site interaction between VN and PAI-1 significantly blocks the formation of higher order complexes. The lower quantity of higher order complexes observed with Q123K are presumably due to the high concentration of the protein (4μM) used during the experiment.

If the loop insertion is the cause of PAI-1/PAI-1 interaction in the complex, use of latent PAI-1, which already has the RCL inserted as the 4th strand of β-sheetA, should presumably block the formation of the complex. This will be valid only if the PAI-1/PAI-1 interaction is 'loop to strand 4A of central β-sheet'-mediated. **Figure-2.17** shows that sedimentation velocity study done using equimolar concentrations of VN and latent-PAI-1 (4μM). While the amount of higher order complexes formed with latent-PAI-1 was much lower than native PAI-1 (around 37%), it was significantly higher compared to the Q123K mutant. 18.3% of the total loading

71
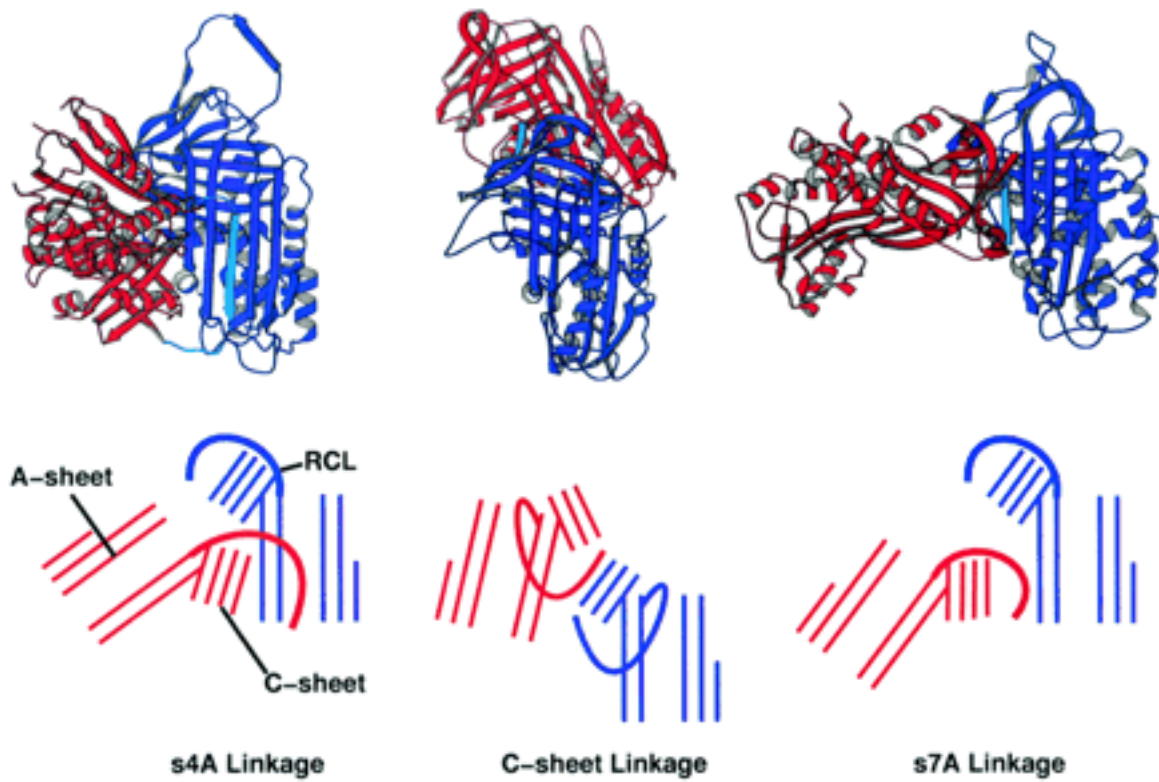
Figure 2. 15: Loop insertion mechanisms for different serpins

Figure-2.15: Multiple ways in which loop insertion may happen between serpin molecules (obtained from Ref: 246). The left panel indicates loop insertion as the 4th strand of β-sheet-A (observed with naturally occurring mutants of α1 antitrypsin). The middle panel indicates loop insertion as a strand of β-sheet-C (observed with the crystal structure of anti-thrombin). The right panel indicates insertion as the 7th stand of β-sheet-A (observed with the crystal structure of PAI-1) [246].
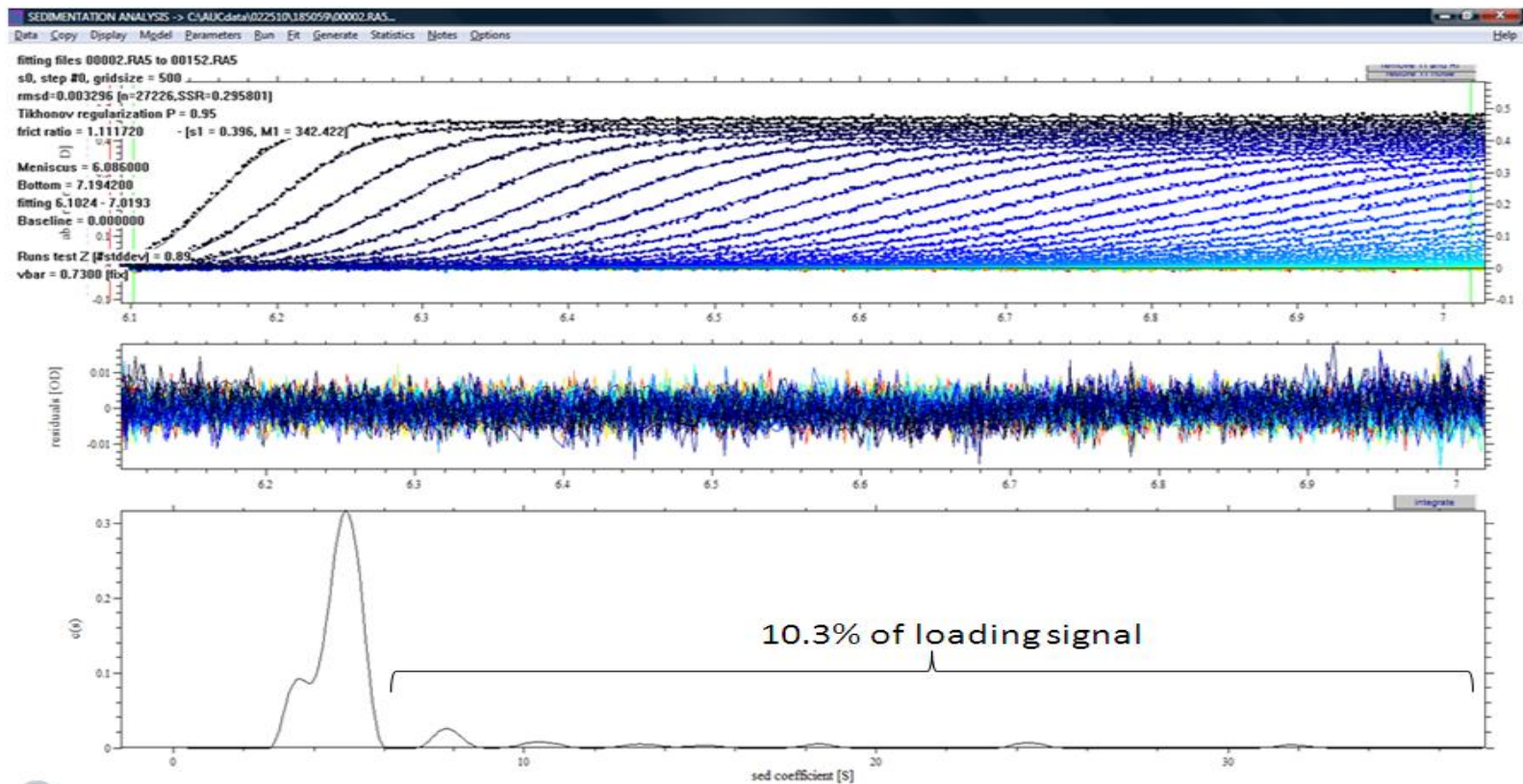
Figure 2. 16: Sedimentation velocity study of oligomeric complex formation between VN and Q123K-PAI-1

Figure-2.16: Proteins (VN and Q123K-PAI-1) were mixed at equimolar concentration (4μM) at 37^0C for 1hr and loaded into the centrifuge cells. Absorbance data were collected at 50000rpm at 25^0C and fitted to c(S) distribution model using SEDFIT. The top-panel indicates the RI noise and TI noise subtracted data fitted to the c(S) distribution model. The numbers indicate the fitted parameters referring to the model. The middle-panel indicates the residual of the fit. The bottom-panel is the distribution plot of different sedimenting species (c(S) vs. S).Integration of the distribution between 6S and 36S indicates that 10.3% of the loading concentration was present as higher order complexes.
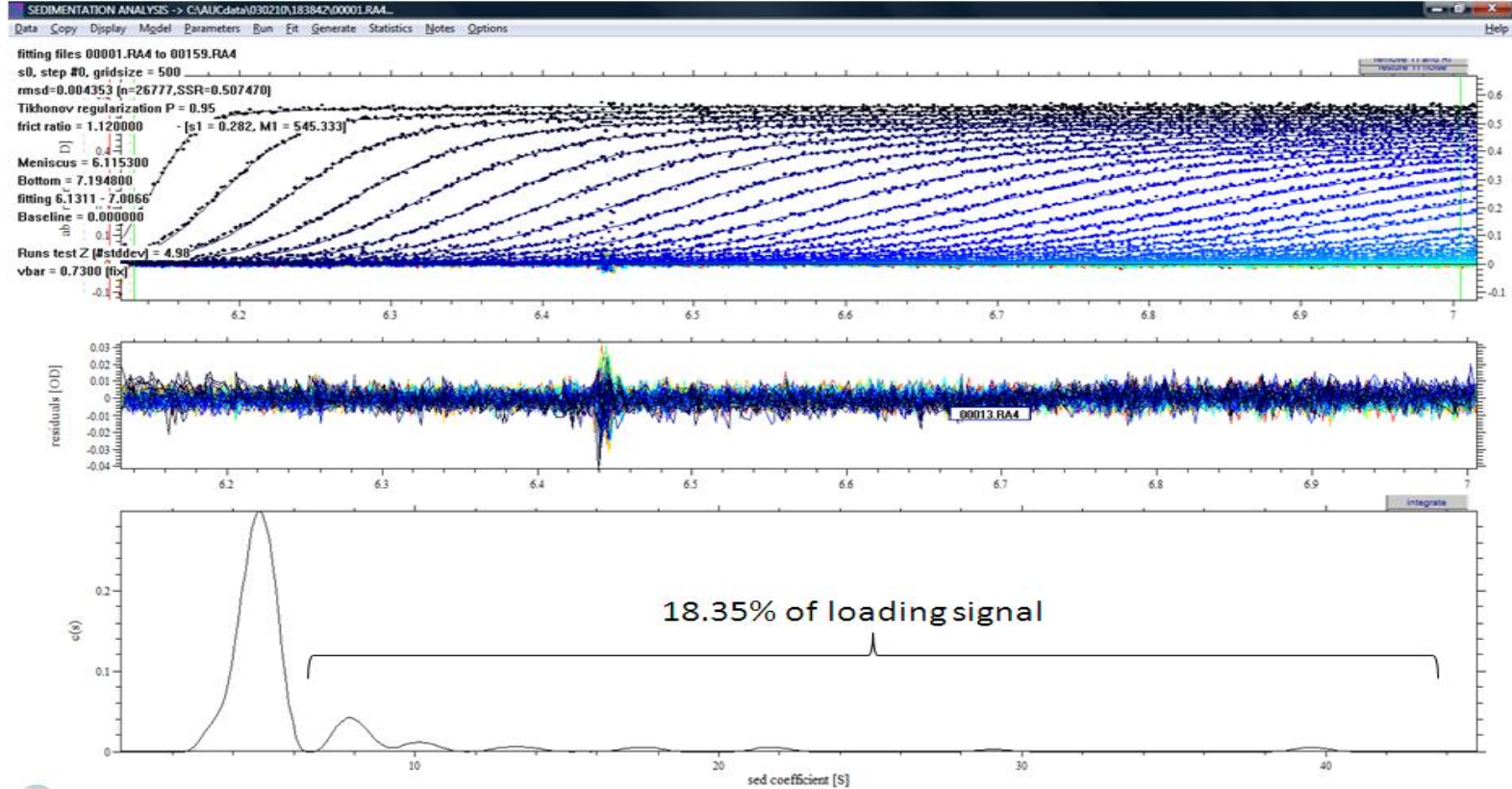
Figure 2. 17: Sedimentation velocity study of oligomeric complex formation between VN and latent-PAI-1

Figure-2.17: Proteins (VN and lat-PAI-1) were mixed at equimolar concentration (4µM) at 37^0C for 1hr and loaded into the centrifuge cells. Absorbance data were collected at 50000rpm at 25^0C and fitted to c(S) distribution model using SEDFIT. The top-panel indicates the RI noise and TI noise subtracted data fitted to the c(S) distribution model. The numbers indicate the fitted parameters referring to the model. The middle-panel indicates the residual of the fit. The bottom-panel is the distribution plot of different sedimenting species (c(S) vs. S). Integration of the distribution between 6S and 44S indicates that 18.3% of the loading concentration was present as higher order complexes.

signal was present between sedimentation coefficient ranges of 6S to 44S. This indicates that it is possible that the interaction between PAI-1 can occur through more than one mechanism.

2.3.II.c. Effect of RCL Peptide Mimics on the Interaction Between VN and PAI-1

In order to further evaluate the concept of RCL insertion as a mechanism for PAI-1/PAI-1 interaction, an alternative approach was utilized. RCL-mimicking peptides have been utilized in a number of cases to interfere with the loop insertion process and study ligand binding interaction with PAI-1 [247-248]. There are two different RCL peptide mimics that are most commonly used. They are: i. octapeptide: N- TVASSSTA –C (mimics P14-P7 residues) and ii. pentapeptide: N- TVASS –C (mimics P14-P10 residues). A crystal structure exists for a cleaved PAI-1 mutant (Ala335Pro) complexed with the pentapeptide [249]. **Figure-2.18 and 3.19** represent the relative positions of the residues that correspond to octapeptide and pentapeptide in the inserted RCL of latent PAI-1, respectively. Each of these RCL peptide mimics was - incubated with native PAI-1 (at ~ 330 fold higher molar concentration) for 1hr at 37^0C and then mixed with an equimolar concentration of monomeric VN (6μM) to test for complex formation. **Figure-2.20** and **Figure-2.21** show the results of sedimentation velocity experiments on mixtures of VN and native PAI-1 in the presence of octapeptide and pentapeptide respectively. With each of these peptides, only about 7% of the loading signal was present as higher order complexes between the sedimentation coefficient values of 6S to 60S. The control experiment performed in the absence of peptides showed that 65% of the loading signal is present as higher order complexes within the same sedimentation coefficient range. Another striking observation was that, with the presence of each peptide, the interaction between VN and PAI-1 was almost completely inhibited. Almost no 1:1 complex between VN and PAI-1 was observed.
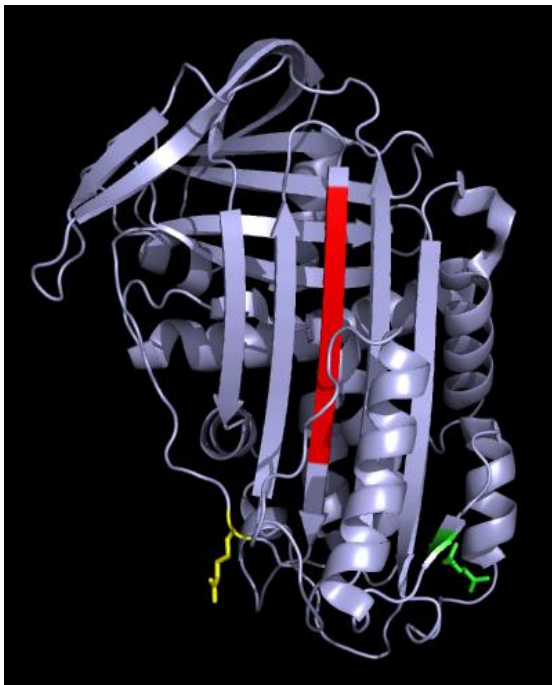
Figure 2. 19: Relative orientation of the octapeptide sequence in latent PAI-1
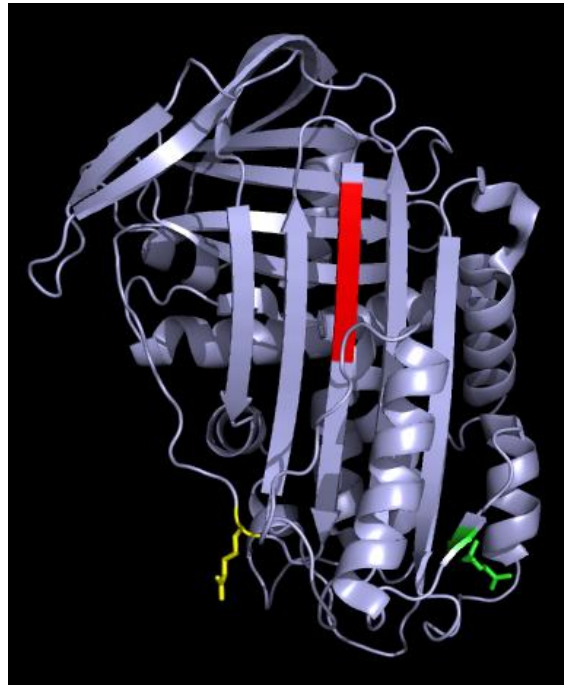
Figure 2. 18: Relative orientation of the pentapeptide sequence in latent PAI-1

Figure-2.18 & 2.19: Crystal structure of latent-PAI-1 with RCL inserted as 4ᵗʰ strand of β-sheet-A [161]. Figure-2.18 shows relative positions of the residues (in red) that correspond to the octapeptide. Figure-2.19 shows the positions of the pentapeptide (in red). In both structures R346 (P1) is shown in yellow and Q123 residue is shown in green.
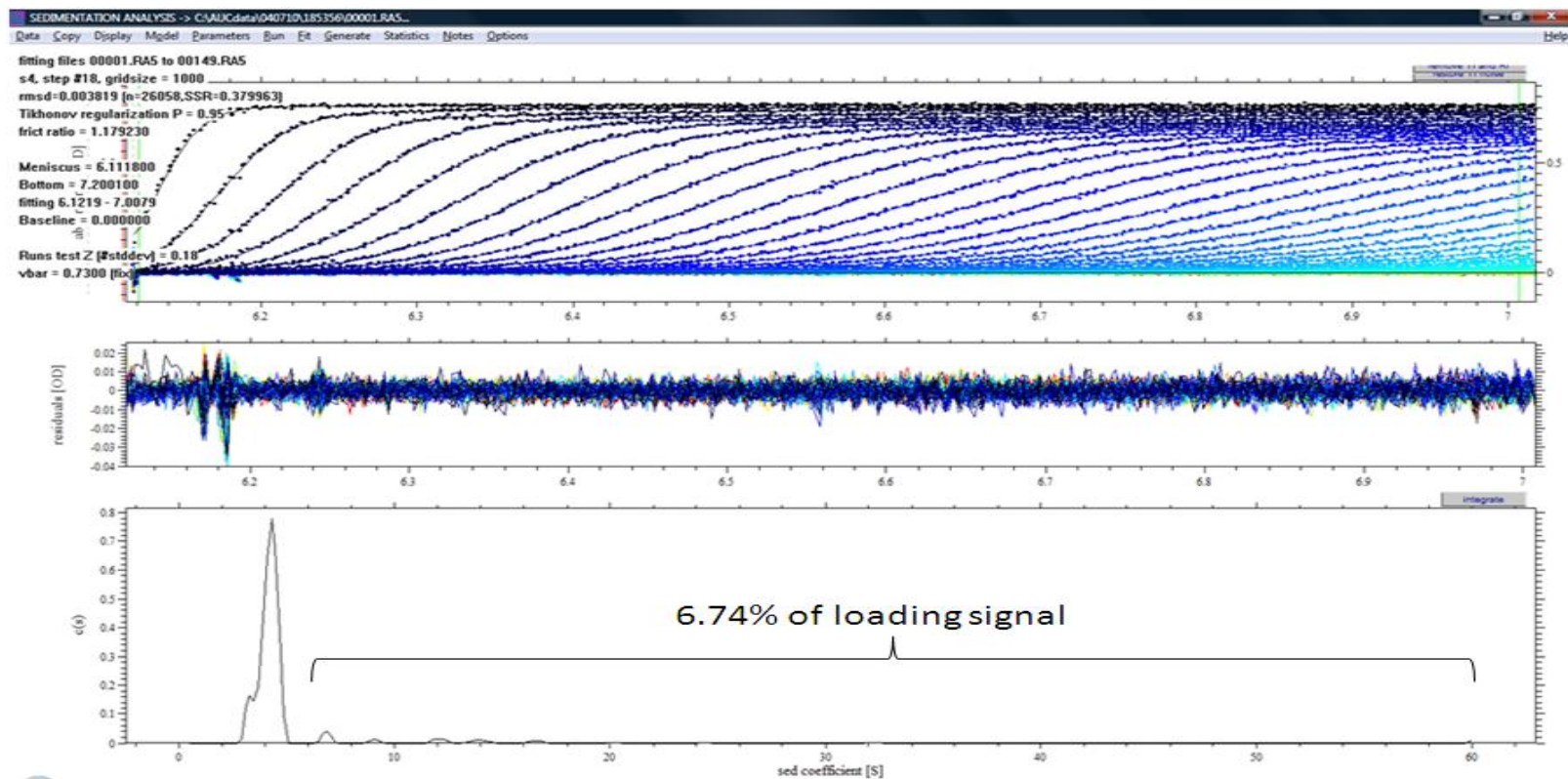
Figure 2. 20: Effect of the octapeptide on the interaction between VN and wtPAI-1: sedimentation velocity study

Figure-2.20: Analysis of the effect of the binary complex between wtPAI-1 (6μM) and octapeptide (2mM) on the oligomerization by AUC. The mixture was incubated at 37^0C for 1hr. This was mixed with 6μM VN and incubated for 1hr at 37^0C prior to loading the centrifuge cells. Absorbance data were collected at 50000rpm at 25^0C and fitted to a c(S) distribution model using SEDFIT. The top-panel indicates the RI noise and TI noise subtracted data fitted to the c(S) distribution model. The numbers indicate the fitted parameters referring to the model. The middle-panel indicates the residual of the fit. The bottom-panel is the distribution plot of different sedimenting species (c(S) vs. S).Integration of the distribution between 6S and 44S indicates that 6.7% of the loading concentration was present as higher order complexes.

77
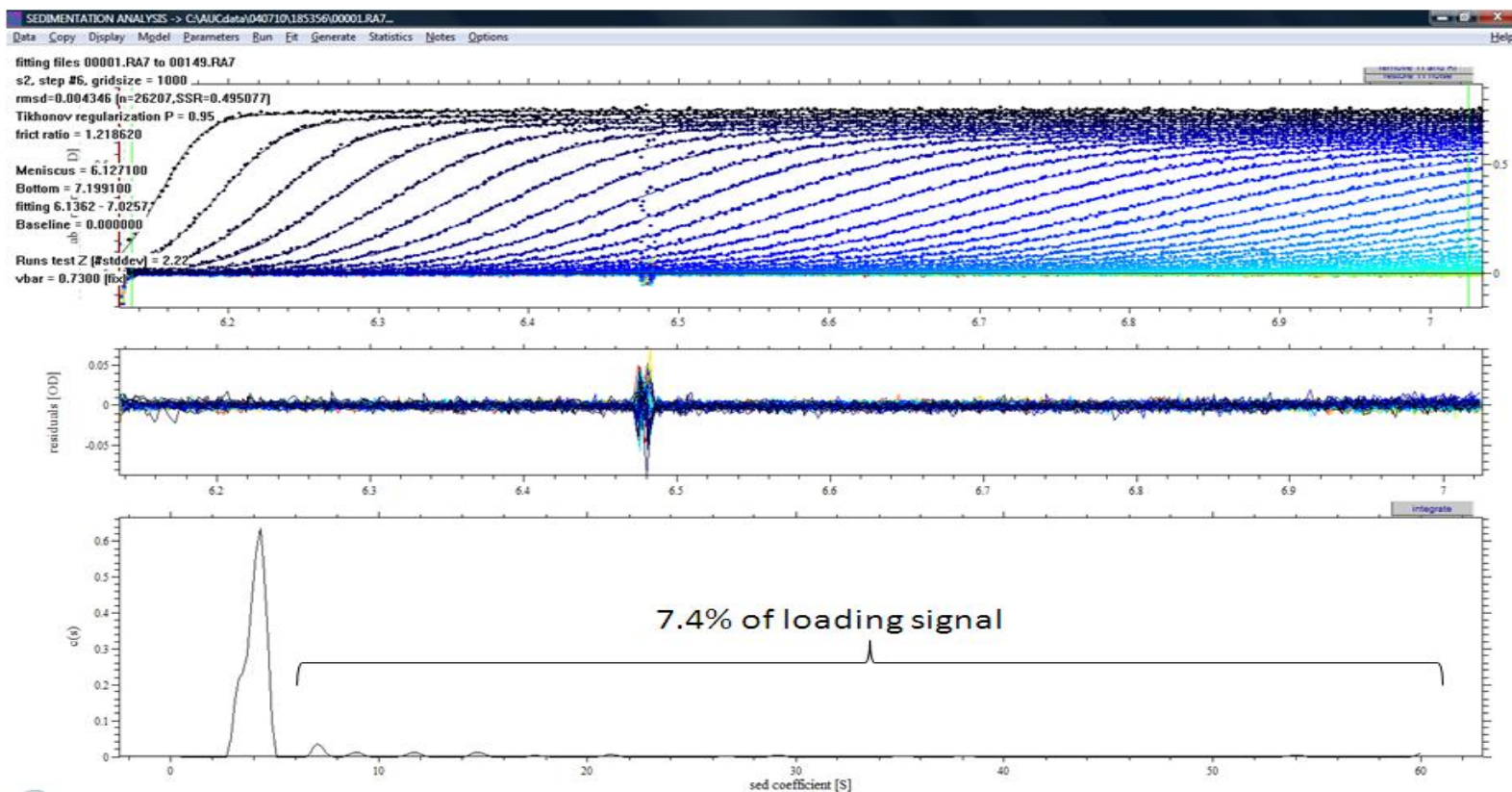
Figure 2. 21: Effect of the pentapeptide on the interaction between VN and wtPAI-1: sedimentation velocity study

Figure-2.21: Analysis of the binary complex between wtPAI-1 (6µM) and octapeptide (2mM) on the oligomerization by AUC. The mixture was incubated at 37^{0}C for 1hr. This was mixed with 6µM VN and incubated for 1hr at 37^{0}C prior to loading the centrifuge cells. Absorbance data were collected at 50000rpm at 25^{0}C and fitted to a c(S) distribution model using SEDFIT. The top-panel indicates the RI noise and TI noise subtracted data fitted to the c(S) distribution model. The numbers indicate the fitted parameters referring to the model. The middle-panel indicates the residual of the fit. The bottom-panel is the distribution plot of different sedimenting species (c(S) vs. S).Integration of the distribution between 6S and 44S indicates that 7.4% of the loading concentration was present as higher order complexes.

78

2.3. III. Characterizing the Binding between PAI-1 and Different Metals

There are multiple factors that influence the stability of PAI-1, including temperature, buffer, salt, pH and different ligands. Recently our lab has found that metal ions are also important regulators of PAI-1 function and stability. This work has been performed in conjunction with Dr. Larry Thompson, a postdoctoral associate of our lab. It was observed that Type-I (Mg^{+2}, Ca^{+2}) and Type-II (Ni^{+2}, Cu^{+2}) metal ions exhibit different effects on the stability of PAI-1. While the effect of type-II metals was strongly destabilizing, type-I metals caused slight stabilization of PAI-1. The effect of these metals was even more interesting in the presence of VN. While the type-I metals did not show much difference in the absence or presence of VN, type-II metals had completely opposite effects. In presence of VN, type-II metals dramatically stabilized PAI-1. **Figure-1.9** (chapter-1) shows the effect of different metals on the stability of PAI-1 in the absence/presence of VN (Thompson et al., submitted). The physiological relevance of this interaction between metals and PAI-1 will be largely dictated by the affinity of their interaction. The goal for these experiments was to establish a reproducible method for characterizing the binding affinity between PAI-1 and different metals.

2.3. III.a. Comparing Ni Binding with wtPAI-1 and PAI-1 Variants Using SPR.

The availability of a NTA (nitrilotriacetic acid)-chip from Biacore offered a way to make use of surface plasmon resonance for this study. NTA is a reagent that is commonly used for immobilized metal affinity chromatography (IMAC). In this chip, NTA is covalently linked with a carboxy-methyl chain and is available for metal binding. Since IMAC was used for purifying recombinant PAI-1, the same principle was utilized here to characterize the metal binding affinity. An assay was standardized as described in the method section. Briefly, metal was loaded

on to the test flow cell, and PAI-1 passed through both test and reference flow cells in order to establish specific metal binding in contrast to background (nonspecific) binding. This assay was then utilized to obtain information on the affinity of the interaction between PAI-1 and Ni. **Figure-2.22** shows the representative sensograms obtained from the injections of varying concentrations of active PAI-1 on immobilized Ni on the NTA chip. Each of these response curves indicates that binding has reached steady state. **Figure-2.23** shows the binding isotherm of active PAI-1 binding to Ni using the steady-state binding response versus PAI-1 concentration. This isotherm was fitted to Langmuir's 1:1 binding equation. The affinity obtained for PAI-1 binding to Ni from these experiments is **6.22 ± 0.05 μM**.

Since type-II metal severely destabilized active PAI-1, it was important for us to determine the affinity of latent-PAI-1 for type-II metals. A titration experiment was carried out for checking latent-PAI-1 binding to Ni. **Figure-2.24** shows the binding isotherm of latent-PAI-1 binding to Ni. The affinity of latent-PAI-1 was found to be **21.8 ± 3.5 μM**. Thus, the latent-PAI-1 has at least three times weaker affinity for Ni binding compared to active-PAI-1. This indicates that the destabilization of active PAI-1 by Ni is not a direct consequence of preferable binding of Ni to the latent form. Binding of Ni most likely causes a conformational change in active PAI-1 that favors the conversion to latent form.

The effect of type-I and type-II metals on PAI-1 stability was essentially the opposite. A plausible explanation of this finding is the presence of different binding sites for type-I and type-II metals. In order to check the presence of multiple binding sites, a competition experiment was designed. Varying concentrations of $MgCl_2$ (type-I metal) was mixed with a fixed concentration
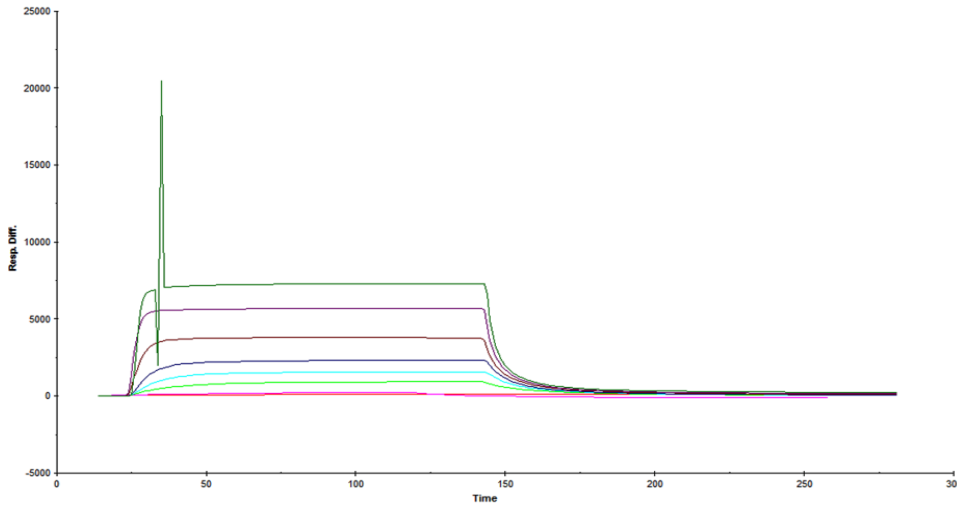
Figure 2. 22: Representative sensogram of titration experiment of PAI-1 binding to Ni-NTA
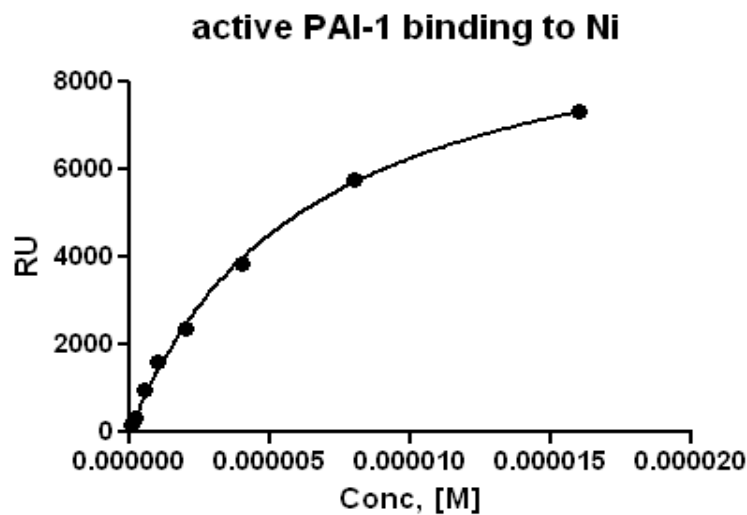
Figure 2. 23: Binding isotherm of wtPAI-1 binding to Ni

Figure-2.22: This figure shows representative sensograms of varying concentrations (serial dilution from1600nM to 100nM) of PAI-1 injected on a Ni-NTA chip (1.5min association and 5min dissociation). Figure-2.23: binding isotherm of wtPAI-1 binding to Ni-NTA. Equilibrium binding responses were plotted against PAI-1 concentration. Data were fitted to Langmuir 1:1binding equation.
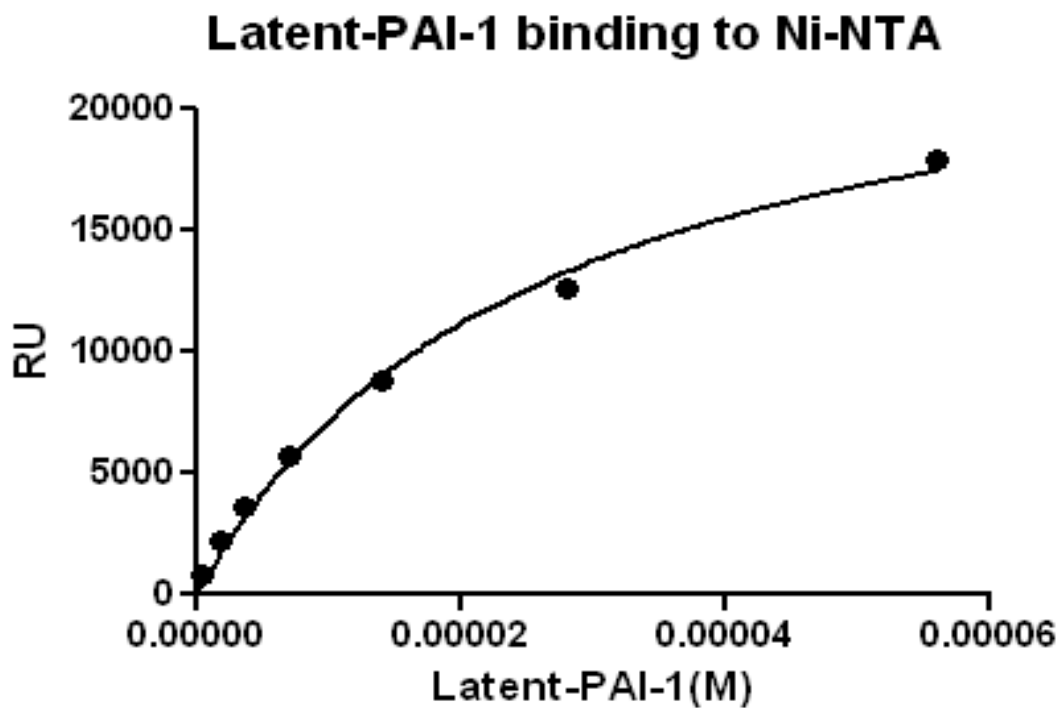
Figure 2. 24: Binding isotherm of latent-PAI-1 binding to Ni: SPR study

Figure-2.24: Varying concentrations of PAI-1 (serial dilution from 56μM to 0.875μM) were run on a Ni-loaded NTA chip. Equilibrium binding responses were plotted against PAI-1 concentrations. Data were fitted to Langmuir 1:1binding equation.

(2μM) of active-PAI-1, and the mixtures were allowed to flow over Ni immobilized on the NTA chip. **Figure-2.25** shows the representative sensograms of PAI-1 binding to Ni in the presence of different concentrations of $MgCl_2$. At high concentrations (millimolar), binding of PAI-1 to Ni (type-II) could be partially blocked by Mg (type-I). This indicates that type-I metal can bind to the type-II metal site, but with much lower affinity.

14-1-B, the constitutively active form of PAI-1, exhibits a half-life of about 145 hrs [164]. Because of this marked stability, this mutant PAI-1 has been used in different studies as an alternative to wild type active PAI-1. Blouse et al. reported that the mutation of the conserved Tryptophan residue (Trp175) by Phenylalanine increased the inherent stability of the structure from a half-life of about 2 hrs to 22 hrs [135]. We aimed to compare the metal binding of these two stable mutants with that of wild type active PAI-1. **Figure-2.26** and **2.27** show the binding isotherm of W175F and 14-1-B binding to Ni, respectively. The affinity of these two mutants for Ni binding were **33.6 ± 2.7 μM** and **38.44 ± 3.2 μM** respectively. This study indicates that wt-PAI-1 possesses an optimal conformation for type-II metal binding.

2.3. III.b. The SPR Based Assay was not Suitable for Measurements with Other Type-II Metals.

We hoped to extend the application of this SPR method for studying other type-II metal binding to PAI-1. Unfortunately, this method could not be applied to other type-II metals like Cu, Co, or Zn. When Cu was used for immobilization, the initial binding to the chip was found to occur normally, but with time it showed gradual leaching off the chip. Cu bound to NTA could not even withstand the mild EDTA wash that was part of the original Ni-binding assay. Omitting

Mg competition for PAI-1 (2uM) binding to Ni

Legend: 0mM MgCl2, 8mM MgCl2, 16mM MgCl2, 33mM MgCl2
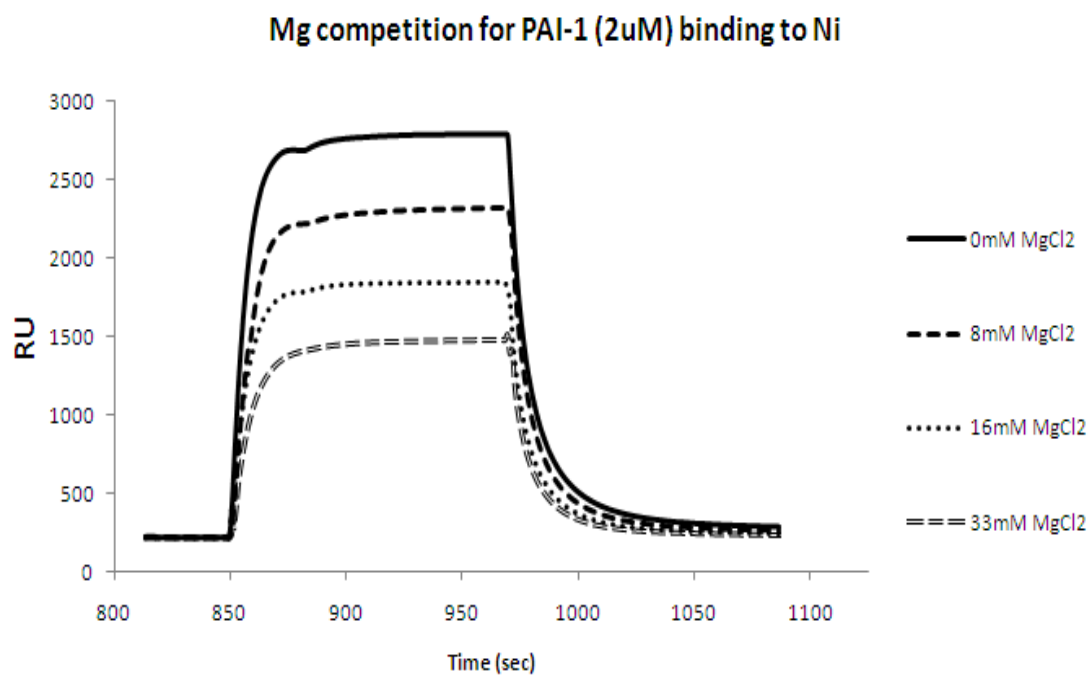
Figure 2. 25: Competition experiment of Mg binding with Ni: SPR study

Figure-2.25: Sensograms showing a competition experiment of Mg binding to PAI-1 with Ni. PAI-1 was mixed with varying concentrations of MgCl2, and the mixtures were run on a Ni-loaded NTA chip. The free concentration of MgCl$_2$, after binding to Tris buffer, is calculated and included in the graph.
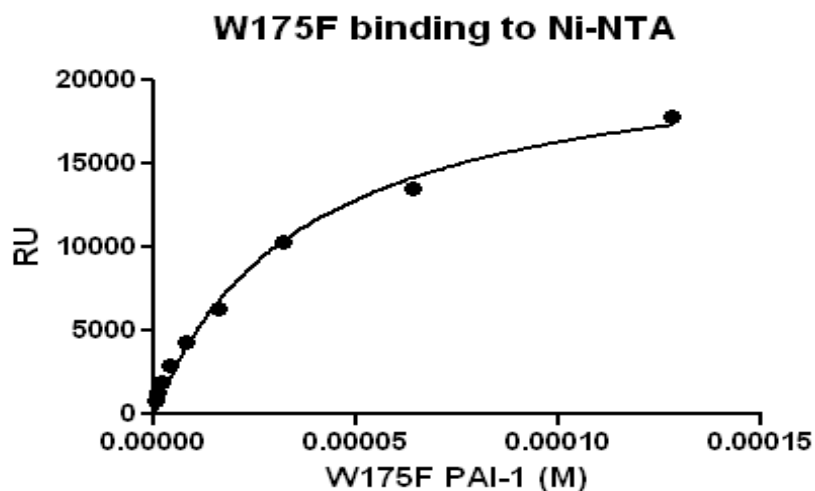
Figure 2. 26: Binding isotherm of W175F-PAI-1 binding to Ni: SPR study
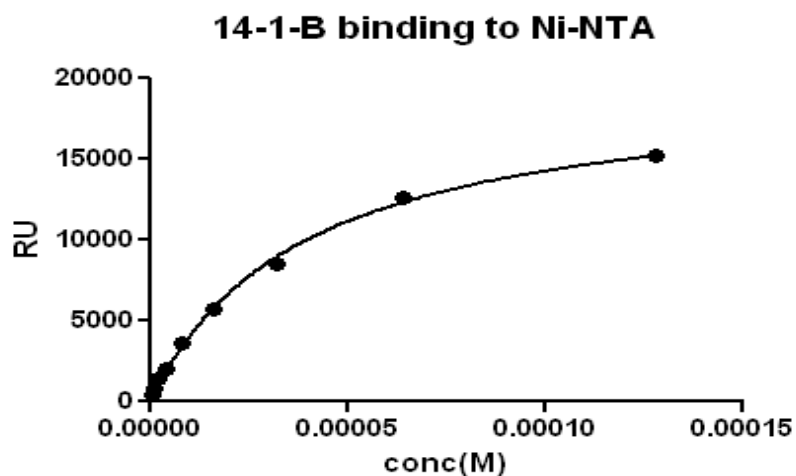
Figure 2. 27: Binding isotherm of 14-1-B binding to Ni: SPR study

Figure-2.26 & 2.27: Binding isotherms of W175F-PAI-1 (Figure-2.26) and 14-1-B (Figure-2.27) binding to Ni-NTA respectively. Varying concentrations of PAI-1 (serial dilution from 128µM to 0.5µM) were run on a Ni-loaded NTA chip. Equilibrium binding responses were plotted against PAI-1 concentrations. Data were fitted to Langmuir 1:1 binding equation.

the EDTA wash stabilized better Cu binding to the chip. However, when PAI-1 was loaded on to the Cu-NTA surface, the initial protein binding followed normal association behavior but it never reached steady state, as shown in **Figure-2.28**. It can be observed that when the PAI-1 injection was made, another interaction phase occurred in parallel that reduced the overall Cu binding. Co and Zn could not be immobilized on the chip even when used at 2mM concentration. On the other hand, when these two metals were separately premixed with PAI-1 and the mixture was loaded directly on to NTA chip, binding could be observed. **Figure-2.29** shows the loading of a mixture of 1μM PAI-1 and 1mM $CoCl_2$ on to NTA chip. It can be observed that binding followed a single phase association pattern and reached steady state. A titration experiment was conducted where different concentrations of $CoCl_2$ were mixed with fixed concentration of PAI-1 and the mixtures were allowed to flow over NTA chip one at a time. Steady state response units were measured and plotted against free Co concentration (**Figure-2.30**). The binding isotherm was fit to a Langmuir's 1:1 binding equation. The dissociation constant obtained from this fitting was 170μM. However, the specificity of the interaction (PAI-1 binding to Co or PAI-1/Co complex binding to NTA) was not clear from this experiment. When the mixture of PAI-1 and Zn was loaded on to NTA chip, the binding interaction was found to exhibit more than one phase of interaction (**Figure-2.31**). It seems that the specific coordination geometry provided by nitrilotriacetic acid is most suitable for studying Ni binding, but less appropriate for the other metals in this situation.

86
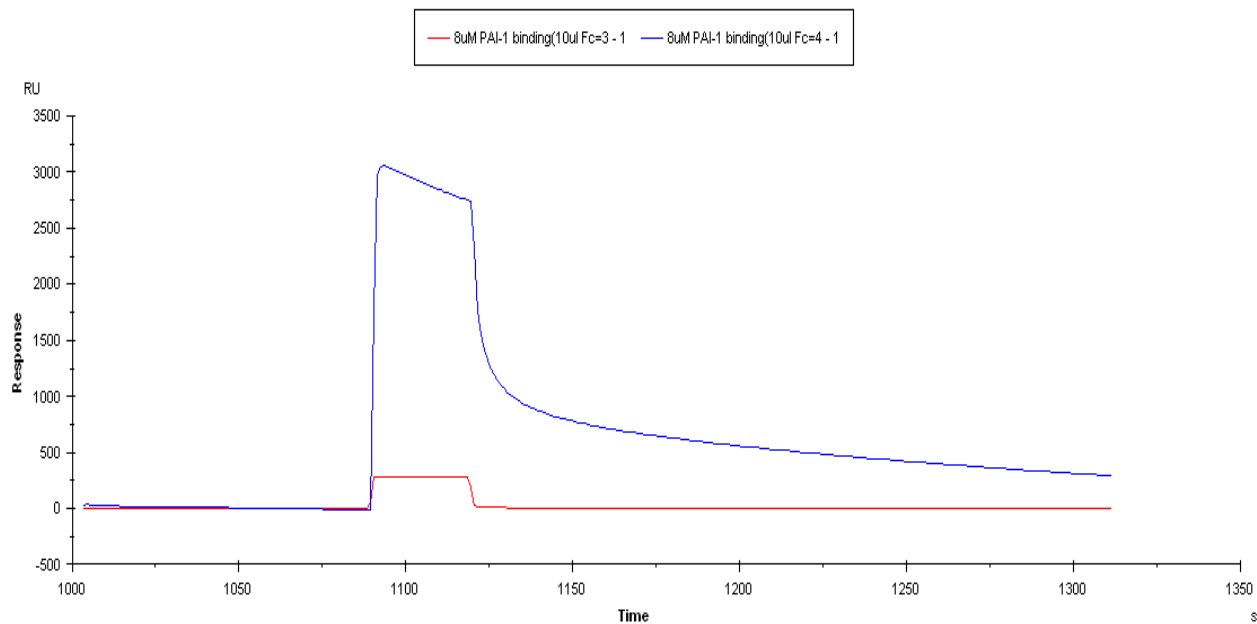
Figure 2. 28: SPR study on wtPAI-1 binding to Cu-NTA

Figure-2.28: 1mM CuCl$_2$ was loaded on to flow cell-4 (test cell) of the NTA chip. No EDTA wash was performed. 1μM PAI-1 was run on both flow cell-3 (reference, shown in red) & flow cell-4 (test, shown in blue). Injection was carried out for 1min, at a 20μl/min flow rate, followed by a dissociation phase. Though PAI-1 binding to flow cell-4 showed rapid association, it never reached steady state.
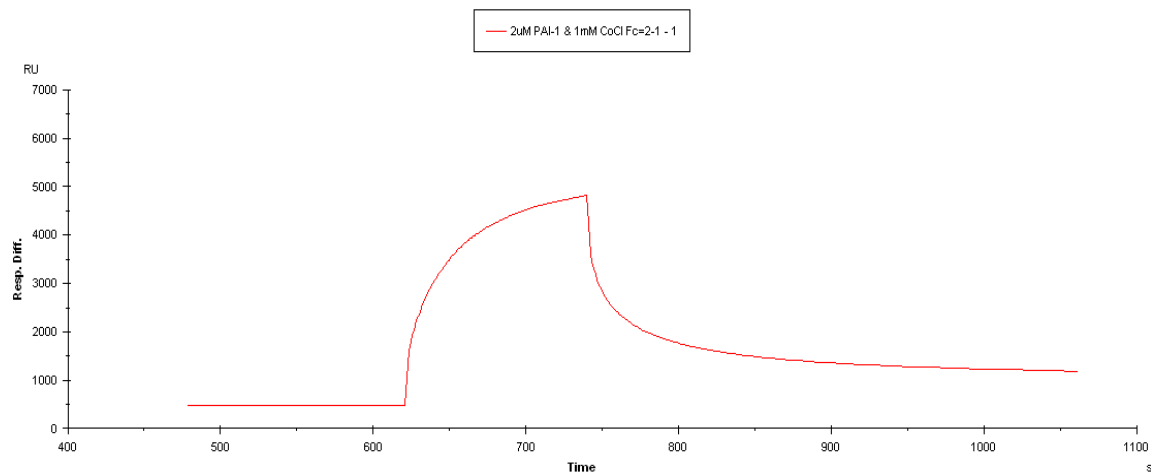
Figure 2. 29: Representative sensogram for Mixture of PAI-1 & CoCl$_2$ to NTA

Binding Isotherm of PAI-1 binding to Co

One site -- Specific binding	
Best-fit values	
Bmax	10897
Kd	0.0001721
Std. Error	
Bmax	1057
Kd	5.846e-005
Goodness of Fit	
Degrees of Freedom	8
R square	0.9134
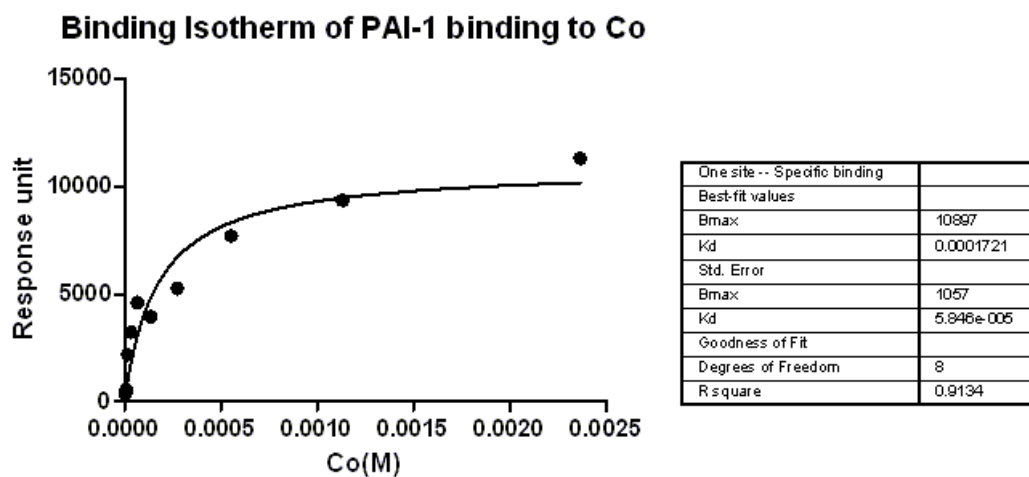
Figure 2. 30: Binding isotherm of mixture of CoCl2 & PAI-1 to NTA

Figure-2.29 & 2.30: 1mM of CoCl$_2$ was mixed with 2μM PAI-1 and the mixture was run on flow cell-2 (test) for 2min at 20μl/min flow rate (Figure-2.29). Binding reached steady state. The bottom panel (Figure-2.30) indicates the result from a titration study where 2μM PAI-1 was mixed with increasing concentrations of CoCl$_2$. The mixtures were run on a NTA chip (test flow cell only) and allowed to reach steady state. Free Co concentration was calculated and used for plotting the binding isotherm.

88
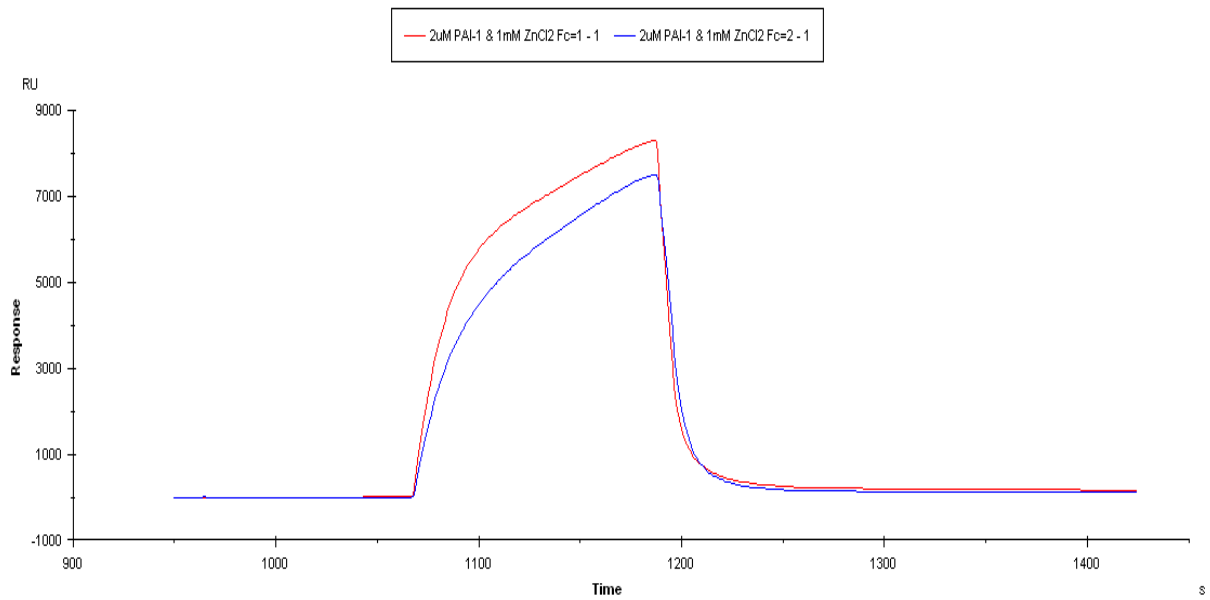
Figure 2. 31: Representative sensogram of mixture of wtPAI-1 & ZnCl$_2$ binding to NTA

Figure-2.31: 1mM ZnCl$_2$ was mixed with 2μM PAI-1 and the mixture was run on both flow cells (FC1- red, FC2- blue) for about 2min at 20μl/min flow rate. Binding to flow cell-1 and flow cell-2 are shown in red and purple, respectively. Binding was found to follow more than one phase of interaction.

2.4. Discussion

2.4. a. Interaction Between VN and PAI-1, Binding Interface and Stoichiometry

Understanding the interaction between VN & PAI-1 has been one of the main objectives of this work. In fact, it has remained as one of the major research areas for our lab for the last few years. We have always recognized the relevance of this interaction based on the vast information in the literature that supports its physiological significance. Thus, we have carefully addressed a number of issues regarding the interaction between these two proteins that have remained controversial. PAI-1 binding to VN has typically been considered to be mediated by the SMB domain of VN. Though there are other groups that suggested the presence of another PAI-1 binding site outside SMB domain [200-202], no confirmatory evidence has been pursued prior to our recent work [204]. The issue of one *versus*. two binding sites on VN appears of great importance, as the simple 1:1 binding between VN and PAI-1 is not enough to explain the reaction mechanism by which these two proteins form higher-order multimers. Our lab has recently provided the most direct evidence in support of the presence of another PAI-1-binding site outside the SMB domain [204]. A deletion mutant of VN lacking the N-terminal SMB domain was found to retain PAI-1 binding activity with a relatively lower affinity ($Kd\sim100nM$) than that of with SMB domain ($Kd\sim1nM$) of VN [204]. Furthermore, using stopped-flow analysis our lab has provided evidence that indicates that the binding interaction between PAI-1 and full length VN involves residues that exist beyond the SMB domain [168]. These studies suggested that the interaction between full length VN and PAI-1 is more complex and involves an extended binding interface.

This stopped-flow analyses in the published work [168] utilized fluorescently labeled PAI-1 in order to probe the structural changes resulting from binding. In this present study we have standardized a method that will allow us to perform strategic incorporation of a nitroxide spin label in the PAI-1 structure. Nitroxide spin labels used in electron paramagnetic resonance (EPR) study are extremely sensitive towards the change in local environment and no other group before us has reported the use of a spin label on PAI-1. We have successfully incorporated the MTSL spin label at the P9 residue of the RCL of PAI-1. Labeling of the P9 residue with the environmentally sensitive fluorescent probe has been utilized before to probe the structural change during latency transition. We have used our MTSL labeled PAI-1 for probing the RCL insertion that happens during the latency transition. The half-life obtained from this study allowed us to validate the idea of probing structural changes of PAI-1 with EPR. We have further utilized the spin-labeled PAI-1 to probe the binding interaction with the isolated SMB domain and full-length VN. We have found that, while the signal of labeled PAI-1 did not change with increasing concentration of the SMB domain, there is a decrease in EPR signal upon the addition of the full-length vitronectin. This preliminary EPR study with SMB and VN falls in line with stopped-flow analyses and suggests once again that the binding interactions that involve these two partners are different from each other. This EPR based method will also allow us to probe the structural change that occurs in PAI-1 with response to metal binding.

In the last few years our lab has also made significant progress in the understanding of the formation of the higher-order PAI-1/vitronectin complexes. By using a variety of techniques (size exclusion chromatography, sedimentation velocity, FRET) we have obtained evidence that leads us to the following conclusions: 1. PAI-1 can induce the multimerization process in dose

91

dependent fashion. 2. Initiation of the multimeric complexes begins with the formation of a

heterotrimer containing two molecules of PAI-1 and one molecule of VN. 3. PAI-1 remains

associated with these multimeric complexes for several hours [203-204, 209-211]. Although

significant advances have been made, we are keen to know more about the mechanism by which

the multimerization occurs. There are many questions that are still in need of answers. What is

the relative contribution of the partner proteins (VN and PAI-1) in initiating the complex

formation? Are the two PAI-1 molecules in the heterotrimer directly connected to VN? How

does the heterotrimer further associate to form even larger multimeric complexes? Our initial

thought was that the heterotrimer formed between VN and PAI-1 (1:2 stoichiometry) contains

two PAI-1 directly occupying two different binding sites on VN. Though the model generated

from the SANS study (**Figure-2.14**) confirms the formation of a heterotrimer between two PAI-1

molecules and one VN molecule, the heterotrimer appears to involve only a single interaction

between VN and PAI-1. The second PAI-1 molecule, on the other hand connects to the first PAI-

1 that is in direct contact with VN. We must be cautious since this SANS study was done with

the W175F-PAI-1 mutant, which is a stable variant of wt-PAI-1[135]. Though sedimentation

velocity studies performed with this mutant and VN in PBS buffer showed a similar pattern of

multimerization as with wtPAI-1 (**Figure-2.13**), for the buffer conditions in which the SANS

experiment (50mM sodium-phosphate, 300mM NaCl, pH-7.4) was done, this mutant was found

to form less amount of multimeric complexes compared to wtPAI-1 (data not shown). Since the

SANS study is highly sensitive to the presence of high molecular weight species and our goal

was to capture the initial part of the multimerization reaction (1:2 and 2:4 complex), formation of

fewer multimeric complexes with W175F-PAI-1 was chosen as a favorable condition for the

SANS experiment. Although our assumption was that the wtPAI-1 and the mutant W175F form higher-order complexes with VN in similar fashion, we need to be careful about the fact that some distinct structural differences exist between these two proteins.

We have addressed the importance of the initial VN/PAI-1 contact for the multimerization reaction (as indicated by the model) by performing sedimentation velocity analysis with the Q123K mutant of PAI-1. Q123K-PAI-1 exhibits low affinity for VN binding and showed a dramatic decrease in the formation of multimeric complexes by comparison with wtPAI-1. We have also devoted significant effort to address the PAI-1/PAI-1 interaction that may occur within the heterotrimer. Serpin-serpin interaction is not uncommon and has been found to happen with serpins like α1-antitrypsin, antithrombin etc [243-245]. Most of these interactions have been found to be mediated by the insertion of RCL of one serpin molecule to the β-sheet region of the other serpin molecule. Examples of loop-sheet interaction have been included in **Figure-2.15** [246]. Under normal condition PAI-1 does not form polymers by loop-sheet interaction like other serpins, but Zhou et al. showed that at low pH both native and latent PAI-1formed dimer via loop-sheet insertion mechanism [246]. Polymerization in native PAI-1 occurs by the insertion of the loop as the 4th β-strand A of the other molecule, whereas for latent PAI-1 the insertion happens to form β-stand1C [246]. It is possible that the binding to VN promotes conformational changes within PAI-1 that are conducive to PAI-1/PAI-1 interaction. Important questions are yet to be answered. Is this interaction at all loop-sheet insertion mediated? Are there other processes involved or it is the combination of more than one process? If the interaction is loop-sheet insertion mediated, is there more than one possible way by which loop-sheet insertion occurs within the higher-order complex of VN and PAI-1 (as indicated in

Figure-2.15)? In order to check if the PAI-1/PAI-1 interaction within the heterotrimer is exclusively mediated by the loop-sheet4A linkage, sedimentation velocity experiment was performed with VN and latent-PAI-1. Latent-PAI-1 does not have an exposed RCL, as it is involved in the formation of 4th β-strand of the central β-sheetA. The sedimentation velocity experiment showed formation of a significant amount of multimeric complexes (**Figure-2.17**) with latent-PAI-1. Zhou et al. proposed that dimerization of latent PAI-1 at low pH happened through the loop-sheet insertion mechanism. They also proposed that the inserted RCL of one latent PAI-1 molecule formed strand-1C of the other latent-PAI-1 molecule [246]. If this is true, then it seems that there is more than one way in which loop-sheet insertion occurs within multimeric complexes of VN and PAI-1. The presence of the inserted RCL in latent-PAI-1 disrupts loop-sheet4A linkage that may normally happen with active PAI-1. However, the loop-sheet1C linkage remains unaffected, although the RCL is fully inserted. It is also possible that latent-PAI-1 forms multimeric complexes through a mechanism totally independent of loop-sheet insertion. In this case the decrease in the amount of multimeric complexes that we observe with latent-PAI-1 compared to active PAI-1 could be due to its relatively lower affinity for VN.

The experiment with latent-PAI-1 indicated that the PAI-1/PAI-1 interaction within the multimeric complexes was not exclusively loop-sheet4A mediated, but the experiments with the RCL peptide mimics virtually completely disrupted the formation of the multimeric complexes between VN and PAI-1. These results can be explained relatively simply. Since the RCL is known to take part in loop-sheet insertion through more than one possible mechanism, these RCL mimicking peptides may be binding to all the possible locations where insertion may happen. As a result, no PAI-1/PAI-1 interaction is possible. Also interesting is the observation

94

that the interaction between VN and PAI-1 was almost completely disrupted in the presence of the peptides. Almost no 1:1 complex was found when VN and wtPAI-1 were mixed at equimolar concentrations (6μM) in the presence of 2mM peptide. A simple binding of the peptides within the groove between strand-3A and 5A may not be enough to explain this finding. While the exact mechanism by which these peptides disrupt the VN/PAI-1 interaction requires further attention, the finding itself has promise. Considering how important the interaction between VN and PAI-1 is and how many different pathophysiological conditions for which this interaction is involved, use of these peptides may represent a new therapeutic prospect.

2.4. b. Immobilization of Metal and Coordination Chemistry

The function of a protein can be regulated in many ways, including post-translational modification, the action of an activator or inhibitor etc. For PAI-1, functional regulation has attained an extra level of sophistication due to its inherently low half-life (1-2hrs at 37^0C) [158-159]. Such a low half-life of PAI-1 activity results because PAI-1 naturally favors the latent conformation [133, 164]. This also provides a means for this delicate balance to be harnessed as a means for regulating the functional activity of PAI-1.

Ligand binding to PAI-1 and the subsequent effect on the conformational flexibility is a subject of keen interest among the serpin biologists. The stabilization of the half-life of PAI-1, although modest under most conditions, has been considered as the major role for its interaction with VN [82, 158, 250]. Though PAI-1 was known to bind to metals, as immobilized metal ion chromatography (IMAC) was used for the purification of recombinant PAI-1 [251], no one has investigated the implications of metal binding on regulating conformational flexibility of PAI-1. Our group now has shown that metals may significantly impact this structural stability of PAI-1

(Thompson et al., submitted). We have investigated the effects of different metals (both type-I and type-II) and found that, while type-I metals (Ca, Mg) do not have much impact on the stability of PAI-1, type-II metals (Ni, Cu, Co) cause substantial reduction in its half-life. In the presence of VN, the effect of type-II metals is the exact opposite (a significant increase in half-life). Thus, metals appear to have a significant impact on the regulation of PAI-1 activity in our body, as transition metals like Cu are naturally present in different tissues, like blood, liver, brain etc [252-255].

The physiological relevance of this metal effect will be dictated by the affinity of such interaction. In this present study, a surface plasmon resonance based assay has been developed for the determination of the affinity of the interaction between PAI-1 and metals. We have utilized an NTA (nitrilotriacetic acid) chip for the immobilization of Ni and successfully obtained affinity information for the binding of wtPAI-1 and its variants with Ni. Currently we are trying to locate the metal binding site on PAI-1 using multiple mutants of PAI-1. This SPR based method will help us to perform rapid screening of PAI-1 mutants for metal binding.

We also hoped to extend this Ni binding study to other type-II metals such as, Cu, Co, Zn. Unfortunately none of these metals could be successfully immobilized on the NTA chip. For example, the initial loading of Cu to the NTA chip could be carried out nicely but the binding was not as stable as for Ni. Running of Tris buffer through immobilized Cu caused slow but continuous leaching of Cu from the chip. During the assay of PAI-1 binding to Ni-NTA, a short pulse of low concentration of EDTA was used following metal immobilization in order to remove unbound/loosely bound Ni in the microfluidic channel. Use of this low concentration of EDTA during the assay with Cu caused even stronger leaching of the metal. When PAI-1 was

run on to Cu loaded chip, the initial phase of that binding showed clear association event that reached a maxima but a steady state was never established, as the protein showed continuous release from the chip surface (as shown in **Figure-2.28**). With Co and Zn successful immobilization could not be achieved even at higher metal concentration (about 2mM). On the other hand, when Co or Zn was premixed with PAI-1 and ran on NTA chip binding of protein could be observed. For Co, binding showed a clear association phase that reached steady state (**Figure-2.29**). We attempted to plot the steady state binding response from Co/PAI-1 mixture binding to NTA with a series of free Co concentration (**Figure-2.30**). This resulted in a saturable binding isotherm that could be fit reasonably well to single-site specific binding equation. We could not draw any conclusion on the affinity information of Co binding to PAI-1 because it was not clear whether the calculated Kd was reporting the binding of Co to PAI-1 or the binding of PAI/Co mixture to NTA. Moreover the goodness of the fit was only moderate. When Zn was mixed with PAI-1 and ran on to NTA chip, protein binding could be observed but the binding was even more complicated to explain as it was not found to follow a single phase interaction (**Figure-2.31**).

Investigating these anomalies with metals in the SPR method was beyond the scope of current study. It is clear that the coordination chemistry involved with each of these metals for binding to NTA and specific amino acid residues that coordinate the metals in PAI-1 had a significant role to play. NTA is commonly used in Ni-based IMAC for the purification of His-tagged proteins. NTA can maintain a strong and stable binding with Ni. NTA is tetradentate and provides four coordination sites for Ni binding. Thus, Ni bound to NTA can coordinate with two additional His molecules of a His-tagged protein (see **Figure-2.32**) [256] to fulfill its six

97

coordination sites. Co also has six coordination sites, but the stability constant for the binding of Co to NTA has been found be much lower [257]. For Co-based IMAC, the TALON resin (from BD biosciences) has been found to be more suitable. The TALON resin provides an optimal geometry that allows for four coordination sites with Co and that result in much tighter binding and much less leaching of the metal. This explains in part why Co immobilization was not successful on the NTA chip. A similar explanation is reasonable for Zn immobilization on NTA as well, but how the metal bound to PAI-1 complements the coordination with NTA chip is unknown. It is possible that the local geometry within PAI-1 favors formation of four coordinate bonds with Co or Zn. Once this stable coordinating conformation was achieved, the bound metal could then bind to two carboxylate groups of NTA. Though the use of Cu in IMAC is not common, there are examples where people used a Cu(II)-IMAC-based ZipTip for the extraction of phosphorylated peptides [258]. However, in this IMAC, instead of NTA, IDA (iminodiacetic acid) was used as the chelating agent, which provides three coordination sites. Burns et al. reported a crystal structure of the ternary complex between Cu^{+2}, NTA and Bisimmidazole ketone (a poly-His analog) [256]. Thus, there are examples of coordination complexes formed between Cu and NTA, but no example is known in which Cu has been used for immobilization on an NTA chip. Understanding the exact chemistry for Cu interaction with the NTA surface that leads to an unstable surface with significant leaching requires further study. It is clear that the SPR method developed will be limited to nickel binding and can be used as a preliminary screen for metal binding to guide further studies on specific stability effects on PAI-1 with other metals.
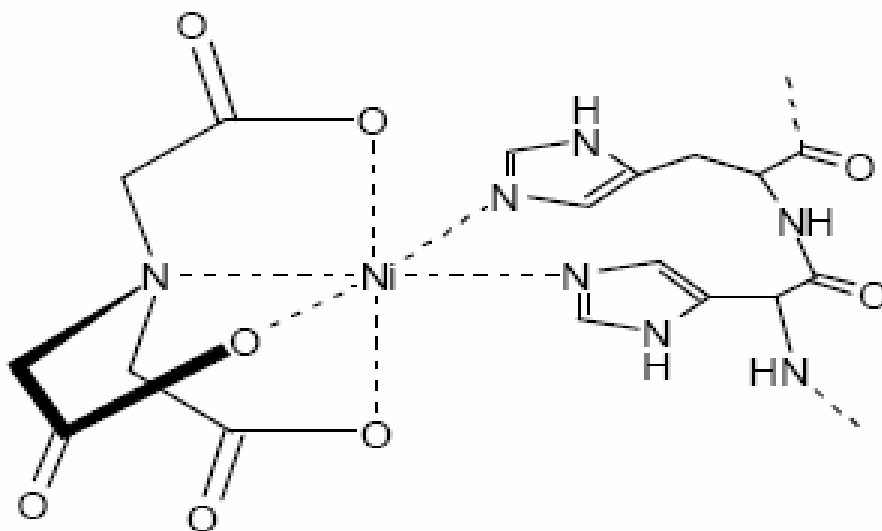
Figure 2. 32: Hexa-coordination geometry of Ni binding NTA and Histidine

Figure-2.32: Coordination of Ni with NTA and two His molecules. NTA being tetradentate provides four coordination sites

CHAPTER-3

How does the interaction between Vitronectin and Plasminogen Activator Inibitor-1 modulate their matrix associated functions?

3. 1. Introduction

Vitronectin is a glycoprotein (459 aa) found in both the circulation and the extracellular matrix (ECM). In blood it circulates mainly as a monomer (0.2-0.4mg/ml, ~0.3-0.6uM), but in the extracellular matrix it exists as a multimer [13-14, 259]. While the exact mechanism for its conformational alteration and compartmentalization is unknown, it is well known that vitronectin has specific and distinct functions in blood and extracellular matrix. The multifunctional nature of this protein results from its ability to recognize various ligands including the thrombin-antithrombin complex (T-AT) [44-45], heparin [46-48], PAI-1 [49-51], complement proteins [52] as well as several cell surface receptors, including integrins and the urokinase plasminogen activator receptor (uPAR) [53-59]. Vitronectin plays important regulatory roles in several different physiological and pathological processes, e.g. - fibrinolysis, thrombosis, coagulation, wound healing, cellular adhesion/migration [61-62, 66]. Regulation of cellular adhesion/migration comes from its ability to act as a matrix protein that can bind to different cell surface receptors like uPAR and certain subclasses of integrins ($\alpha v\beta 3$ and $\alpha v\beta 5$) [92].

PAI-1 is a member of the serpin (Serine protease inhibitor) family of proteins. Like VN, PAI-1 is also found in both circulation and the extracellular matrix. The two main target serine proteases that are inactivated by PAI-1 are urokinase plasminogen activator (uPA) and tissue plasminogen activator (tPA) [80]. PAI-1 regulates the formation of plasmin and thus plays

animportant role in the control of coagulation, fibrinolysis and thrombolysis [180, 260]. Such **protease-dependent** effects of PAI-1 have remained in the limelight for a long time. Currently a significant emphasis is also being given to its **protease-independent** effects. One of the important protease-independent functions of PAI-1 is the regulation of cell surface receptor interaction with ECM-associated VN. PAI-I is known to physically interfere with the interaction of uPAR and integrin receptors with VN. It has been found that exogenously added PAI-1 blocked uPAR mediated binding of U937, endothelial and uPAR-transfected 293 cells to multimeric 'denatured' VN [53, 226]. On the other hand uPAR-mediated migration of U937 and melanoma cells through multimeric 'denatured' VN was blocked by PAI-1 [226, 228]. PAI-1 has been also found to cause blocking of binding and migration of smooth muscle cells (SMC) through multimeric 'denatured' VN in a αvβ3 dependent manner [229]. There is evidence in favor of PAI-1 being pro-angiogenic and pro-tumorigenic [191, 231]. On the other hand there is also some evidence that indicates that PAI-1 may inhibit angiogenesis [232] and such inhibition was found to be dependent on its ability to interact with VN. McMahon et al. reported a study where they showed that PAI-1-mediated effect on tumor formation and angiogenesis is dose-dependent [233]. While at low concentrations PAI-1 acted as pro-angiogenic, at high concentrations it was anti-angiogenic [233]. A similar dose-dependent effect of PAI-1 on angiogenesis was also observed in a study by Devy et al [261]. In this study they showed that the increase in angiogenesis observed at physiological concentrations of PAI-1 was not dependent on its ability to interact with VN [261]. Therefore a significant amount of controversy exists about how PAI-1 regulates VN-mediated cell-matrix interactions.

Though it appears that multimerization of VN happens in a biological setting, most of the *in vitro* studies have been performed with 'denatured' VN (formed by heat or chaotropic agents) as an alternative to the matrix-associated multimeric form of vitronectin. 'Denatured' multimeric VN was found to possess the conformational sensitivity usually observed with matrix-associated, multimeric VN [44, 77]. However, multimeric VN formed in a biologically relevant process may have significant structural/functional differences compared to 'denatured' VN. There are a number of biomolecules that may initiate the process of transition to the multimeric conformation of VN, e.g. – the thrombin-antithrombin-III (TAT) complex, the terminal complement complex (C5b-C7) and PAI-1 [44, 205-206]. In our study we have relied on purifying monomeric VN from blood and then investigating its conversion to a matrix-associated form in the presence of PAI-1 as a co-factor. We have confirmed that PAI-1 induces multimerization of VN in a concentration-dependent fashion, and we are also confident that PAI-1 remains associated with this multimeric complex for several hours [203, 209-211]. With these findings as a basis, we hypothesize: 1. that PAI-1 acts a biological partner for the transformation of VN into the matrix-associated form, and 2. the multimeric complexes formed by the interaction between these two proteins significantly influence their matrix associated functions. Furthermore, we hypothesize that: 3. the multimeric complexes formed by this more biologically feasible process modulate cellular binding/migration, and 4. such modulation is sensitive to the pericellular microenviroment constituted of other matrix components, cell types and the set of receptors expressed on the cell surface.

3. 2. Materials and methods

3.2. a. Proteins and antibodies

Recombinant wtPAI-1 and its mutant Q123K were expressed in the *E. coli* Rosetta2(DE3 media)pLysS strain, grown in TB and induced at 15^0C. Purification was carried out through a three-step column chromatography that included cation-exchange (SP-Sepharose column), immobilized metal ion affinity (Ni-IDA) and size-exclusion chromatography (Sephacryl S-100) (Thompson et al., unpublished). The entire purification was carried out at 4^0C. Correctly folded recombinant somatomedin-B (SMB) domain was expressed and purified as described in the work by Thompson et al. (unpublished). Heparan sulfate proteoglycan (HSPG) was purchased from SIGMA. Collagen-I & IV were purchased from BD Biosciences. Purified recombinant integrins were purchased from Millipore Corp. Purified recombinant urokinase-plasminogen activator inhibitor (uPAR) was purchased from R & D systems. Monoclonal antibodies against VN (1E9, made in mouse) were obtained from Molecular Innovation. All the antibodies (monoclonal and polyclonal) against integrins were purchased from Millipore corp. Monoclonal antibodies against uPAR were purchased from R & D systems. Peroxidase conjugated anti mouse/rabbit IgG was purchased from Vector Labs and Alexa-488 conjugated goat anti-mouse IgG was purchased from Invitrogen.

3.2. b. Purification of monomeric vitronectin

Monomeric vitronectin was purified from human plasma using a procedure that is a modified version of the protocol designed by Dahlback & Podack [32]. This method was standardized in collaboration with Dr. Lawrence Thompson, a former postdoctoral associate of our lab. 3litre plasma was subject to $BaCl_2$ precipitation step and then $(NH_4)_2SO_4$ was added to

plasma at 50% saturation. After an overnight incubation, the precipitate was harvested by centrifugation, resuspended in 1L of phosphate buffer containing DTNB (20 mM NaH_2PO_4, 0.1 mM EDTA, and 1 mM dinitrothiobenzoate (DTNB) pH 7.0) and centrifuged again. The supernatant was dialyzed twice against 22 L of the same buffer without DTNB at 4^0C. Protein was then loaded onto a DEAE Sephacel column (5 x 21.5 cm), washed with the same phosphate buffer, and the eluted with a linear 0-0.5M NaCl gradient with a total volume of 4.4 L. Throughout the protein purification procedure, fractions to be pooled that contained vitronectin were determined using a quantitative immunoaffinity column coupled with the 1E934 monoclonal antibody (see below). In two batches, pooled fractions from the DEAE column were chromatographed on a blue Sepharose column (5 x 17.5 cm) using a linear 0.15-3.0 M NaCl gradient with a total volume of 4.4 L. Fractions containing vitronectin from each blue-Sepharose step were pooled separately and dialyzed against Tris buffer (20 mM Tris, pH 7.4, containing 20 mM NaCl and 0.1 mM EDTA) for chromatography on heparin-Sepharose. Dialyzed protein from each batch of blue-Sepharose chromatography was loaded on to heparin-Sepharose column (2.5 x 15 cm). After loading, protein was eluted from the heparin-Sepharose column using a linear gradient from 0.02 to 1.0 M NaCl with a total volume of 0.8 L. The protein pool from the heparin column was concentrated by ultrafiltration to ~8 mL, and then chromatographed in two aliquots on a high-resolution Sephacryl S-200 gel filtration column (2.5 x 115 cm) equilibrated in PBS, pH 7.4. 3ml fraction was collected from the Sephacryl S-200 gel filtration column at flow rate of 0.5ml/min. Vitronectin containing fractions were pooled and stored at 4 ^{0}C under saturating concentrations of $(NH_4)_2SO_4$ (70%) prior to use. Vitronectin concentration was

determined at 280 nm using $\varepsilon_{280} = 1.0$ mL·mg^{-1}· cm^{-1} [262] and a molecular weight = 62,000 g/mol [27].

In order to optimize the yield of vitronectin and to follow the purification steps using a quantitative method, the total amount of protein recovered in each step was monitored using the BCA assay, while the total amount of vitronectin was determined by immunoaffinity chromatography using a mouse antihuman vitronectin monoclonal antibody (1E934) column. Briefly, 2 mg of antibody 1E934 was covalently linked to 1 mL of NHS-activated Sepharose following the standard protocol and used in HPLC. Several standard amounts of purified monomeric human vitronectin were loaded onto the column, washed for 5 min with PBS pH 7.4, and then eluted with 100 mM NaH$_2$PO$_4$ pH 3.0. Elution of vitronectin was monitored at 220 nm. A standard curve was generated by injecting known amount of vitronectin to the antibody column. Area of the eluted peak was utilized for plotting the standard curve. This method gave a linear range from 0 to 19 μg of vitronectin. Quantification using the 1E934 antibody indicated that 3 L of human plasma typically contained 0.2-0.3 mg/mL vitronectin, which was in good agreement with previous measurements [3, 6, 31]. A typical final yield of vitronectin from 3 L of human plasma using this modified purification method was ~9%-10% (approximately 60-70 mg).

3.2. c. Cell culture

The human fibrosarcoma cell line (HT1080) was purchased from American Tissue Culture Collection (ATCC) and maintained in Eagle's Minimum Essential Medium (EMEM) (purchased from ATCC) supplemented with 10% Fetal bovine serum (FBS, purchased from ATCC) and 1% penicillin-streptomycin solution (ATCC). The EA.hy 926 cell line was a kind

gift from Dr. John Biggerstaff's lab at University of Tennessee, Knoxville. This is an

immortalized hybridoma cell line created by the fusion between A459 cell (human lung

carcinoma) and human umbilical vascular endothelial cell (HUVEC) [263]. This cell line was

found to express factor-VIII related antigen (VIII-R:Ag), which is considered to be one of the

highly differentiated properties of the vascular endothelium. The fibrinolytic properties of this

cell line have also been found to be comparable with HUVE cell [264]. This cell line has been

successfully used in a number of studies as an effective alternative to HUVE cell [265-266].

Thus this cell line was used as an endothelial cell for this study. The EA.hy926 cell line was

maintained in Dulbecco's Modified Eagle Medium (DMEM) containing high amount of D-

glucose (4500mg/L), 25mM HEPES, L-glutamine and no sodium-pyruvate (purchased from

GIBCO). This media was supplemented with 10% FBS (heat inactivated) (Atlanta Biologicals)

and 1% penicillin-streptomycin solution (ATCC). Heat inactivation of the FBS was carried out

by heating the thawed serum at 56^0C water-bath for 30 min. Both of these cell lines were

maintained at 37^0C in the cell-culture incubator containing 5% CO_2.

3.2. d. In vitro matrix binding assay

All the *in vitro* protein binding assays were carried out in high-binding, half area, flat

bottom, transparent, 96-well plates from Costar. For studying the binding of monomeric VN and

its complex with PAI-1 to matrix components, plates were initially coated with either HSPG or

Col-IV. For HSPG coating, the matrix was dissolved in a binding buffer containing 50mM Tris,

100mM NaCl, 1mM $CaCl_2$ and 1mM $MgCl_2$ (pH- 7.4) at 5µg/ml concentration. Dissolved

matrix was allowed to coat the surface of the 96-well plate for 1.5hr at 37^0C. For collagen-IV,

the matrix was dissolved in 10mM acetic acid at 3.6 µg/ml concentration and allowed to coat the

surface of the plate at room temperature for 1hr. Following coating, unbound matrix was washed by the binding buffer at least three times. Coating with GAG molecules was carried out at 4^0C overnight. Coating concentration was 25µg/ml for each GAG molecule, made in 1X PBS. Blocking of matrix or GAG-coated plate was carried out by 0.2% gelatin solution (made in binding buffer) for 1hr at 37^0C. Monomeric VN (or SMB domain) was mixed with wtPAI-1 and its variants at indicated concentrations in binding buffer containing 0.1% Tween-20 and the mixture was incubated at 37^0C for 1hr to allow complex formation. A preformed mixture of these proteins was allowed to bind to the matrix coated (blocked) plate for 1hr at 37^0C. Unbound protein was removed by washing (3X) with 0.1% Tween-20 containing buffer. Probing of VN or SMB binding to the matrix-coated plate was carried out immunochemically. For all the steps that involved antibody binding, 1X PBS containing 0.3%BSA was used as buffer. For probing VN, either Bunny-11 (a polyclonal antibody, used at 1:5000 dilution) or 1E9 (a monoclonal antibody, used at 1:2000) was used as primary antibody. For SMB, 1E9 (1:1000 dilution) was used. Primary antibody was allowed to incubate for 1hr at 37^0C followed by 3X washing with antibody binding buffer. Peroxidase conjugated anti-mouse/anti-rabbit IgG was used as secondary antibody. Secondary antibody (1:2000 dilution) was added to plate and incubated for 1hr at 37^0C followed by 3X washing with antibody binding buffer. Color was developed by adding 100µl of 50mM sodium-citrate (pH-5.5) solution containing 0.6mg/ml ABTS (SIGMA) and 1:1000 dilution of 30% H_2O_2 (Fisher) to each well of the plate and the absorbance data from each well was collected in Synergy Labtek plate reader at 405nm wavelength. **Figure-3.1** includes a schematic presentation of all the basic steps of this matrix binding assay.
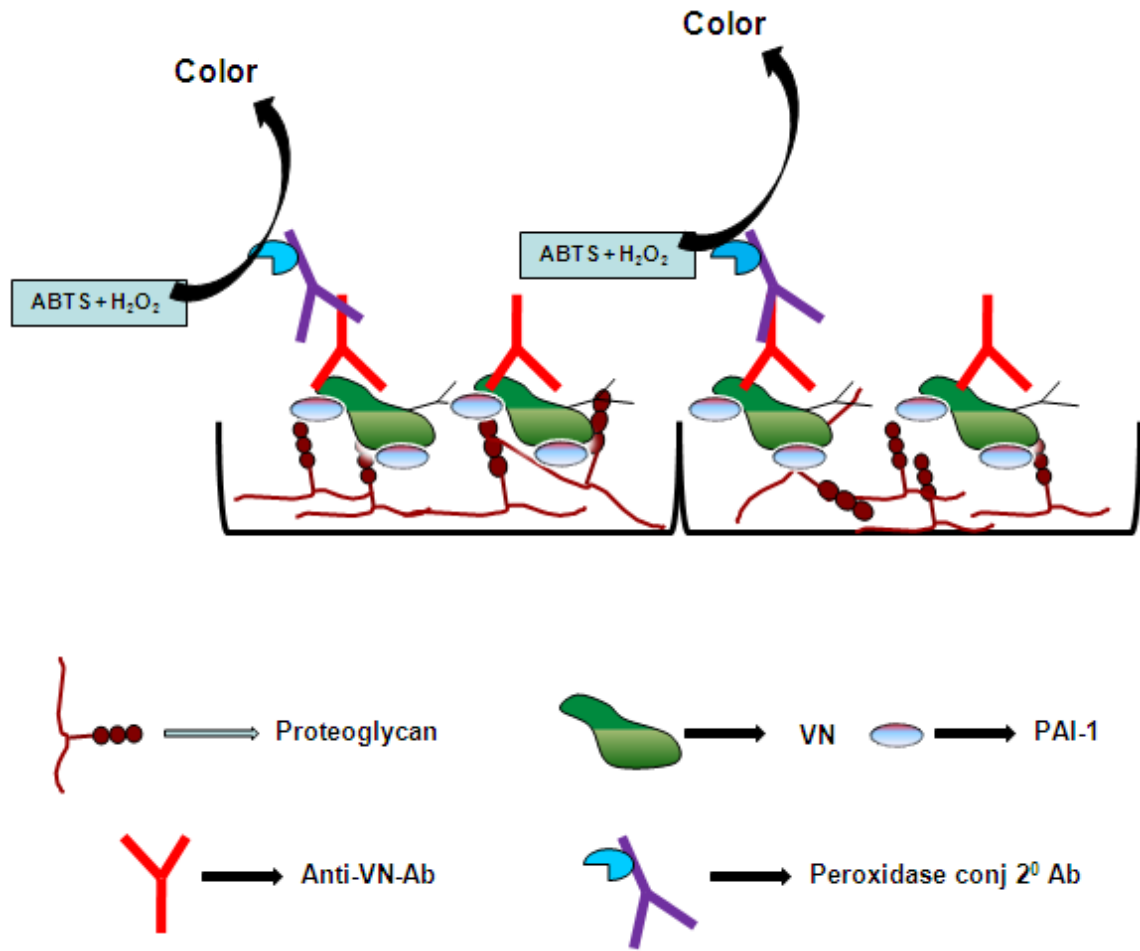
Figure 3. 1: Basic scheme for matrix binding assay

Figure-3.1: This figure includes the schematic presentation of the important steps for the matrix binding assay. When collagen was included in the assay, it replaced proteoglycan for coating the plate.

3.2. e. *In vitro* receptor binding assay

For characterizing the binding of the VN/PAI-1 complex with cell surface receptors, two different approaches were taken. In one approach, the receptor was directly coated on to the 96-well plate, and in the second approach the receptor was maintained in solution phase during the assay. For the direct coating of uPAR or integrin, the receptor was dissolved in binding buffer containing 50mM Tris, 100mM NaCl, 1mM $CaCl_2$ and 1mM $MgCl_2$ (pH- 7.4) at 5µg/ml concentration. Coating was allowed for 1hr at 37^0C followed by 3X washing with binding buffer. Blocking and incubation of VN/PAI-1 complex were carried out in the same manner as described in the previous section (matrix binding assay). VN binding was probed immunochemically (1E9 as primary antibody) as described in the previous section.

For binding assays with receptors in the solution phase, VN and PAI-1 were mixed in 0.1% Tween-20 containing binding buffer, incubated for 1hr at 37^0C and then added to plate with/out matrix coating followed by incubation for 1hr at 37^0C. When monomeric VN and its complex with PAI-1 were directly added to the plate, blocking with gelatin was carried out after VN/PAI-1 coating. When monomeric VN and its complex with PAI-1were added to the matrix-coated plate, blocking was carried out following matrix coating. Unbound proteins were removed by 3X washing with binding buffer. Binding solutions of uPAR and integrin (20µg/ml and 10µg/ml respectively) were made in binding buffer containing 0.1%Tween-20 and the receptors were allowed to bind to VN/PAI-1on the plate at 37^0C for 1-1.5hr as when indicated. For all the steps that involved antibody binding, 1X PBS containing 0.3%BSA, 0.5mM $CaCl_2$ and 0.5mM $MgCl_2$ was used as buffer. Unbound receptors were removed by 3X washing with this antibody binding buffer. For integrin binding, a polyclonal antibody (made in rabbit) directed against the

c-terminal domain of αv-subunit was used at 1:100 dilution. For uPAR binding a monoclonal

antibody (made in mouse) against uPAR was used at 1:100 dilution. Primary antibody binding

was carried out at 37^0C for 1hr followed by 3X washing with antibody binding buffer.

Peroxidase conjugated anti-mouse/anti-rabbit IgG was used as secondary antibody. This

antibody was used at 1:1000 dilution and incubation was carried out at 37^0C for 1hr followed by

3X washing with antibody binding buffer. Color was developed as described in the previous

section (matrix binding assay).

For all binding assays the average reading obtained from each treatment condition

(normalized with respect to background) was plotted along with the standard error. Statistical

significance was determined by two-tailed Student's t-tests. P-values <0.05 were considered

significant.

3.2. f. Cell binding assay

For cell binding assay, coating of matrix (HSPG or Col-IV), blocking of the coated

surface and incubation of preformed complex between VN and PAI-1 on to coated matrix were

carried out as described in the matrix binding assay. High-binding, solid side, transparent flat

bottom, 96-well plates from Costar were used for this assay. Cells were incubated overnight in

the absence/presence of growth factors, under serum free condition. VEGF (Vascular endothelial

growth factor) and bFGF (basic fibroblast growth factor) were used at 10ng/ml concentration and

PMA (phorbol 12-myristate13-acetate) was used at 100ng/ml concentration. Cells were detached

from the surface by 1% trypsin/EDTA solution and complete media (with serum) was used for

neutralizing the trypsin. Cells were resuspended in serum-free media at required concentration.

When Col-IV was used for coating the plate, 100µl of cell suspension containing 10^5cells/ml was

added to each well followed by incubation at 37^0C for 30min. When HSPG was used for coating

the plate, 100µl of cell suspension containing $5*10^5$cells/ml was added to each well followed by

incubation at 37^0C for 1.5hr. Unbound cells were removed and labeling of bound cells was

carried out by adding 100µl serum-free media containing 1µg/ml calcein to each well followed

by incubation at 37^0C for 30min. Incubation of the cells during binding assay was always carried

out in the cell-culture incubator. Free label and the unbound cells were removed by washing 2X

with serum free media. Fluorescent cells bound to the surface were observed under the Zeis

microscope using excitation and emission optics suitable for fluorescin. Photographs of the

randomly selected multiple fields (15 to 18) were taken from each well. Each treatment condition

was repeated in triplicates. The average number of cells bound/0.13mm^2 (area of each field) was

plotted (along with the standard error) with respect to each treatment condition. Statistical

significance was determined by two-tailed Student's t-tests. P-values <0.05 were considered

significant.

3.2. g. Cell migration assay

Migration experiments were carried out using FluoroBlok cell culture inserts of 8µm pore

size, purchased from BD Bioscience. These inserts are made of polyethylene terephthalate (PET)

membrane containing a dye that blocks transmission of the light between the range of 490-

700nm. If a suitable fluorescent dye is chosen, selective observation of the top or the bottom of

the insert can be achieved. Thus, use of this insert allows efficient counting of the migrated cells

that are bound at the bottom of the insert. Migration experiments on these inserts also require the

use of companion 24-well cell-culture plate obtained from BD Bioscience. Coating of the insert

with matrix components was carried out as described in the previous sections. Premixing of VN

and PAI-1 was carried out the in the binding buffer (same as mentioned in the matrix binding section) that contained 0.3%BSA instead of 0.1% Tween-20. Mixing was carried out for 1hr at 37^0C followed by incubation onto the inserts for 1hr at 37^0C as described before. Cells were treated and prepared as described in the cell binding assay section. When Col-IV was used for coating the plate, 150µl of cell suspension containing 10^6cells/ml was added to each insert and when HSPG was used for coating the plate, 150µl of cell suspension containing $2*10^5$cells/ml was added to each insert. 500µl serum-free media was added to the bottom of the each insert. Migration was carried out overnight in the cell culture incubator. Labeling of the cells was carried out by adding 500µl serum-free media containing 1µg/ml calcein to the bottom of each insert followed by incubation at 37^0C for 30min. Media containing free calcein was replaced by 500µl serum-free media and the calcein-labeled migrated cells were observed under the microscope (Zeiss). Photographs of the randomly selected multiple fields (15 to 18) from the bottom of each insert were taken. Each treatment condition was repeated in triplicates. Average number of cells migrated/0.13mm^2 (area of each field) was plotted (along with standard error) with respect to each treatment condition. Statistical significance was determined by two-tailed Student's *t*-tests. *P*-values <0.05 were considered significant. **Figure-3.2** represents the basic scheme for the migration experiments.

3.2. h. Flow cytometry

Cells were incubated overnight in the absence/presence of growth factors, under serum free condition. VEGF (Vascular endothelial growth factor) and bFGF (basic fibroblast growth factor) were used at 10ng/ml concentration, and PMA (phorbol 12-myristate13-acetate) was used at 100ng/ml concentration. Cells were detached from the surface by 1% trypsin/EDTA solution,
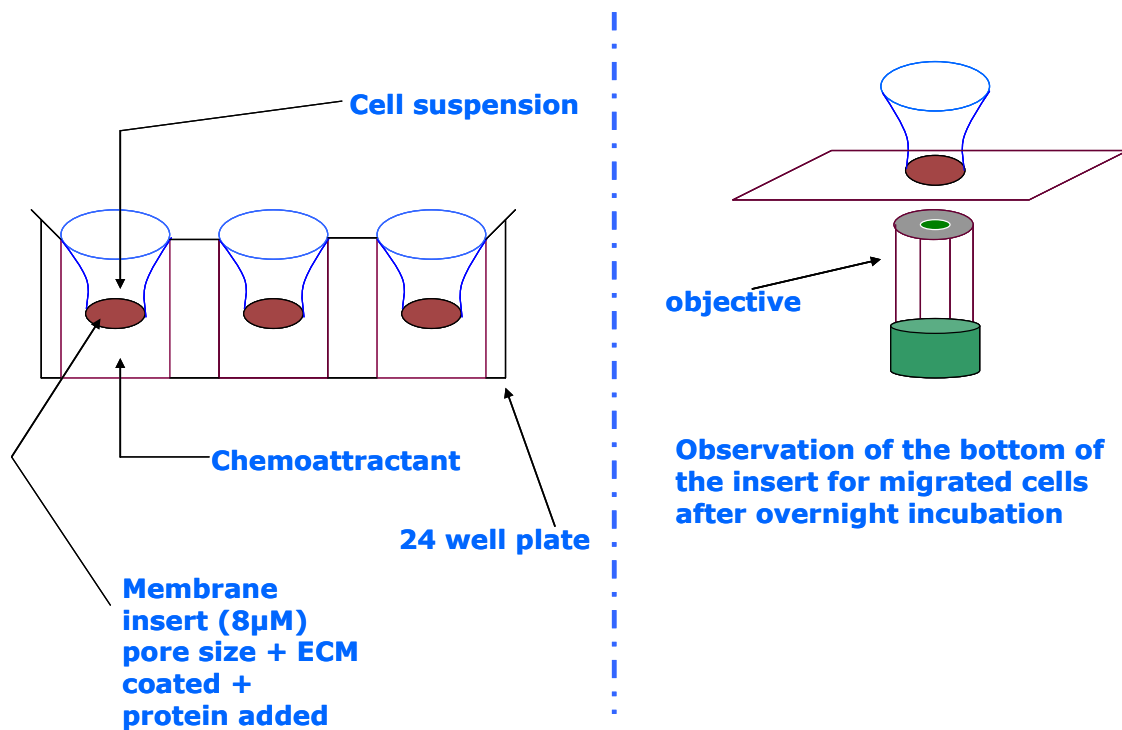
Figure 3. 2: Basic scheme of migration experiments

Figure-3.2: During the migration experiment, cells are added on to the top chamber of the fluoroblok membrane insert. To the bottom chamber, fresh media is added. The presence of migrated cells is observed on the bottom of the insert under the microscope. Photographs of multiple fields were taken and the number of cells migrated per 0.13mm^2 area is plotted.

and complete media (with serum) was used for neutralizing the trypsin. Cells were resuspended in serum-free media, and 100μl of cell suspension containing at least 10^6 cells for each treatment condition were added to the wells of a 96-well round bottom plate. Staining of the cell surface receptors was carried out in this plate. For each treatment condition, samples were taken in duplicates. Cells were incubated with primary antibody against uPAR at 1:40 dilution and αvβ3, αvβ5, α5β1 & α2β1 at 1:100 dilutions. Dilutions were carried out in FACS buffer, and incubation with primary antibody was carried out for 1hr on ice. Unbound antibodies were removed by washing 2X with FACS buffer followed by incubation with Alexa-488 conjugated goat anti-mouse IgG (1:200 dilution) for 1hr on ice. Unbound antibodies were removed by washing 2X with FACS buffer. Stained cells were fixed by 1% paraformaldehyde for 20min at room temperature. Cells were washed 2X with FACS buffer and content of each well was transferred into FACS tube containing 1ml of FACS buffer. Receptor expression was observed in FACS-Calibur instrument and the data was analyzed by Flow-Jo.

3. 3. Results

3.3. a. Multimeric Complexes Formed by the Interaction of PAI-1 and VN Exhibit Increased Association with Matrix Components.

In most of the published work in which PAI-1 was checked for its effect on cellular adhesion and migration, 'denatured' multimeric VN was used to mimic its matrix associated multimeric form and PAI-1 was added exogenously in order to affect interaction of VN with cell surface receptors. There are many pathophysiological conditions where PAI-1 is found to be co-localized with VN in the matrix [49, 212, 225, 267] and so we believe a more realistic approach

114

is to include PAI-1 as a part of the multimeric complex. Since we know that PAI-1 initiates multimerization of VN and remains associated with the complex for a long period of time, we have opted to test a preformed complex of VN and PAI-1 in all of our studies and compare its effect with monomeric VN. Furthermore, instead of using VN directly as a binding substrate, we have included other matrix components in our *in vitro* experiments; these include Col-IV, Col-I and HSPG (heparan sulfate proteoglycan) to probe the specific role of PAI-1/VN complex in a more relevant context. Col-IV is an important basement membrane component that provides tensile strength [268-269]. Col-IV interacts with VN, and it was found that the conformationally altered, multimeric VN interacted better with collagen [104]. HSPG is also an integral basement membrane component and is found in almost any mammalian tissue [270-271]. One of the many proposed functions of basement membrane associated HSPG is to interact with other matrix components, like laminin, fibronectin, and Col-IV [272-273]. In this study we test whether HSPG can interact with both monomeric and multimeric forms of VN.

Figure-3.3 & 3.4 show the dose-dependent increase in VN binding to Col-IV or HSPG respectively as PAI-1 concentrations are varied. We observed that the multimeric complex of VN and PAI-1 had a higher propensity to associate with the mixture of Col-IV and HSPG (**Figure-3.5**). This finding is consistent with our hypothesis, i.e. as more multimeric complexes are being formed by the interaction of increasing concentration of PAI-1, an increase in VN binding is observed with the individual components or mixture of matrix substituents.

Finqure-3.3-3.5: 100nM VN was mixed with increasing concentrations of PAI-1. The mixtures were allowed to bind to Col-IV (Figure-3.3) and HSPG (Figure-3.4) respectively and then probed for VN binding immunochemically. For Figure-3.5, the plate was coated with Col-IV, followed by coating with HSPG. 20nM VN was mixed with increasing concentrations of PAI-1 and the complexes were allowed to bind to the matrix. VN binding was probed immunochemically.

Association of VN/wt-PAI-1 complex with Col-IV
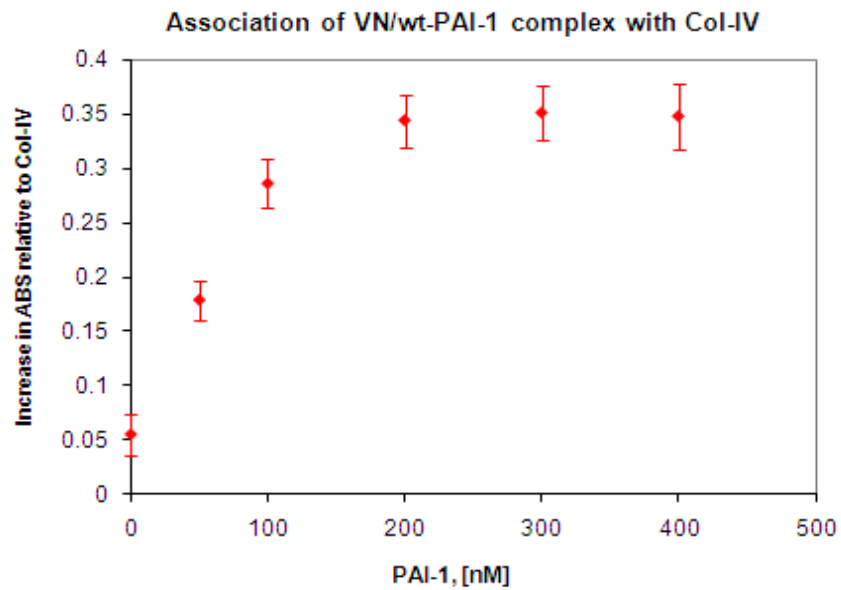
Figure 3. 3: Association of VN/PAI-1 complex with Col-IV- dose dependency

116
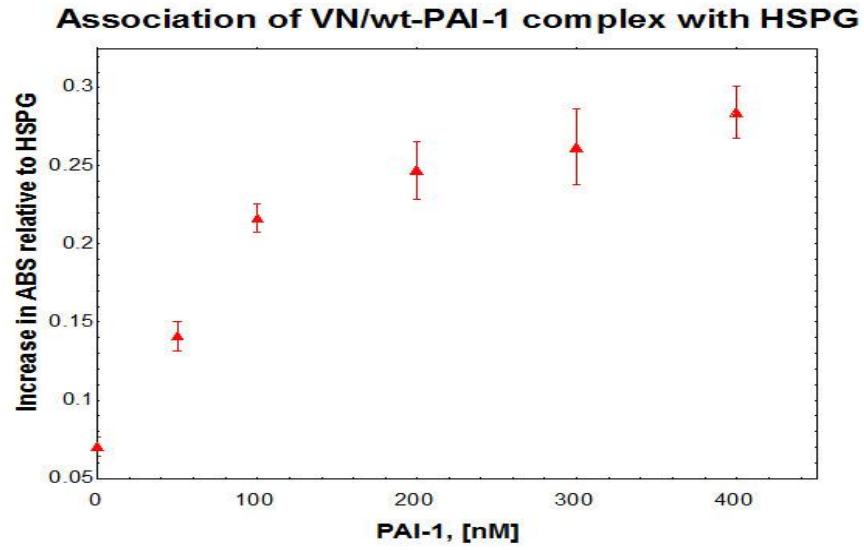
Figure 3. 4: Association of VN/PAI-1 complex with HSPG- dose dependency
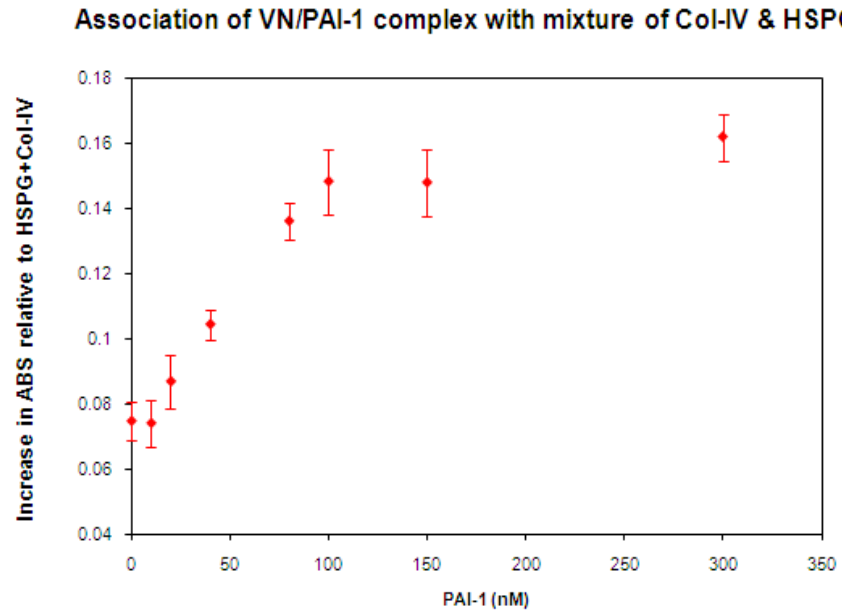
Figure 3. 5: Association of VN/PAI-1 complex with Col-IV- dose dependency

117

3.3. b. Formation of a Complex with Full Length VN is Critical for Increased Association with Matrix

It has generally been thought the interaction between VN and PAI-1 is mediated through the SMB domain of VN. The crystal structure of recombinant SMB domain bound to 14-1-B shows a single-turn 3-^{10} α-helix of SMB interacting with helix-F and part of the central β-sheet of 14-1-B [22]. Recently we have found that the interaction between these two proteins actually extends beyond this observed surface. By rapid reaction kinetics experiments done to test the binding of VN and strategically labeled (fluorescent) PAI-1, under conditions where only 1:1 binding was allowed, it was observed that the interaction between these two proteins is biphasic. Binding between PAI-1 and the isolated SMB, in contrast, was monophasic [168]. This data showed that interaction with full length VN is more complex and involves multiple interactions. We hypothesize that such multiple interactions between PAI-1 and full length VN are critical for the assembly of multimeric complexes and thus for increased association of VN with matrix components. In order test this idea, matrix-binding experiments have been carried out with complexes formed with PAI-1 and fully functional isolated SMB domain. **Figures-3.6 & 3.7** show binding data where SMB was mixed with two different concentrations of PAI-1, and the binding of the complex was compared to SMB alone on HSPG and Col-IV respectively. As expected, no significant increase in binding of SMB was observed upon mixing with PAI-1. The complex formed between PAI-1 and full length VN was used as positive control.

Since it is the multimeric complex of VN that is commonly found to be localized in the extracellular matrix and PAI-1 is the biological partner that causes such conformational transitions that lead to relocalization of VN, disruption of the interaction between these proteins

118
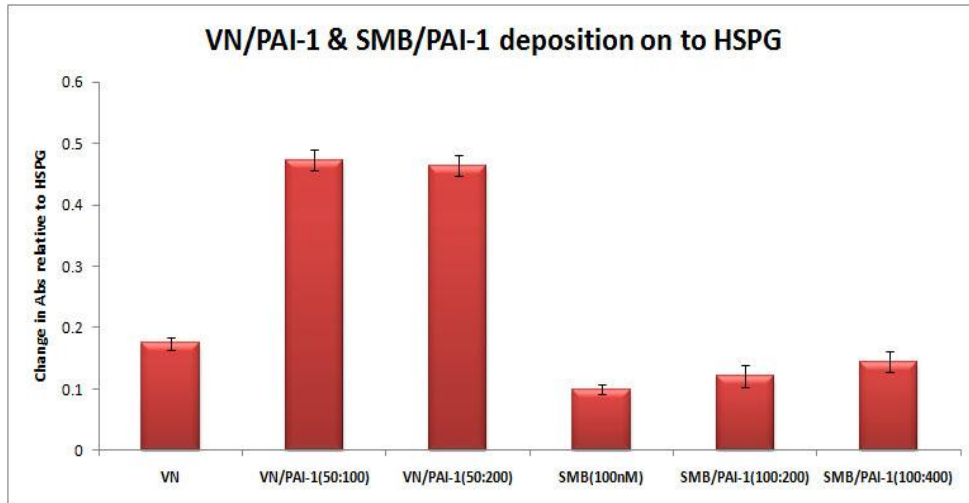
Figure 3. 6: Association of SMB/PAI-1 complex with HSPG
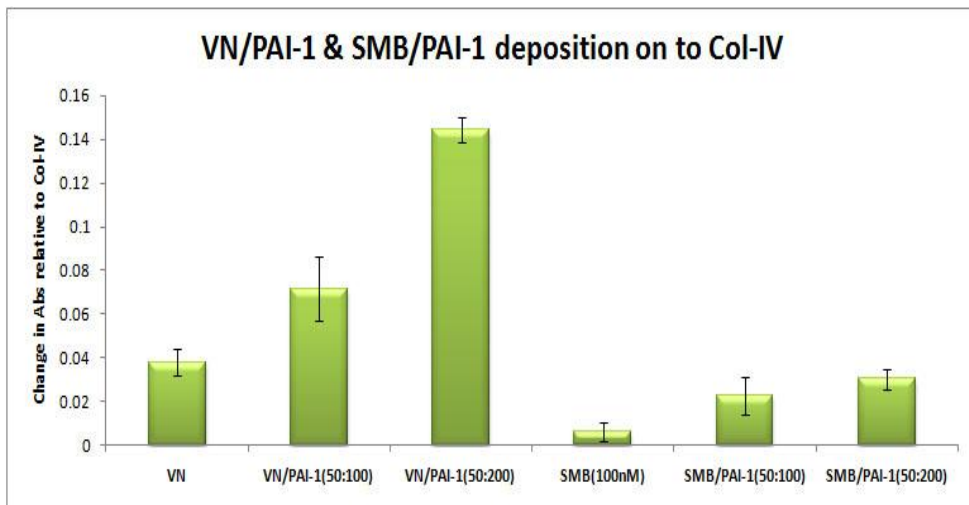
Figure 3. 7: Association of SMB/PAI-1 complex with Col-IV

Figure-3.6 & 3.7: 50nM VN and 100nM SMB were mixed with two different concentrations of PAI-1 corresponding to 1:1 and 1:2 stoichiometry. The VN/PAI-1 complex and SMB/PAI-1 complexes were added to HSPG (Figure-3.6) and Col-IV (Figure-3.7). Binding of VN and SMB to the matrix was probed immunochemically.

119

can be a useful therapeutic strategy. Recently we have found two peptides (an octapeptide and a pentapeptide, mimicking the RCL of PAI-1) that can completely disrupt the interaction between VN and PAI-1 and inhibit the formation of oligomeric complexes. (A detailed description of these two peptides and the experiments will be included under the Chapter-3.) In order to check the potential of these peptides to disrupt matrix association, we have performed these matrix binding experiments on the complex formed between VN and PAI-1 in the presence/absence of the octapeptide. **Figures-3.8 & 3.9** show the results of these binding experiments to HSPG or Col-IV respectively. As expected, the presence of the octapeptide completely disrupted the increased association of VN with matrix components.

Mutating glutamate-123 residue of PAI-1 by replacement with arginine (Q123K) has been found to severely weaken the affinity for the primary site interaction with VN [197]. A sedimentation velocity study done with monomeric VN and Q123K-PAI-1, mixed at equimolar concentrations, showed that this mutant essentially lacked the ability to form multimeric complexes (discussed in chapter-3). In order to check the effect of this mutant on influencing the association of VN with matrix components, similar matrix binding experiments were done. **Figure-3.8 & 3.9** contain data that show that Q123K mutant of PAI-1 cannot promote increased association of VN with Col-IV and HSPG.

3.3. c. Increased Association of VN Is Not Glycosaminoglycan (GAG) Mediated.

Glycosaminoglycans (GAGs) are long unbranched polysaccharides comprised of repeating disaccharide units. The disaccharide units are usually made of one hexose or
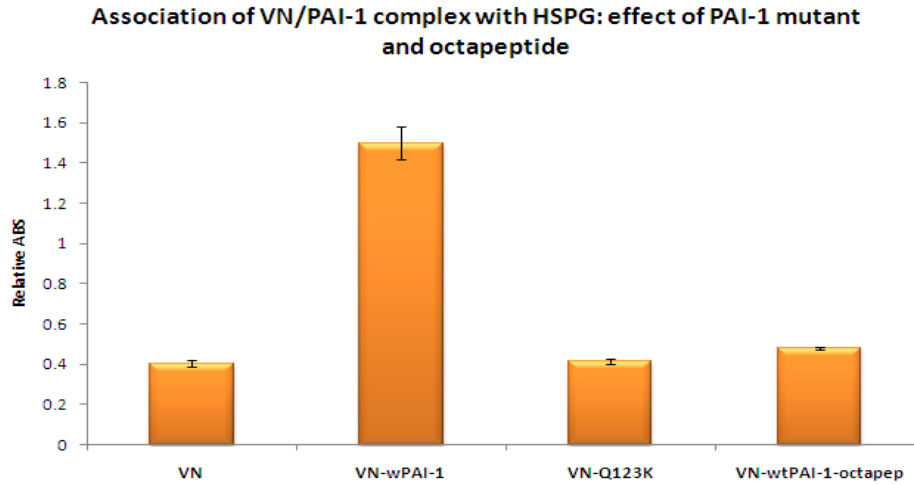
Figure 3. 8: Effect of octapetide and Q123K-PAI-1 on VN/PAI-1 complex binding to HSPG
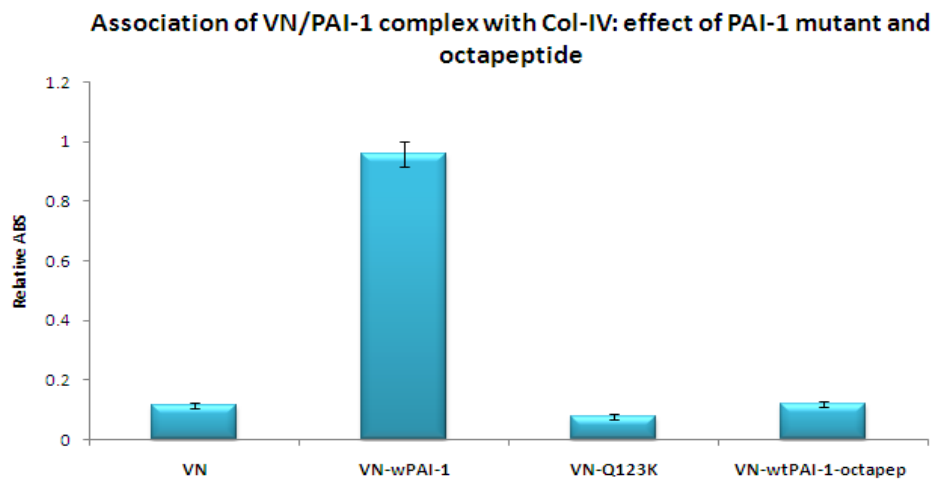
Figure 3. 9: Effect of octapetide and Q123K-PAI-1 on VN/PAI-1 complex binding to Vol-IV

Figure-3.8.a & 3.9: 50nM VN was mixed with a 100nM concentration of the Q123K mutant of PAI-1 or 100nM wtPAI-1 in the absence or presence of 2mM octapeptide. Mixtures were added to HSPG (Figure-3.8) and Col-IV (Figure-3.9) respectively. Binding of VN and SMB was quantified immunochemically using 1E9. monoclonal antibody (1:2000 dilution).

hexuronic acid residue and one hexosamine (6-C sugar made containing nitrogen). Heparin, the natural anticoagulant found in our body is a common example of GAG. There are many other types of GAGs, including heparin sulfate, chondroitin sulfate, dermatan sulfate etc. HSPG, the matrix component that we have used in our study is a proteoglycan that contains heparan sulfate as the GAG molecule. Col-IV is also heavily glycosylated [274]. The anticoagulant property of heparin comes from its ability to increase the rate of antithrombin-III mediated inactivation of thrombin [70]. VN is known to act as a scavenger of heparin and thus reduces the rate of antithrombin-III-mediated inactivation of thrombin [5, 74]. Studies have shown that multimeric VN exhibits increased binding affinity for heparin [48, 275]. Our lab showed that this apparent increased binding of multimeric VN to heparin is attributed to avidity (e.g. multi-valent effects) rather than differences in affinity. Thus, it was observed that the affinity of monomeric VN was similar to that of a single unit of the multimer [276]. Nevertheless, the overall effective binding to heparin was higher with 'denatured' multimeric VN. In order to test whether the increased association of the PAI-1/VN complex with the matrix is GAG mediated, we have performed binding studies with different types of GAG molecules. **Figure-3.10** compares monomeric VN and VN/PAI-1 for their ability to interact with different types of GAG molecules. Though monomeric VN was found to bind to all the different GAG molecules used, the multimeric complex formed between VN and PAI-1 did not show any increased association. This finding indicates that increased association of the complex to matrices and/or tissues is not GAG mediated.

122
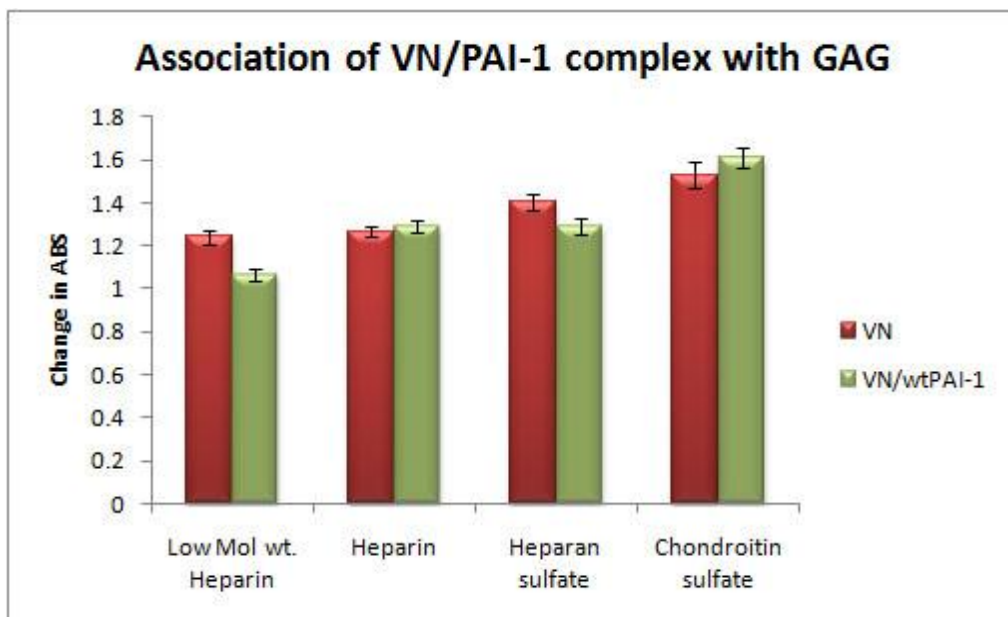
Figure 3. 10: Association of VN/PAI-1 complex with different GAG

Figure-3.10: A plate designed for GAG binding was coated with different GAGs as indicated. For each GAG molecule coating concentration was 25µg/ml. Coating was carried out overnight at 4⁰C. VN was incubated with 100nM wt-PAI-1 and the mixtures were added to plate coated with GAGs. Binding of VN was quantified immunochemically using 1E9 monoclonal antibody.

3.3. d. The Multimeric Complex Formed Between VN/PAI-1 Associate More with Cell Surface Receptors.

VN interacts with several surface receptors, e.g. - uPAR αvβ3 and αvβ5. *In vitro* studies indicate that binding of uPAR to 'denatured' multimeric VN is inhibited by the addition of PAI-1[226-227]. Other studies indicate that binding of αvβ3 to 'denatured' multimeric VN is inhibited by PAI-1 added exogenously [229, 277]. Unfortunately, no one except for our lab has chosen to compare the interaction of receptors and VN with that of the multimeric complex formed by the interaction of VN and PAI-1. Previously our lab has shown that the multimeric complexes formed by the interaction between VN and PAI-1 associate more with αvβ3 and GPIIaIIIb (a platelet integrin) compared to monomeric VN [209]. We further pursued this strategy to add to our existing knowledge on: 1. the biological relevance of multimeric complexes formed between VN and PAI-1; 2. the effect of PAI-1 on the interaction between VN and cell surface receptors while associated with VN within the multimeric complexes.

Figure-3.11 shows the dose-dependent increase in VN binding to suPAR (soluble uPAR with no GPI link) with increasing concentrations of PAI-1. This is an experiment that explicitly checked binding of VN to a uPAR-coated plate. The side panel shows the basic schematic of the binding assay. In this study we did not see any interference with VN binding to suPAR by PAI-1. In fact, the multimeric complexes formed between VN and PAI-1 exhibit increased binding compared to native monomeric VN. **Figure-3.12 & 3.13** show binding experiments to test association of uPAR with the VN/PAI-1 complex associated with matrix components. In these experiments monomeric VN and the complex between PAI-1 and VN were incubated with Col-IV and HSPG, and uPAR was added to the plate following VN binding. The binding of uPAR
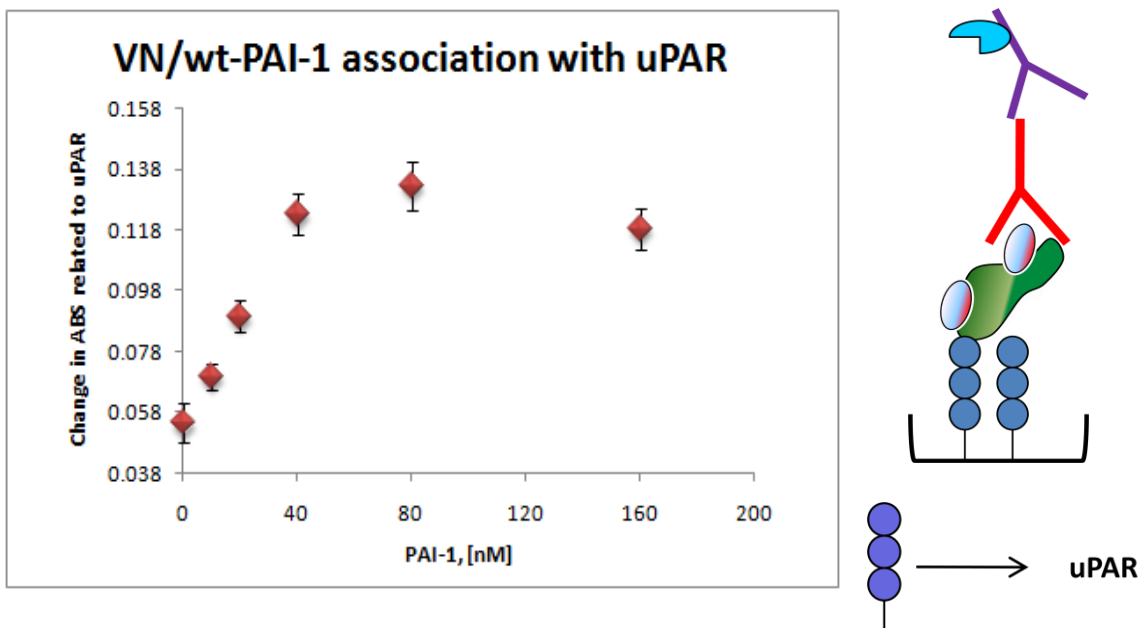
Figure 3. 11: Association of VN/PAI-1 complex with uPAR- dose dependency

Figure-3.11: 20nM VN was mixed with varying concentrations of PAI-1 and incubated at 37^0C for 1hr. Mixtures were added to a uPAR coated plate. Binding of VN to uPAR was quantified immunochemically using the 1E9 monoclonal antibody against VN. The right panel shows the basic scheme of this experiment. The symbol for uPAR is defined. For all the other symbols, refer to Figure-3.1.
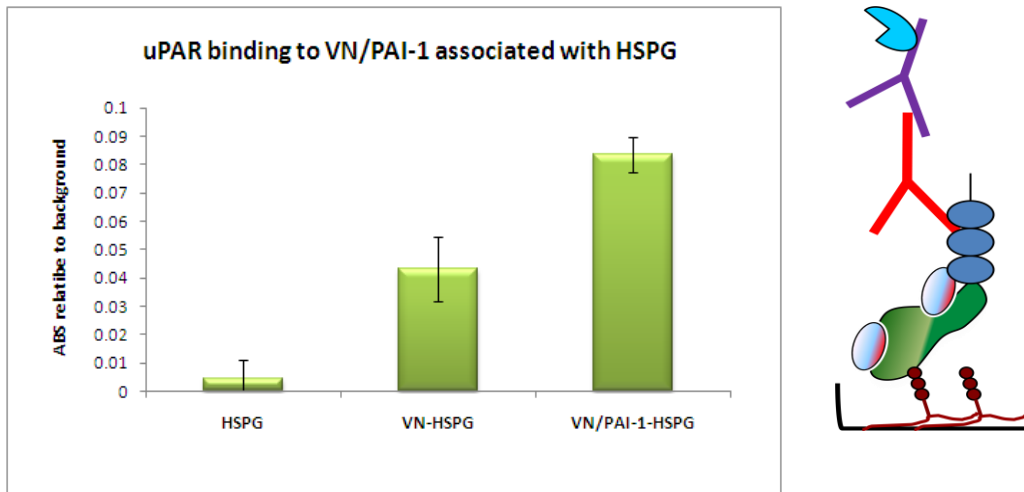
Figure 3. 12: uPAR binding to VN/PAI-1 complex associated with HSPG
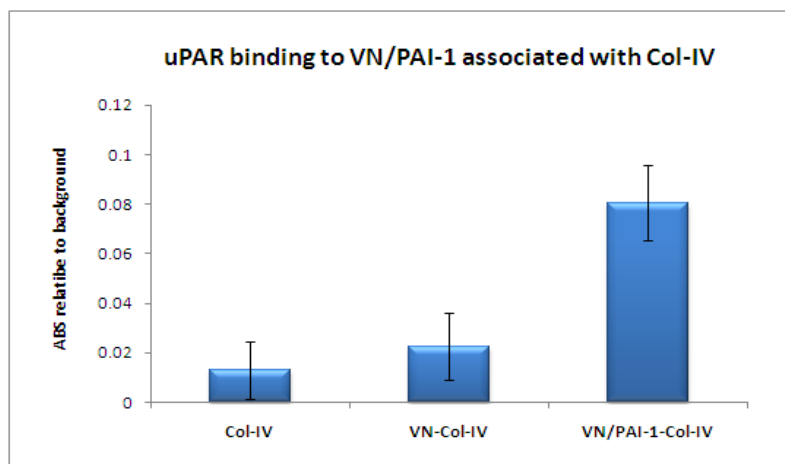
Figure 3. 13: uPAR binding to VN/PAI-1 complex associated with Col-IV

Figure-3.12 & 3.13: 100nM VN was mixed with 200nM wtPAI-1 and the mixtures were then added to HSPG (Figure-3.12) and Col-IV (Figure-3.13) coated plate. Soluble uPAR was added and binding of uPAR to the VN/PAI-1 complex was probed immunochemically using an antibody directed against uPAR. The right panel shows the basic scheme of this experiment. For all the symbols refer to Figure-3.1 and 3.11.

was probed by an antibody that recognizes a non-VN binding epitope on uPAR. While uPAR

binding could not be detected to native VN under the given conditions, a significant increase in

binding was observed to the VN/PAI-1 complex associated with Col-IV or HSPG. A previous

study showed that the affinity of uPAR binding to native VN was lower than with 'denatured'

multimeric VN [278]. It may be that a significantly higher concentration of native VN is needed

to demonstrate binding of uPAR. Nevertheless, a significant increase in binding of uPAR to the

VN/PAI-1 complex compared to monomeric VN indicates that the presence of PAI-1 is not

inhibitory to uPAR binding. uPAR binding to native VN and the VN/PAI-1 complex directly

coated on to a 96-well plate was also checked (data not shown). Once again no binding could be

observed to native VN under these conditions, but binding was much higher with the VN/PAI-1

complex. Though a significant difference in binding was observed with the VN/PAI-1 complex,

the difference was more prominent when the VN/PAI-1 complex was associated with matrix

components.

     Figure-3.14 shows tests of binding of the VN/PAI-1 complex to αvβ3, αvβ5 and α5β1.

We observe that multimeric complexes formed between VN and PAI-1 show increased

association with both αvβ3 and αvβ5 compared to monomeric VN. Once again, no inhibition of

VN binding to these integrins was observed in the presence of PAI-1. In this figure, we also see

that monomeric VN binds to α5β1, and this binding increase in the presence of the VN/PAI-1

complex. α5β1 is primarily known as a fibronectin receptor [279-280] that recognizes an RGD

sequence on fibronectin [280]. α5β1 shares some functions with αvβ3. Like αvβ3, expression of

α5β1 is minimal in quiescent endothelial cells, but activated endothelial cells show significant
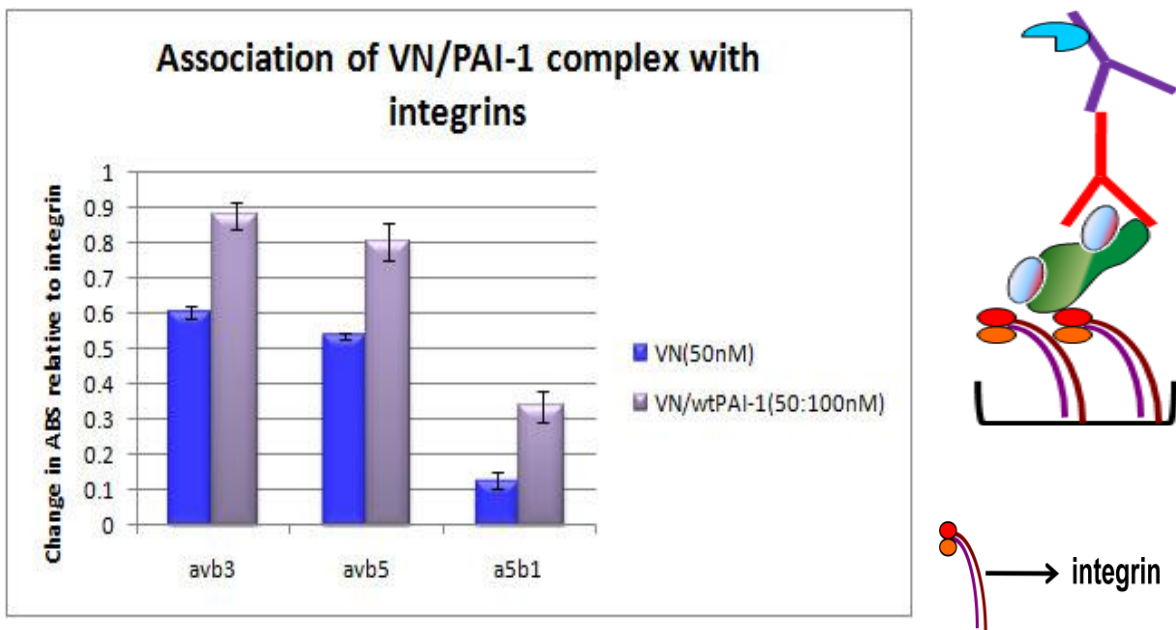
Figure 3. 14: Association of VN/PAI-1 complex with αvβ3, αvβ5 and α5β1

Figure-3.14: 50nM VN was mixed with 100nM PAI-1 and added to αvβ3, αvβ5 or α5β1 coated plates. 50nM VN alone or in complex with 100nM PAI-1 were added to integrin coated plates. Binding of VN was quantified immunochemically using the 1E9 monoclonal antibody against VN. The right panel shows the basic scheme of this experiment. The symbol for integrin is defined. For all the other symbols, refer to Figure-3.1.

increase in the expression of α5β1. Similarly, expression of α5β1 on endothelial cells can be

upregulated by bFGF or TNF-α [281]. **Figure-3.15 & 3.16** show results that further confirm the

specific interaction of VN and α5β1. **Figure-3.15** compares the binding of monomeric VN alone

or in complex with PAI-1 (equimolar mixture). Monomeric VN shows a concentration-

dependent increase in binding to α5β1, whereas at each concentration, the presence of an

equimolar amount of PAI-1 resulted in a further increase in binding. **Figure-3.16** shows the dose

dependent increase in VN binding with increasing concentrations of PAI-1. **Figure-3.17** probes

for αvβ5 binding to native VN and the VN/PAI-1 complex coated on a 96-well plate. Probing of

αvβ5 binding was carried out using an antibody that recognizes the C-terminal domain of αv

integrin. A schematic presentation of the binding strategy is shown in the side panel. Though no

detectable binding of αvβ5 could be observed with monomeric VN, a significant increase was

observed with the VN/PAI-1 complex. The absence of binding to monomeric VN could be due to

a weak affinity. Seiffert et al. showed that 'denatured' multimeric VN has much higher affinity

for αvβ3 [277]. A similar issue may play a role here with αvβ5. This study shows that the

presence of PAI-1 in the multimeric complex does not inhibit αvβ5 binding to VN. Strikingly,

when the binding of αvβ5 to VN/PAI-1 associated with matrix components was checked, no

binding was detected to either native VN or VN/PAI-1 under similar experimental conditions. It

appears that in the environment where αvβ5 is associated with multimeric VN in the context of

other matrix components, the C-terminal domain of αvβ5 is not accessible to the antibody.
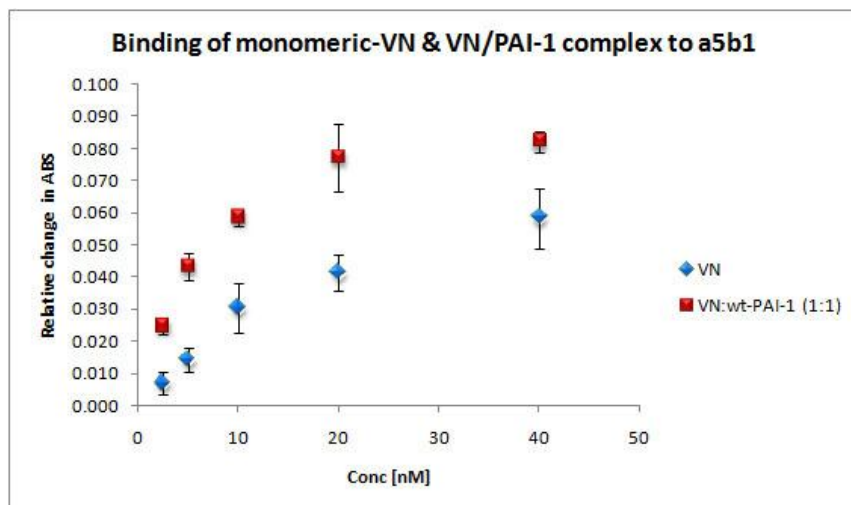
Figure 3. 15: Comparison of VN/PAI-1 complex and monomeric VN binding to α5β1
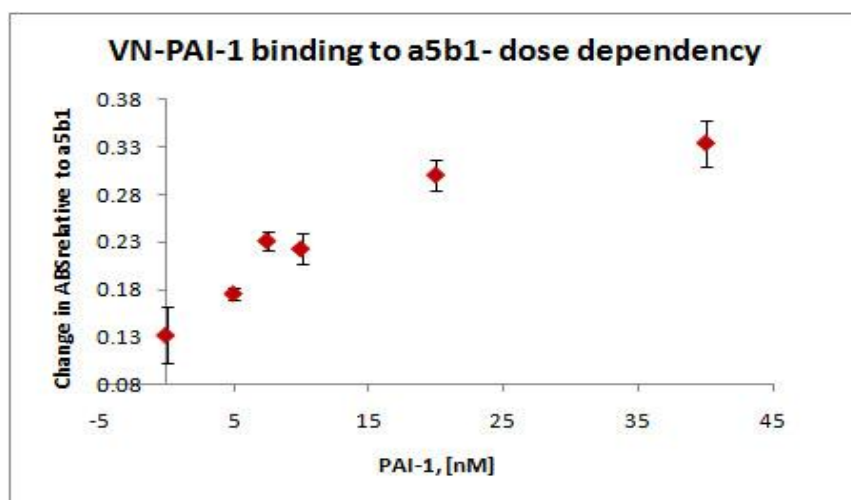
Figure 3. 16: association of VN/PAI-1 with α5β1- dose dependency

Figure-3.15: A series of VN concentrations was mixed with wtPAI-1 in an equimolar concentration, and the binding of the VN/PAI-1 complex to an α5β1 coated plate is compared to that of a VN alone. Figure-3.16: 10nM VN was mixed with varying concentrations of PAI-1 and added to α5β1 coated plate. The binding of VN was probed immunochemically.
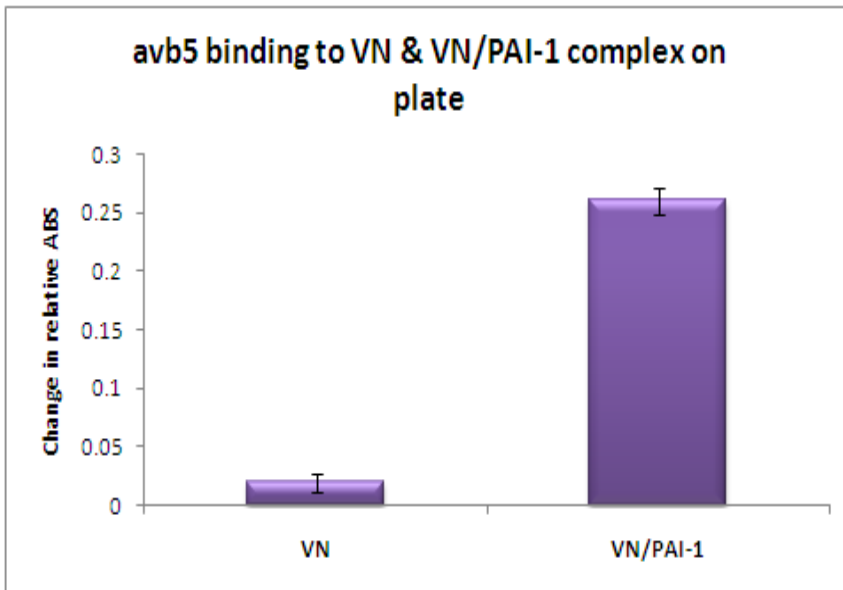
Figure 3. 17: αvβ5 binding to VN and VN/PAI-1 complex

Figure-3.17: 100nM VN alone or mixed with 200nM PAI-1 were added to a plate. αvβ5 was added to VN or VN/PAI-1 coated plate and the binding of the integrin was probed by an antibody against the C-terminus of the αv subunit (1:100 dilution). The right panel shows the basic scheme of this experiment. For all the symbols refer to Figure-3.1 & 3.14.

3.3. e. Effect of the VN/PAI-1 Complex on Cellular Adhesion and Migration: Testing the Role of the Surrounding Environment.

Previous studies showed that PAI-1 promoted migration of U937 cells and melanoma cells through VN in a uPAR-dependent manner [226, 228]. On the other hand, PAI-1 was found to inhibit migration of SMC, WISH and Hep2 cells lines on VN in a αvβ3 mediated fashion [229-230]. The particular effect of the interaction between PAI-1 and VN on cellular migration/adhesion may thus be influenced by cell type and variability in cell surface receptors. In order to explore the effect of specific cell types, we have included two different cell lines in our study. They are HT1080 (fibrosarcoma) and EA.hy 926 (endothelial cell), cells relevant in different aspects of angiogenesis, as discussed above [191, 231-233]. Angiogenesis is the process of new blood vessel formation. In this process, activated endothelial cells migrate from the existing blood vessel to the tumor site and initiate new blood vessel formation. Formation of new blood vessels is key for the development and progression of the tumor [282-283]. VN is thought to play an important role in the regulation of angiogenesis. The absence of VN was found to decrease angiogenesis in mice [66]. There are a number of inhibitors of angiogenesis, designed to disrupt the interaction of αvβ3 and αvβ5 with VN, currently being studied in clinical trial [99, 284-285]. Thus, the use of these two cell lines is relevant in the context of angiogenesis.

It is known that cytokines and growth factors can regulate the expression of receptors on the cell surface. Waltz et al. found that stimulation of the monocytic cell line U937 with TGFβ1 and Vitamin-D3 (Cholecalciferol) caused expression of uPAR on the cell surface. In other studies, the use of bFGF increases expression of αvβ3 in HDMEC (human dermal microvascular endothelial cell) [286]. Phorbol 12-myristate 13-acetate (PMA), which is known to be a

132

tumorigenic substance, was also found to cause an increase in αvβ3 expression in HDMEC [287]. Angiogenesis is initiated by the activation of endothelial cells. Often times this activation results from the change in receptor expression on the cell surface mediated by the effect of different growth factors. Brooks et al. reported that bFGF and TNF-α (tumor necrosis factor-α) can induce angiogenesis by increasing the expression of αvβ3 on the vascular endothelial [288]. Such angiogenesis could be blocked by a specific antibody against αvβ3. On the other hand, Friedlander et al. showed that angiogenesis induced by VEGF and TGF-β (transforming growth factor-β) was blocked by an antibody against αvβ5 [96]. Thus, angiogenesis induced by these two growth factors was proposed to be αvβ5-mediated. In our study we have used bFGF and VEGF as possible modulators of the receptor expression on the cell surface of the two cell lines. We have also used PMA for influencing receptor expression. Our rationale was to determine the specific regulation of receptors on our chosen cell types due to stimulation with bFGF, VEGF and PMA. Among the many growth factors available, it was logical to choose those that are known to cause changes in other systems. However, it should be noted that there were no previous studies to establish the effects of these particular cytokines and chemicals on these cell lines. **Figure-3.18** contains the basic scheme of all the cell based experiments. Briefly, each cell line (1080 and 926) was separately treated with different stimulants (bFGF, VEGF and PMA) under serum free conditions. As control, each cell line was also left under serum free condition with no treatment. Each cell line subject to separate treatment condition was utilized for cell binding and migration assay. For all binding and migration experiments matrix conditions were generated by using either Col-IV or HSPG as the base matrix component. VN alone and its complex with PAI-1 were then allowed to bind to Col-IV or HSPG to complete two different sets

133
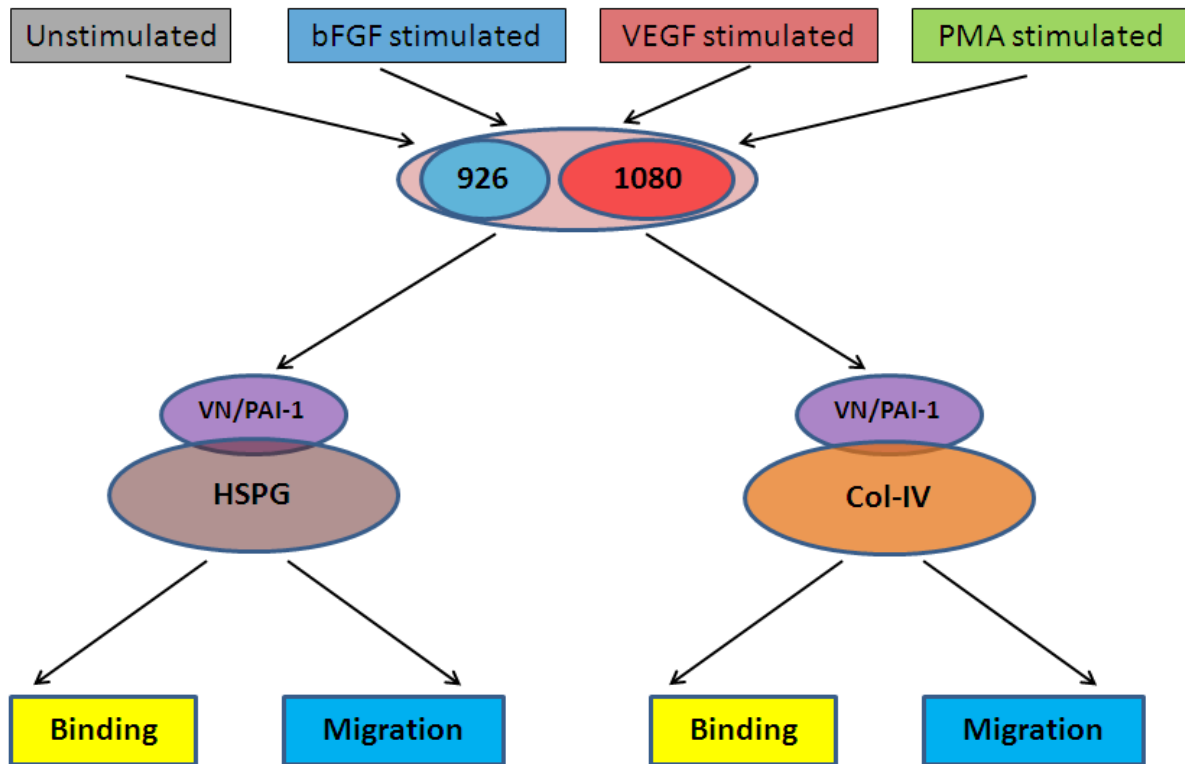
Figure 3. 18: Basic scheme for the cell binding and migration experiments

Figure-3.18: 926 cells and HT1080 cells were treated with growth factors and PMA separately. As a control, untreated cells were also used. Specific matrix conditions were generated by adding VN or the VN/PAI-1 complex to either plates coated with HSPG or Col-IV. Cells treated with different conditions were subject to both binding and migration study in the presence of specific matrix condition.

of matrix preparation. Both 1080 and 926 cell lines that have already been treated with different conditions were then subject to cell binding assay and cell migration assay separately under two different sets of matrix conditions. While EA.hy926 cells were checked for adhesion to the VN/PAI-1 complex associated with HSPG, no differential effect in cell binding was observed between the VN/PAI-1 complex and monomeric VN. This was true under all conditions. **Figure-3.19 -3.22** show binding of unstimulated, bFGF-, VEGF- and PMA-stimulated EA.hy926 cells to VN/PAI-1 complex associated with HSPG, respectively. For almost all the conditions tested the presence of the VN/PAI-1 complex neither inhibited nor promoted cellular binding compared to VN alone ($P>0.05$). However, VN alone increased cell binding relative to HSPG ($P<0.05$). Another striking observation was that when PAI-1 was associated with HSPG, a significant increase in binding compared to HSPG ($P<0.05$)) could be observed, as found with VN alone or with the VN/PAI-1 complex. When HT1080 cell line was used for studying the effect of different stimulation conditions on cell binding to VN/PAI-1 complex associated with HSPG very similar results were obtained as with EA.hy926 cell line. Presence of VN/PAI-1 complex showed no significant difference in terms of number of cell bound compared to VN alone ($P>0.05$). When VN alone was mixed with HSPG significant increase in binding was observed compared to that of HSPG alone.

926 Cell binding to VN or the VN/PAI-1 complex associated with Col-IV was dominated by the presence of Col-IV. Considerable amount of cell binding was observed to Col-IV within 30 minutes of incubation and there was no additional influence of the presence of VN or the VN/PAI-1 complex under all the conditions tested ($P>0.05$). **Figure-3.23 - 3.26** show the result

135

Figure-3.19- 3.22: A 50nM concentration of VN was incubated with 100nM wt-PAI-1, and the mixtures were added to plates coated with HSPG. Unstimulated (Figure-3.19), bFGF stimulated (Figure-3.20), VEGF stimulated (Figure-3.21) and PMA stimulated (Figure-3.22) 926 cells were added to wells and bound cells were labeled with calcein. The number of cells bound per 0.13mm^2 area is plotted. *P<0.05
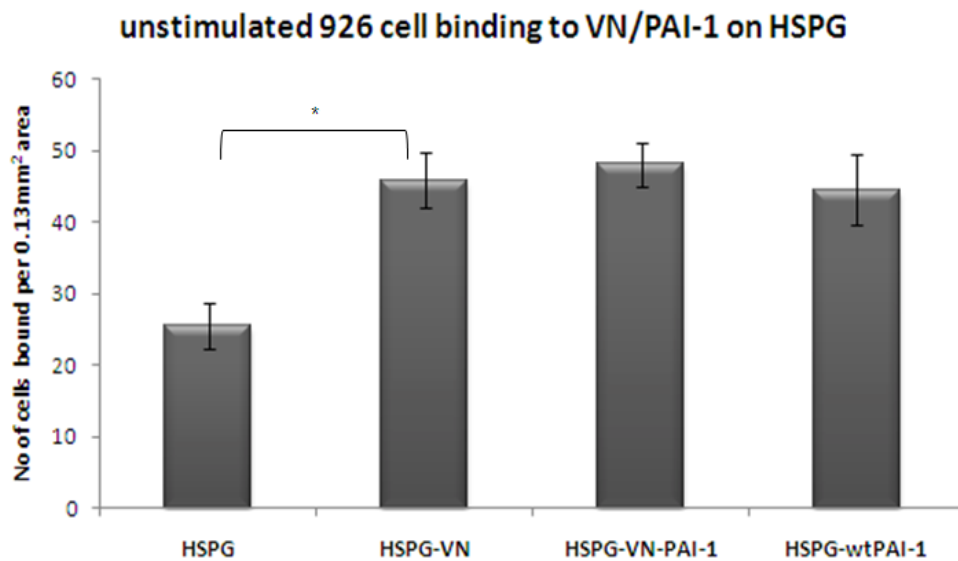
Figure 3. 19: Unstimulated 926 cell binding to VN/PAI-1 complex associated with HSPG
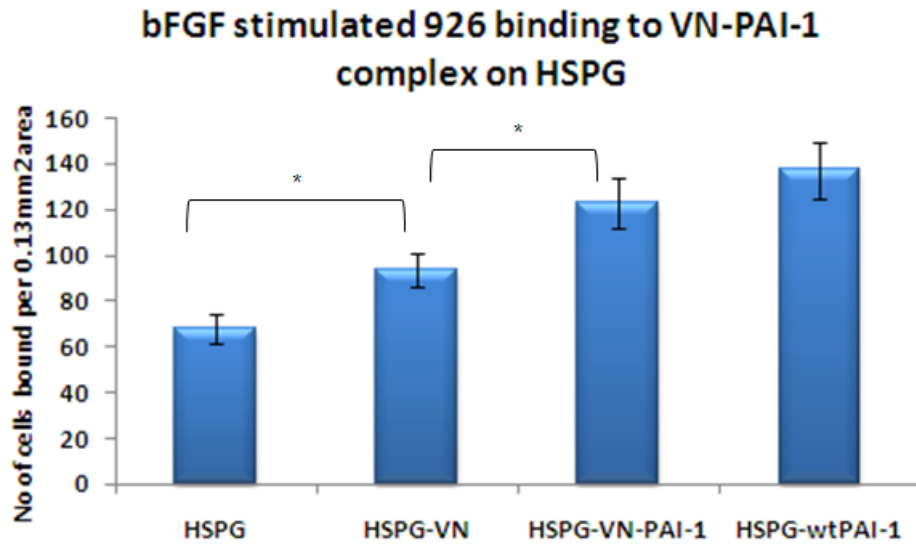
Figure 3. 20: bFGF stimulated 926 cell binding to VN/PAI-1 complex associated with HSPG
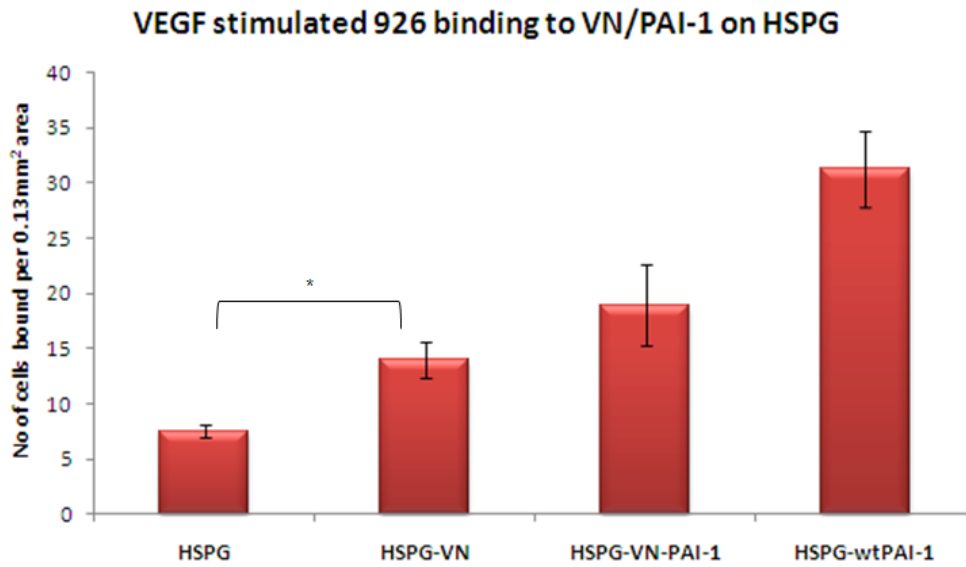
Figure 3. 21:VEGF stimulated 926 cell binding to VN/PAI-1 complex associated with HSPG
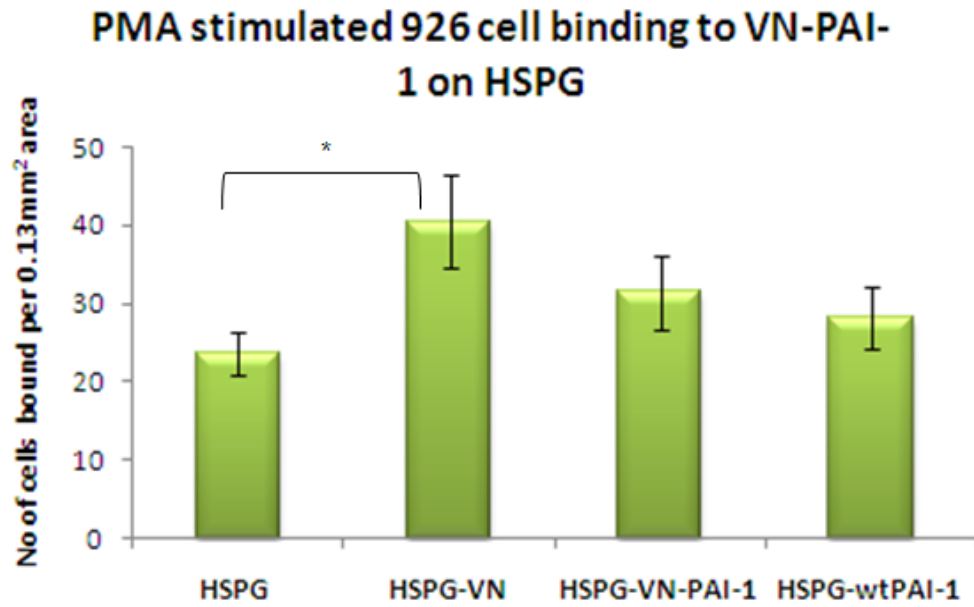
Figure 3. 22: PMA stimulated 926 cell binding to VN/PAI-1 complex associated with HSPG

Figure-3.23 -3.26: A 50nM concentration of VN was incubated with 100nM wt-PAI-1, and the mixtures were added to plates coated with Col-IV. Unstimulated (Figure-3.23), bFGF stimulated (Figure-3.24), VEGF stimulated (Figure-3.25) and PMA stimulated (Figure-3.26) 926 cells were added to wells and bound cells were labeled with calcein. The number of cells bound per $0.13mm^2$ area is plotted.
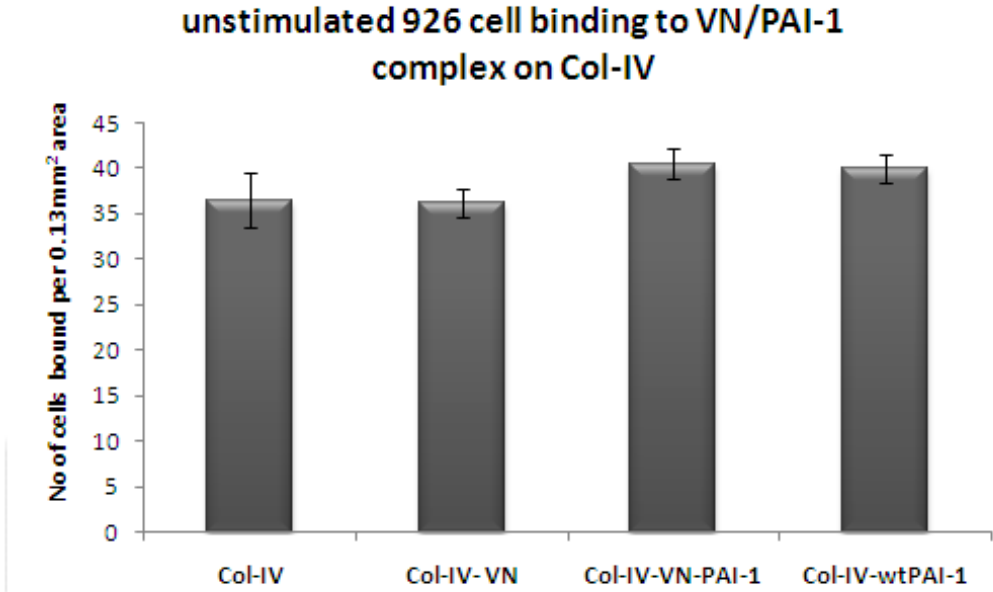
Figure 3. 23: Unstimulated 926 cell binding to VN/PAI-1 complex associated with Col-IV
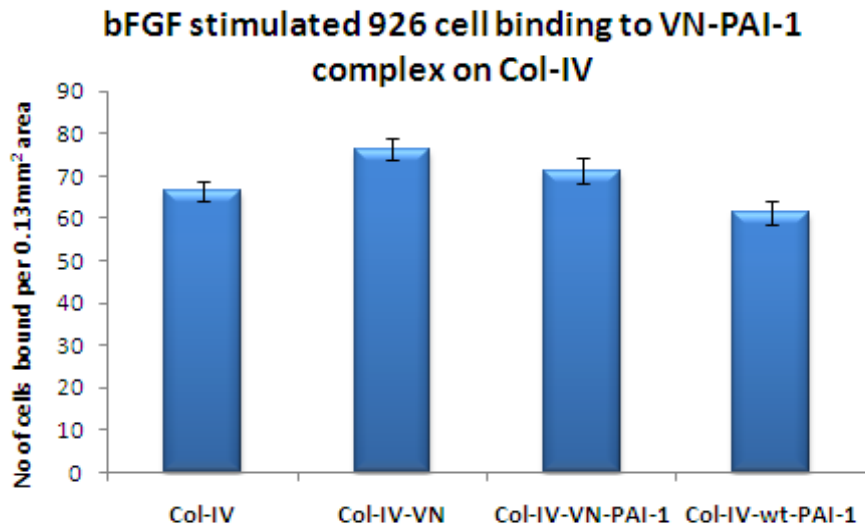
Figure 3. 24: bFGF stimulated 926 cell binding to VN/PAI-1 complex associated with Col-IV
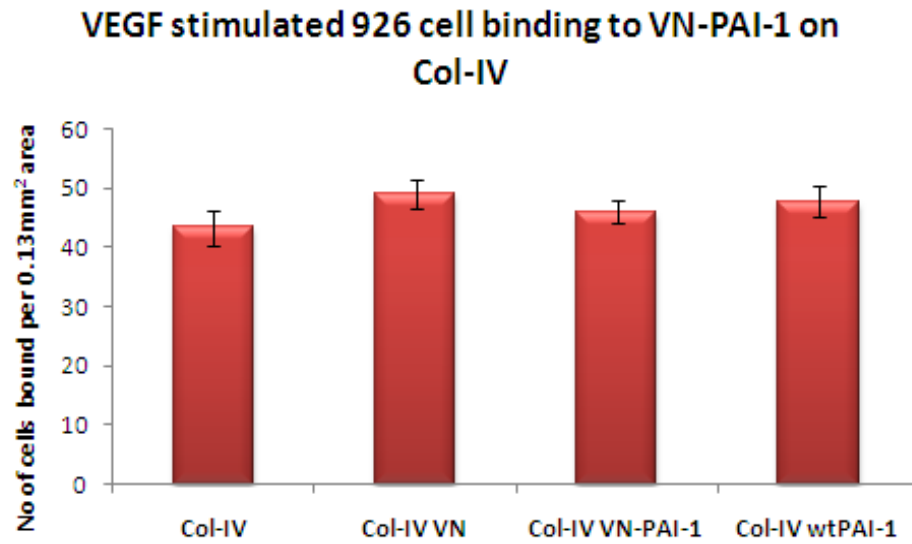
Figure 3. 25: VEGF stimulated 926 cell binding to VN/PAI-1 complex associated with Col-IV

PMA stimulated 926 cell binding to VN/PAI-1 complex on Col-IV
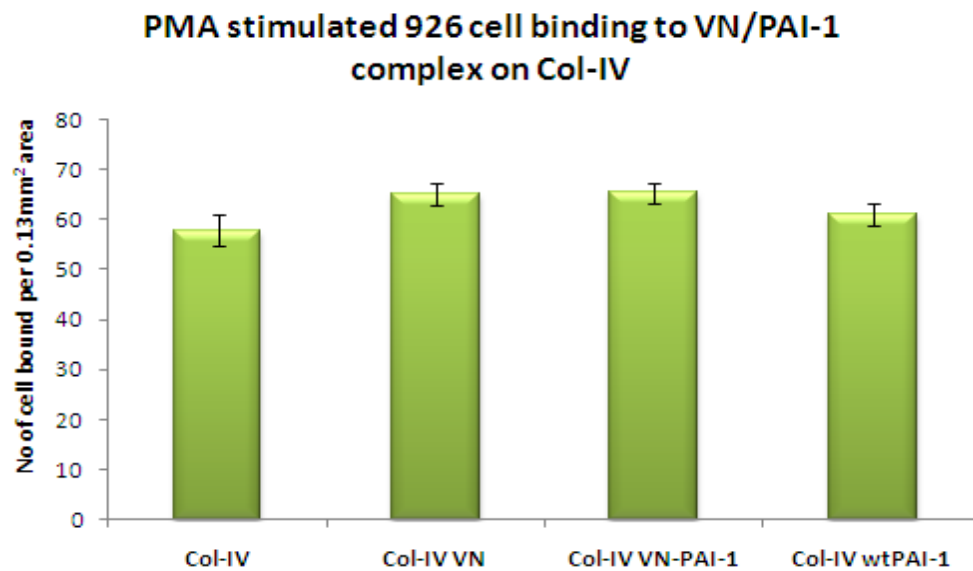
Figure 3. 26: PMA stimulated 926 cell binding to VN/PAI-1 complex associated with Col-IV

of unstimulated, bFGF-, VEGF- and PMA-stimulated EA.hy926 binding to VN/PAI-1 associated with Col-IV. Similar results were obtained with HT1080 cells (data not shown).

Figure-3.27 & 3.28 show the migration of VEGF-stimulated 1080 cells and PMA-stimulated 926 cells on VN or the VN/PAI-1 complex associated with Col-IV, respectively. Both of these results show that, with VN bound to Col-IV, migration was increased several fold. With wtPAI-1, there was essentially no effect on migration. The effect of the multimeric complex is the opposite. With VEGF stimulated 1080 cells, a statistically significant ($P < 0.05$) **increase** in migration compared to VN alone could be observed, whereas with PMA stimulated 926 cells presence of the VN/PAI-1 complex on Col-IV caused statistically significant **decrease** ($P < 0.05$) in migration. **Tables-3.1 & 3.2** summarize the effects of the VN/PAI-1 complexes relative to VN alone on the migration of 1080 and 926 cells under all the tested conditions, respectively. In general, the effect of VN associated with the matrix components was pro-migratory. PAI-1 by itself had no effect on migration, which indicates that other binding partners like VN were required to produce protease-independent effects on migration. The effect of the multimeric complex formed by the interaction between VN and PAI-1 was subject to the specific microenvironment in which it was found. While only a few stimulating conditions showed difference in migration between monomeric VN and the VN/PAI-1 complex, most of the stimulating conditions tested showed that PAI-1 associated with VN in the multimeric complex can have no effect on migration. Conditions under which migration with VN/PAI-1 complex was found to be different from VN alone with statistical significance ($P < 0.05$) have been highlighted in **Tables-3.1 & 3.2**.
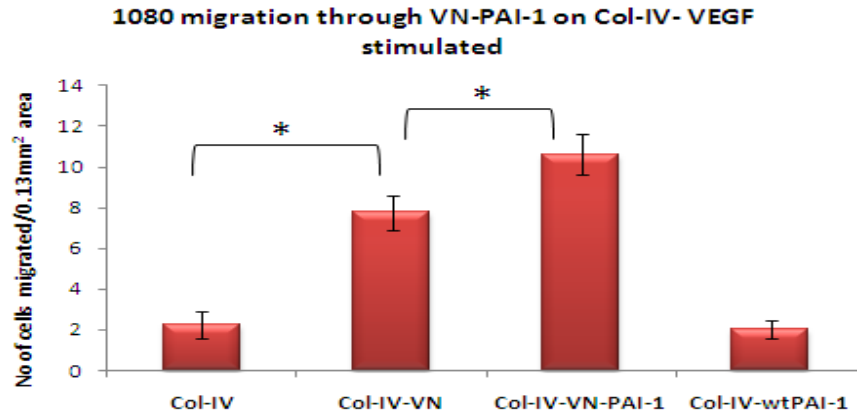
Figure 3. 27: VEGF stimulated 1080 cell migration through VN/PAI-1 complex on Col-IV
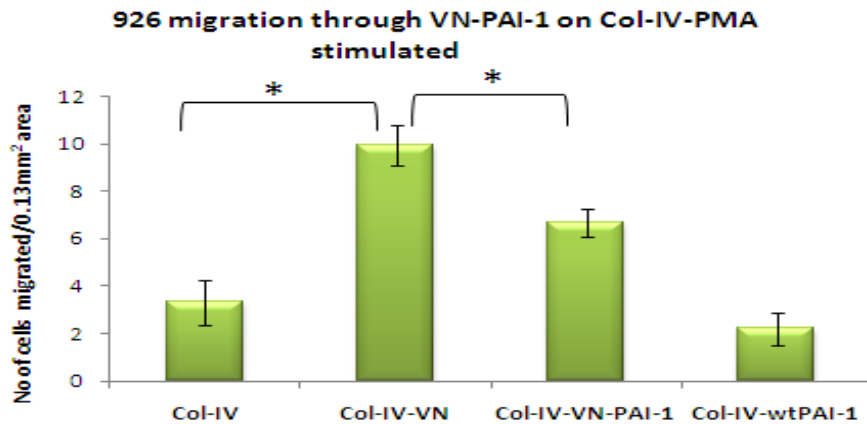
Figure 3. 28: PMA stimulated 926 cell migration through VN/PAI-1 complex on Col-IV

> **Figure-3.27- 3.28: A 100nM concentration of VN was incubated with 200nM wt-PAI-1, and the mixtures were added to inserts coated with Col-IV. VEGF stimulated (Figure-3.27) 1080cells and PMA (Figure-3.28) stimulated 926 cells were added to inserts and migration was continued overnight. Cells were labeled with calcein and the number of cells migrated per 0.13mm^2 area is plotted.**
> ***P<0.05**

Table- 3. 1: Summary of 1080 cell migration experiments

GROWTH FACTOR	CELL LINE	MATRIX	EFFECT OF VN/PAI-1 COMPLEX ON MIGRATION
Unstimulated	1080	HSPG	No difference relative to VN
Unstimulated	1080	Col-IV	No difference relative to VN
bFGF	1080	HSPG	No difference relative to VN
bFGF	1080	Col-IV	No difference relative to VN
VEGF	1080	HSPG	No difference relative to VN
VEGF	1080	Col-IV	Significant increase in migration relative to VN
PMA	1080	HSPG	No difference relative to VN
PMA	1080	Col-IV	No difference relative to VN

Table- 3. 2: Summary of 926 cell migration experiments

GROWTH FACTOR	CELL LINE	MATRIX	EFFECT OF VN/PAI-1 COMPLEX ON MIGRATION
Unstimulated	926	HSPG	Significant decrease in migration relative to VN
Unstimulated	926	Col-IV	No difference relative to VN
bFGF	926	HSPG	No difference relative to VN
bFGF	926	Col-IV	Significant increase in migration relative to VN
VEGF	926	HSPG	No difference relative to VN
VEGF	926	Col-IV	No difference relative to VN
PMA	926	HSPG	No difference relative to VN
PMA	926	Col-IV	Significant decrease in migration relative to VN

3.3. f. Flow Cytometry Study: Receptor Expression on Cell Surface

Cell-matrix interactions are mediated between different matrix components and cell surface receptors, such as uPAR and integrins. We have tested the effect of the VN/PAI-1 complex under a number of possible conditions, and the results obtained from such analyses were exciting and to some extent unexpected. At this point it was important to examine the receptor expression profile of 1080 and 926 cells under all the conditions tested. There are a total of ~24 different kinds of integrin heterodimers [93] expressed on human cells. So it was necessary to carefully select receptors for studying at flow cytometry. Many studies indicate the importance of uPAR on the cell surface for the regulation of PAI-1-mediated effects on cellular adhesion and migration via VN [226-227]. For these reasons, checking uPAR expression was an obvious requirement. Among all the different integrins, the ones that are primarily involved in VN recognition are αvβ3 and αvβ5. We have observed the role of αvβ3 in regulating the PAI-1 mediated effect on adhesion and migration through VN [229-230]. We are also aware that bFGF and VEGF are the known modulators of the expression of αvβ3 and αvβ5 on endothelial cells, respectively. Therefore, we decided to evaluate the expression of these two integrins. We observed in our cell binding assays that there was no considerable effect of VN or the VN/PAI-1 complex while Col-IV was the substratum. It is possible that the expression of specific collagen receptors dominates over the expression of VN receptors. There are four known Collagen receptors (α1β1, α2β1, α10β1 and α11β1) [93]. Out of these, α2β1 has been found to be present in endothelial cells and is known to recognize different kinds of collagens, including Col-IV [289-290], so we decided to check the expression of α2β1. We also checked the expression of α5β1 because we found that VN interacts with this receptor, and we observed that this interaction

145

was even more prominent with the VN/PAI-1 complex. Moreover bFGF was found to cause increase in expression of α5β1 on endothelial cell surface [281].

Figure-3.29 & 3.30 show the basal level (unstimulated condition) expression of all the five receptors on 926 and 1080 cells respectively. As observed except for uPAR, all of the other four receptors were expressed in both the cell lines. Expression of α2β1 was the highest among all the five receptors on 1080 lines, followed by α5β1, αvβ5, αvβ3 and uPAR in the order of their expression level. For 926 cells α5β1 expression was the highest under basal conditions, followed by α2β1, αvβ3, αvβ5 and uPAR in the order of their expression level. Figure-3.31-3.35 and Figure-3.36-3.40 show the expression profiles of each chosen receptor (uPAR, αvβ3, αvβ5, α5β1 and α2β1) in the absence or presence of growth factor stimulation on 926 and 1080 cells respectively. Each panel shows the signal from unstained cells (histogram in gray color). The signal from unstained cell is due to auto-fluorescence. Expression of each receptor under different treatment conditions can be compared relative to this background signal. No uPAR expression was observed on these two cell lines, even under the influence of growth factor stimulation. Expression of αvβ3 did not change under the influence of growth factors on both of the cell lines. Expression of αvβ5 slightly increased in both cell lines with the application of bFGF and VEGF. While PMA caused a greater increase in expression of αvβ5 on 1080, this increase was not observed with 926 cells. Under any given stimulation condition, expression of α2β1 was much higher compared to that of αvβ3 and αvβ5 on both cell lines. Growth factor stimulation had no effect on the expression of α2β1. Expression of α5β1 was also much higher compared to that of αvβ3 and αvβ5 on both cell lines under any stimulation condition. While bFGF and VEGF had no effect on its expression, application of PMA caused a moderate

146

Basal receptor expression
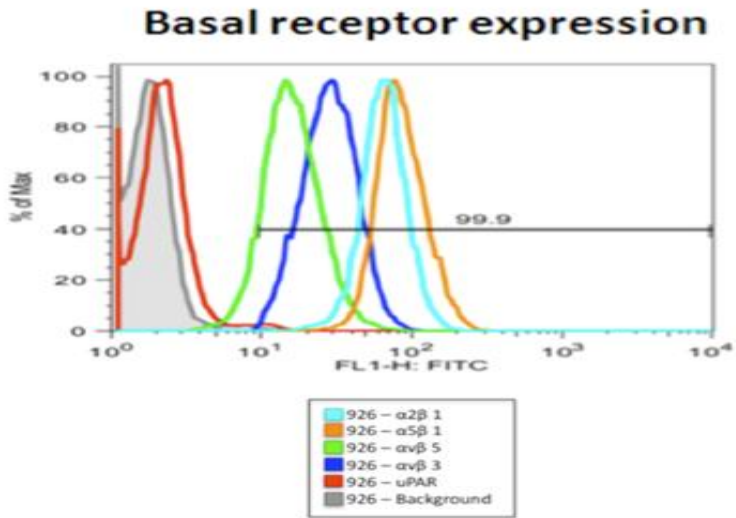
Figure 3. 29: Basal receptor expression- 926 cells

Basal receptor expression
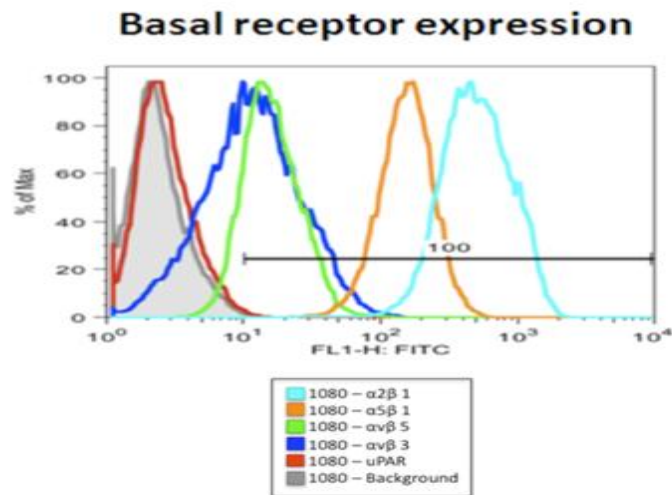
Figure 3. 30: Basal receptor expression- 1080 cells

Figure-3.29- 3.30: Results of the flow cytometry study to compare the basal expression level of uPAR (red), αvβ3 (blue), αvβ5 (green), α5β1 (brown) and α2β1 (turquoise) on unstimulated 926 cells (Figure-3.29) and 1080 (Figure-3.30) cells. The histogram shown in the gray color indicates the unstained cells. The line indicates the average percentage of the population showing signal over background.

Figure 3. 31: uPAR expression on 926 cells- growth factor stimulation
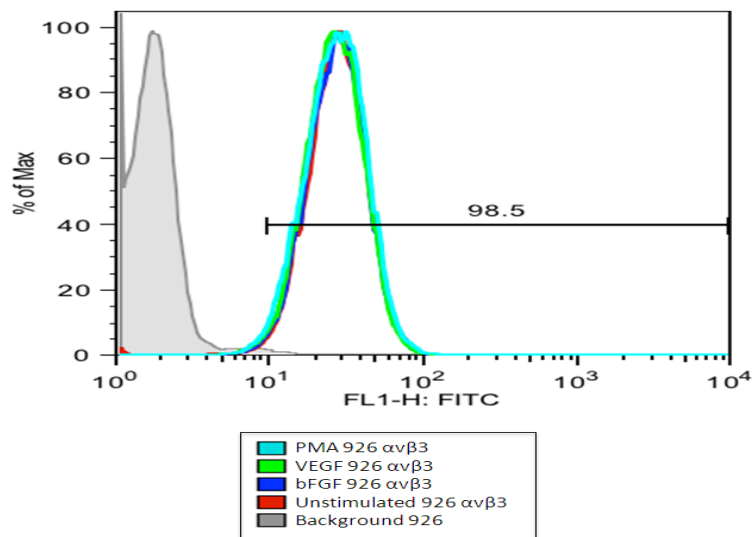
Figure 3. 32: αvβ3 expression on 926 cells- growth factor stimulation
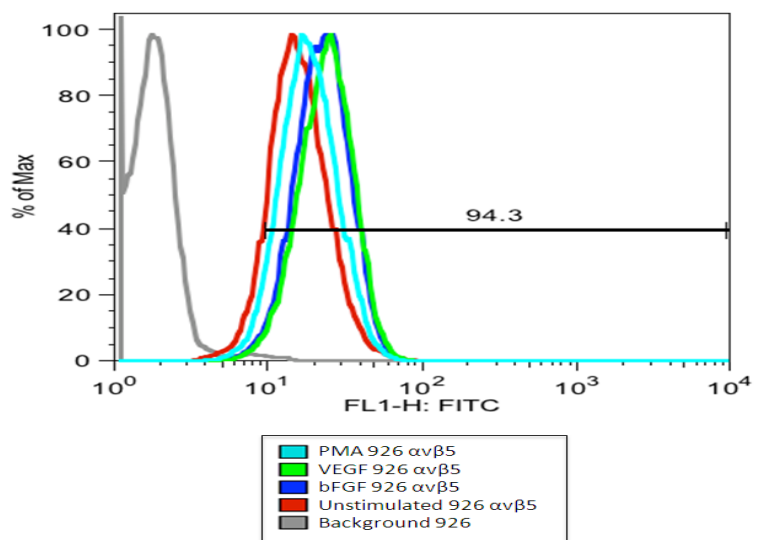
Figure 3. 33: αvβ5 expression on 926 cells- growth factor stimulation
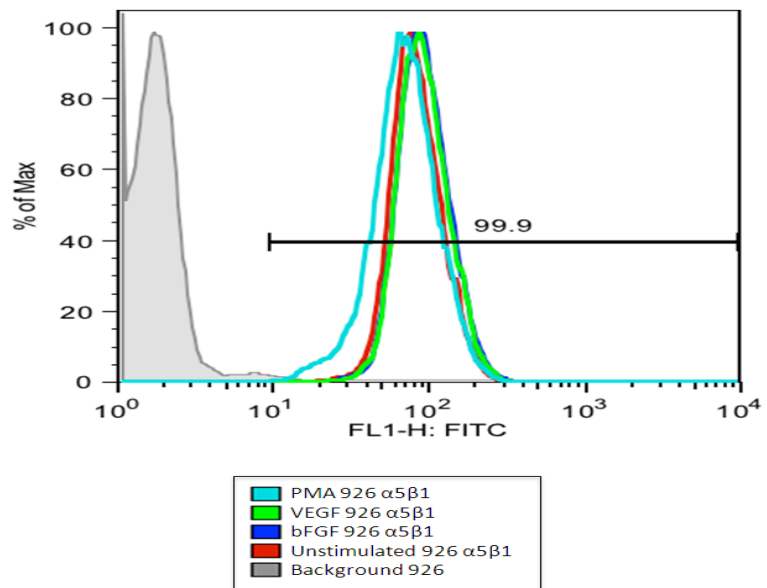
Figure 3. 34: α5β1 expression on 926 cells- growth factor stimulation
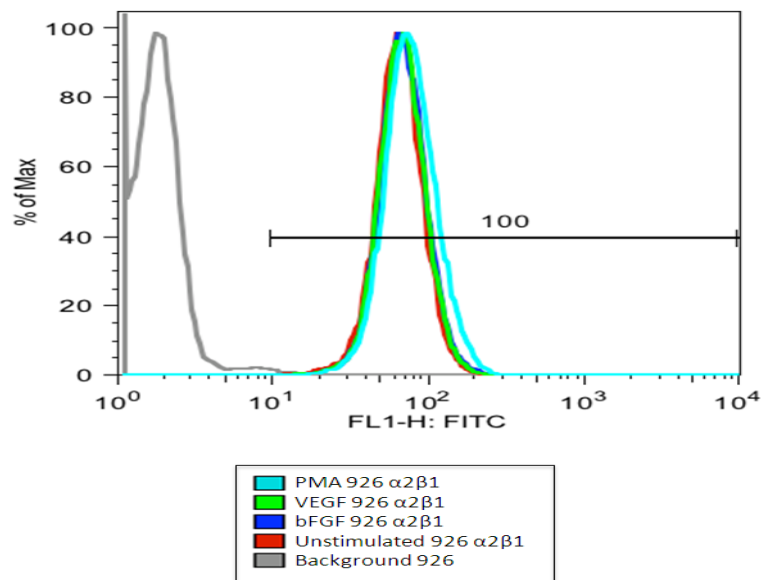
Figure 3. 35: α2β1 expression on 926 cells- growth factor stimulation

Figure-3.36-3.40: A flow cytometry study to check expression of uPAR (Figure-3.36), αvβ3 (Figure-3.37), αvβ5 (Figure-3.38), α5β1 (Figure-3.39) and α2β1 (Figure-3.40) on unstimulated (red), bFGF (blue), VEGF (green) and PMA (turquoise) stimulated 1080 cells. The histogram shown in gray color indicates the unstained cells. The line indicates the average percentage of the population showing signal over background.
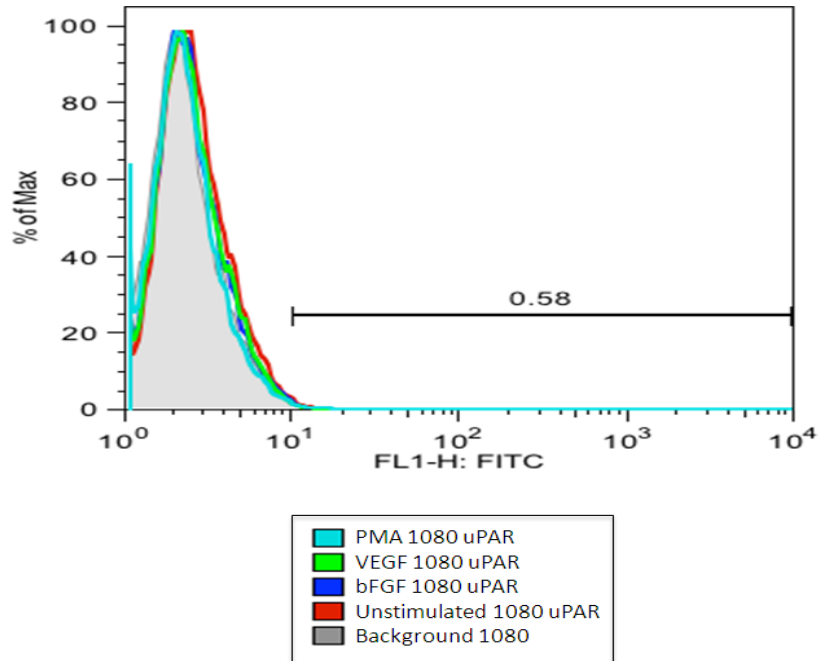
Figure 3. 36: uPAR expression on 1080 cells- growth factor stimulation
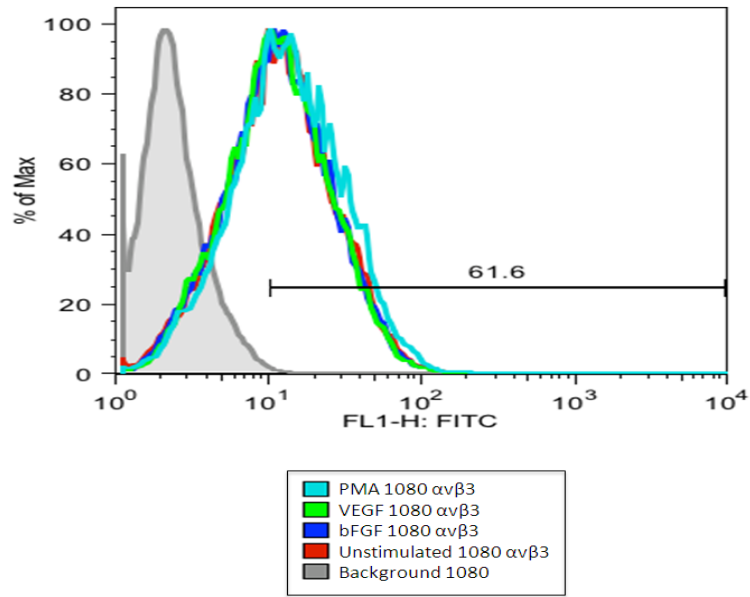
Figure 3. 37: αvβ3 expression on 1080 cells- growth factor stimulation
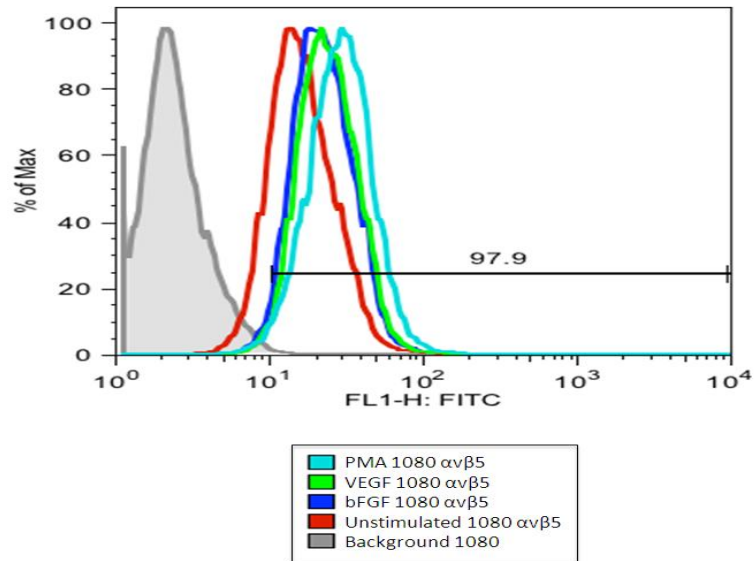
Figure 3. 38: αvβ5 expression on 1080 cells- growth factor stimulation
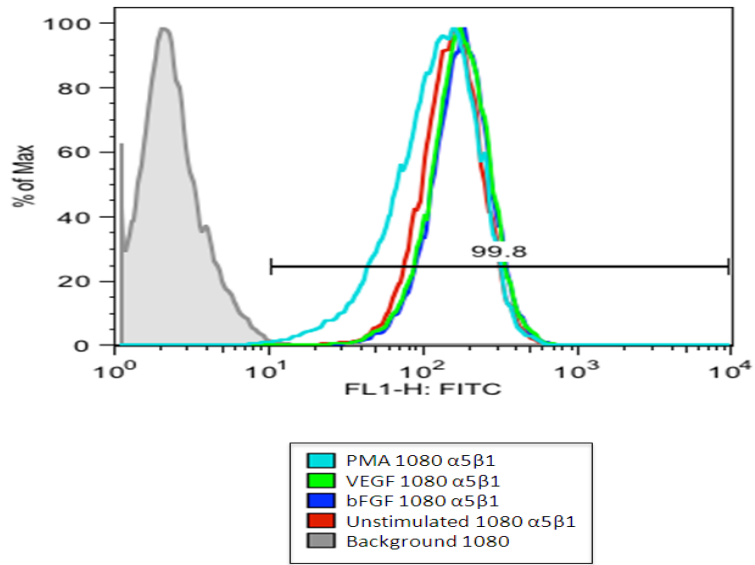
Figure 3. 39: α5β1 expression on 1080 cells- growth factor stimulation
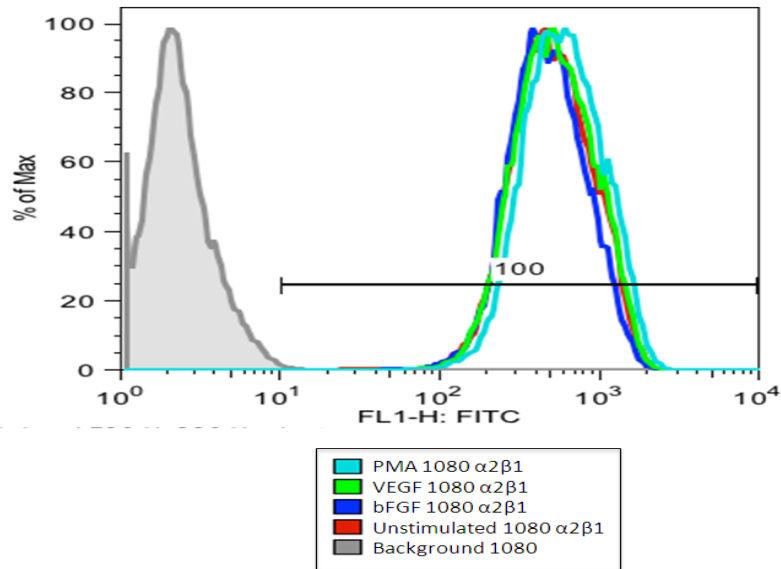
Figure 3. 40: α2β1 expression on 1080 cells- growth factor stimulation

153

decrease in the expression of α5β1 on 926 cells and a slight increase in expression on 1080 cells. Overall it appears that none of the stimulants actually caused a dramatic change in the expression pattern of any of the receptors tested.

3. 4. Discussion

3.4. a. 'Denatured' Multimeric VN vs. 'Biological' Multimeric VN

VN is an important biomolecule involved in various physiological processes. It is found in both the circulation and the extracellular matrix. This molecule shows a preferred conformation and functions specific to its localization. While it exists as a monomer in the circulation, the preferred conformation in the extracellular matrix is multimeric [13-14, 259]. Volker et al. showed that while multimeric VN could readily bind with the monolayer of porcine endothelial cells and the associated subcellular matrix, native monomeric plasma VN showed little binding [259]. Extracellular matrix-associated VN plays an important role in the regulation of cellular adhesion and migration. Though the mechanism of such compartmentalization is not known, the general idea is that a conformational change is required for the transition of the monomeric plasma form into its multimeric matrix associated form. There are studies that indicate that a number of biological molecules may initiate the process of this conformational transition, including thrombin-antithrombin-III (TAT) complex, terminal complement complex (C5b-C7) and PAI-1 [44, 205-206]. Conformational changes initiated by the binding of these molecules expose an epitope that is not found in monomeric plasma form of VN and is recognizable by monoclonal antibodies like, 8E6. Conformational changes also expose the binding sites for heparin. Among these biomolecules, PAI-1 has been considered to be primarily responsible for the conformational transition of VN. Seiffert et al. showed that PAI-1 mixed with

154

monomeric plasma VN causes a conformational transition and multimerization of the latter [206]. This conformational alteration induced by PAI-1 was recognized by the conformational sensitive antibody like 8E6.

Despite the fact that there are a number of biomolecules that can potentially cause the conformational transition of VN, most of the studies related to the matrix-associated form of VN have been limited to the use of a 'denatured' form of VN, formed by various physical methods. Treatment of the plasma form of monomeric VN with urea, guanidine chloride or heat result in the conversion into the homomultimeric form also known as the 'denatured' form of multimeric VN. This 'denatured' form of vitronectin was found to possess the conformational sensitivity usually observed with matrix associated multimeric VN [44, 77]. The main assumption involved in the use of these approaches is that the 'denatured' form of multimeric VN is similar to the naturally occurring matrix associated form of VN. While this approach has been found to be valuable in the understanding the role of VN in regulating cell-matrix interactions, its physiological relevance is questionable. In fact, Seiffert et al found out that platelet-associated multimeric VN is structurally and conformationally distinct from 'denatured' multimeric VN [207]. Their study indicated that platelet-released multimeric VN was significantly smaller in size compared to 'denatured' multimeric VN, and the conformationally sensitive epitopes (for mAb 153, 1244 and 8E6) were more pronouncedly expressed in 'denatured' VN than platelet released VN. Thorough examination and comparison between the multimeric form of 'denatured' VN and the multimeric form produced by biologically relevant processes is still lacking. Thus, the primary motive of our study has been to understand the role of the matrix-associated form of VN in cellular adhesion and migration. These studies have used multimers

155

produced under conditions that more likely replicate the physiological scenario. We consider that PAI-1 is a potential biological factor that can cause the transition of monomeric VN into its matrix-associated multimeric form, and we have used multimeric complexes formed by the interaction of VN and PAI-1 for all our experiments.

In the last few years, our lab has produced data that show that PAI-1 mixed with monomeric VN induces multimerization [209-211]. Also, we have established that PAI-1 remains associated with these multimeric complexes for several hours under *in vitro* conditions.[209-210]. For these reasons, we refer to these multimeric complexes formed between VN and PAI-1 as 'biological' multimeric complexes. In this present study we have mixed PAI-1 and VN so that the 'biological' multimeric complex is formed, and then have used these complexes to check their ability to associate with matrix components like HSPG and Col-IV. A previous sedimentation velocity study showed that VN mixed with various concentrations of PAI-1 yielded multimeric complexes in a dose-dependent fashion [210]. Following the same principle, VN was mixed with differing concentrations of PAI-1 to test the hypothesis that the 'biological' multimeric complexes formed between VN and PAI-1 will associate more readily with matrix components. The extent of association with the matrix components should be proportional to the amount of multimeric complexes present. Consistently, it was observed that increasing concentrations of PAI-1 increased the amount of VN associated with both HSPG and Col-IV in a dose-dependent fashion. This observation supports our hypothesis and suggests that these 'biological' multimeric complexes formed by the interaction between VN and PAI-1 have practical relevance for determining the localization and function of VN in tissues. Another observation is that these 'biological' multimeric complexes did not show an enhanced propensity

to associate with different GAGs, especially heparin. 'Denatured' multimeric VN has previously been presumed to bind heparin better than monomeric VN [48]. However, the 'biological' multimeric complexes formed by the interaction between VN and PAI-1 did not show this tendency, indicating that the assumption regarding 'denatured' VN being an adequate mimic of multimeric vitronectin in the ECM has flaws and should be re-examined.

We have also determined that the successful multimerization requires an interaction between PAI-1 and full length VN. Limiting the interactions to PAI-1 binding to the primary binding site within the SMB domain is not sufficient to cause increased association with the matrix components. The isolated SMB domain mixed with PAI-1 did not exhibit increased association with HSPG or Col-IV, compared to SMB alone. Thus interaction between PAI-1 and full length VN with the more extensive binding interfaces that we have characterized before [168] is required to ensure the successful transition into the multimeric form. If the interaction between these two proteins is inhibited, the conformational transition from the monomeric form to the multimeric form is impaired. We have recently found that an octapeptide that mimics the reactive center loop of PAI-1, while mixed with this protein, almost completely disrupts the interaction between VN and PAI-1, using a sedimentation velocity analysis that showed that almost no higher order multimeric complexes were produced in the presence of this octapeptide (discussed in detail in chapter-2). When VN and PAI-1 were mixed in the presence of this octapeptide and association of VN to matrix components was probed, no increase in VN binding could be observed compared to VN alone. Once again, this result supports our hypothesis that the interaction between VN and PAI-1 that leads to the transformation into the higher order multimeric complexes is required for showing increased association with the matrix components.

157

This octapeptide is supposed to insert within the groove formed between the strand β3A and β5A of PAI-1 and thus block the SMB domain mediated interaction of VN with PAI-1. Once this interaction is blocked formation of higher order multimeric complexes is also inhibited and no increased association of VN with the matrix components is observed. Similar results were obtained when VN was mixed with a mutant of PAI-1 (Q123K) that has very low affinity for VN binding. The sedimentation velocity study shows that this mutant (discussed in detail in chapter-2) while mixed with VN forms very low amount of multimeric complexes compared to wtPAI-1. Once again we can see that blocking the interaction between VN and PAI-1 interfere with the amount of multimeric complexes formed, and that, in turn, is affecting how much increased association of VN could be expected towards matrix components.

3.4. b. Does PAI-1 Always Negatively Interfere with the Interaction Between VN and Cell Surface Receptors?

The most widely accepted role for PAI-1 regarding the interaction between VN and its common cell surface receptors is as a general inhibitor that disrupts the interactions of vitronectin with molecules such as uPAR or integrins. According to previous studies, the interaction between uPAR and 'denatured' multimeric VN was inhibited by exogenously added PAI-1 [226-227]. The uPAR-binding site on the SMB domain appears to overlap with the PAI-1-binding site, so that PAI-1 and uPAR compete for binding to VN [103]. Similar results were observed with VN binding to αvβ3; binding of 'denatured' multimeric VN to αvβ3 was blocked by the addition of PAI-1 [229, 277]. Though the RGD domain responsible for integrin recognition does not appear to be directly blocked by PAI-1 binding [22] in the crystal structure

158

between the SMB domain and the 14-1-B form of PAI-1, steric interference resulting from the proximity of the PAI-1-binding and integrin-binding sites has been thought to be the cause of the inhibitory effect of PAI-1 on the VN-integrin interaction. The interaction of PAI-1 with VN has been proposed to be a molecular switch [186, 227, 229]. According to Smith and his group, PAI-1 binding to monomeric VN causes a conformational change and an opening up of the cryptic cell adhesion site (for integrin binding) on VN, but that site remains inaccessible as long as PAI-1 is bound. This model assumed that, once PAI-1 is released, the cell adhesion site becomes available on VN and integrin binding can occur [277]. Release of PAI-1 from VN can be initiated by the interaction of the cell surface bound urokinase also. Binding of protease by the serpin causes significant decrease in affinity of PAI-1 for VN and may lead to release of PAI-1 from matrix associated VN [186, 232]. Seiffert et al. performed some studies where they used PAI-1 to cause multimerization of VN, but waited for 16hrs until PAI-1 was released from these multimeric complexes. These multimeric complexes of VN showed increased binding to αvβ3, but such binding could be blocked by exogenously added PAI-1[277]. In this current study we have taken a more realistic approach by using 'biological' multimeric VN that remains associated with PAI-1. Use of this 'biological' multimeric complex of VN formed by the interaction with PAI-1 allowed us to check what physiological roles they play and also revisit the role of PAI-1 in regulating the interaction between VN and its receptors, while present as a part of the 'biological' multimeric complexes.

Testing for receptor-ligand binding with the receptor immobilized on the plate is a common method that we have employed to test for the ability of the multimeric complexes to recognize immobilized uPAR. Monomeric VN was mixed with varying concentrations of PAI-1,

and the resulting multimeric complexes tested for binding to uPAR. With increasing

concentrations of PAI-1, binding of VN to uPAR increased in a dose-dependent fashion. Thus, in

these measurements, the presence of PAI-1 within the complexes did not inhibit the interaction

between VN and uPAR, although the time scale of the experiment (only a few hours) ensures

that PAI-1 remains in the multimeric complexes during the experiment. In an alternative

approach, we directly probed the binding of uPAR to the 'biological' multimeric complex bound

to the plate directly or associated with other matrix components, such as HSPG or Col-IV. For

directly probing uPAR binding, an antibody was chosen that recognized an epitope that does not

interfere with the interaction between uPAR and VN. This approach again showed that uPAR

binding to the 'biological' multimeric complex of VN was not blocked by the presence of PAI-1.

Presence of PAI-1 in the matrix (both Col-IV and HSPG), following addition of VN/PAI-1

complex was confirmed in separate study by using an antibody against PAI-1 (data not shown).

Little uPAR binding could be detected with monomeric VN associated with matrix components

or directly with the plate; however, this finding is not altogether surprising and can presumably

be explained by the proposed difference in binding affinity between monomeric VN and

multimeric VN for uPAR [278]. Clearly, uPAR binding was observed for the 'biological'

multimeric complexes formed between VN and PAI-1, but it is not clear how the interaction

between uPAR and VN occurs in the presence of PAI-1, as the two binding sites are known to

overlap. It is possible that another uPAR binding site, which lies at the C-terminal heparin

binding domain, as proposed by Waltz et al. [226], becomes more exposed following the

conformational transition.

We have also tested the ability of these 'biological' multimeric complexes to recognize different integrin receptors. Previously we have shown that these complexes associate more readily than VN alone with αvβ3 and αIIbβ3 integrins [209]. In this current study, we observed that PAI-1 present in the multimeric complexes also did not block VN binding to integrins αvβ5. Furthermore, we found that monomeric VN could interact with α5β1, a known fibronectin receptor. Though the interaction was weaker compared to that of with αvβ3 and αvβ5, these 'biological' multimeric complexes showed an increased association with α5β1 compared to monomeric VN. In an alternative approach, we also probed αvβ5 binding to monomeric VN and 'biological' multimeric VN directly bound to the plate. Though not much binding was observed with monomeric VN, binding increased several fold with multimeric VN. Lack of binding to monomeric VN once again is thought to be due to an affinity issue, with monomeric VN exhibiting a lower affinity than the 'biological' complexes. Surprisingly, no binding of αvβ5 to either monomeric or multimeric VN could be detected while the proteins were present with other matrix components like HSPG and Col-IV. There is a possibility that the epitope for the C-terminally directed antibody against the αv subunit is not easily accessible by the antibody under this situation. Another possibility is that the specific activation state of αvβ5 that we are dealing with under the current experimental conditions is not suitable for tight binding to the matrix associated monomeric or multimeric VN. In other words the binding site for αvβ5 binding on monomeric VN or 'biological' multimeric VN has very low affinity while they are associated with the matrix components like Col-IV and HSPG.

3.4. c. PAI-1 Effects on Cellular Adhesion and Migration: Significance of the Pericellular Environment.

The effect of PAI-1 and its interaction with VN on the regulation of cellular adhesion and migration is an interesting subject. There is still no a consensus on the role of these two proteins and their interaction in the regulation of cell-matrix interactions. The literature is full of opposing claims made by different groups. Some studies say that PAI-1 inhibits cell binding to VN but promotes migration, while others say that PAI-1 inhibits migration through VN [226-227, 229-230]. Though the effect of PAI-1 on migration has been found to be variable, as far as its effect on cell binding is concerned, most of the studies indicate that PAI-1 acts as an antiadhesive molecule when cell binding occurs through VN. The majority of these studies were aimed at understanding the role of exogenously added PAI-1 in regulating cellular adhesion and migration mediated by 'denatured' multimeric VN. Our approach has been different from these studies in two ways; first, it is more reflective of natural environment because PAI-1 is present and bound to vitronectin, and second, it is thorough in looking at a wide variety of biological settings with different cell types and tissue components. We have compared the role of monomeric VN and 'biological' multimeric VN on cellular adhesion and migration in the context of other matrix components such as HSPG and Col-IV. Also, we have placed emphasis on modulating the pericellular microenvironments in which adhesion and migration are happening, as we believe the specific role the multimeric complex formed between VN and PAI-1 may have on cellular adhesion and migration is sensitive to the surrounding environment. The specific microenvironment in which the adhesion or migration takes place is comprised of different matrix components, different cell types and different receptors expressed on their surface. The

choice of cancer fibroblast (HT1080) and endothelial (EA.hy926) cells for our work has provided the context of a cellular environment for angiogenesis. We have also used PMA and different growth factors, including bFGF and VEGF, in order to modulate receptor expression on the cell surface. The choice of growth factors was based on previous studies that showed changes in receptor expression on the surface of HDMEC (endothelial cells) [96, 288].

The results of our adhesion studies do not support the majority of studies in the literature. The presence of 'biological' multimeric complexes on either HSPG or Col-IV neither inhibited nor promoted cellular attachment relative to VN alone. With HSPG, VN caused some increase in binding of the 'biological' complexes, while the presence of Col-IV did not lead to differential effects for VN or its multimeric form on cellular adhesion or migration. This result was similar with both cell lines, and the presence of growth factors also did not cause a difference in adhesion. When isolated PAI-1 was associated with Col-IV, it had no effect on adhesion or migration, but PAI-1 associated with HSPG appeared to increase cell binding to some extent and this increase in binding was the same for the multimeric complexes. VN was found to promote migration under all conditions, whereas isolated PAI-1 bound to the matrix components had no effect on migration. The effect of the 'biological' multimeric complex on migration was variable. While under most conditions it neither promoted nor inhibited migration relative to VN alone, under a few conditions it exhibited both promigratory and antimigratory effect. For example with Col-IV as the matrix component, VEGF stimulated 1080 cells showed a statistically significant **increase** (P<0.05) in migration, whereas PMA stimulated 926 cells showed a statistically significant **decrease** (P<0.05) in migration compared to VN alone.

There are examples from other studies where VN was found to promote migration of different cell lines, such as SMCs (smooth muscle cell line) and keratinocytes [291-292]. There are also other studies in which PAI-1 had no effect on cellular attachment but caused a decrease in cellular migration. Stefansson et al. showed that PAI-1 did not have any effect on cellular attachment of SMCs while 'denatured' multimeric VN was associated with matrigel, an artificial ECM mimic. However, under similar conditions, PAI-1 blocked migration of SMCs via 'denatured' multimeric VN associated with matrigel [229]. Stefansson et al. suggested that the lack of an effect of PAI-1 on cellular attachment was due to the presence of receptors that recognized matrix components other than VN. Following a similar line of rationale, we performed a flow cytometry study to test for the expression of a number of receptors (uPAR, αvβ3, αvβ5, α5β1, α2β1) on the surface in the two cell lines upon growth factor treatment. Under any condition, irrespective of growth factor stimulation and among all the receptors tested, α2β1, the collagen receptor, showed very high expression in both the cell lines. Because of this abundance of the collagen receptors, it is possible that no differential effect of monomeric or multimeric VN could be observed using Col-IV as the matrix substratum. Another striking observation from flow cytometry was that uPAR was not found to be expressed in either of the cell lines under any of the conditions tested. Since uPAR is a cell surface receptor that recognizes only VN among all the matrix components, the absence of this receptor may account for the relative insensitivity of the cells to the presence of monomeric or multimeric VN in the matrix. The effect of uPAR could be exclusively tested using cells like U937, which show high levels of uPAR expression on the surface [293].

164

Though some increase in cell binding could be observed with monomeric VN while associated with HSPG, the presence of the 'biological' multimeric complex with HSPG did not promote additional cell binding. We know from our matrix binding assay that such 'biological' multimeric complexes of VN associate more with matrix components like HSPG. While the presence of more VN was expected to provide more binding sites for cell surface receptor interaction, no increase in cell binding was observed. It may appear that the multimeric form of VN is providing multiple contact points for a single cell. Integrin clustering at focal adhesions at the leading edge of cells is a common phenomenon that provides added strength of binding [294]. So the presence of the multimeric VN might be associated with the strength of binding by providing multiple connection points for integrins expressed at the focal adhesion surface of the cell. This would result in the increase in the strength of the cell binding rather than the total number of binding. Alternatively, it may be that the binding of one cell masks multimeric complexes so that they are inaccessible for further cellular attachment. Regardless, the presence of PAI-1 in the multimeric complexes did not inhibit cellular attachment, and this appears opposite to with the prevailing opinion in the literature from studies with a different experimental design.

While the results for cellular adhesion followed a general pattern with respect to the effect of 'biological' multimeric complexes of VN, the results regarding migration were more variable. Once again, that signifies a more complicated process. As expected, the increase in the cell migration due to the presence of monomeric VN in the substratum was several-fold higher relative to the ECM components alone. However, the change in migration due to the presence of the 'biological' multimeric complex of VN was significant only in some cases, but not dramatic

165

compared to the levels observed with monomeric VN. A flow cytometry study told us that none

of the growth factors had any notable effect on the expression pattern of any of the receptors

tested. Any changes observed were moderate. Perhaps other integrin receptors are more

significantly affected under the given conditions. What we have observed demonstrates that PAI-

1, while associated with the matrix as a part of the 'biological' multimeric complex of VN, will

not necessarily promote or inhibit migration. The specific effect of PAI-1 on the regulation of

cellular adhesion and/or migration, while acting as a biological partner for the conformational

and oligomeric transition of VN, is strongly influenced by the pericellular environment.

CHAPTER-4

Evaluating the Role of Vitronectin in the Pathogenesis of *Candida albicans* Infection

4. 1. Introduction

Vitronectin (VN) is a glycoprotein found in both the circulation and extracellular matrix [13-14, 259] that has important functional roles in controlling hemostasis and different pathological conditions. The multifunctional nature of this protein results from its ability to recognize different ligands, e.g. the thrombin-antithrombin complex (T-AT) [44-45], heparin [46-48], PAI-1 [49-51], complement proteins [52] and cell surface receptors like integrins and the urokinase plasminogen activator receptor (uPAR) [53-59]. The circulating pool of VN has a role in regulating coagulation, fibrinolysis, wound healing, and thrombosis [61-62, 66]. On the other hand, extracellular matrix associated VN has an important role in controlling cell-matrix interactions and cell signaling [13]. Regulation of the cell-matrix interactions results from its ability to act as a matrix protein that can bind to different cell surface receptors like uPAR and certain subclasses of integrins ($\alpha v \beta 3$ and $\alpha v \beta 5$) [92] that govern cellular adhesion and migration.

In last few years, researchers have begun to understand the importance of VN in pathogenic infections. A number of studies have been published indicating the significance of VN in the regulation of host-pathogen interactions. For example, Duensing et al. for the first time showed that VN was required for the internalization of *Neisseria gonorrhoeae* by CHO cells [295]. Later, Dehio et al showed that the internalization of *Neisseria gonorrhoeae* into epithelial

cells (HeLa cells) was mediated by VN, and the process also required binding of VN to integrin αvβ5 (primarily) and αvβ3 [296]. Li et al. proposed that the infection of *Staphylococcus epidermidis,* the most common infection to be found in patients undergoing shunt implantations, is mediated by the vitronectin [297]. They showed that VN adsorbed on the surface of the shunt provides sites for bacterial adhesion and colonization [297]. Bergmann et al. established the importance of VN as a host cell component in the uptake of *Streptococcus pneumoniae* [298], demonstrating that VN bound on the cell surface mediated adherence and invasion of the bacteria in to the epithelial and endothelial cells [298]. They also showed in that study that the internalization of the pathogen inside the host cells occurs in an αvβ3-dependent manner.

Involvement of VN in fungal pathogenesis has also become evident in the last few years. Fungal infection (such as *Candida albicans, Cryptococcus neoformans, Pneumocystis carinii*) in the lung is known to cause increase in the secretion of inflammatory mediators such as tumor necrosis-α (TNF-α) [299-301]. For many of these fungal infections, release of TNF-α happens following the binding of the macrophage through the β-glucan present on the fungal cell wall [301-302]. It has also been demonstrated that VN increases macrophage recognition by *P. Carinii* and *C. albicans* [303-304]. Olson et al. showed that VN could bind to the β-glucan present on the cell wall of *Pneumocystis carinii* and this interaction in turn helped fungal binding to the macrophages and the subsequent release of TNF-α [305]. Spreghini et al. reported the presence of VN receptors on the surface of *C. albicans* that were antigenically and functionally related to the mammalian αvβ3 and αvβ5 receptors [108]. The application of the antibodies that block the function of αvβ3 and αvβ5 interfered with the interaction of *C. albicans* with VN; when VN was added exogenously, the interaction of the pathogen with the endothelial cells was

blocked [108]. Santoni et al. used immunochemical analysis to show that αvβ3- and αvβ5-like

receptors were present on the surface of the germ tube of *C. albicans* [306]. Binding of these

germ tubes to VN and to endothelial cells (EAhy.926 cells) could be significantly blocked by the

addition of RGD based peptides and function blocking antibody against αvβ3 and αvβ5 [306].

Based on the potential involvement of VN in fungal pathogenesis and the presence of

integrin αvβ3, αvβ5 like receptors on the cell surface of C. albicans, our lab began a

collaboration with Dr. Jeffrey Becker to use a genetic approach to further explore the role of VN

in the progression of *C. albicans* pathogenesis. A systemic infection with *C. albicans* (strain:

SC5314) was carried out in control mice (C57BL/6) and VN knock-out mice generated in the

background of C57BL/6. This knock-out line was generated by David Ginsburg and his group

and was found to be normal in terms of development, fertility and survival [307]. Infection with

C. albicans resulted in a marked difference in terms of survival between the wild type and the

knock-out mice. **Figure-4.1** shows the results on the survival of these two strains upon injection

with an inoculum of 1×10^5 and 5×10^4 cells of the SC5314 strain of *C. albicans*. This figure

clearly shows a significant difference in survival between the strains upon *C .albicans* infection

and also indicates that the VN knock-out mice are more tolerant to the *C. albicans* infection.

Increased survival of the VN knock-out mice could be due to a variety of reasons.

Perhaps the absence of VN did not allow the pathogen to interact with the host cells, and as a

result it took a longer time for the infection to progress. It is also possible that the increased

death rate of the wild type mice was due to the adverse immune response resulting from the

infection. The absence of VN in the knock-out mice might interfere with the adverse

manifestation of the immune reaction, leading to increased survival. The requirement of VN

Figure 4. 1: Composite survival curve- *Candida* infection

Figure-4.1: Composite survival curve of *C. albicans* infection on wild type and VN knock-out mice from two different experiments. In one experiment, the inoculum containing 10^5 cells was injected to each mouse, and the other experiment had $5x10^4$ cells injected to each mouse. These data show a significant difference in survival between VN knock-out and wild type mice. VN knock-out mice were found to be more tolerant to *C. albicans* infection. These data are attributed to Sara Kauffman, Christine Schar, Cynthia Peterson and Jeff Becker.

for recognition of macrophages and subsequent release of TNF-α has been shown with *C. albicans* and other types of fungi [303-304, 308]. The purpose of this current study is to understand the increased survival in the the absence of VN. We are currently focusing on comparing neutrophil invasion, cytokine expression and colonization of *C. albicans* in different tissues, including lung, kidney, blood and spleen.

4. 2. Materials and method

4.2. a. Infection of mice with *C. albicans*

For all the *C .albicans* infection experiments, only male mice were used. Vitronectin knock-out mice (generated at the background of C57BL/6) were initially provided by David Ginsburg (Univ. of Michigan, Ann Arbor). They were maintained and bred in our animal facility at University of Tennessee, Knoxville. Wild type C57BL/6 mice were purchased from Harlan Sprague Dawley, Indianapolis, IN. For infection studies, C57BL/6 mice were purchased so that their age matched the knock-out mice. The age of the mice ranged between 7-8 weeks during infection. Infection was carried out with the virulent strain of *C. albicans.* , SC5314. The night before the infection, SC5314 was cultured in 50ml YEPD media with constant shaking at 30^0C. After overnight culture, cells were harvested and washed twice with 1XPBS, and a final suspension of 10^6cells/ml was made in 1XPBS (phosphate buffer saline) in a sterile environment. 100µl of this cell suspension was injected using a 0.5 cc insulin syringe (purchased from BD Bioscience) through the dorsal tail vein of each mouse (10^5cells/mouse). The Falcon tube in which the original cell suspension was stored was shaken from time to time in order to maintain the uniformity of the cell suspension. In each group (wild type and knock-out) there were at least 24 mice were included for the infection study.

4.2. b. Collection of tissue for the analysis of fungal burden, cytokine expression and myeloperoxidase assay.

Following infection, mice from each group (wild type and knock-out) were sacrificed on day 6, 8, 11 and 14. An equal number of mice were sacrificed (five) at each time point, except for day-14. On day-14 there were always more knock-out mice present than wild type due to their increased survival. In another set of infections, tissues were collected at day 5, 9 and 14. Various tissues were collected, including lung, kidney, spleen and blood. Collection of blood was carried out following a terminal procedure. Briefly, mice were anaesthetized, and blood was collected through retro-orbital bleeding into BD Microtainer tubes that are designed to enhance coagulation. Tubes containing blood were stored in ice. From the collected blood, 50µl was mixed with 450µl DI (deionized) water and stored for the fungal burden assay. Following collection of blood, mice were killed by vertebral dislocation, and kidney, lung and spleen were harvested. Kidney and spleen from each mouse were stored in sterile tubes for fungal burden and cytokine analysis. For each mouse and for each type of tissue, a separate tube was used. Each tube contained 1ml of sterile 1XPBS mixed with protease cocktail inhibitor (purchased from Roche). Lung from each mouse was divided approximately into two portions. One portion was collected in a tube containing 0.5ml of 1XPBS mixed with protease cocktail inhibitor and the other portion was wiped on clean tissue to remove excess blood and then collected into a tube for myeloperoxidase assay. Tubes containing tissues were left at -80^{0}C for further analysis.

4.2. c. Fungal burden and cytokine expression analysis

For the fungal burden analysis of blood, the mixture of 50µl blood and 450µl DI water that was made during tissue collection was directly mixed with 3ml of noble-agar (liquefied at 55^0C), and the mixture was plated on to YEPD plates and incubated for 48hours at 30^0C. The number of colony forming units present on each plate was counted. The rest of the blood that was stored in the BD Microtainer tube was centrifuged at 4^0C for 10min at 15000rpm, and the separated serum was collected from the top and stored at -80^0C fro cytokine analysis.

For fungal burden analysis on kidney and spleen tubes were thawed and weight of the tissue in each tube was measured. The specific weight of the tissue from each tube was obtained as follows:

(Weight of tissue in each tube) =

(Weight of the whole tube with tissue & buffer) – (Weight of the tube with buffer only)

In order to obtain the 'weight of the tube with buffer only', five empty tubes were filled with 1ml 1XPBS mixed with protease cocktail inhibitor and weighed to calculated the average weight. Tissues were then sliced into small pieces using a razor blade, and the sliced tissues were homogenized by a polytron homogenizer for 30-45 seconds. 10µl of homogenized kidney from each sample was transferred to tubes containing 0.5ml DI water for the fungal burden assay. For the spleen, 50ul of the homogenized tissues was used for fungal burden assay. The content of each tube collected for the fungal burden assay was mixed with 3ml noble agar (liquefied at 55^0C), and the mixture was directly plated on to a YEPD plate followed by incubation for 48 hours at 30^0C. After 48hours, the number of colony forming units (CFU) from each plate was counted, and the fungal burden in terms of number of CFU/gm of tissue was plotted for each

group of mice at each time point. The rest of the homogenized tissues were centrifuged at 12000rpm for 15min, and the supernatants were stored at -80^{0}C for cytokine analysis.

For cytokine analysis the homogenized tissue (frozen) samples were sent to Dr. Chad Steele's lab at University of Alabama, Birmingham and the analysis, was done following a multiplex procedure using a 23-plex kit purchased from Biorad. This kit allows analysis of 23 different cytokines at the same. The basic scheme of the method is depicted in **Figure-4.2**. Briefly the tissue extract is incubated with antibody-coupled beads. For each different cytokine, a specific antibody is used. The mixture is then centrifuged to pull down the bead-coupled antibody attached to the specific cytokine. Biotinylated detection antibody is then added to the mixture to test for binding to the cytokine that is attached to the bead-coupled antibody. Following incubation, PE (phycoerythrin) conjugated streptavidin is added and read in a Bio-plex suspension array system.

4.2. c. Myeloperoxidase assay

The following reagents were made for myeloperoxidase assay.

MPO buffer

50mM potassium-phosphate, pH-6.5. Stored at room temperature.

HTAB buffer:

0.5% hexadecyltrimethylammonium bromide (HTAB) (w/v) made in MPO buffer. Stored at room temperature.

O-dianisidine HCl solution
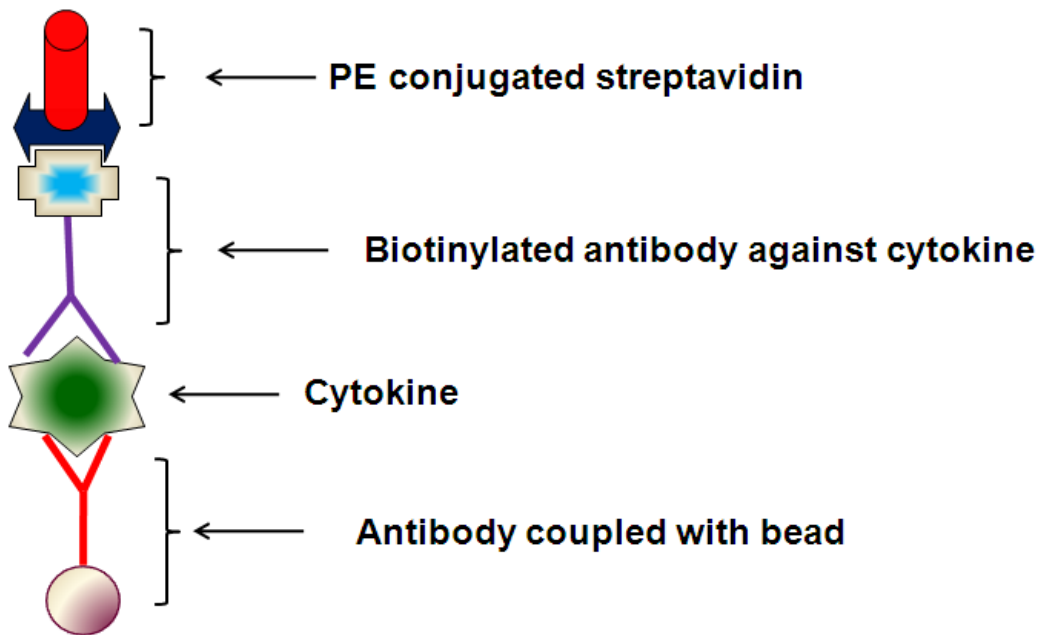
Figure 4. 2: Basic scheme for multiplex analysis

Figure-4.2: Basic scheme of multiplex analysis for checking cytokine expression. Antibody coupled to the bead is used to isolate a specific cytokine. Another specific antibody conjugated with biotin is then allowed to bind to the cytokine. Streptavidin conjugated PE is then added to bind to the biotinylated Ab and read at Bioplex system.

175

16.7 mg O-dianisidine-HCL was dissolved in 90ml DI water and 10ml MPO buffer. The container was wrapped with an aluminium foil and stored in dark at 4^0C.

Lung tissue for myeloperoxidase assay was stored in sterile tubes at -80^0C. Tissue was thawed and the weight of the tissue was measured similarly to what has been described before.

(Weight of tissue in each tube) =

(Weight of the whole tube with tissue) – (Weight of the empty tube)

Five empty tubes were taken and each of these tubes was weighed and the calculated average weight was used as 'weight of the empty tube'. 1ml of HTAB buffer was added to each tube, and the tissue from each tube was sliced using a razor blade. The sliced tissue was homogenized using a polytron homogenizer for ~ 30-45 seconds. 30µl of the homogenized tissue was transferred to a tube containing 500µl of DI water, and this mixture was used to check the fungal burden in lung following the same method as described for kidney and spleen above. The rest of the homogenized tissue was centrifuged at 12000rpm for 30min at 4^0C. The supernatant was collected, distributed in smaller aliquots and stored at -80^0C for the future analysis of myeloperoxidase activity.

For performing the assay for myeloperoxidase activity, the aliquots of lung tissue samples were thawed. A portion of the thawed aliquot was diluted 8-fold and used for measuring the total protein concentration in that sample using the Bio-Rad DC protein assay. This assay was done in 96-well plates, and the absorbance of the reacted samples was measured in a plate reader following the protocol from the manufacturer. A standard curve was generated using the protein-standards provided with the kit. This standard curve was used for calculating the total protein concentration in the lung tissue extract. For each ELISA plate, a separate standard curve

was generated. Each sample was measured in triplicate. In order to calculate the crude myeloperoxidase activity in the lung, 5µl of the lung homogenate from each sample added to the wells of a 96-well plate. The same aliquot that was used for total protein concentration measurement was used for measuring myeloperoxidase activity. O-dianisidine HCl solution was warmed at 37^0C and mixed with 0.3% hydrogen-peroxide (1:600 dilution, final concentration 0.0005% hydrogen peroxide.). 200µl of the mixture was added to each well containing 5µl of the lung homogenate, and the plate was read at 450nm using the Synergy Labtek plate reader following a kinetic assay condition (total run time: 10min, each cycle: 30sec with 3sec shaking before each cycle). Each sample was measured in triplicate. The absorbance at 10min (when the myeloperoxidase reaction has ended) for each sample was normalized with respect to the total protein concentration for that sample and the average normalized myeloperoxidase activity for each time point was plotted for each group of mice (wild type and knock-out).

4. 3. Results and discussion

4.3. a. Fungal Burden Analysis Shows no Difference between Wild-type and Knock-out Mice

Systemic infection of mice with *C* . *albicans* results in the distribution of the pathogen in a wide variety of tissues, including kidney, heart, spleen, thymus, brain and liver [309]. Out of these tissues, the kidney has been found to be the site for most extensive fungal colonization [309-310]. Thus, the kidney was our first choice for comparing the fungal burden between *C* .*albicans* infected male wild type and VN knock-out mice. **Figure-4.3** shows the number of colony forming units (CFU) present per gram of kidney tissue at different post infection time
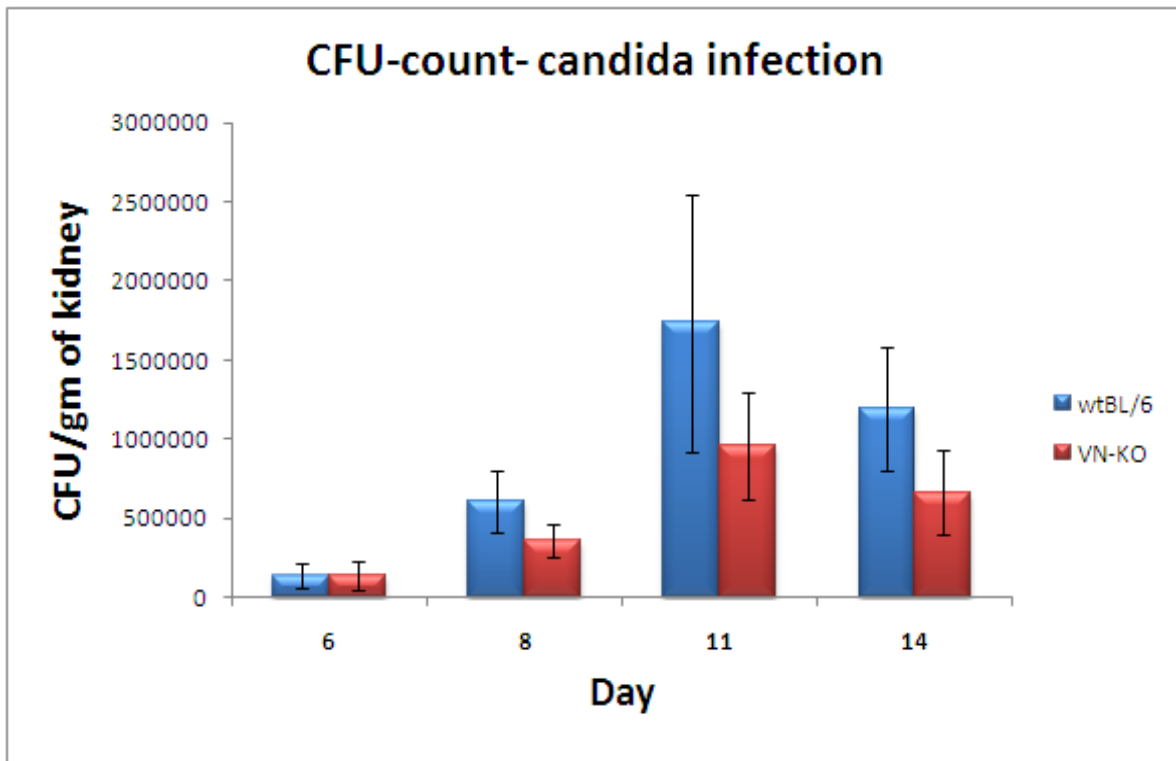
Figure 4. 3: Fungal burden analysis on kidney upon *Candida* infection

Figure-4.3: Colony forming units (CFU) of *C. albicans* present per gram of kidney. Male wild type and VN-knock-out mice were infected with inoculum containing 10^5 viable *C. albicans* cells. Mice were sacrificed at day 5, 8, 11 & 14, and both kidneys were collected. At each time point, a minimum of 5 mice were sacrificed from each group. Fungal burden analysis was performed on each of those mice, and the average CFU/gm kidney tissue is plotted for each time point and for each group of mice.

points for both groups of mice. Statistically there is no difference (P<0.05) in terms of fungal burden between the wild type and the knock-out mice in the kidney. We have also performed fungal burden analysis on spleen, lung and blood. Little to no colony forming units could be observed for blood, spleen and lung on the YEPD plate, even after 48hours of incubation. The absence of colony forming unit within the lung is in line with what Rozell et al. found in their study of *C. albicans* infection in mice [309]. Lung collected from the mice at day two post-infection did not show any presence of *C. albicans*; even at day fourteen post-infection we did not observe presence of *C. albicans* in lung. Though we did not observe any colony forming unit from spleen extract at any of our selected time points, Rozell et al. observed the presence of *C. albicans* in spleen at two day post-infection [309]. It appears that by day five, which is our first time point, significant clearance of the pathogen has been achieved in spleen. Rozell et al. found that though *C. albicans* was present in the heart tissue at day one post-infection and caused severe damage to the cardiac myocytes, from day two post-infection and afterwards very little *C. albicans* was found in the heart due to clearance of the pathogen by neutrophilic granulocytes [309]. A similar mechanism is likely in the spleen also.

The fungal burden assay performed on the above mentioned tissues did not show any difference in terms of colonization, irrespective of the presence and absence of VN. Kidney, being the primary site for *C. albicans* colonization upon systemic infection, was found to be equally loaded with the pathogen in both wild type and VN knock-out mice at each time point. Overall, the number of colony forming units increased with time as expected. Fungal burden is not always correlated with death though. Warenda et al. showed that *Candida* strains that were mutant for septin (a family of cytoskeletal proteins that is important for the proper

179

morphogenesis of *C. albicans*) could colonize nicely within kidney but could not propagate the invasion [311]. Silver staining of the kidney of the mice infected with septin-mutant strains of *Candida* showed localized growth of the pathogen mainly in the uretar space but did not show any sign of invasion [311]. This resulted in no difference in fungal burden but the mutant strains were less virulent. It will be interesting to see if such localized colonization is happening with VN knock-out mice.

Adhesion of the fungus to the host is considered important for the colonization and virulence of fungal pathogens like *C. albicans* [312]. Since VN has been found to be involved in recognizing receptors on the fungal cell surface and integrin αvβ3 and αvβ5 like receptors were found to be present on the surface of *C. albicans* [305-306], our initial idea was that absence of VN is interfering with the colonization of *C. albicans* in mouse tissue and causing increased tolerance to the infection in knock-out mice, but these findings with fungal burden analysis performed at different tissues suggest that absence of VN may not directly interfere with the colonization of the pathogen..

4.3. b. Myeloperoxidase Activity in the Infected Lung

When neutrophils invade the site of inflammation, a number of lysozomal enzymes are secreted [313-314]. One of these enzymes is myeloperoxidase (MPO), which has been found to have antimicrobial and cytotoxic properties [315-316]. Bradley et al. reported that neutrophils involved in phagocytosis release active MPO in the surrounding extracellular matrix at the site of bacterial infection [313]. MPO also acts intracellularly during lysozomal degradation of the phagocytosed pathogen [317]. The primary function of MPO is to generate reactive oxygen from hydrogen-peroxide. Reactive oxygen then acts on chloride and generates highly oxidative

180

hypochlorous acid (HOCl), which further acts on the bacterial system and causes killing of the bacteria [318-319]. Zhang et al. reported that MPO at the site of inflammation generates reactive intermediates that can cause lipid peroxidation. Lipid peroxidation results in cellular dysfunction due to disruption of the membrane integrity [320]. In this study, Zhang et al. showed that MPO can generate reactive intermediates like tyrosyl radicals and nitrogen dioxide ,which in turn may cause lipid peroxidation [320]. Since MPO is primarily secreted by the activated neutrophils, measurement of MPO activity has been utilized as an indicator of neutrophil invasion at the site of infection or inflammation. For example, Mullane et al. reported the use of MPO activity as a measurement for neutrophil invasion at the site of ischemic myocardium [321].

Neutrophils are the effector cells in innate immunity that play a major role in the early stages of the *C. albicans* infection [309, 322]. MPO produced by activated neutrophils contributes to the host defense mechanism against fungal infection [323]. Aratani et al. reported that pulmonary or systemic infection with *Candida. albicans* or *Aspergillus. fumigatus* results in a severe effect in the mice that are null mutants for MPO [324-325]. It has been also found that patients with congenital MPO deficiency show an increased rate of infection with *C. albicans* [326]. Due to the importance of neutrophil function in the defense against *C. albicans* infection and the inherent relationship between neutrophil infiltration and MPO activity, we decided to compare neutrophil invasion in the lung between wild type and knock-out mice following *C. albicans* infection. Lung tissue was collected at day 5, 9 and 14, and half of the lung tissue from each mouse was used for measuring the MPO activity. **Figure-4.4** shows the result of the comparison of MPO activity between the two groups of mice at different time points. No difference in MPO activity in the lung was observed between wild type and VN knock-out mice

181
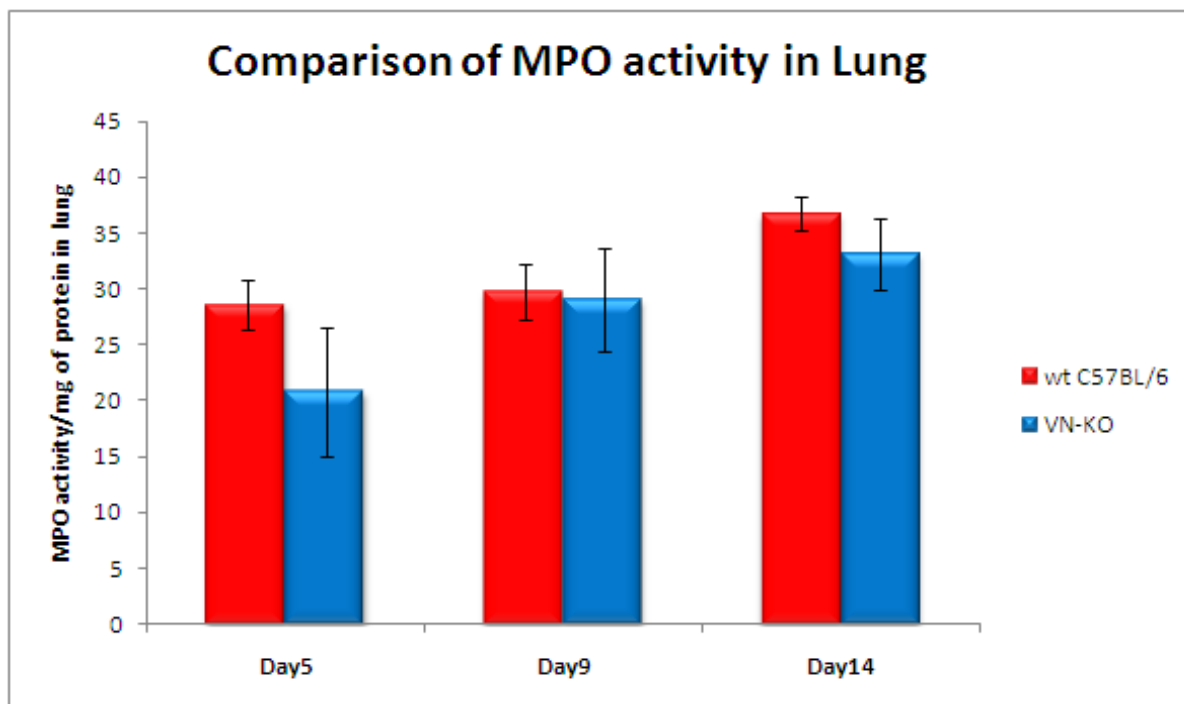
Figure 4. 4: Myeloperoxidase assay in lung upon *Candida* infection

Figure-4.4: Myeloperoxidase activity per mg of total protein in lung. Male wild type and VN-knock-out mice were infected with inoculum containing 10^5 viable *C. albicans* cells. Mice were sacrificed at day 5, 9 & 14, and half of the lung from each mouse was collected. At each time point a minimum of 5 mice were sacrificed from each group. Total amount of protein present in the lung sample collected from each mouse was measured using the kit from Biorad. MPO activity was measured using H_2O_2 and O-dianisidine-HCl and normalized with respect to the total amount protein in that sample.

at all the time points checked. Also, MPO activity did not increase with time. This is reminiscent of what we observed with the fungal burden assay in which there was no measurable number of colony-forming units in the lung for both groups of mice following *C. albicans* infection. Since the neutrophil is the primary line of defense against *C. albicans* infection, the absence of fungal burden correlates with no change in MPO activity over time. It appears that lung is not the best tissue for evaluating the change in neutrophil invasion following systemic *C. albicans* infection. Since kidney is normally found to have the highest fungal burden content, our next study will include the MPO assay on kidney tissue.

4.3. c. Analysis of Cytokine Expression

Cytokines are important modulators of the immune system and play important roles in response to pathogenic attack. Specific cytokines expressed by tissues dictate the fate of the host response to the *C. albicans* infection [327]. For example, infection with *C. albicans* has been found to induce expression of interleukin-6 (IL-6), interleukin-8 (IL-8) and monocyte chemoattractant protein-1 (MCP-1) from endothelial cells, and thus affects the inflammatory response and augments the host defense against the infection [328]. Expression of cytokines in response to *C. albicans* causes activation of the candidacidal activity of effector immune cells, including lymphocytes, neutrophil, macrophages, etc [329-330]. A number of different cytokines can be expressed in response to different kinds of *C. albicans* infections, which include oral, vaginal and systemic infections [330].

Ashman et al. have provided a comprehensive review on different types of cytokines that are expressed in response to different kinds of *C. albicans* infections, including how these cytokines influence the activation of different effector immune cells [330]. For example,

expression of interferon-γ (IFN-γ) in response to *C. albicans* infection in mice causes activation of polymorphonuclear leukocytes (PMNL) and macrophages and that promote killing of *C. albicans* cells [330-333]. Application of recombinant IFN-γ has been found to play a protective role in the acute disseminated *C. albicans* infection in mice by activating PMNL [334]. Injury by *C. albicans* on endothelial cells plays a major role in assisting the microbe in its invasion into the surrounding tissue from the circulation. It has been found that application of IFN-γ protects the endothelial cells from the *C. albicans* induced damage by reducing the extent of phagocytosis of the microbe by the endothelial cells [335-336].

T-helper-1 (Th1) and T-helper-2 (Th2) lymphocytes have an important role in determining the fate of *C. albicans* following infection. While the type-1 immunity obtained from Th1 provides protection to both mucocutaneous and disseminated *C. albicans* infection, type-2 immunity (from Th2 cells) is unprotective and results in the greater susceptibility of the host towards disseminated infection by suppressing the type-1 immunity [337]. There are specific types of cytokines that are involved in mediating type-1 and type-2 immunity. Th1 cells release cytokines like IFN-γ, IL-2, IL-12, lymphotoxin-1 (LT-1), which induces type-1 immunity by activating the phagocytic activity of immune cells. Th2 cells, on the other hand, release cytokines including IL-4, IL-5, IL-9, IL-10, IL-13, which act by deactivating the phagocytic activity of the immune cells [337-339]. The ability of the fungus to undergo the yeast to hyphae transformation provides a specific advantage to *C. albicans* over other fungi in terms of activating the type-2 immune response, which is ineffective and in turn suppresses the type-1 response [339]. *C. albicans* in its hyphal phase inhibits IL-12 production (important for type-1 immunity) and increases the production of IL-4 (important for type-2 response) [340-341].

184

TNF-α is another cytokine that plays an important role in responding to the *C. albicans* infection. This cytokine exhibits harmful effects as a mediator of the inflammatory response in sepsis that happens during endotoxemia or gram negative bacterial infection [342-343]. However, with *C. albicans* infection, TNF-α has been found to play a protective role, as inhibition of this cytokine by antibody or pharmacological inhibitors has deleterious effects on the outcome of the *C. albicans* infection [344-345]. By performing a systemic *C. albicans* infection in TNF-α knock-out mice, Netea et al. reported that TNF-α mediated an increased host resistance against this infection that results from the activation of neutrophil and phagocytosis of the microbes [346]. Another cytokine that may have important role in *C. albicans* infection is granulocyte-colony stimulating factor (G-CSF). G-CSF has been found to cause an increase in amount and an enhancement of the microbicidal property of PMNL under *in vitro* conditions [347-348]. Kullberg et al. reported that application of recombinant G-CSF during systemic infection increases the host resistance by enhancing the activation and recruitment of PMNL in the infected organs [349].

Considering the potential involvement of this large set of cytokines in mediating the host response to *C. albicans* infection, we aimed to check the expression of different cytokines in response to the *C. albicans* infection in wild type and VN knock-out mice. The availability of the multi-plex system allows us to check the expression of an array of cytokines within specific tissues. **Table-4.1** shows the summary of the results of 23 different cytokine expression assays in the kidney and spleen tissues of *C. albicans* infected wild type and VN knock-out mice. Most of the tested cytokines do not show any marked difference between the two groups of mice. For example IFN-γ, which plays such an important role in providing type-1 immunity, was found to

185

show no difference in expression between the two different groups of mice in both tissues tested (see **Figure-4.5 & 4.6**). Also, many of the cytokines tested that are involved in type-1 and type-2 immunity (e.g. – IL-2, IL-10) showed no change in expression between both groups of mice.

There are some cytokines that showed changes in the expression between two groups of mice, but explanation of those changes may require input from other experiments. For example, G-CSF which is known to have protective role in *C. albicans* infection, showed no change in expression between the two groups of mice and stayed at same level until day-11 of infection. On day-14, both groups of mice showed significant decreases in expression of G-CSF compared to day-11 in both of the tissues tested. These decreases in expression at day-14 may not be attributed to the clearance of the microbes from the organ, since on day-14 the kidney maintained considerable fungal burden. Some other cytokines showed differences between two groups of mice, but only at certain time points after infection. For example, MIP-1α showed increase in expression with wild type mice but only at day-11 and with kidney tissue. No other time point showed any difference in kidney. Expression of TNF-α showed perhaps the most consistent results among all the cytokines. In the kidney, the expression of TNF-α was significantly higher at day-8 for both groups of mice. After day-8, the expression stayed same for the knock-out mice, but for wild type mice the expression was significantly lower (see **Figure-4.7**). Considering the important protective role TNF-α has against *C. albicans* infection, the decrease in expression of this cytokine may partially explain the increased mortality of wild type mice. In spleen, the expression of this cytokine was highest on day-6 for both groups of mice, but then decreased at the subsequent time points (see **Figure-4.8**). The significant decrease in the expression of TNF-α at the later time points correlates nicely with the clearance of the microbes

186

from the tissue, as fungal burden in the spleen did not exist at these time points. Though fungal burden in the spleen was absent even at day-6 post infection, the relatively higher expression of TNF-α at this time point is presumably due to an initial spike that occurred in response to the primary phase of infection. Cytokine expression analysis at earlier time point may be more informative in this regard.

The overall results obtained from the cytokine expression analyses on kidney and spleen were not sufficient to explain the apparent difference in mortality between wild type and VN-knock-out mice. While certain results from this analysis are interesting, a much better understanding of the situation is anticipated from cytokine expression analysis performed on other tissues, such as blood serum, lung etc. Another important area that requires attention is sepsis. Spellberg et al. reported that the major cause of death in mice suffering from disseminated candidiasis is progressive sepsis [350]. They reported the presence of certain symptoms, including hypotension, tachycardia, hypothermia, metabolic acidosis, acidemia, hypoglycemia that clearly established the role of sepsis in the infection mediated death. In our next study, we will monitor some of these hemodynamic parameters to characterize progression of sepsis in both groups of mice upon *C. albicans* infection.

Table 4. 1: Summary of cytokine expression analysis in kidney and spleen

CYTOKINE	Comparison of cytokine expression between wild type and VN knock-out mice	
	KIDNEY	**SPLEEN**
IL-1a	No noticeable difference	No noticeable difference
IL-1b	No noticeable difference	No noticeable difference
IL-2	No noticeable difference	No detectable signal was obtained
IL-4	No noticeable difference	No detectable signal was obtained
IL-5	No noticeable difference	No detectable signal was obtained
IL-6	No noticeable difference	No detectable signal was obtained
IL-9	No noticeable difference	No noticeable difference
IL-10	No noticeable difference	No noticeable difference
IL-12(p40)	Expression was significantly higher in wild type mice only at day-14	Expression was significantly higher in wild type mice only at day-14
IL-12(p70)	No noticeable difference	No detectable signal was obtained
IL-13	No noticeable difference	No noticeable difference

CYTOKINE	Comparison of cytokine expression between wild type and VN knock-out mice	
	KIDNEY	**SPLEEN**
IL-17	No noticeable difference between the groups. A general trend of increase in expression observed with both group of mice	No detectable signal was obtained
Eotaxin	No noticeable difference	No detectable signal was obtained
G-CSF	No noticeable difference between the groups. At day-14 expression went down for both group of mice	No noticeable difference between the groups. At day-14 expression went down for both group of mice
GM-CSF	No noticeable difference between the groups. At day-14 expression went down for both group of mice	No noticeable difference
IFN-γ	No noticeable difference	No noticeable difference
KC	No noticeable difference except for day-8 when VN-knock-out show higher expression. Expression for wild type mice stay unchanged, where as for knock-out mice it seems to reach peak at day-8 followed by a decrease	No noticeable difference except for day-8 when VN-knock-out mice show higher expression. Expression for wild type mice stay unchanged, where as for knock-out mice it seems to reach peak at day-8 followed by a decrease
MCP-1 (M-CAF)	No noticeable difference	No noticeable difference
MIP-1a	No noticeable difference except for day-11 when wild type mice show higher expression.	No noticeable difference except for day-11 when wild type mice show higher expression.

189

CYTOKINE	Comparison of cytokine expression between wild type and VN knock-out mice	
	KIDNEY	SPLEEN
MIP-1b	No noticeable difference	No noticeable difference
RANTES	No noticeable difference between the groups. Expression is highest at day-6 and then decrease	No noticeable difference
TNF-α	Expression reaches a peak for both groups of mice at day-8. While expression for knock-out mice stay same after that, for wild type mice it came down and remained lower than knock-out mice	No noticeable difference between the groups. Expression is highest at day-6 but then goes down for both group of mice
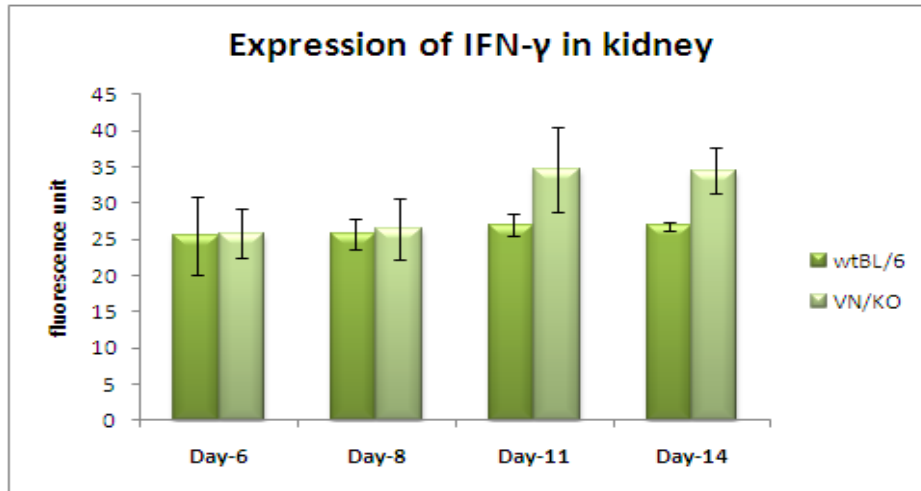
Figure 4. 5: Expression of IFN-γ in kidney upon Candida infection
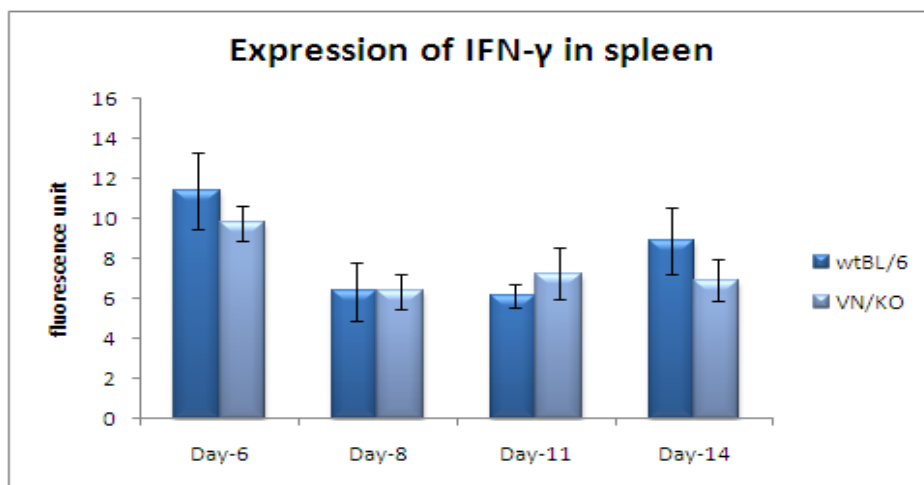
Figure 4. 6: Expression of IFN-γ in spleen upon Candida infection

Figure-4.5 & 4.6: IFN-γ expression analysis in the kidney (Figure-4.5) and spleen (Figure-4.6) following *C. albicans* infection. Male wild type and VN-knock-out mice were infected with inoculum containing 10^5 viable *C. albicans* cells. Mice were sacrificed at day 5, 8, 11 & 14, and both kidneys and spleen were collected. At each time point a minimum of 5 mice were sacrificed from each group. Expression of IFN-γ was analyzed using the 23-plex kit from Biorad.
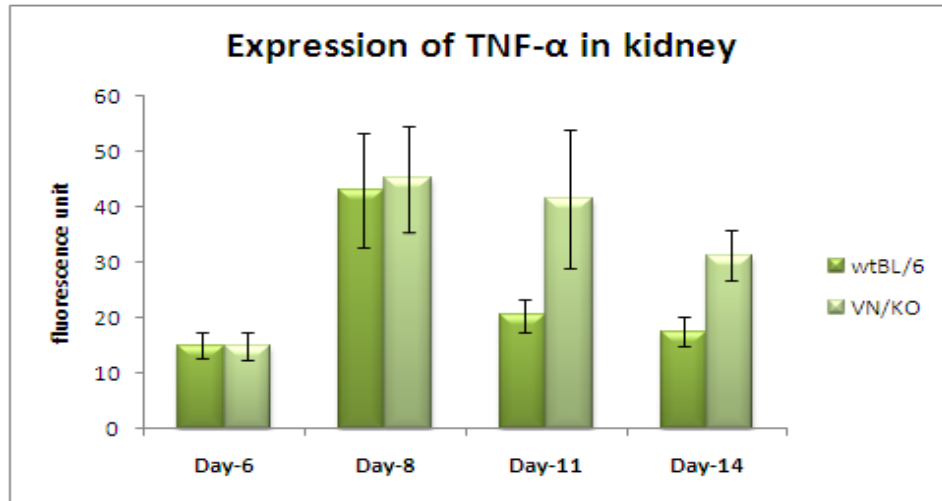
Figure 4. 7: Expression of TNF-α in kidney upon Candida infection
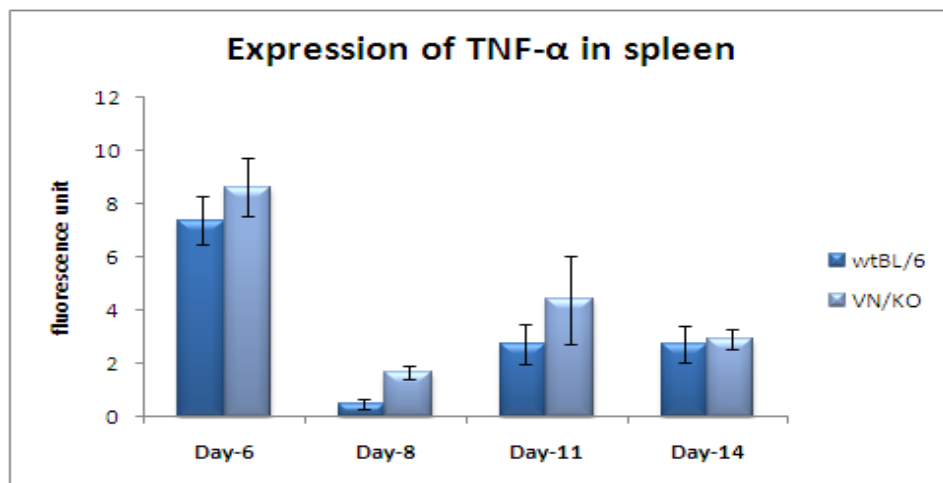
Figure 4. 8: Expression of TNF-α in spleen upon Candida infection

Figure-4.7 & 4.8: TNF-α expression analysis in the kidney (Figure-4.7) and spleen (Figure-4.8) following *C. albicans* infection. Male wild type and VN-knock-out mice were infected with inoculum containing 10^5 viable *C. albicans* cells. Mice were sacrificed at day 5, 8, 11 & 14, and both kidneys and spleen were collected. At each time point a minimum of 5 mice were sacrificed from each group of mice. Expression of TNF-α was analyzed using the 23-plex kit from Biorad.

CHAPTER-5

Summary and Future Studies

Vitronectin (VN) and Plasminogen Activator Inhibitro-1 (PAI-1) are two blood proteins that are well known for their involvement in a wide variety of biological processes. Both of these proteins are found in the extracellular matrix (ECM) also. Though in the circulation VN exist as monomer, it exists as a multimer in the ECM. VN can recognize a number of different ligands like the thrombin-antithrombin complex (T-AT) [44-45], heparin [46-48], PAI-1 [49-51], complement proteins [52] and several cell surface receptors, including integrins and the urokinase plasminogen activator receptor (uPAR) [53-59]. The ability to recognize such a wide variety of ligands makes this protein required in several physiological processes, including thrombus formation, coagulation, fibrinolysis, pericellular proteolysis, wound healing, inhibition of the membrane attack complex, and cellular adhesion/migration [8, 60-66, 81-82, 91-92]. On the other hand, PAI-1 is a member of the serine protease inhibitor family of proteins whose physiological functions can be broadly classified into two main categories- **protease dependent** and **protease independent activities**. Under protease dependent functions, PAI-1 is primarily involved in the regulation of plasmin formation from inactive plasminogen by inhibiting tissue-plasminogen activator-1 (tPA) and urokinase-plasminogen activator-1(uPA) [79-80]. PAI-1-mediated regulation of plasmin formation plays regulatory roles in several patho-physiological processes like coagulation, fibrinolysis, thrombolysis and renal diseases such as nephritic syndrome and hemolytic uremic syndrome [109, 112, 170-172, 175, 177].

In the last two decades, protease-independent functions of PAI-1 have drawn attention and been heavily investigated. In this context, PAI-1 function is not directly related to its ability to inhibit proteases like uPA or tPA. For example, binding of PAI-1 to receptor-bound uPA on the cell surface causes internalization of the ternary complex of PAI-1/uPA/uPAR via receptor-mediated endocytosis process [180-182]. PAI-1 has been also found to be involved in the internalization of the tPA/PAI-1 complex [188]. Thus, such protease-independent activities of PAI-1 play important roles in the turnover of its target proteases.

Many of the protease-independent functions of PAI-1 are mediated by its interaction with VN. One of the areas where this interaction has generated a much interest is in cellular adhesion and migration. A major part of this dissertation work has been devoted to the understanding of the interaction between these two proteins and how such interaction regulates their extracellular-matrix associated functions. PAI-1 has been found to interfere with the interaction of matrix associated VN with cell surface receptors (like uPAR and integrin) and thus regulate cell-matrix interactions. Though considerable effort has been made in this area, a significant amount of controversy still exists regarding how the interaction between PAI-1 and VN regulates cellular adhesion and migration. Some studies suggest that PAI-1 inhibits cell binding to VN but promotes migration, while others indicate that PAI-1 inhibits migration that would be mediated by VN [226-227, 229-230]. Our main goal in this current research has been to attempt to mimic the natural biological environment under which these proteins interact. Most of the studies in the literature have been aimed at understanding the role of exogenously added PAI-1 in regulating cellular adhesion and migration mediated by 'denatured' multimeric VN. In our studies, we have used multimeric VN formed by a process that is relevant to actual biological settings. We have

194

used PAI-1 as a biological factor for the transition of monomeric VN into its multimeric counterpart, and then have evaluated the association of this 'biological' multimeric VN with the extracellular matrix. The ECM is made of a number of components. As a protein that binds a broad array of ligands, VN interacts with other matrix components like Col-IV [104] and thus associates with the ECM. While associated with the matrix, it interacts with cell surface receptors. We evaluated the relevance of this 'biological' multimeric form of VN by checking its ability to interact with matrix components such as Col-IV and HSPG. Our results show that multimeric complexes of VN formed in the presence of PAI-1 associate more with the matrix. We also report for the first time that VN can interact with HSPG.

PAI-1has been considered to promote the matrix partitioning of VN because these two proteins are co-localized in extracellular matrix [21, 192-193]. The observed increased association of this 'biological' multimeric form of VN with matrix components is significant, providing strong evidence for the role of PAI-1 in regulating compartmentalization of VN from the circulation to the matrix. We have also evaluated the interaction of this complex with a variety of cell surface receptors including uPAR and different integrins. Our study indicates that the 'biological' multimeric complex of VN interacts more with the receptors tested compared to monomeric VN. The fact that this multimeric form of VN, while still bound with PAI-1, interacts with uPAR and integrins is in contrast to current thinking. Here we are able to show that PAI-1, while associated with VN within the multimeric complex, does not block receptor interaction with VN. This is an important finding since PAI-1 and VN are found to be co-localized under many physiological conditions. This result indicates that their effects on cell-matrix interaction

195

while part of the same multimeric complexes may be significantly different from what is observed when one of the proteins is added in isolation exogenously.

We have taken a thorough approach in evaluating components in the pericellular environment for understanding the role of the interaction between these two proteins on the regulation of cell-matrix interaction. The effect of the 'biological' multimeric complex of VN formed in the presence of PAI-1 on cellular adhesion and migration was checked in the context of different matrix components, different cell types and different growth factor conditions that may modulate the receptor expression pattern on the cell surface. Our results indicate that the effect that the VN/PAI-1 complex has on cell-matrix interactions is largely dictated by the specific cell type and the pericellular conditions. Though most of the studies have indicated that PAI-1 blocks cellular interactions with VN, our findings indicate that PAI-1 within the 'biological' multimeric complex of VN has no effect on cellular adhesion. However, the effect on cellular migration has been found to be variable.

VN as a constituent of the ECM is involved in the modulation of cell-matrix interactions in various important patho-physiological processes like angiogenesis [66]. Targeting the interaction between VN and cell surface receptors for VN is a subject of therapeutic interest. Thiolutin is an example of a drug that was used for preventing tumor cell induced angiogenesis by blocking the interaction of VN and $\alpha v\beta 3$ on the surface of HUVEC [351]. There are a number of inhibitors of angiogenesis (targeted to prevent cancer), designed to act as antagonists of $\alpha v\beta 3$ and $\alpha v\beta 5$, the two most common receptors for VN, that have been subject to clinical trials [99, 284-285]. One example is cilengitide, a RGD based inhibitor of $\alpha v\beta 3$. Though it showed tremendous promise in the initial phases, most of the trials with this drug failed at the clinical

196

level. Out of different types of cancers tried at the phase-II level, it showed promise only with patients of glioblastoma multiforme (GMB); currently it is being tested in phase-III clinical trials [284, 352]. This example tells us the importance of understanding the underlying biology for designing effective therapeutic strategies. In our study the main goal has been to understand the biological role that VN and PAI-1 have in a nearly natural cell-matrix environment.

Another important aspect of this study involving the interaction between VN and PAI-1 is the finding of the unique function of reactive center mimicking peptides. These peptides were found to almost completely disrupt the interaction between VN and PAI-1 and they blocked the formation of higher order multimeric complexes. It was found that increased association of VN to Col-IV and HSPG that is normally induced by binding to PAI-1 was completely inhibited in the presence of these peptides. This finding of a new function for these peptides represents tremendous potential, considering how important the role the interaction between VN and PAI-1 is in several biological processes. For example, the interaction between VN and PAI-1 has been implicated in the development of renal fibrotic disease. Expression of PAI-1 becomes very high in renal fibrotic condition and is thought to be one of the major causes for the loss of matrix turn over. VN significantly contributes to the progression of this disease by localizing PAI-1 in the fibrotic matrix [223-225]. Disrupting the interaction between PAI-1 and VN thus is desirable, and compounds such as the peptide mimetics that accomplish this may have clinical benefit.

Another important goal of this dissertation work was to understand the role of VN in *Candida* pathogenesis. This was pursued in continuation of a very interesting finding from our lab where VN knock-out mice were found to be more tolerant against *Candida* infection compared to wild type C57BL/6 mice. In this dissertation work, our goal was to investigate how

197

the absence of the vitronectin gene acts to increased survival. We have studied at different aspects of infection pathogenesis, and we have performed assays to compare cytokine expression levels in different tissues. We have also evaluated neutrophil invasion in the lung, and we have performed fungal burden analysis on different tissues. Though we have not obtained conclusive evidence that would clearly explain the role of VN in *Candida* infection, our approach has demonstrated that there are not obvious differences in expected inflammatory markers. Addressing the specific role that VN may have in *Candida* pathogenesis will thus require a thorough investigation of all possible aspects involved with fungal infection. In this dissertation work we have been able to pursue some of them.

A significant portion of this dissertation work was involved in developing methods for understanding the structure and dynamics PAI-1. We have for the first time reported the use of an electron paramagnetic resonance (EPR) based method for understanding the structural change in PAI-1 that happens naturally or due to ligand binding. We have been able to strategically place the nitroxide spin level on PAI-1 (at the P9 position) and have shown that this spin label can be successfully used for monitoring the conformational transition that happens during the latency transition. This spin labeled PAI-1 can be further utilized for understanding the conformational transitions that may happen in the reactive center loop upon metal binding. A spin label may also be placed in other positions for specifically probing ligand binding to PAI-1.

We have also developed a surface plasmon resonance (SPR) based method for analyzing metal binding to PAI-1. Using this method useful affinity information has been generated for PAI-1 (and its mutants) binding to nickel. Though this method could not be extended for metals other than nickel, it will serve the important purpose for screening different mutants of PAI-1 for

198

metal binding in order to identify the metal-binding site in the protein. Our lab is currently in the process of generating many different mutants of PAI-1 for locating the metal binding sites. This SPR based method will provide a quick of way screening these mutants for metal binding.

Future Experiments

- **On functional aspects of VN/PAI-1 complex**
    - Specific role of uPAR will be tested on the effect of VN/PAI-1 complex in cellular adhesion and migration. U937 cells will be cultured, and uPAR expression will be induced by TGF-β and Vitamin-D3. Expression of uPAR will be confirmed by flow cytometry. uPAR expressing U937 cells will be used for studying cell adhesion and migration under the conditions where VN/PAI-1 complex is associated with Col-IV and HSPG.
    - Effect of the VN/PAI-1 complex on cellular adhesion and migration will be tested under 3-dimensional matrix conditions.
    - Role of the VN/PAI-1 complex in angiogenesis will be tested by using the standard endothelial tube formation assay system from BD bioscience.

- **On structural aspects of the VN/PAI-1 complex**
    - Effect of the octapeptide and pentapeptide on formation of complexes will be tested using latent-PAI-1 with VN in sedimentation velocity experiments.
    - Dose dependent effects of the octapeptide will be tested on the inhibition of the multimerization reaction between VN and wtPAI-1.
    - Effect of the triple mutant of PAI-1 (R115E, R118E, Q123K), which is defective in binding to VN, will be tested for its effect on forming multimeric complex

199

with VN. This mutant should be capable of taking part in the PAI-1/PAI-1

interaction as observed in the SANS model.

- **On EPR studies**

  o P9 labeled mutant will be utilized for monitoring the insertion dynamics of the

    reactive center loop upon metal binding

  o Spin label will be incorporated at different positions of the reactive center loop

    and will be monitored for changes that occur during the insertion of the loop

    during the latency transition and also during ligand binding.

  o Spin lapel will be also put at V328. This residue sits at the base of the reactive

    center loop. It does not get inserted during the latency transition, but may show

    significant movement during the process. Spin label at this residue can tell us

    about structural events at the base of the loop during insertion. It will be also

    used for studying the effect of ligand binding on loop insertion.

- **On the role of VN in *Candida* pathogenesis**

  o Neutrophil invasion in kidney will be checked by performing myeloperoxidase

    assay on both wild type and knock-out mice.

  o Cytokine expression analysis will be carried out on blood and lung.

  o Symptoms for sepsis (e.g. - hypotension, tachycardia, hypothermia, metabolic

    acidosis, acidemia, and hypoglycemia) will be checked in both wild type and

    knock-out mice upon *Candida* infection.

o Role of VN will be further checked by performing survival study under condition where *Candida* and VN were co-injected in knock-out mice. This will test if the presence of VN is needed during the onset infection.

o The potential involvement of integrin like receptors on the surface of *Candida. albicans* in the colonization of the microbes inside the body will be tested by injecting *Candida* along with cyclic-RGD peptide to wild type C57BL/6 mice.

REFERENCES

1.	Holmes, R., *Preparation from human serum of an alpha-one protein which induces the immediate growth of unadapted cells in vitro.* J Cell Biol, 1967. **32**(2): p. 297-308.
2.	Barnes, D., et al., *Effects of a serum spreading factor on growth and morphology of cells in serum-free medium.* J Supramol Struct, 1980. **14**(1): p. 47-63.
3.	Barnes, D.W., et al., *Characterization of human serum spreading factor with monoclonal antibody.* Proc Natl Acad Sci U S A, 1983. **80**(5): p. 1362-6.
4.	Podack, E.R. and H.J. Muller-Eberhard, *Isolation of human S-protein, an inhibitor of the membrane attack complex of complement.* J Biol Chem, 1979. **254**(19): p. 9808-14.
5.	Tomasini, B.R. and D.F. Mosher, *Vitronectin.* Prog Hemost Thromb, 1991. **10**: p. 269-305.
6.	Shaffer, M.C., T.P. Foley, and D.W. Barnes, *Quantitation of spreading factor in human biologic fluids.* J Lab Clin Med, 1984. **103**(5): p. 783-91.
7.	Hayman, E.G., et al., *Serum spreading factor (vitronectin) is present at the cell surface and in tissues.* Proc Natl Acad Sci U S A, 1983. **80**(13): p. 4003-7.
8.	Podack, E.R., W.P. Kolb, and H.J. Muller-Eberhard, *The SC5b-7 complex: formation, isolation, properties, and subunit composition.* J Immunol, 1977. **119**(6): p. 2024-9.
9.	Preissner, K.T., et al., *Physicochemical, immunochemical and functional comparison of human S-protein and vitronectin. Evidence for the identity of both plasma proteins.* Biochem Biophys Res Commun, 1986. **134**(2): p. 951-6.
10.	Jenne, D. and K.K. Stanley, *Molecular cloning of S-protein, a link between complement, coagulation and cell-substrate adhesion.* EMBO J, 1985. **4**(12): p. 3153-7.
11.	Suzuki, S., et al., *Complete amino acid sequence of human vitronectin deduced from cDNA. Similarity of cell attachment sites in vitronectin and fibronectin.* EMBO J, 1985. **4**(10): p. 2519-24.
12.	Tomasini, B.R. and D.F. Mosher, *On the identity of vitronectin and S-protein: immunological crossreactivity and functional studies.* Blood, 1986. **68**(3): p. 737-42.
13.	Schvartz, I., D. Seger, and S. Shaltiel, *Vitronectin.* Int J Biochem Cell Biol, 1999. **31**(5): p. 539-44.
14.	Seiffert, D., *Constitutive and regulated expression of vitronectin.* Histol Histopathol, 1997. **12**(3): p. 787-97.
15.	Kemkes-Matthes, B., et al., *S protein/vitronectin in chronic liver diseases: correlations with serum cholinesterase, coagulation factor X and complement component C3.* Eur J Haematol, 1987. **39**(2): p. 161-5.
16.	Conlan, M.G., et al., *Plasma vitronectin polymorphism in normal subjects and patients with disseminated intravascular coagulation.* Blood, 1988. **72**(1): p. 185-90.
17.	Barnes, D.W. and J. Reing, *Human spreading factor: synthesis and response by HepG2 hepatoma cells in culture.* J Cell Physiol, 1985. **125**(2): p. 207-14.
18.	Cooper, S. and M.F. Pera, *Vitronectin production by human yolk sac carcinoma cells resembling parietal endoderm.* Development, 1988. **104**(4): p. 565-74.
19.	Hetland, G., et al., *S-protein is synthesized by human monocytes and macrophages in vitro.* Scand J Immunol, 1989. **29**(1): p. 15-21.
20.	Parker, C.J., et al., *Vitronectin (S protein) is associated with platelets.* Br J Haematol, 1989. **71**(2): p. 245-52.

21. Preissner, K.T., et al., *Identification of and partial characterization of platelet vitronectin: evidence for complex formation with platelet-derived plasminogen activator inhibitor-1.* Blood, 1989. **74**(6): p. 1989-96.

22. Zhou, A., et al., *How vitronectin binds PAI-1 to modulate fibrinolysis and cell migration.* Nat Struct Biol, 2003. **10**(7): p. 541-4.

23. Kamikubo, Y., et al., *Disulfide bonding arrangements in active forms of the somatomedin B domain of human vitronectin.* Biochemistry, 2004. **43**(21): p. 6519-34.

24. Mayasundari, A., et al., *The solution structure of the N-terminal domain of human vitronectin: proximal sites that regulate fibrinolysis and cell migration.* J Biol Chem, 2004. **279**(28): p. 29359-66.

25. Kjaergaard, M., et al., *Solution structure of recombinant somatomedin B domain from vitronectin produced in Pichia pastoris.* Protein Sci, 2007. **16**(9): p. 1934-45.

26. Xu, D., et al., *Model for the three-dimensional structure of vitronectin: predictions for the multi-domain protein from threading and docking.* Proteins, 2001. **44**(3): p. 312-20.

27. Lynn, G.W., et al., *A model for the three-dimensional structure of human plasma vitronectin from small-angle scattering measurements.* Biochemistry, 2005. **44**(2): p. 565-74.

28. Li, X., et al., *Defining the native disulfide topology in the somatomedin B domain of human vitronectin.* J Biol Chem, 2007. **282**(8): p. 5318-26.

29. Fryklund, L. and H. Sievertsson, *Primary structure of somatomedin B: a growth hormone-dependent serum factor with protease inhibiting activity.* FEBS Lett, 1978. **87**(1): p. 55-60.

30. Barnes, D.W. and J. Silnutzer, *Isolation of human serum spreading factor.* J Biol Chem, 1983. **258**(20): p. 12548-52.

31. Preissner, K.T., R. Wassmuth, and G. Muller-Berghaus, *Physicochemical characterization of human S-protein and its function in the blood coagulation system.* Biochem J, 1985. **231**(2): p. 349-55.

32. Dahlback, B. and E.R. Podack, *Characterization of human S protein, an inhibitor of the membrane attack complex of complement. Demonstration of a free reactive thiol group.* Biochemistry, 1985. **24**(9): p. 2368-74.

33. Tollefsen, D.M., C.J. Weigel, and M.H. Kabeer, *The presence of methionine or threonine at position 381 in vitronectin is correlated with proteolytic cleavage at arginine 379.* J Biol Chem, 1990. **265**(17): p. 9778-81.

34. Zhuang, P., et al., *Characterization of the denaturation and renaturation of human plasma vitronectin. II. Investigation into the mechanism of formation of multimers.* J Biol Chem, 1996. **271**(24): p. 14333-43.

35. Zhao, Y. and D.C. Sane, *Expression of a recombinant baculovirus for vitronectin in insect cells: purification, characterization of post-translational modifications and functional studies of the recombinant protein.* Arch Biochem Biophys, 1993. **304**(2): p. 434-42.

36. Sano, K., et al., *Changes in glycosylation of vitronectin modulate multimerization and collagen binding during liver regeneration.* Glycobiology, 2007. **17**(7): p. 784-94.

37. Jenne, D., et al., *Sulfation of two tyrosine-residues in human complement S-protein (vitronectin).* Eur J Biochem, 1989. **185**(2): p. 391-5.

38.   Korc-Grodzicki, B., et al., *Vitronectin is phosphorylated by a cAMP-dependent protein kinase released by activation of human platelets with thrombin.* Biochem Biophys Res Commun, 1988. **157**(3): p. 1131-8.

39.   Chain, D., et al., *The phosphorylation of the two-chain form of vitronectin by protein kinase A is heparin dependent.* FEBS Lett, 1990. **269**(1): p. 221-5.

40.   Schvartz, I., et al., *The PKA phosphorylation of vitronectin: effect on conformation and function.* Arch Biochem Biophys, 2002. **397**(2): p. 246-52.

41.   Seger, D., Z. Gechtman, and S. Shaltiel, *Phosphorylation of vitronectin by casein kinase II. Identification of the sites and their promotion of cell adhesion and spreading.* J Biol Chem, 1998. **273**(38): p. 24805-13.

42.   Seger, D., R. Seger, and S. Shaltiel, *The CK2 phosphorylation of vitronectin. Promotion of cell adhesion via the alpha(v)beta 3-phosphatidylinositol 3-kinase pathway.* J Biol Chem, 2001. **276**(20): p. 16998-7006.

43.   Gechtman, Z. and S. Shaltiel, *Phosphorylation of vitronectin on Ser362 by protein kinase C attenuates its cleavage by plasmin.* Eur J Biochem, 1997. **243**(1-2): p. 493-501.

44.   Tomasini, B.R. and D.F. Mosher, *Conformational states of vitronectin: preferential expression of an antigenic epitope when vitronectin is covalently and noncovalently complexed with thrombin-antithrombin III or treated with urea.* Blood, 1988. **72**(3): p. 903-12.

45.   de Boer, H.C., et al., *Ternary vitronectin-thrombin-antithrombin III complexes in human plasma. Detection and mode of association.* J Biol Chem, 1993. **268**(2): p. 1279-83.

46.   Barnes, D.W., J.E. Reing, and B. Amos, *Heparin-binding properties of human serum spreading factor.* J Biol Chem, 1985. **260**(16): p. 9117-22.

47.   Lane, D.A., et al., *Structural requirements for the neutralization of heparin-like saccharides by complement S protein/vitronectin.* J Biol Chem, 1987. **262**(34): p. 16343-8.

48.   Hayashi, M., et al., *Activation of vitronectin (serum spreading factor) binding of heparin by denaturing agents.* J Biochem, 1985. **98**(4): p. 1135-8.

49.   Owensby, D.A., et al., *Binding of plasminogen activator inhibitor type-1 to extracellular matrix of Hep G2 cells. Evidence that the binding protein is vitronectin.* J Biol Chem, 1991. **266**(7): p. 4334-40.

50.   Lawrence, D.A., et al., *Characterization of the binding of different conformational forms of plasminogen activator inhibitor-1 to vitronectin. Implications for the regulation of pericellular proteolysis.* J Biol Chem, 1997. **272**(12): p. 7676-80.

51.   Arroyo De Prada, N., et al., *Interaction of plasminogen activator inhibitor type-1 (PAI-1) with vitronectin.* Eur J Biochem, 2002. **269**(1): p. 184-92.

52.   Tschopp, J., et al., *The heparin binding domain of S-protein/vitronectin binds to complement components C7, C8, and C9 and perforin from cytolytic T-cells and inhibits their lytic activities.* Biochemistry, 1988. **27**(11): p. 4103-9.

53.   Kanse, S.M., et al., *The urokinase receptor is a major vitronectin-binding protein on endothelial cells.* Exp Cell Res, 1996. **224**(2): p. 344-53.

54.   Huang, X., et al., *The integrin alphavbeta6 is critical for keratinocyte migration on both its known ligand, fibronectin, and on vitronectin.* J Cell Sci, 1998. **111 (Pt 15)**: p. 2189-95.

55. Dahm, L.M. and C.W. Bowers, *Vitronectin regulates smooth muscle contractility via alphav and beta1 integrin.* J Cell Sci, 1998. **111 (Pt 9)**: p. 1175-83.

56. Memmo, L.M. and P. McKeown-Longo, *The alphavbeta5 integrin functions as an endocytic receptor for vitronectin.* J Cell Sci, 1998. **111 (Pt 4)**: p. 425-33.

57. Schnapp, L.M., et al., *The human integrin alpha 8 beta 1 functions as a receptor for tenascin, fibronectin, and vitronectin.* J Biol Chem, 1995. **270**(39): p. 23196-202.

58. Nishimura, S.L., D. Sheppard, and R. Pytela, *Integrin alpha v beta 8. Interaction with vitronectin and functional divergence of the beta 8 cytoplasmic domain.* J Biol Chem, 1994. **269**(46): p. 28708-15.

59. Boettiger, D., et al., *Distinct ligand-binding modes for integrin alpha(v)beta(3)-mediated adhesion to fibronectin versus vitronectin.* J Biol Chem, 2001. **276**(34): p. 31684-90.

60. Jenne, D., F. Hugo, and S. Bhakdi, *Interaction of complement S-protein with thrombin-antithrombin complexes: a role for the S-protein in haemostasis.* Thromb Res, 1985. **38**(4): p. 401-12.

61. Podor, T.J., et al., *Incorporation of vitronectin into fibrin clots. Evidence for a binding interaction between vitronectin and gamma A/gamma' fibrinogen.* J Biol Chem, 2002. **277**(9): p. 7520-8.

62. Eitzman, D.T., et al., *Plasminogen activator inhibitor-1 and vitronectin promote vascular thrombosis in mice.* Blood, 2000. **95**(2): p. 577-80.

63. Konstantinides, S., et al., *Plasminogen activator inhibitor-1 and its cofactor vitronectin stabilize arterial thrombi after vascular injury in mice.* Circulation, 2001. **103**(4): p. 576-83.

64. Reheman, A., et al., *Vitronectin stabilizes thrombi and vessel occlusion but plays a dual role in platelet aggregation.* J Thromb Haemost, 2005. **3**(5): p. 875-83.

65. Plow, E.F., *Vitronectin: back into the spotlight.* J Thromb Haemost, 2005. **3**(5): p. 873-4.

66. Jang, Y.C., et al., *Vitronectin deficiency is associated with increased wound fibrinolysis and decreased microvascular angiogenesis in mice.* Surgery, 2000. **127**(6): p. 696-704.

67. Rosenberg, R.D. and P.S. Damus, *The purification and mechanism of action of human antithrombin-heparin cofactor.* J Biol Chem, 1973. **248**(18): p. 6490-505.

68. Bjork, I. and B. Nordenman, *Acceleration of the reaction between thrombin and antithrombin III by non-stoichiometric amounts of heparin.* Eur J Biochem, 1976. **68**(2): p. 507-11.

69. Kowalski, S. and T.H. Finlay, *Heparin and the inactivation of thrombin by antithrombin III.* Thromb Res, 1979. **14**(2-3): p. 387-97.

70. Peterson, C.B. and M.N. Blackburn, *Antithrombin conformation and the catalytic role of heparin. II. Is the heparin-induced conformational change in antithrombin required for rapid inactivation of thrombin?* J Biol Chem, 1987. **262**(16): p. 7559-66.

71. Olson, S.T., et al., *Binding of high affinity heparin to antithrombin III. Stopped flow kinetic studies of the binding interaction.* J Biol Chem, 1981. **256**(21): p. 11073-9.

72. McKay, E.J. and C.B. Laurell, *The interaction of heparin with plasma proteins. Demonstration of different binding sites for antithrombin III complexes and antithrombin III.* J Lab Clin Med, 1980. **95**(1): p. 69-80.

73. Peterson, C.B. and M.N. Blackburn, *Antithrombin conformation and the catalytic role of heparin. I. Does cleavage by thrombin induce structural changes in the heparin-binding region of antithrombin?* J Biol Chem, 1987. **262**(16): p. 7552-8.

74. Preissner, K.T. and G. Muller-Berghaus, *S protein modulates the heparin-catalyzed inhibition of thrombin by antithrombin III. Evidence for a direct interaction of S protein with heparin.* Eur J Biochem, 1986. **156**(3): p. 645-50.

75. Podack, E.R., B. Dahlback, and J.H. Griffin, *Interaction of S-protein of complement with thrombin and antithrombin III during coagulation. Protection of thrombin by S-protein from antithrombin III inactivation.* J Biol Chem, 1986. **261**(16): p. 7387-92.

76. Essex, D.W., et al., *Protein disulfide isomerase catalyzes the formation of disulfide-linked complexes of vitronectin with thrombin-antithrombin.* Biochemistry, 1999. **38**(32): p. 10398-405.

77. Stockmann, A., et al., *Multimeric vitronectin. Identification and characterization of conformation-dependent self-association of the adhesive protein.* J Biol Chem, 1993. **268**(30): p. 22874-82.

78. Wells, M.J. and M.A. Blajchman, *In vivo clearance of ternary complexes of vitronectin-thrombin-antithrombin is mediated by hepatic heparan sulfate proteoglycans.* J Biol Chem, 1998. **273**(36): p. 23440-7.

79. Huntington, J.A. and R.W. Carrell, *The serpins: nature's molecular mousetraps.* Sci Prog, 2001. **84**(Pt 2): p. 125-36.

80. Lawrence, D., et al., *Purification of active human plasminogen activator inhibitor 1 from Escherichia coli. Comparison with natural and recombinant forms purified from eucaryotic cells.* Eur J Biochem, 1989. **186**(3): p. 523-33.

81. Declerck, P.J., et al., *Purification and characterization of a plasminogen activator inhibitor 1 binding protein from human plasma. Identification as a multimeric form of S protein (vitronectin).* J Biol Chem, 1988. **263**(30): p. 15454-61.

82. Hansen, M., M.N. Busse, and P.A. Andreasen, *Importance of the amino-acid composition of the shutter region of plasminogen activator inhibitor-1 for its transitions to latent and substrate forms.* Eur J Biochem, 2001. **268**(23): p. 6274-83.

83. Thompson, R.A. and P.J. Lachmann, *Reactive lysis: the complement-mediated lysis of unsensitized cells. I. The characterization of the indicator factor and its identification as C7.* J Exp Med, 1970. **131**(4): p. 629-41.

84. Hammer, C.H., A. Nicholson, and M.M. Mayer, *On the mechanism of cytolysis by complement: evidence on insertion of C5b and C7 subunits of the C5b,6,7 complex into phospholipid bilayers of erythrocyte membranes.* Proc Natl Acad Sci U S A, 1975. **72**(12): p. 5076-80.

85. Podack, E.R., et al., *Membrane attack complex of complement: a structural analysis of its assembly.* J Exp Med, 1980. **151**(2): p. 301-13.

86. Podack, E.R., et al., *The C5b-6 complex: reaction with C7, C8, C9.* J Immunol, 1978. **121**(2): p. 484-90.

87. Podack, E.R. and H.J. Muller-Eberhard, *Binding of desoxycholate, phosphatidylcholine vesicles, lipoprotein and of the S-protein to complexes of terminal complement components.* J Immunol, 1978. **121**(3): p. 1025-30.

88. Podack, E.R., J. Tschoop, and H.J. Muller-Eberhard, *Molecular organization of C9 within the membrane attack complex of complement. Induction of circular C9 polymerization by the C5b-8 assembly.* J Exp Med, 1982. **156**(1): p. 268-82.

89. Podack, E.R. and J. Tschopp, *Polymerization of the ninth component of complement (C9): formation of poly(C9) with a tubular ultrastructure resembling the membrane attack complex of complement.* Proc Natl Acad Sci U S A, 1982. **79**(2): p. 574-8.

90. Tschopp, J., E.R. Podack, and H.J. Muller-Eberhard, *Ultrastructure of the membrane attack complex of complement: detection of the tetramolecular C9-polymerizing complex C5b-8.* Proc Natl Acad Sci U S A, 1982. **79**(23): p. 7474-8.

91. Podack, E.R., K.T. Preissner, and H.J. Muller-Eberhard, *Inhibition of C9 polymerization within the SC5b-9 complex of complement by S-protein.* Acta Pathol Microbiol Immunol Scand Suppl, 1984. **284**: p. 89-96.

92. Felding-Habermann, B. and D.A. Cheresh, *Vitronectin and its receptors.* Curr Opin Cell Biol, 1993. **5**(5): p. 864-8.

93. Barczyk, M., S. Carracedo, and D. Gullberg, *Integrins.* Cell Tissue Res, 2010. **339**(1): p. 269-80.

94. Hess, S., et al., *The versatility of adhesion receptor ligands in haemostasis: morpho-regulatory functions of vitronectin.* Thromb Haemost, 1995. **74**(1): p. 258-65.

95. Kanse, S.M., et al., *Promotion of leukocyte adhesion by a novel interaction between vitronectin and the beta2 integrin Mac-1 (alphaMbeta2, CD11b/CD18).* Arterioscler Thromb Vasc Biol, 2004. **24**(12): p. 2251-6.

96. Friedlander, M., et al., *Definition of two angiogenic pathways by distinct alpha v integrins.* Science, 1995. **270**(5241): p. 1500-2.

97. Friedlander, M., et al., *Involvement of integrins alpha v beta 3 and alpha v beta 5 in ocular neovascular diseases.* Proc Natl Acad Sci U S A, 1996. **93**(18): p. 9764-9.

98. Colevas, A.D., O. Scharf, and M. Schoenfeldt, *Clinical trials referral resource. Current clinical trials of cilengitide, an alpha(v) antagonist in clinical development as an anticancer agent.* Oncology (Williston Park), 2004. **18**(14): p. 1778, 1781-2, 1784.

99. Wu, H., et al., *Stepwise in vitro affinity maturation of Vitaxin, an alphav beta3-specific humanized mAb.* Proc Natl Acad Sci U S A, 1998. **95**(11): p. 6037-42.

100. Ploug, M., et al., *Structural analysis of the interaction between urokinase-type plasminogen activator and its receptor: a potential target for anti-invasive cancer therapy.* Biochem Soc Trans, 2002. **30**(2): p. 177-83.

101. Llinas, P., et al., *Crystal structure of the human urokinase plasminogen activator receptor bound to an antagonist peptide.* EMBO J, 2005. **24**(9): p. 1655-63.

102. Huai, Q., et al., *Structure of human urokinase plasminogen activator in complex with its receptor.* Science, 2006. **311**(5761): p. 656-9.

103. Huai, Q., et al., *Crystal structures of two human vitronectin, urokinase and urokinase receptor complexes.* Nat Struct Mol Biol, 2008. **15**(4): p. 422-3.

104. Gebb, C., et al., *Interaction of vitronectin with collagen.* J Biol Chem, 1986. **261**(35): p. 16698-703.

105. Panetti, T.S. and P.J. McKeown-Longo, *Receptor-mediated endocytosis of vitronectin is regulated by its conformational state.* J Biol Chem, 1993. **268**(16): p. 11988-93.

106.   Panetti, T.S. and P.J. McKeown-Longo, *The alpha v beta 5 integrin receptor regulates receptor-mediated endocytosis of vitronectin.* J Biol Chem, 1993. **268**(16): p. 11492-5.

107.   Bhattacharya, S., et al., *Soluble ligands of the alpha v beta 3 integrin mediate enhanced tyrosine phosphorylation of multiple proteins in adherent bovine pulmonary artery endothelial cells.* J Biol Chem, 1995. **270**(28): p. 16781-7.

108.   Spreghini, E., et al., *Evidence for alphavbeta3 and alphavbeta5 integrin-like vitronectin (VN) receptors in Candida albicans and their involvement in yeast cell adhesion to VN.* J Infect Dis, 1999. **180**(1): p. 156-66.

109.   Binder, B.R., et al., *Plasminogen activator inhibitor 1: physiological and pathophysiological roles.* News Physiol Sci, 2002. **17**: p. 56-61.

110.   Schneiderman, J., et al., *Increased type 1 plasminogen activator inhibitor gene expression in atherosclerotic human arteries.* Proc Natl Acad Sci U S A, 1992. **89**(15): p. 6998-7002.

111.   Thogersen, A.M., et al., *High plasminogen activator inhibitor and tissue plasminogen activator levels in plasma precede a first acute myocardial infarction in both men and women: evidence for the fibrinolytic system as an independent primary risk factor.* Circulation, 1998. **98**(21): p. 2241-7.

112.   Kohler, H.P. and P.J. Grant, *Plasminogen-activator inhibitor type 1 and coronary artery disease.* N Engl J Med, 2000. **342**(24): p. 1792-801.

113.   Wiman, B., et al., *The role of the fibrinolytic system in deep vein thrombosis.* J Lab Clin Med, 1985. **105**(2): p. 265-70.

114.   Duffy, M.J., et al., *Urokinase plasminogen activator: a prognostic marker in multiple types of cancer.* J Surg Oncol, 1999. **71**(2): p. 130-5.

115.   Dublin, E., et al., *Immunohistochemical expression of uPA, uPAR, and PAI-1 in breast carcinoma. Fibroblastic expression has strong associations with tumor pathology.* Am J Pathol, 2000. **157**(4): p. 1219-27.

116.   Juhan-Vague, I., et al., *Plasminogen activator inhibitor-1, inflammation, obesity, insulin resistance and vascular risk.* J Thromb Haemost, 2003. **1**(7): p. 1575-9.

117.   Juhan-Vague, I., M.C. Alessi, and P.E. Morange, *Hypofibrinolysis and increased PAI-1 are linked to atherothrombosis via insulin resistance and obesity.* Ann Med, 2000. **32 Suppl 1**: p. 78-84.

118.   Appel, S.J., J.S. Harrell, and M.L. Davenport, *Central obesity, the metabolic syndrome, and plasminogen activator inhibitor-1 in young adults.* J Am Acad Nurse Pract, 2005. **17**(12): p. 535-41.

119.   Mavri, A., M.C. Alessi, and I. Juhan-Vague, *Hypofibrinolysis in the insulin resistance syndrome: implication in cardiovascular diseases.* J Intern Med, 2004. **255**(4): p. 448-56.

120.   Zhang, W.J., J. Wojta, and B.R. Binder, *Notoginsenoside R1 counteracts endotoxin-induced activation of endothelial cells in vitro and endotoxin-induced lethality in mice in vivo.* Arterioscler Thromb Vasc Biol, 1997. **17**(3): p. 465-74.

121.   Keeton, M.R., et al., *Identification of regulatory sequences in the type 1 plasminogen activator inhibitor gene responsive to transforming growth factor beta.* J Biol Chem, 1991. **266**(34): p. 23048-52.

122.   Westerhausen, D.R., Jr., W.E. Hopkins, and J.J. Billadello, *Multiple transforming growth factor-beta-inducible elements regulate expression of the plasminogen activator inhibitor type-1 gene in Hep G2 cells.* J Biol Chem, 1991. **266**(2): p. 1092-100.

123.   Dennler, S., et al., *Direct binding of Smad3 and Smad4 to critical TGF beta-inducible elements in the promoter of human plasminogen activator inhibitor-type 1 gene.* EMBO J, 1998. **17**(11): p. 3091-100.

124.   Chen, Y.Q., et al., *Sp1 sites mediate activation of the plasminogen activator inhibitor-1 promoter by glucose in vascular smooth muscle cells.* J Biol Chem, 1998. **273**(14): p. 8225-31.

125.   Maiello, M., et al., *Increased expression of tissue plasminogen activator and its inhibitor and reduced fibrinolytic potential of human endothelial cells cultured in elevated glucose.* Diabetes, 1992. **41**(8): p. 1009-15.

126.   Pandolfi, A., et al., *Glucose and insulin independently reduce the fibrinolytic potential of human vascular smooth muscle cells in culture.* Diabetologia, 1996. **39**(12): p. 1425-31.

127.   Schneider, D.J., T.K. Nordt, and B.E. Sobel, *Stimulation by proinsulin of expression of plasminogen activator inhibitor type-I in endothelial cells.* Diabetes, 1992. **41**(7): p. 890-5.

128.   Sironi, L., et al., *Plasminogen activator inhibitor type-1 synthesis and mRNA expression in HepG2 cells are regulated by VLDL.* Arterioscler Thromb Vasc Biol, 1996. **16**(1): p. 89-96.

129.   Vaughan, D.E., S.A. Lazos, and K. Tong, *Angiotensin II regulates the expression of plasminogen activator inhibitor-1 in cultured endothelial cells. A potential link between the renin-angiotensin system and thrombosis.* J Clin Invest, 1995. **95**(3): p. 995-1001.

130.   Alderman, M.H., et al., *Association of the renin-sodium profile with the risk of myocardial infarction in patients with hypertension.* N Engl J Med, 1991. **324**(16): p. 1098-104.

131.   Brown, N.J., M. Agirbasli, and D.E. Vaughan, *Comparative effect of angiotensin-converting enzyme inhibition and angiotensin II type 1 receptor antagonism on plasma fibrinolytic balance in humans.* Hypertension, 1999. **34**(2): p. 285-90.

132.   Hekman, C.M. and D.J. Loskutoff, *Bovine plasminogen activator inhibitor 1: specificity determinations and comparison of the active, latent, and guanidine-activated forms.* Biochemistry, 1988. **27**(8): p. 2911-8.

133.   Cale, J.M. and D.A. Lawrence, *Structure-function relationships of plasminogen activator inhibitor-1 and its potential as a therapeutic agent.* Curr Drug Targets, 2007. **8**(9): p. 971-81.

134.   Sherman, P.M., et al., *Identification of tissue-type plasminogen activator-specific plasminogen activator inhibitor-1 mutants. Evidence that second sites of interaction contribute to target specificity.* J Biol Chem, 1995. **270**(16): p. 9301-6.

135.   Blouse, G.E., et al., *Mutation of the highly conserved tryptophan in the serpin breach region alters the inhibitory mechanism of plasminogen activator inhibitor-1.* Biochemistry, 2003. **42**(42): p. 12260-72.

136.   Shieh, B.H., J. Potempa, and J. Travis, *The use of alpha 2-antiplasmin as a model for the demonstration of complex reversibility in serpins.* J Biol Chem, 1989. **264**(23): p. 13420-3.

137. Lawrence, D.A., et al., *Serpin-protease complexes are trapped as stable acyl-enzyme intermediates.* J Biol Chem, 1995. **270**(43): p. 25309-12.

138. Lawrence, D.A., et al., *Serpin reactive center loop mobility is required for inhibitor function but not for enzyme recognition.* J Biol Chem, 1994. **269**(44): p. 27657-62.

139. Kaslik, G., et al., *Effects of serpin binding on the target proteinase: global stabilization, localized increased structural flexibility, and conserved hydrogen bonding at the active site.* Biochemistry, 1997. **36**(18): p. 5455-64.

140. Stratikos, E. and P.G. Gettins, *Major proteinase movement upon stable serpin-proteinase complex formation.* Proc Natl Acad Sci U S A, 1997. **94**(2): p. 453-8.

141. Dementiev, A., et al., *Canonical inhibitor-like interactions explain reactivity of alpha1-proteinase inhibitor Pittsburgh and antithrombin with proteinases.* J Biol Chem, 2003. **278**(39): p. 37881-7.

142. Huntington, J.A., R.J. Read, and R.W. Carrell, *Structure of a serpin-protease complex shows inhibition by deformation.* Nature, 2000. **407**(6806): p. 923-6.

143. Egelund, R., et al., *An ester bond linking a fragment of a serine proteinase to its serpin inhibitor.* Biochemistry, 1998. **37**(18): p. 6375-9.

144. Crowther, D.C., D.L. Evans, and R.W. Carrell, *Serpins: implications of a mobile reactive centre.* Curr Opin Biotechnol, 1992. **3**(4): p. 399-407.

145. Carrell, R.W., D.L. Evans, and P.E. Stein, *Mobile reactive centre of serpins and the control of thrombosis.* Nature, 1991. **353**(6344): p. 576-8.

146. Stein, P.E., et al., *Crystal structure of ovalbumin as a model for the reactive centre of serpins.* Nature, 1990. **347**(6288): p. 99-102.

147. Stein, P.E., et al., *Crystal structure of uncleaved ovalbumin at 1.95 A resolution.* J Mol Biol, 1991. **221**(3): p. 941-59.

148. Schulze, A.J., et al., *Structural aspects of serpin inhibition.* FEBS Lett, 1994. **344**(2-3): p. 117-24.

149. Carrell, R.W. and P.E. Stein, *The biostructural pathology of the serpins: critical function of sheet opening mechanism.* Biol Chem Hoppe Seyler, 1996. **377**(1): p. 1-17.

150. Skriver, K., et al., *Substrate properties of C1 inhibitor Ma (alanine 434----glutamic acid). Genetic and structural evidence suggesting that the P12-region contains critical determinants of serine protease inhibitor/substrate status.* J Biol Chem, 1991. **266**(14): p. 9216-21.

151. Huber, R. and R.W. Carrell, *Implications of the three-dimensional structure of alpha 1-antitrypsin for structure and function of serpins.* Biochemistry, 1989. **28**(23): p. 8951-66.

152. Loebermann, H., et al., *Human alpha 1-proteinase inhibitor. Crystal structure analysis of two crystal modifications, molecular model and preliminary analysis of the implications for function.* J Mol Biol, 1984. **177**(3): p. 531-57.

153. Stein, P. and C. Chothia, *Serpin tertiary structure transformation.* J Mol Biol, 1991. **221**(2): p. 615-21.

154. Egelund, R., et al., *Type-1 plasminogen-activator inhibitor -- conformational differences between latent, active, reactive-centre-cleaved and plasminogen-activator-complexed forms, as probed by proteolytic susceptibility.* Eur J Biochem, 1997. **248**(3): p. 775-85.

155. Beauchamp, N.J., et al., *Antithrombins Wibble and Wobble (T85M/K): archetypal conformational diseases with in vivo latent-transition, thrombosis, and heparin activation.* Blood, 1998. **92**(8): p. 2696-706.

156. Lomas, D.A., et al., *Preparation and characterization of latent alpha 1-antitrypsin.* J Biol Chem, 1995. **270**(10): p. 5282-8.

157. Carrell, R.W., et al., *Biological implications of a 3 A structure of dimeric antithrombin.* Structure, 1994. **2**(4): p. 257-70.

158. Lindahl, T.L., O. Sigurdardottir, and B. Wiman, *Stability of plasminogen activator inhibitor 1 (PAI-1).* Thromb Haemost, 1989. **62**(2): p. 748-51.

159. Tucker, H.M., et al., *Engineering of plasminogen activator inhibitor-1 to reduce the rate of latency transition.* Nat Struct Biol, 1995. **2**(6): p. 442-5.

160. Mottonen, J., et al., *Structural basis of latency in plasminogen activator inhibitor-1.* Nature, 1992. **355**(6357): p. 270-3.

161. Stout, T.J., et al., *Structures of active and latent PAI-1: a possible stabilizing role for chloride ions.* Biochemistry, 2000. **39**(29): p. 8460-9.

162. Hekman, C.M. and D.J. Loskutoff, *Endothelial cells produce a latent inhibitor of plasminogen activators that can be activated by denaturants.* J Biol Chem, 1985. **260**(21): p. 11581-7.

163. Lambers, J.W., et al., *Activation of human endothelial cell-type plasminogen activator inhibitor (PAI-1) by negatively charged phospholipids.* J Biol Chem, 1987. **262**(36): p. 17492-6.

164. Berkenpas, M.B., D.A. Lawrence, and D. Ginsburg, *Molecular evolution of plasminogen activator inhibitor-1 functional stability.* EMBO J, 1995. **14**(13): p. 2969-77.

165. Sharp, A.M., et al., *The active conformation of plasminogen activator inhibitor 1, a target for drugs to control fibrinolysis and cell adhesion.* Structure, 1999. **7**(2): p. 111-8.

166. Sancho, E., et al., *Conformational studies on plasminogen activator inhibitor (PAI-1) in active, latent, substrate, and cleaved forms.* Biochemistry, 1995. **34**(3): p. 1064-9.

167. Mangs, H., G.C. Sui, and B. Wiman, *PAI-1 stability: the role of histidine residues.* FEBS Lett, 2000. **475**(3): p. 192-6.

168. Blouse, G.E., et al., *Interactions of Plasminogen Activator Inhibitor-1 with Vitronectin Involve an Extensive Binding Surface and Induce Mutual Conformational Rearrangements (dagger).* Biochemistry, 2009.

169. Blasi, F., J.D. Vassalli, and K. Dano, *Urokinase-type plasminogen activator: proenzyme, receptor, and inhibitors.* J Cell Biol, 1987. **104**(4): p. 801-4.

170. Hoylaerts, M., et al., *Kinetics of the activation of plasminogen by human tissue plasminogen activator. Role of fibrin.* J Biol Chem, 1982. **257**(6): p. 2912-9.

171. Higgins, D.L. and G.A. Vehar, *Interaction of one-chain and two-chain tissue plasminogen activator with intact and plasmin-degraded fibrin.* Biochemistry, 1987. **26**(24): p. 7786-91.

172. Wagner, O.F., et al., *Interaction between plasminogen activator inhibitor type 1 (PAI-1) bound to fibrin and either tissue-type plasminogen activator (t-PA) or urokinase-type plasminogen activator (u-PA). Binding of t-PA/PAI-1 complexes to fibrin mediated by both the finger and the kringle-2 domain of t-PA.* J Clin Invest, 1989. **84**(2): p. 647-55.

173. Marder, V.J. and S. Sherry, *Thrombolytic therapy: current status (1).* N Engl J Med, 1988. **318**(23): p. 1512-20.

174. Chesebro, J.H., et al., *Thrombolysis in Myocardial Infarction (TIMI) Trial, Phase I: A comparison between intravenous tissue plasminogen activator and intravenous streptokinase. Clinical findings through hospital discharge.* Circulation, 1987. **76**(1): p. 142-54.

175. Sprengers, E.D., J.W. Akkerman, and B.G. Jansen, *Blood platelet plasminogen activator inhibitor: two different pools of endothelial cell type plasminogen activator inhibitor in human blood.* Thromb Haemost, 1986. **55**(3): p. 325-9.

176. Kruithof, E.K., G. Nicolosa, and F. Bachmann, *Plasminogen activator inhibitor 1: development of a radioimmunoassay and observations on its plasma concentration during venous occlusion and after platelet aggregation.* Blood, 1987. **70**(5): p. 1645-53.

177. Levi, M., et al., *Inhibition of plasminogen activator inhibitor-1 activity results in promotion of endogenous thrombolysis and inhibition of thrombus extension in models of experimental thrombosis.* Circulation, 1992. **85**(1): p. 305-12.

178. Gelehrter, T.D. and R. Sznycer-Laszuk, *Thrombin induction of plasminogen activator-inhibitor in cultured human endothelial cells.* J Clin Invest, 1986. **77**(1): p. 165-9.

179. Margaglione, M., et al., *Abnormally high circulation levels of tissue plasminogen activator and plasminogen activator inhibitor-1 in patients with a history of ischemic stroke.* Arterioscler Thromb, 1994. **14**(11): p. 1741-5.

180. Estreicher, A., et al., *The receptor for urokinase type plasminogen activator polarizes expression of the protease to the leading edge of migrating monocytes and promotes degradation of enzyme inhibitor complexes.* J Cell Biol, 1990. **111**(2): p. 783-92.

181. Cubellis, M.V., T.C. Wun, and F. Blasi, *Receptor-mediated internalization and degradation of urokinase is caused by its specific inhibitor PAI-1.* EMBO J, 1990. **9**(4): p. 1079-85.

182. Argraves, K.M., et al., *The very low density lipoprotein receptor mediates the cellular catabolism of lipoprotein lipase and urokinase-plasminogen activator inhibitor type I complexes.* J Biol Chem, 1995. **270**(44): p. 26550-7.

183. Nykjaer, A., et al., *Purified alpha 2-macroglobulin receptor/LDL receptor-related protein binds urokinase.plasminogen activator inhibitor type-1 complex. Evidence that the alpha 2-macroglobulin receptor mediates cellular degradation of urokinase receptor-bound complexes.* J Biol Chem, 1992. **267**(21): p. 14543-6.

184. Nykjaer, A., et al., *Regions involved in binding of urokinase-type-1 inhibitor complex and pro-urokinase to the endocytic alpha 2-macroglobulin receptor/low density lipoprotein receptor-related protein. Evidence that the urokinase receptor protects pro-urokinase against binding to the endocytic receptor.* J Biol Chem, 1994. **269**(41): p. 25668-76.

185. Moestrup, S.K., et al., *Epithelial glycoprotein-330 mediates endocytosis of plasminogen activator-plasminogen activator inhibitor type-1 complexes.* J Biol Chem, 1993. **268**(22): p. 16564-70.

186. Stefansson, S., et al., *Plasminogen activator inhibitor-1 contains a cryptic high affinity binding site for the low density lipoprotein receptor-related protein.* J Biol Chem, 1998. **273**(11): p. 6358-66.

187. Nykjaer, A., et al., *Recycling of the urokinase receptor upon internalization of the uPA:serpin complexes.* EMBO J, 1997. **16**(10): p. 2610-20.

188. Orth, K., et al., *Complexes of tissue-type plasminogen activator and its serpin inhibitor plasminogen-activator inhibitor type 1 are internalized by means of the low density lipoprotein receptor-related protein/alpha 2-macroglobulin receptor.* Proc Natl Acad Sci U S A, 1992. **89**(16): p. 7422-6.

189. Andreasen, P.A., et al., *The urokinase-type plasminogen activator system in cancer metastasis: a review.* Int J Cancer, 1997. **72**(1): p. 1-22.

190. Pappot, H., et al., *Plasminogen activator inhibitor type 1 in cancer: therapeutic and prognostic implications.* Biol Chem Hoppe Seyler, 1995. **376**(5): p. 259-67.

191. Bajou, K., et al., *Absence of host plasminogen activator inhibitor 1 prevents cancer invasion and vascularization.* Nat Med, 1998. **4**(8): p. 923-8.

192. Wiman, B., et al., *Plasminogen activator inhibitor 1 (PAI) is bound to vitronectin in plasma.* FEBS Lett, 1988. **242**(1): p. 125-8.

193. Seiffert, D., N.N. Wagner, and D.J. Loskutoff, *Serum-derived vitronectin influences the pericellular distribution of type 1 plasminogen activator inhibitor.* J Cell Biol, 1990. **111**(3): p. 1283-91.

194. Seiffert, D. and D.J. Loskutoff, *Evidence that type 1 plasminogen activator inhibitor binds to the somatomedin B domain of vitronectin.* J Biol Chem, 1991. **266**(5): p. 2824-30.

195. Deng, G., et al., *The PAI-1/vitronectin interaction: two cats in a bag?* Thromb Haemost, 1995. **74**(1): p. 66-70.

196. Royle, G., et al., *A method for defining binding sites involved in protein-protein interactions: analysis of the binding of plasminogen activator inhibitor 1 to the somatomedin domain of vitronectin.* Anal Biochem, 2001. **296**(2): p. 245-53.

197. Lawrence, D.A., et al., *Localization of vitronectin binding domain in plasminogen activator inhibitor-1.* J Biol Chem, 1994. **269**(21): p. 15223-8.

198. Padmanabhan, J. and D.C. Sane, *Localization of a vitronectin binding region of plasminogen activator inhibitor-1.* Thromb Haemost, 1995. **73**(5): p. 829-34.

199. Muehlenweg, B., et al., *Epitope mapping of monoclonal antibodies directed to PAI-1 using PAI-1/PAI-2 chimera and PAI-1-derived synthetic peptides.* Thromb Res, 2000. **98**(1): p. 73-81.

200. Mimuro, J., et al., *Identification of the plasminogen activator inhibitor-1 binding heptapeptide in vitronectin.* Biochemistry, 1993. **32**(9): p. 2314-20.

201. Kost, C., et al., *Mapping of binding sites for heparin, plasminogen activator inhibitor-1, and plasminogen to vitronectin's heparin-binding region reveals a novel vitronectin-dependent feedback mechanism for the control of plasmin formation.* J Biol Chem, 1992. **267**(17): p. 12098-105.

202. Gechtman, Z., et al., *The cluster of basic amino acids in vitronectin contributes to its binding of plasminogen activator inhibitor-1: evidence from thrombin-, elastase- and plasmin-cleaved vitronectins and anti-peptide antibodies.* Biochem J, 1997. **325 (Pt 2)**: p. 339-49.

203. Podor, T.J., et al., *New insights into the size and stoichiometry of the plasminogen activator inhibitor type-1.vitronectin complex.* J Biol Chem, 2000. **275**(33): p. 25402-10.

204. Schar, C.R., et al., *A deletion mutant of vitronectin lacking the somatomedin B domain exhibits residual plasminogen activator inhibitor-1-binding activity.* J Biol Chem, 2008. **283**(16): p. 10297-309.

205. Hogasen, K., T.E. Mollnes, and M. Harboe, *Heparin-binding properties of vitronectin are linked to complex formation as illustrated by in vitro polymerization and binding to the terminal complement complex.* J Biol Chem, 1992. **267**(32): p. 23076-82.

206. Seiffert, D. and D.J. Loskutoff, *Type 1 plasminogen activator inhibitor induces multimerization of plasma vitronectin. A suggested mechanism for the generation of the tissue form of vitronectin in vivo.* J Biol Chem, 1996. **271**(47): p. 29644-51.

207. Seiffert, D. and R.R. Schleef, *Two functionally distinct pools of vitronectin (Vn) in the blood circulation: identification of a heparin-binding competent population of Vn within platelet alpha-granules.* Blood, 1996. **88**(2): p. 552-60.

208. Booth, N.A., et al., *Lysis of platelet-rich thrombi: the role of PAI-1.* Ann N Y Acad Sci, 1992. **667**: p. 70-80.

209. Minor, K.H. and C.B. Peterson, *Plasminogen activator inhibitor type 1 promotes the self-association of vitronectin into complexes exhibiting altered incorporation into the extracellular matrix.* J Biol Chem, 2002. **277**(12): p. 10337-45.

210. Minor, K.H., et al., *A mechanism for assembly of complexes of vitronectin and plasminogen activator inhibitor-1 from sedimentation velocity analysis.* J Biol Chem, 2005. **280**(31): p. 28711-20.

211. Balbo, A., et al., *Studying multiprotein complexes by multisignal sedimentation velocity analytical ultracentrifugation.* Proc Natl Acad Sci U S A, 2005. **102**(1): p. 81-6.

212. Stoop, A.A., F. Lupu, and H. Pannekoek, *Colocalization of thrombin, PAI-1, and vitronectin in the atherosclerotic vessel wall: A potential regulatory mechanism of thrombin activity by PAI-1/vitronectin complexes.* Arterioscler Thromb Vasc Biol, 2000. **20**(4): p. 1143-9.

213. Inuzuka, S., et al., *The significance of colocalization of plasminogen activator inhibitor-1 and vitronectin in hepatic fibrosis.* Scand J Gastroenterol, 1997. **32**(10): p. 1052-60.

214. Nakamura, T., et al., *The localization of plasminogen activator inhibitor-1 in glomerular subepithelial deposits in membranous nephropathy.* J Am Soc Nephrol, 1996. **7**(11): p. 2434-44.

215. Ehrlich, H.J., et al., *Thrombin neutralizes plasminogen activator inhibitor 1 (PAI-1) that is complexed with vitronectin in the endothelial cell matrix.* J Cell Biol, 1991. **115**(6): p. 1773-81.

216. Rezaie, A.R., *Vitronectin functions as a cofactor for rapid inhibition of activated protein C by plasminogen activator inhibitor-1. Implications for the mechanism of profibrinolytic action of activated protein C.* J Biol Chem, 2001. **276**(19): p. 15567-70.

217. Ehrlich, H.J., et al., *Alteration of serpin specificity by a protein cofactor. Vitronectin endows plasminogen activator inhibitor 1 with thrombin inhibitory properties.* J Biol Chem, 1990. **265**(22): p. 13029-35.

218. Stefansson, S., D.A. Lawrence, and W.S. Argraves, *Plasminogen activator inhibitor-1 and vitronectin promote the cellular clearance of thrombin by low density lipoprotein receptor-related proteins 1 and 2.* J Biol Chem, 1996. **271**(14): p. 8215-20.

219. van Aken, B.E., et al., *Localization of vitronectin in the normal and atherosclerotic human vessel wall.* Histochem Cell Biol, 1997. **107**(4): p. 313-20.
220. Smith, E.B., L. Crosbie, and S. Carey, *Prothrombin-related antigens in human aortic intima.* Semin Thromb Hemost, 1996. **22**(4): p. 347-50.
221. Schnaper, H.W., *Balance between matrix synthesis and degradation: a determinant of glomerulosclerosis.* Pediatr Nephrol, 1995. **9**(1): p. 104-11.
222. Stetler-Stevenson, W.G., *Dynamics of matrix turnover during pathologic remodeling of the extracellular matrix.* Am J Pathol, 1996. **148**(5): p. 1345-50.
223. Barnes, J.L., R.J. Mitchell, and E.S. Torres, *Expression of plasminogen activator-inhibitor-1 (PAI-1) during cellular remodeling in proliferative glomerulonephritis in the rat.* J Histochem Cytochem, 1995. **43**(9): p. 895-905.
224. Keeton, M., et al., *Expression of type 1 plasminogen activator inhibitor in renal tissue in murine lupus nephritis.* Kidney Int, 1995. **47**(1): p. 148-57.
225. Huang, Y., et al., *A mutant, noninhibitory plasminogen activator inhibitor type 1 decreases matrix accumulation in experimental glomerulonephritis.* J Clin Invest, 2003. **112**(3): p. 379-88.
226. Waltz, D.A., et al., *Plasmin and plasminogen activator inhibitor type 1 promote cellular motility by regulating the interaction between the urokinase receptor and vitronectin.* J Clin Invest, 1997. **100**(1): p. 58-67.
227. Deng, G., et al., *Is plasminogen activator inhibitor-1 the molecular switch that governs urokinase receptor-mediated cell adhesion and release?* J Cell Biol, 1996. **134**(6): p. 1563-71.
228. Stahl, A. and B.M. Mueller, *Melanoma cell migration on vitronectin: regulation by components of the plasminogen activation system.* Int J Cancer, 1997. **71**(1): p. 116-22.
229. Stefansson, S. and D.A. Lawrence, *The serpin PAI-1 inhibits cell migration by blocking integrin alpha V beta 3 binding to vitronectin.* Nature, 1996. **383**(6599): p. 441-3.
230. Kjoller, L., et al., *Plasminogen activator inhibitor-1 represses integrin- and vitronectin-mediated cell migration independently of its function as an inhibitor of plasminogen activation.* Exp Cell Res, 1997. **232**(2): p. 420-9.
231. Gutierrez, L.S., et al., *Tumor development is retarded in mice lacking the gene for urokinase-type plasminogen activator or its inhibitor, plasminogen activator inhibitor-1.* Cancer Res, 2000. **60**(20): p. 5839-47.
232. Stefansson, S., et al., *Inhibition of angiogenesis in vivo by plasminogen activator inhibitor-1.* J Biol Chem, 2001. **276**(11): p. 8135-41.
233. McMahon, G.A., et al., *Plasminogen activator inhibitor-1 regulates tumor growth and angiogenesis.* J Biol Chem, 2001. **276**(36): p. 33964-8.
234. Vaughan, D.E., et al., *Dynamic structural and functional relationships in recombinant plasminogen activator inhibitor-1 (rPAI-1).* Biochim Biophys Acta, 1993. **1202**(2): p. 221-9.
235. Edelhoch, H., *Spectroscopic determination of tryptophan and tyrosine in proteins.* Biochemistry, 1967. **6**(7): p. 1948-54.
236. Magyar, J.S. and H.A. Godwin, *Spectropotentiometric analysis of metal binding to structural zinc-binding sites: accounting quantitatively for pH and metal ion buffering effects.* Anal Biochem, 2003. **320**(1): p. 39-54.

237. Anwar, Z.M. and H.A. Azab, *Ternary complexes in solution. Comparison of the coordination tendency of some biologically important zwitterionic buffers toward the binary complexes of some transition metal ions and some amino acids.* Journal of Chemical and Engineering Data, 1999. **44**(6): p. 1151-1157.

238. Scheller, K.H., et al., *Metal Ion-Buffer Interactions .2. Stability of Binary and Ternary Complexes Containing 2-[Bis(2-Hydroxyethyl)Amino]-2(Hydroxymethyl)-1,3-Propanediol (Bis-Tris) and Adenosine 5'-Triphosphate (Atp).* European Journal of Biochemistry, 1980. **107**(2): p. 455-466.

239. Schuck, P., *Size-distribution analysis of macromolecules by sedimentation velocity ultracentrifugation and lamm equation modeling.* Biophys J, 2000. **78**(3): p. 1606-19.

240. Dam, J. and P. Schuck, *Calculating sedimentation coefficient distributions by direct modeling of sedimentation velocity concentration profiles.* Methods Enzymol, 2004. **384**: p. 185-212.

241. Shore, J.D., et al., *A fluorescent probe study of plasminogen activator inhibitor-1. Evidence for reactive center loop insertion and its role in the inhibitory mechanism.* J Biol Chem, 1995. **270**(10): p. 5395-8.

242. Schar, C.R., et al., *Characterization of a site on PAI-1 that binds to vitronectin outside of the somatomedin B domain.* J Biol Chem, 2008. **283**(42): p. 28487-96.

243. Lomas, D.A., et al., *The mechanism of Z alpha 1-antitrypsin accumulation in the liver.* Nature, 1992. **357**(6379): p. 605-7.

244. Bruce, D., et al., *Thromboembolic disease due to thermolabile conformational changes of antithrombin Rouen-VI (187 Asn-->Asp).* J Clin Invest, 1994. **94**(6): p. 2265-74.

245. Eldering, E., et al., *COOH-terminal substitutions in the serpin C1 inhibitor that cause loop overinsertion and subsequent multimerization.* J Biol Chem, 1995. **270**(6): p. 2579-87.

246. Zhou, A., et al., *Polymerization of plasminogen activator inhibitor-1.* J Biol Chem, 2001. **276**(12): p. 9115-22.

247. Eitzman, D.T., et al., *Peptide-mediated inactivation of recombinant and platelet plasminogen activator inhibitor-1 in vitro.* J Clin Invest, 1995. **95**(5): p. 2416-20.

248. Kvassman, J.O., D.A. Lawrence, and J.D. Shore, *The acid stabilization of plasminogen activator inhibitor-1 depends on protonation of a single group that affects loop insertion into beta-sheet A.* J Biol Chem, 1995. **270**(46): p. 27942-7.

249. Xue, Y., et al., *Interfering with the inhibitory mechanism of serpins: crystal structure of a complex formed between cleaved plasminogen activator inhibitor type 1 and a reactive-centre loop peptide.* Structure, 1998. **6**(5): p. 627-36.

250. Gils, A., et al., *Biochemical importance of glycosylation of plasminogen activator inhibitor-1.* Thromb Haemost, 2003. **90**(2): p. 206-17.

251. Day, D.D., *Method for Making Purified Plasminogen Activator Inhibitor Type-1 (PAI-1) and Purified PAI-1 Made Therefrom*, U. States, Editor. 2006, Molecular Innovations, Inc.: USA.

252. Nalbandyan, R.M., *Copper in brain.* Neurochem Res, 1983. **8**(10): p. 1211-32.

253. Kramer, M.L., et al., *Prion protein binds copper within the physiological concentration range.* J Biol Chem, 2001. **276**(20): p. 16711-9.

254. Linder, M.C. and M. Hazegh-Azam, *Copper biochemistry and molecular biology.* Am J Clin Nutr, 1996. **63**(5): p. 797S-811S.
255. Osterberg, R., *Physiology and pharmacology of copper.* Pharmacol Ther, 1980. **9**(1): p. 121-46.
256. Burns, C.J., Field, L.D., Hambley, T.W., Lin, T., Ridley, D.D., Turner, P., Wilkinson, M.P., *X-Ray crystal structural determination of copper(II)-nitrilotriacetic acid-bis(N-methylimidazol-2-yl)ketone ternary complex.* ARKIVOC, 2001(vii): p. 157-165.
257. Steinert, K., Artz, C., and R. Fabis, Ribbe, A, *Comparison of chelating resins for purification of 6xHis-tagged proteins.* QIAGEN News, 1996. **5**.
258. Napper, S., et al., *Selective extraction and characterization of a histidine-phosphorylated peptide using immobilized copper(II) ion affinity chromatography and matrix-assisted laser desorption/ionization time-of-flight mass spectrometry.* Anal Chem, 2003. **75**(7): p. 1741-7.
259. Volker, W., et al., *Binding and processing of multimeric vitronectin by vascular endothelial cells.* J Histochem Cytochem, 1993. **41**(12): p. 1823-32.
260. Vassalli, J.D., A.P. Sappino, and D. Belin, *The plasminogen activator/plasmin system.* J Clin Invest, 1991. **88**(4): p. 1067-72.
261. Devy, L., et al., *The pro- or antiangiogenic effect of plasminogen activator inhibitor 1 is dose dependent.* FASEB J, 2002. **16**(2): p. 147-54.
262. Zhuang, P., M.N. Blackburn, and C.B. Peterson, *Characterization of the denaturation and renaturation of human plasma vitronectin. I. Biophysical characterization of protein unfolding and multimerization.* J Biol Chem, 1996. **271**(24): p. 14323-32.
263. Edgell, C.J., C.C. McDonald, and J.B. Graham, *Permanent cell line expressing human factor VIII-related antigen established by hybridization.* Proc Natl Acad Sci U S A, 1983. **80**(12): p. 3734-7.
264. Emeis, J.J. and C.J. Edgell, *Fibrinolytic properties of a human endothelial hybrid cell line (Ea.hy 926).* Blood, 1988. **71**(6): p. 1669-75.
265. Thornhill, M.H., J. Li, and D.O. Haskard, *Leucocyte endothelial cell adhesion: a study comparing human umbilical vein endothelial cells and the endothelial cell line EA-hy-926.* Scand J Immunol, 1993. **38**(3): p. 279-86.
266. Saijonmaa, O., et al., *Endothelin-1 is expressed and released by a human endothelial hybrid cell line (EA.hy 926).* Biochem Biophys Res Commun, 1991. **181**(2): p. 529-36.
267. Podor, T.J., et al., *Type 1 plasminogen activator inhibitor binds to fibrin via vitronectin.* J Biol Chem, 2000. **275**(26): p. 19788-94.
268. Kadler, K.E., et al., *Collagens at a glance.* J Cell Sci, 2007. **120**(Pt 12): p. 1955-8.
269. Than, M.E., et al., *The 1.9-A crystal structure of the noncollagenous (NC1) domain of human placenta collagen IV shows stabilization via a novel type of covalent Met-Lys cross-link.* Proc Natl Acad Sci U S A, 2002. **99**(10): p. 6607-12.
270. Heremans, A., et al., *Matrix-associated heparan sulfate proteoglycan: core protein-specific monoclonal antibodies decorate the pericellular matrix of connective tissue cells and the stromal side of basement membranes.* J Cell Biol, 1989. **109**(6 Pt 1): p. 3199-211.
271. Hassell, J.R., et al., *Isolation of a heparan sulfate-containing proteoglycan from basement membrane.* Proc Natl Acad Sci U S A, 1980. **77**(8): p. 4494-8.

272. Fujiwara, S., et al., *Structure and interactions of heparan sulfate proteoglycans from a mouse tumor basement membrane.* Eur J Biochem, 1984. **143**(1): p. 145-57.

273. Gallagher, J.T., M. Lyon, and W.P. Steward, *Structure and function of heparan sulphate proteoglycans.* Biochem J, 1986. **236**(2): p. 313-25.

274. Wang, S.Y., M.A. Roguska, and L.J. Gudas, *Defective post-translational modification of collagen IV in a mutant F9 teratocarcinoma cell line is associated with delayed differentiation and growth arrest in response to retinoic acid.* J Biol Chem, 1989. **264**(26): p. 15556-64.

275. Preissner, K.T. and G. Muller-Berghaus, *Neutralization and binding of heparin by S protein/vitronectin in the inhibition of factor Xa by antithrombin III. Involvement of an inducible heparin-binding domain of S protein/vitronectin.* J Biol Chem, 1987. **262**(25): p. 12247-53.

276. Zhuang, P., A.I. Chen, and C.B. Peterson, *Native and multimeric vitronectin exhibit similar affinity for heparin. Differences in heparin binding properties induced upon denaturation are due to self-association into a multivalent form.* J Biol Chem, 1997. **272**(11): p. 6858-67.

277. Seiffert, D. and J.W. Smith, *The cell adhesion domain in plasma vitronectin is cryptic.* J Biol Chem, 1997. **272**(21): p. 13705-10.

278. Okumura, Y., et al., *Kinetic analysis of the interaction between vitronectin and the urokinase receptor.* J Biol Chem, 2002. **277**(11): p. 9395-404.

279. Humphries, J.D., A. Byron, and M.J. Humphries, *Integrin ligands at a glance.* J Cell Sci, 2006. **119**(Pt 19): p. 3901-3.

280. Aota, S., M. Nomizu, and K.M. Yamada, *The short amino acid sequence Pro-His-Ser-Arg-Asn in human fibronectin enhances cell-adhesive function.* J Biol Chem, 1994. **269**(40): p. 24756-61.

281. Kim, S., et al., *Regulation of angiogenesis in vivo by ligation of integrin alpha5beta1 with the central cell-binding domain of fibronectin.* Am J Pathol, 2000. **156**(4): p. 1345-62.

282. Kumar, C.C., *Integrin alpha v beta 3 as a therapeutic target for blocking tumor-induced angiogenesis.* Curr Drug Targets, 2003. **4**(2): p. 123-31.

283. Weidner, N., et al., *Tumor angiogenesis and metastasis--correlation in invasive breast carcinoma.* N Engl J Med, 1991. **324**(1): p. 1-8.

284. Reardon, D.A., et al., *Cilengitide: an integrin-targeting arginine-glycine-aspartic acid peptide with promising activity for glioblastoma multiforme.* Expert Opin Investig Drugs, 2008. **17**(8): p. 1225-35.

285. Trikha, M., et al., *CNTO 95, a fully human monoclonal antibody that inhibits alphav integrins, has antitumor and antiangiogenic activity in vivo.* Int J Cancer, 2004. **110**(3): p. 326-35.

286. Sepp, N.T., et al., *Basic fibroblast growth factor increases expression of the alpha v beta 3 integrin complex on human microvascular endothelial cells.* J Invest Dermatol, 1994. **103**(3): p. 295-9.

287. Swerlick, R.A., et al., *Expression and modulation of the vitronectin receptor on human dermal microvascular endothelial cells.* J Invest Dermatol, 1992. **99**(6): p. 715-22.

288. Brooks, P.C., R.A. Clark, and D.A. Cheresh, *Requirement of vascular integrin alpha v beta 3 for angiogenesis.* Science, 1994. **264**(5158): p. 569-71.

289. Choi, S., et al., *Small molecule inhibitors of integrin alpha2beta1.* J Med Chem, 2007. **50**(22): p. 5457-62.

290. McCall-Culbreath, K.D. and M.M. Zutter, *Collagen receptor integrins: rising to the challenge.* Curr Drug Targets, 2008. **9**(2): p. 139-49.

291. Brown, S.L., et al., *Stimulation of migration of human aortic smooth muscle cells by vitronectin: implications for atherosclerosis.* Cardiovasc Res, 1994. **28**(12): p. 1815-20.

292. Kim, J.P., et al., *Vitronectin-driven human keratinocyte locomotion is mediated by the alpha v beta 5 integrin receptor.* J Biol Chem, 1994. **269**(43): p. 26926-32.

293. Waltz, D.A., L.Z. Sailor, and H.A. Chapman, *Cytokines induce urokinase-dependent adhesion of human myeloid cells. A regulatory role for plasminogen activator inhibitors.* J Clin Invest, 1993. **91**(4): p. 1541-52.

294. Roca-Cusachs, P., et al., *Clustering of alpha(5)beta(1) integrins determines adhesion strength whereas alpha(v)beta(3) and talin enable mechanotransduction.* Proc Natl Acad Sci U S A, 2009. **106**(38): p. 16245-50.

295. Duensing, T.D. and J.P. van Putten, *Vitronectin mediates internalization of Neisseria gonorrhoeae by Chinese hamster ovary cells.* Infect Immun, 1997. **65**(3): p. 964-70.

296. Dehio, M., et al., *Vitronectin-dependent invasion of epithelial cells by Neisseria gonorrhoeae involves alpha(v) integrin receptors.* FEBS Lett, 1998. **424**(1-2): p. 84-8.

297. Li, D.Q., F. Lundberg, and A. Ljungh, *Characterization of vitronectin-binding proteins of Staphylococcus epidermidis.* Curr Microbiol, 2001. **42**(5): p. 361-7.

298. Bergmann, S., et al., *Integrin-linked kinase is required for vitronectin-mediated internalization of Streptococcus pneumoniae by host cells.* J Cell Sci, 2009. **122**(Pt 2): p. 256-67.

299. Castro, M., et al., *Candida albicans induces the release of inflammatory mediators from human peripheral blood monocytes.* Inflammation, 1996. **20**(1): p. 107-22.

300. Cross, C.E. and G.J. Bancroft, *Ingestion of acapsular Cryptococcus neoformans occurs via mannose and beta-glucan receptors, resulting in cytokine production and increased phagocytosis of the encapsulated form.* Infect Immun, 1995. **63**(7): p. 2604-11.

301. Hoffman, O.A., J.E. Standing, and A.H. Limper, *Pneumocystis carinii stimulates tumor necrosis factor-alpha release from alveolar macrophages through a beta-glucan-mediated mechanism.* J Immunol, 1993. **150**(9): p. 3932-40.

302. Hoffman, O.A., E.J. Olson, and A.H. Limper, *Fungal beta-glucans modulate macrophage release of tumor necrosis factor-alpha in response to bacterial lipopolysaccharide.* Immunol Lett, 1993. **37**(1): p. 19-25.

303. Neese, L.W., et al., *Vitronectin, fibronectin, and gp120 antibody enhance macrophage release of TNF-alpha in response to Pneumocystis carinii.* J Immunol, 1994. **152**(9): p. 4549-56.

304. Limper, A.H. and J.E. Standing, *Vitronectin interacts with Candida albicans and augments organism attachment to the NR8383 macrophage cell line.* Immunol Lett, 1994. **42**(3): p. 139-44.

305. Olson, E.J., et al., *Fungal beta-glucan interacts with vitronectin and stimulates tumor necrosis factor alpha release from macrophages.* Infect Immun, 1996. **64**(9): p. 3548-54.

306.   Santoni, G., et al., *Involvement of alpha(v)beta3 integrin-like receptor and glycosaminoglycans in Candida albicans germ tube adhesion to vitronectin and to a human endothelial cell line.* Microb Pathog, 2001. **31**(4): p. 159-72.

307.   Zheng, X., et al., *Vitronectin is not essential for normal mammalian development and fertility.* Proc Natl Acad Sci U S A, 1995. **92**(26): p. 12426-30.

308.   Limper, A.H., et al., *Vitronectin binds to Pneumocystis carinii and mediates organism attachment to cultured lung epithelial cells.* Infect Immun, 1993. **61**(10): p. 4302-9.

309.   Rozell, B., P.O. Ljungdahl, and P. Martinez, *Host-pathogen interactions and the pathological consequences of acute systemic Candida albicans infections in mice.* Curr Drug Targets, 2006. **7**(4): p. 483-94.

310.   Rogers, T. and E. Balish, *Experimental Candida albicans infection in conventional mice and germfree rats.* Infect Immun, 1976. **14**(1): p. 33-8.

311.   Warenda, A.J., et al., *Candida albicans septin mutants are defective for invasive growth and virulence.* Infect Immun, 2003. **71**(7): p. 4045-51.

312.   Yang, Y.L., *Virulence factors of Candida species.* J Microbiol Immunol Infect, 2003. **36**(4): p. 223-8.

313.   Bradley, P.P., R.D. Christensen, and G. Rothstein, *Cellular and extracellular myeloperoxidase in pyogenic inflammation.* Blood, 1982. **60**(3): p. 618-22.

314.   Olsen, R.L., et al., *Molecular forms of myeloperoxidase in human plasma.* Biochem J, 1986. **237**(2): p. 559-65.

315.   Klebanoff, S.J., *Myeloperoxidase-halide-hydrogen peroxide antibacterial system.* J Bacteriol, 1968. **95**(6): p. 2131-8.

316.   Edelson, P.J. and Z.A. Cohn, *Peroxidase-mediated mammalian cell cytotoxicity.* J Exp Med, 1973. **138**(1): p. 318-23.

317.   Klebanoff, S.J., *Myeloperoxidase: contribution to the microbicidal activity of intact leukocytes.* Science, 1970. **169**(950): p. 1095-7.

318.   Thomas, E.L., *Myeloperoxidase-hydrogen peroxide-chloride antimicrobial system: effect of exogenous amines on antibacterial action against Escherichia coli.* Infect Immun, 1979. **25**(1): p. 110-6.

319.   Winterbourn, C.C., M.C. Vissers, and A.J. Kettle, *Myeloperoxidase.* Curr Opin Hematol, 2000. **7**(1): p. 53-8.

320.   Zhang, R., et al., *Myeloperoxidase functions as a major enzymatic catalyst for initiation of lipid peroxidation at sites of inflammation.* J Biol Chem, 2002. **277**(48): p. 46116-22.

321.   Mullane, K.M., R. Kraemer, and B. Smith, *Myeloperoxidase activity as a quantitative assessment of neutrophil infiltration into ischemic myocardium.* J Pharmacol Methods, 1985. **14**(3): p. 157-67.

322.   Kullberg, B.J., *Trends in immunotherapy of fungal infections.* Eur J Clin Microbiol Infect Dis, 1997. **16**(1): p. 51-5.

323.   Tuite, A., A. Mullick, and P. Gros, *Genetic analysis of innate immunity in resistance to Candida albicans.* Genes Immun, 2004. **5**(7): p. 576-87.

324.   Aratani, Y., et al., *Differential host susceptibility to pulmonary infections with bacteria and fungi in mice deficient in myeloperoxidase.* J Infect Dis, 2000. **182**(4): p. 1276-9.

325.   Aratani, Y., et al., *Severe impairment in early host defense against Candida albicans in mice deficient in myeloperoxidase.* Infect Immun, 1999. **67**(4): p. 1828-36.

326. Lanza, F., *Clinical manifestation of myeloperoxidase deficiency.* J Mol Med, 1998. **76**(10): p. 676-81.

327. He, H., et al., *Mutative expression in Candida albicans infection and cytokine signaling network in gene knockout mice.* Eur J Clin Microbiol Infect Dis, 2010.

328. Filler, S.G., et al., *Candida albicans stimulates cytokine production and leukocyte adhesion molecule expression by endothelial cells.* Infect Immun, 1996. **64**(7): p. 2609-17.

329. Dongari-Bagtzoglou, A. and P.L. Fidel, Jr., *The host cytokine responses and protective immunity in oropharyngeal candidiasis.* J Dent Res, 2005. **84**(11): p. 966-77.

330. Ashman, R.B. and J.M. Papadimitriou, *Production and function of cytokines in natural and acquired immunity to Candida albicans infection.* Microbiol Rev, 1995. **59**(4): p. 646-72.

331. Morrison, C.J., et al., *Activation of murine polymorphonuclear neutrophils for fungicidal activity by recombinant gamma interferon.* J Leukoc Biol, 1987. **41**(5): p. 434-40.

332. Brummer, E., C.J. Morrison, and D.A. Stevens, *Recombinant and natural gamma-interferon activation of macrophages in vitro: different dose requirements for induction of killing activity against phagocytizable and nonphagocytizable fungi.* Infect Immun, 1985. **49**(3): p. 724-30.

333. Brummer, E. and D.A. Stevens, *Candidacidal mechanisms of peritoneal macrophages activated with lymphokines or gamma-interferon.* J Med Microbiol, 1989. **28**(3): p. 173-81.

334. Kullberg, B.J., et al., *Recombinant interferon-gamma enhances resistance to acute disseminated Candida albicans infection in mice.* J Infect Dis, 1993. **168**(2): p. 436-43.

335. Ibrahim, A.S., et al., *Interferon-gamma protects endothelial cells from damage by Candida albicans.* J Infect Dis, 1993. **167**(6): p. 1467-70.

336. Fratti, R.A., et al., *Gamma interferon protects endothelial cells from damage by Candida albicans by inhibiting endothelial cell phagocytosis.* Infect Immun, 1996. **64**(11): p. 4714-8.

337. Romani, L., *Innate and adaptive immunity in Candida albicans infections and saprophytism.* J Leukoc Biol, 2000. **68**(2): p. 175-9.

338. Romani, L., F. Bistoni, and P. Puccetti, *Initiation of T-helper cell immunity to Candida albicans by IL-12: the role of neutrophils.* Chem Immunol, 1997. **68**: p. 110-35.

339. Spellberg, B. and J.E. Edwards, *The Pathophysiology and Treatment of Candida Sepsis.* Curr Infect Dis Rep, 2002. **4**(5): p. 387-399.

340. Chiani, P., C. Bromuro, and A. Torosantucci, *Defective induction of interleukin-12 in human monocytes by germ-tube forms of Candida albicans.* Infect Immun, 2000. **68**(10): p. 5628-34.

341. d'Ostiani, C.F., et al., *Dendritic cells discriminate between yeasts and hyphae of the fungus Candida albicans. Implications for initiation of T helper cell immunity in vitro and in vivo.* J Exp Med, 2000. **191**(10): p. 1661-74.

342. Beutler, B., I.W. Milsark, and A.C. Cerami, *Passive immunization against cachectin/tumor necrosis factor protects mice from lethal effect of endotoxin.* Science, 1985. **229**(4716): p. 869-71.

343. Tracey, K.J., et al., *Anti-cachectin/TNF monoclonal antibodies prevent septic shock during lethal bacteraemia.* Nature, 1987. **330**(6149): p. 662-4.

344. Steinshamn, S. and A. Waage, *Tumor necrosis factor and interleukin-6 in Candida albicans infection in normal and granulocytopenic mice.* Infect Immun, 1992. **60**(10): p. 4003-8.

345. Netea, M.G., et al., *Pharmacologic inhibitors of tumor necrosis factor production exert differential effects in lethal endotoxemia and in infection with live microorganisms in mice.* J Infect Dis, 1995. **171**(2): p. 393-9.

346. Netea, M.G., et al., *Increased susceptibility of TNF-alpha lymphotoxin-alpha double knockout mice to systemic candidiasis through impaired recruitment of neutrophils and phagocytosis of Candida albicans.* J Immunol, 1999. **163**(3): p. 1498-505.

347. Cohen, A.M., et al., *In vivo activation of neutrophil function in hamsters by recombinant human granulocyte colony-stimulating factor.* Infect Immun, 1988. **56**(11): p. 2861-5.

348. Roilides, E., et al., *Granulocyte colony-stimulating factor enhances the phagocytic and bactericidal activity of normal and defective human neutrophils.* J Infect Dis, 1991. **163**(3): p. 579-83.

349. Kullberg, B.J., et al., *Recombinant murine granulocyte colony-stimulating factor protects against acute disseminated Candida albicans infection in nonneutropenic mice.* J Infect Dis, 1998. **177**(1): p. 175-81.

350. Spellberg, B., et al., *Mice with disseminated candidiasis die of progressive sepsis.* J Infect Dis, 2005. **192**(2): p. 336-43.

351. Minamiguchi, K., et al., *Thiolutin, an inhibitor of HUVEC adhesion to vitronectin, reduces paxillin in HUVECs and suppresses tumor cell-induced angiogenesis.* Int J Cancer, 2001. **93**(3): p. 307-16.

352. Weller, M., et al., *Will integrin inhibitors have proangiogenic effects in the clinic?* Nat Med, 2009. **15**(7): p. 726; author reply 727.

APPENDIX

Cell types and their culture conditions

Cell Type	Culture Condition	Comments
HT1080 (fibrosarcoma)	MEM + 10%FBS + 1X penicillin-streptomycin solution (from 100X stock)	Adherent type of culture grows in monolayer. This cell line grows pretty fast but doesn't like too much of overgrowth. Sensitive to cell-cell contact. Once they come off the surface they do not re-adhere. Purchased from ATCC.
EA.hy926 (immortalized endothelial cell)	DMEM + 10%FBS + 1X penicillin-streptomycin solution (from 100X stock) + 1X HAT (from 500X stock)	Hybrid of A549 (lung carcinoma celli line) and HUVEC. Contains more than 46 chromosomes. Expresses factor-VIII related antigen that is characteristic feature of endothelial cell. Media is purchased from GIBCO which already contains HEPES but no Na-pyruvate. Use FBS-premium from Atlanta Biologicals and heat denature the FBS before use (56^0C for 30 min) Obtained from Dr. John Biggerstaff's lab.
HEK293 (human embryonic kidney fibroblast)	DMEM + 10%FBS + 1X penicillin-streptomycin solution (from 100X stock) + 20mM HEPES	Adherent type of culture grows in monolayer. This cell line grows fairly well and okay with overgrowth. As long as the media is regularly changed they can tolerate cell-cell contact better than 1080 cells. Purchased from ATCC.
NIH3T3 (mouse embryonic kidney fibroblast)	DMEM + 10%FBS + 1X penicillin-streptomycin solution (from 100X stock) + 20mM HEPES	Adherent type of culture grows in monolayer. Cell growth is nice. Growth needs to be maintained within 70%. Greater confluency will change the property of the cell. Obtained from Dr. Wang's lab.
U937 (monocyte)	RPMI-1640 + 10%FBS + 1X penicillin-streptomycin solution (from 100X stock) + 20mM HEPES	Suspension type of culture. Maximum growth allowed $2*10^6$/ml. Subculture can be started with a concentration of 10^5/ml Purchased from ATCC.

Cell Type	Culture Condition	Comments
HUVEC (primary endothelial cell)		Primary cell line. Grows for only few passages (5-6 passages). Growth rate is not very fast. Purchased from CAMBREX Biosc.
MEF (mouse embryonic fibroblast)	DMEM + 10%FBS + 1X penicillin-streptomycin solution (from 100X stock) + 20mM HEPES	Adherent type of culture grows in monolayer. This cell line grows fairly well. Shows high level of LRP expression. Obtained from Dr. Dudley Strickland's lab.
PEA13	DMEM + 10%FBS + 1X penicillin-streptomycin solution (from 100X stock) + 20mM HEPES	Adherent type of culture grows in monolayer. This cell line grows fairly well. **LRP is not expressed.** Obtained from Dr. Dudley Strickland's lab.
HEK293-β3	DMEM + 10%FBS + 1X penicillin-streptomycin solution (from 100X stock) + 20mM HEPES	This is integrin β3 transfected HEK293 cells. Grows like HEK293 cells. Obtained from Dr. Jeff Smith's lab.
HEK293-β5	DMEM + 10%FBS + 1X penicillin-streptomycin solution (from 100X stock) + 20mM HEPES	This is integrin β5 transfected HEK293 cells. Grows like HEK293 cells. Obtained from Dr. Jeff Smith's lab.

VITA

Sumit Goswami was born on August 9th, 1976 in Calcutta (Kolkata) a city of historical importance of India. He graduated from high school in 1995. He received his Bachelor degree in Pharmaceutical Sciences from Jadavpur University, Calcutta, India in the year 2001. After completing his Bachelor degree with Honors, he joined Department of Biotechnology in Jadavpur University and finished his Masters Biotechnology in the year 2003. After finishing his Masters he moved to United States with his wife and in fall 2003, he joined the PhD program in the Biochemistry Cellular and Molecular Biology Department (BCMB) at The University of Tennessee, Knoxville. He continued as a graduate student under the supervision of Dr. Cynthia B. Peterson and finished his PhD with a major in Biochemistry Cellular and Molecular Biology on summer 2010.